Geodynamic evolution of the Eastern Pelagonian Zone in north-western Greece and the Republic of Macedonia.

Implications from U/Pb, Rb/Sr, K/Ar, $^{40}Ar/^{39}Ar$ geochronology and fission track thermochronology.

D I S S E R T A T I O N

zur Erlangung des Grades eines Doktors
der Naturwissenschaften

der Geowissenschaftlichen Fakultät
der Eberhardt-Karls-Universität Tübingen

vorgelegt von

Thomas Most
aus Rüsselsheim

2003

Tag der mündlichen Prüfung: 3. Februar 2003

Dekan: Prof. Dr. Dr. h.c. Muharrem Satir

1. Berichterstatter: Prof. Dr. Wolfgang Frisch

2. Berichterstatter: Priv. Doz. Dr. Joachim Kuhlemann

Vorwort

Zu allererst möchte ich mich bei Prof. Dr. Wolfgang Frisch bedanken, der mir die vorliegende Arbeit ermöglicht hat. Seine stetige Diskussionsbereitschaft und seine kritischen und konstruktiven Kommentare haben sehr zum Gelingen dieser Arbeit beigetragen. Bedanken möchte ich mich auch dafür, daß er mir bei meinen Arbeiten immer viel Freiraum ließ und meine Initiativen stets unterstützte. Außerdem ermöglichte er mir die Teilnahme an vielen internationalen Tagungen und Weiterbildungen, sowie erste Einblicke in die Lehre. Die gemeinsamen Geländearbeiten und Tavernenbesuche in Griechenland werden mir unvergessen bleiben.

PD Dr. Joachim Kuhlemann möchte ich für die Übernahme des Korreferats und für die vielen Anregungen und Diskussionen danken.

Prof. Dr. Blazo Boev (Institute of Mining and Geochemistry; St. Cyrils University Skopje, Republik Mazedonien) leistete umfangreiche logistische Unterstützung in Mazedonien. Ohne seine persönliches Engagement, vor allem bei den mazedonischen Behörden, wäre dieses Projekt nie möglich gewesen. Dafür möchte ich ihm an dieser Stelle noch einmal ganz herzlich danken.

Unvergeßlich bleibt mir auch die gemeinsame Geländearbeit mit Prof. Dr. Adamantios Kilias (Institue of Geology, Aristotle University Thessaloniki, Griechenland) und meinem griechischen Leidenskameraden Astelios Avgerinas. Sie beide legten großen Wert darauf, daß neben der Erforschung der Geologie Griechenlands auch der Besuch von Kafenions und Tavernen nicht zu kurz kam.

Dr. István Dunkl hat mich in die Spaltspurenanalysen eingewiesen und ist mir über die ganze Zeit immer mit Rat und Tat zur Seite gestanden. Außerdem übernahm er auch die Ar/Ar Messungen in Bern. Dafür möchte ihm ganz besonders danken.

Dr. Kadosa Balogh (Institute of Nuclear Research, Debreccen, Ungarn) führte die K/Ar Messungen durch. Dr. Igor Villa (Mineralogisches Institut, Universität Bern) ermöglichte die Ar/Ar Messungen.

Dr. Wolfgang Siebel hat die U/Pb und Rb/Sr Datierungen durchgeführt und mich in die knifflige Technik der hierfür notwendigen Probenpräparation eingeführt. Besonders bedanken möchte ich mich aber vor allem bei ihm, für seine stetige Diskussions- und Hilfsbereitschaft in allen Fragen der Geochronologie.

Dr. Mathias Westphal führte mich in die Bedienung der Mikrosonde ein und stand immer mit Rat und Tat zur Seite, wenn die Sonde anders wollte, als ich. Und das war recht häufig der Fall. Außerdem hat er mir sehr viele Anregungen für meine Arbeit gegeben und war immer bereit meine Daten mit mir zu diskutieren. Dafür herzlichen Dank.

PD Dr. Thomas Wenzel half bei den Mikrosondenmessungen der Apatite.

Besonders bedanken will ich mich auch bei unseren TA´s Gerlinde Höckh, Dagmar Kost und Doris Mühlbayer Renner. Ohne ihre tatkräftige Unterstützung hätte die Probenaufbereitung der Altersproben mit Sicherheit um einiges länger gebraucht. Besonderes danken muß ich auch Thomas Piepenbrink für die super schnelle Grobpräparation meiner Proben. Frau Indra Gill-Kopp hat die Dünn- und Mikrosondenschliffe hergestellt.

Beim Land Baden-Württemberg (Graduierten-Stipendium), dem Deutschen Akademischen Austausch-Dienst und der Deutschen Forschungsgemeinschaft möchte ich mich für die großzügige finanzielle Unterstützung des Projektes bedanken.

Unvergeßlich bleiben mir auch die vielen (häufig weniger wissenschaftlichen) Diskussionen und Gespräche mit Ines Dünkel, Uwe Dünkel, Horst Hann, Bernd Kaufmann, Franz Moser, Martina Schwab und Conny Spiegel.

Mein ganz besonderer Dank gilt meiner Frau Petra Most, die mich auch bei den Geländearbeiten in Mazedonien und Griechenland begleitet und unterstützt hat. Ohne sie hätte es mit Sicherheit nur halb soviel Spaß gemacht.

Zusammenfassung

Die Pelagonische Zone ist eine ca. 420 km lange und 60 km breite NNW-SSE streichende Einheit der zentralen Helleniden. Sie ist in der Republik Mazedonien, in Albanien und auf dem griechischen Festland aufgeschlossen. Im W schließt sich die Pindos Zone, im Osten die Vardar Zone an. Das Arbeitsgebiet liegt in der kaum untersuchten nördlichen Pelagonischen Zone (Nordwest Griechenland und Republik Mazedonien).

Aufgrund der Unterschiede in der lithologischen, strukturellen und metamorphen Entwicklung wird die nördliche Pelagonische Zone in Nordwest-Griechenland, der Republik Mazedonien und Albanien weiter unterteilt, in eine West und Ostpelagonische Zone. Das kristalline Basement der Westpelagonischen Zone besteht aus Graniten, Gneisen und Glimmerschiefern, welche von spätjurassischen Ophioliten und unmetamorphen paläozoischen Gesteinen überlagert werden. Die Ostpelagonische Zone zeigt eine Antiklinalstruktur und besteht aus einer unteren Einheit (hauptsächlich Granitoide und Gneise) und einer oberen Einheit (metaklastische und metakarbonatische Sequenz).

Die vorliegende Arbeit konzentriert sich auf die Ostpelagonische Zone, wobei ergänzend Proben aus der Westpelagonischen Zone und der Vardar Zone untersucht worden. Die geochronologischen, struktur-geologischen und petrologischen Untersuchungen wurden mit dem Ziel durchgeführt, neue Daten für die Rekonstruktion der geodynamische Entwicklung zur Verfügung zu stellen.

U/Pb Zirkon Datierungen an ostpelagonischen Graniten zeigen zwei magmatische Ereignisse während des späten Paläozoikums an, welche mit der Schließung der Paleotethys im Zusammenhang stehen.

In der West und Ostpelagonischen Zone, sowie in der Vardar Zone konnten mit Hilfe von K/Ar, Ar/Ar und Rb/Sr Datierungen fünf unterschiedliche tektonometamorphe Ereignisse während der alpidischen Orogenese datiert werden.
Ein blauschieferfazielles Ereignis D_1 (~150 Ma) ist in den liegenden Einheiten eines allochtonen Marmors in der Ostpelagonischen Zone erhalten. Minimale Drücke um 12.5 kbar wurden mit der Phengit-Barometrie abgeschätzt.
Bedingungen der oberen Grünschiefer bis Amphibolitfazies wurden während D_2 (148-130 Ma; spätes Jura – frühe Kreide) in der Ostpelagonischen Zone erreicht. Der Metamorphosegrad nimmt dabei von der oberen in Richtung der unteren Einheit kontinuierlich zu. Geothermobarometrische Untersuchungen ergaben maximale Temperaturen <650° C bei minimalen Drücken zwischen 6 und 10 kbar. Strukturgeologische Daten zeigen eine Transportrichtung der tektonischen Decken nach NE während D_2 an.
Während der mittleren Kreide (110-90 Ma) wurden die obere Einheit der Ostpelagonischen Zone und die Almopias Einheit der Vardar Zone durch ein weiteres Ereignis (D_3) erneut überprägt. Die begleitende Metamorphose erreichte die Bedingungen der Grünschieferfazies. Dabei wurde die obere Einheit der Ostpelagonischen Einheit nur schwach, die Almopias Einheit hingegen penetrativ überprägt. Während D_3 erfolgte der Deckentransport in Richtung SW.

NE gerichtete Bewegungen unter grünschieferfaziellen Bedingungen markieren das vierte Ereignis (D_4) während des Campan. Die zeitgleiche Deformation in der Ostpelagonische Zone lief unter semi-duktilen bis bruchhaften Bedingungen ab.

Nach W gerichtete Bewegungen um 65 Ma (D_5) in der Almopias Einheit der Vardar Zone werden von einer schwachen grünschieferfaziellen Metamorphose begleitet. Dieses Ereignis markiert zugleich das letzte duktile Überschiebungsereignis im Arbeitsgebiet.

Zirkon und Apatit Spaltspurendatierungen erlauben die zeitliche Rekonstruktion der bruchhaften Deformationsgeschichte. Identische Zirkonspaltspurenalter zwischen 86 und 63 Ma aus der Vardar Zone und der Ostpelagonischen Zone zeigen eine zeitgleiche Abkühlung dieser Einheiten unter 240° C an. In der Westpelagonischen Zone liegen die Zirkonspaltspurenalter zwischen 53 und 39 Ma. Die Abkühlung der Gesteine unter 100° C wird von den Apatitspaltspurenaltern angezeigt. Sie werden von der Vardar Zone (60 Ma) in Richtung Westpelagonische Zone (30 Ma) kontinuierlich jünger. Zusammen mit den strukturgeologischen Daten zeigen sie die paläozäne bis oligozäne Bildung eines nach W gerichteten Überschiebungskomplexes an. Nach NE gerichtete Extensionsbewegungen markieren das Endstadium der Entwicklung der Ostpelagonischen Zone nach dem mittleren Oligozän.

Summary

The Pelagonian Zone is a ca. 420 km long and 60 km broad NNW-SSE striking part of the central Hellenides, which is exposed in the Republic of Macedonia, Albania and the Greek mainland. It is flanked by the Pindos Zone in the W and the Vardar Zone in the E. The study area is located in the poorly studied northern Pelagonian Zone in north-western Greece and the Republic of Macedonia.

According to differences in their lithology, structural and metamorphic evolution the northern Pelagonian Zone in north-western Greece, the Republic of Macedonia and Albania is subdivided into a West and East Pelagonian Zone. The crystalline basement of the West Pelagonian Zone consists of granites, gneisses and micaschists, which are superimposed by Late Jurassic ophiolites and unmetamorphosed Paleozoic rocks. The East Pelagonian Zone has an anticlinal shape and comprises a lower unit (mainly granitoids and gneisses) and an upper unit (metaclastic and metacarbonatic sequence).

This study is concentrated on the East Pelagonian Zone, whereas additional samples derived from the West Pelagonian Zone and Vardar Zone were also investigated. Geochronological, structural and petrological investigations were carried out to provide new data for the geodynamic reconstruction of this part of the Hellenic orogen.

U/Pb zircon age determinations on East Pelagonian granites gave two different magmatic events during the Late Paleozoic, which were related to the closure of the Paleo-Tethyian ocean.

In the West and East Pelagonian Zone and the Vardar Zone five different tectonometamorphic events, which are related to the Alpine orogeny, were dated by K/Ar, Ar/Ar and Rb/Sr.

Blueschist facies conditions during D_1 (~150 Ma) are preserved at the bottom of an allochtonous marble in the East Pelagonian Zone. Minimum pressures of 12.5 kbar were estimated by phengite geobarometry.
Upper greenschist to amphibolite facies conditions were reached during D_2 (148-130 Ma; Late Jurassic – Early Creatceous) in the East Pelagonian Zone, whereas the metamorphic grade increases from the upper unit towards to the lower unit. Geothermobarometric investigations gave maximum temperatures <650° C at minimum pressures between 6 and 10 kbar. Structural data indicates top to NE directed nappe transport during D_2.
During Middle Cretaceous (110-90 Ma) the upper unit of the East Pelagonian Zone and the Almopias Unit of the Vardar Zone were effected by D_3. The accompanied metamorphism reached middle greenschist facies conditions. The East Pelagonian Zone was only weakly affected in the upper unit, whereas the Almopias Unit was penetrative overprinted by D_3. During D_3, nappe transport occurred top to SW.
D_4 (Campanian) is marked by top to NE directed nappe transport under greenschist facies conditions in the West Pelagonian Zone. In the East Pelagonian Zone the deformation occurred only under semi-ductile to brittle conditions.
Westward directed movements around 65 Ma, which are accompanied by a lower greenschist facies metamorphism (D_5), mark the latest ductile event caused by thrusting in the Almopias Unit of the Vardar Zone.

Zircon and apatite fission track thermochronology enable the reconstruction of the brittle deformation history. Zircon FT ages between 86-63 Ma obtained from the East Pelagonian Zone and the Vardar Zone indicate contemporaneous cooling below 240°C of these units. In the West Pelagonian Zone zircon FT ages between 53 and 39 Ma were obtained. The apatite FT ages indicate cooling off rocks below 100° C. They continuously decrease from the Vardar Zone (60 Ma) towards to the West Pelagonian Zone (30 Ma). Together with structural geological data they indicate the formation of westward propagating thrust complex during Paleocene to Oligocene time. Extensional NE directed movements mark the final stage in the evolution of the East Pelagonian Zone after the Middle Oligocene.

Contents

1 Aim of study

During the last decades numerous research projects were dedicated to the geodynamic evolution of the Pelagonian Zone, especially along the Greek coastline (Olympos, Ossa, Pelion, Evvia, Kranea and Pieria). In contrast to this, minor strenghts were put on the Pelagonian Zone outcropping in north-western Greece, Albania and the Republic of Macedonia. Especially the part situated in the Republic of Macedonia was hardly open to international researchers for the last decades, for political reasons. Therefore, no comprehensive reconstruction of the evolution of the Pelagonian Zone of the Hellenides as well as their northern continuations in the Dinarides is available until today.

The aim of this study is to provide new data from this poorly studied part of the Hellenides and to reinitiate the research in this part of the Hellenic orogen. This might help to enable a complete reconstruction of the geodynamic evolution of the Dinaridic – Hellenidic realm in the future. Furthermore it is purposed to clarify if the East Pelagonian Zone also represent a metamorphic core complex like the further south situated tectonic windows of the Olympos-Ossa, Kranea and Pelion region.

The study presented here is especially focused on geochronology and thermochronology. Where necessary accompanying structural geological and petrological investigations were carried out, which provide a base for the future. Note that the latter are not primary targets of this study and they do not substitute further detailed investigations.

2 Geological setting and framework

2.1 The Hellenides

The present structure of the Hellenides and their northern continuation, the Dinarides, is the result of a Mesozoic to Cenozoic orogeny, related to the ongoing convergence between the Apulian and European plates.
A primary description as well as a first tectonic subdivision of the Hellenides and the Dinarides was carried out by Phillipson (1896, 1898) and Kossmat (1924) and was later elaborated by Renz (1940) and Medwenitsch (1956c, 1956a, 1956b). The present subdivision of the Hellenides into NNW-SSE trending zones (Fig. 1.1A) is related to the structural geological and sedimentological investigations of Aubouin et al. (1959), Aubouin et al. (1963, 1976), Celet and Ferriere (1978), Jacobshagen et al. (1978) as well as Jacobshagen (1986).

after Aubouin et. al (1959)		after Jacobshagen (1986)	Major tectonic units
Hellenides	external	Foreland	Preapulian Zone (PRAZ)
		West Hellenic nappes	Ionios Zone (IZ) Gavrovo-Tripolitza Zone (GTZ)
	internal	Central Hellenic nappes and Median Crystalline belt	Pindos Zone (PDZ) Parnass Zone (PNZ) Subpelagonian Zone (SBPZ) Pelagonian Zone (PZ) Attic-Cycladic-Crystalline Belt (ACCB)
		Internal Hellenic nappes	Vardar Axios Zone (VZ) Ophiolites
		Hinterland	Serbomacedonian Massif (SRM) Rhodope Massif (RM)

Tab. 1.1: Comparison of the subdivision of the Hellenides into major tectonic units (from W to E) after Jacobshagen (1986) and Aubouin et al. (1959). Abbreviations are given in parentheses.

The Apulian platform forms the foreland of the Hellenic orogen, which is exposed on islands (e.g. Paxos) situated west of the Greek mainland. The Hellenic hinterland is represented by the crystalline of the Serbomacedonian and the Rhodope Massif (Fig. 1.1A).
The west vergent nappe system of the Hellenic orogen comprises the following major tectonic units (from W to E, cf. Tab. 1.1 and Fig. 1.1A):
The Preapulian Zone is made of carbonates (Triassic to Early Tertiary) and forms the eastern margin of the Apulian platform. Late Permian to Early Tertiary semipelagic sediments of a shelf basin characterise the Ionios Zone. The Gavrovo-Tripolitza Zone comprises Late Permian to Paleocene neritic carbonates, deposited on a rise between the Ionios and the Pindos Zone. Both, the Ionios as well as the Gavrovo-Tripolitza Zone are overlain by the Westhellenic flysch (Eocene to Miocene). The geodynamic interpretation of the Pindos Zone is not finally cleared. The sedimentary succession starts with Triassic carbonates and continues with deep sea sediments. Occurrences of Jurassic ophiolites in the Pindos Zone are rare. The model of Jacobshagen (1986) suggests a deep

sea marine setting on thinned continental crust without production of oceanic crust and spreading. Contrary to this the occurrence of MORB-type oceanic crust in the Pindos Zone is safety proven by e.g. Robertson (1991) and Smith (1993).

In the Subpelagonian Zone unmetamorphosed rocks are superimposed by ophiolites. The ophiolite complexes (Vourinos, Orthris and Vermion) are regarded as allochtonous remnants of obducted oceanic crust from the Pindos ocean (e.g. Barton, 1976; Robertson, 1991). In contrast to this Zimmerman (1972) assume, that the Vourinos ophiolite was probably originated in the Vardar Zone.

The Pelagonian Zone forms the central part of the Hellenides and is regarded as a pre-Alpine crystalline massif covered by Mesozoic platform carbonates. The Attic-Cycladic-Crystalline Belt (ACCB) is thought to be the southern continuation of the Pelagonian Zone.

The Vardar Zone (also referred to as Vardar-Axios Zone) represents the eastern Hellenic and Dinaridic ophiolite belt and comprises MORB-type oceanic crust (Permian to Jurassic) as well as Paleozoic and Mesozoic sediments. The Serbomacedonian and the Rhodope massif are predominately composed of crystalline rocks and are regarded as a continental slope and rise during Jurassic and Cretaceous time.

According to Jacobshagen (1986) the Alpine evolution of the Hellenic orogen is dominated by four different orogenic cycles (Tab. 1.2), each of them is accompanied by folding, nappe transport and regional metamorphism. The presence of an additional orogenic cycle during Late Cretaceous times is assumed by Jacobshagen (1986).

Orogenic cycle	Duration	Thermochronologic age [Ma]
Neohellenic	Miocene - recent	25 - present
Mesohellenic	Eocene - Oligocene	55 - 25
Eohellenic	Tithonian - Albian	144 - 100
Cimmeric	pre Tithonian	before 144

Tab. 1.2: Major cycles of the Hellenic orogeny after Jacobshagen (1986).

The current boundaries of the Aegean region are formed by the subduction of the African plate below the Eurasian plate (Fig. 1.1A). It is assumed that the subduction was initiated in response to continued convergence between Africa and Eurasia after Apulia became sutured to Eurasia.

The timing of the onset of subduction is uncertain. Depending on the used method the start of subduction is thought to took place between 50 and 4 Ma.

Meulenkamp et al. (1988) and Spakman et al. (1988) suggested an onset of subduction between 26 and 40 Ma due to their seismic tomographic investigations. Based on the oldest rocks of island arc affinity in the Aegean, Le Pichon and Angelier (1979) calculated an age around 13 Ma. The Late Miocene to Early Pliocene volcanism in the Aegean is thought to mark the start of subduction according to Taymaz et al. (1990).

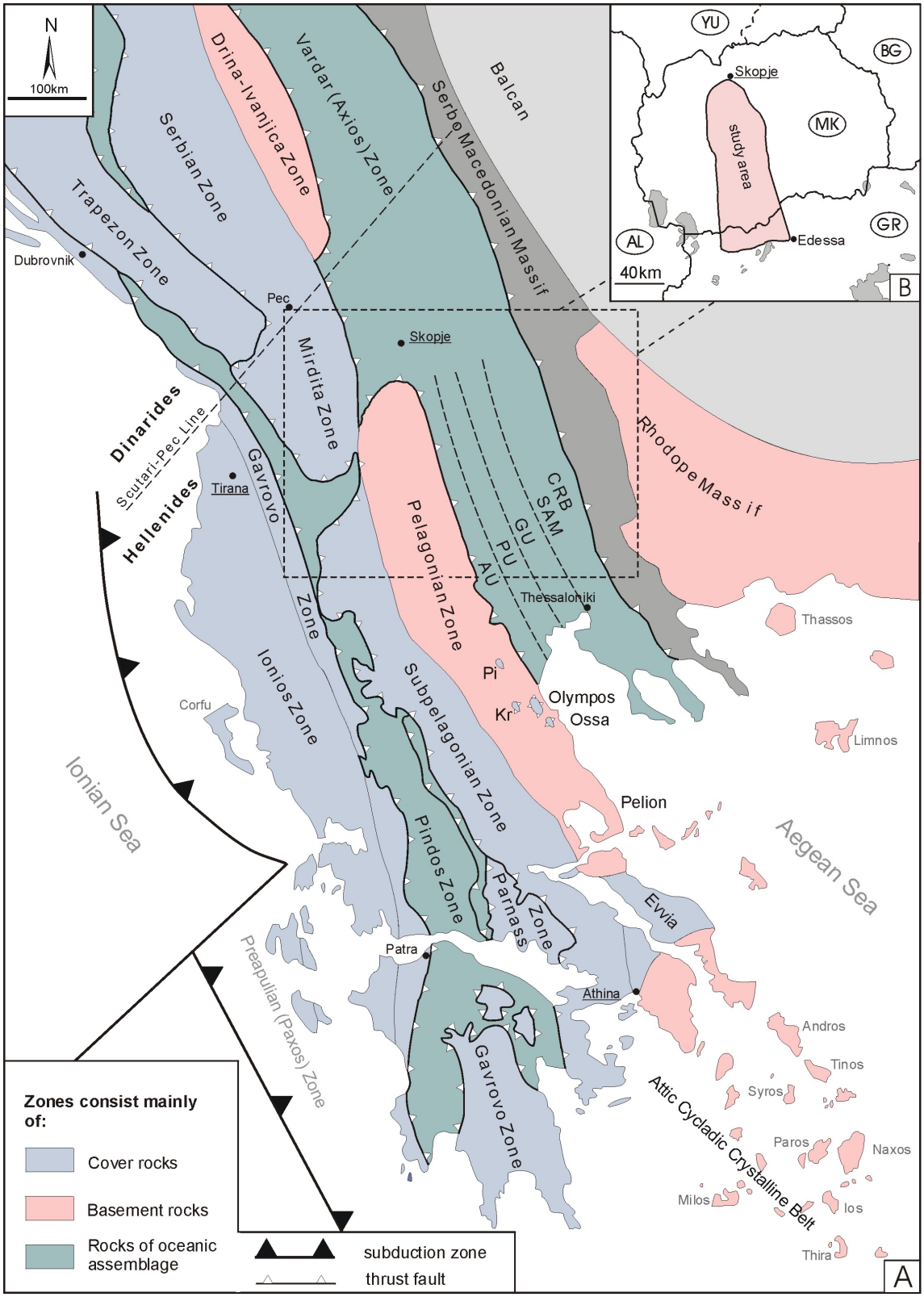

Fig. 1.1: A: Compiled geological sketch map of the major tectonic units of the Dinarides and Hellenides. **B:** location of the main study area in NW Greece and the Republic of Macedonia (modified after Aubouin et al., 1959). Abbreviations: AL = Albania; AU = Almopias Unit; BG = Bulgaria; CRB = Circum Rhodope Belt; GR = Greece; GU = Guevguelije Unit; Kr = Kranea; MK = Republic of Macedonia; Pi = Pierien Mt.; PU = Paikon Unit; SAM = Serbo Macedonian Massif; YU = Serbia.

2.2 The Pelagonian Zone

Kossmat (1924) established the term 'Pelagonian massif' as a descriptive term for the crystalline basement of the Balkan peninsula, named by the plain between Prilep and Bitola (located in the Republic of Macedonia). Later, the crystalline basement and the overlying Mesozoic cover rocks were combined by the term Pelagonian Zone (PZ; Brunn, 1956), which is exposed out from Skopje (Rep. Macedonia) to northern Evvia (Greece), covering an area of 420 km length and up to 60 km width. The northern Dinaridic continuation of the Pelagonian Zone is referred to as Drina-Ivanjica or Golija Zone (see Fig. 1.1A).

The polymetamorphic crystalline basement of the Pelagonian Zone comprises granites, micaschists, para- and orthogneisses as well as amphibolites and is exposed to the surface in tectonic windows like the Olympos-Ossa (Schermer, 1992), Pelion (Lips et al., 1999), Rizomata (Kilias and Mountrakis, 1985) and Kranea windows (Kilias et al., 1991; Sfeikos, 1992). Jacobshagen (1986) supposes a pre-Alpine, probably Hercynian formation age for the crystalline basement, based on U/Pb zircon data around 300 Ma obtained from various granitoids of the Pelagonian Zone (cf. Yardwood and Aftalion, 1976; Koroneos et al., 1993; DeBono et al., 1999; Vavassis et al., 1999; Avgerinas et al., 2001; Reischmann et al., 2001). Alpine nappe formation within the Pelagonian Zone is safely proven by the discovery of Eocene nummulites in the lowest tectonic units of the Olympos area (Godfriaux, 1962).
The western margin of the PZ is covered by an Late Permian to Early Tertiary metaclastic sequence containing metapelites, meta conglomerates, meta-arkoses and calc schists with intercalations of meta-volcanics (Mountrakis et al., 1983). Towards to the W, the PZ is superimposed by unmetamorphosed Paleozoic and Mesozoic clastics and limestones of the Subpelagonian Zone (Aubouin, 1959).

The whole Pelagonian Zone underwent a common Variscan geodynamic evolution. During the Alpine orogeny the crystalline basement as well as the cover rocks of the Pelagonian Zone underwent different regional tectonometamorphic evolutions. Therefore, the Pelagonian Zone is subdivided into a southern- and northern Pelagonian Zone (Fig 1.1A). The southern Pelagonian Zone (SPZ) is exposed between Macedonia and Evvia. The northern Pelagonian Zone (NPZ) is exposed in north-western Greece (Macedonia), the Republic of Macedonia and Albania. A simplified geological map of the northern Pelagonian Zone is presented in Fig. 1.3.

According to Mountrakis (1984), the NPZ can be further subdivided into a West Pelagonian Zone (WPZ; in Albania referred to as Korap Zone) and an East Pelagonian Zone (EPZ), related to differences in their lithology as well as their metamorphic and structural geological evolution.

The East Pelagonian Zone consists of various crystalline rocks. Dumurdzanov (1985) subdivided the East Pelagonian Zone into a lower unit (granites, migmatites, micaschists, gneisses and intercalated amphibolites) and an upper unit (micaschists, gneisses, marbles and intercalated amphibolites). The metamorphic grade increases from upper greenschist facies conditions (epidote amphibolite facies) at the margins to amphibolite facies conditions towards to the central part (Selecka Mountains) of the East Pelagonian Zone. Jacobshagen (1986) assumed a pre-Alpine age for the amphibolite facies event, which is probably related to the intrusions of the granites. The oc-

currence of two different greenschist facies metamorphic events (I: around 130-140 Ma, II: around 100 Ma) during the Eohellenic orogeny was successfully proved by Borsi and Ferrara (in: Mercier, 1973).
In contrast to this, Arsovski et al. (1977) and Arsovski and Dumurdzanov (1984) suppose a Proterozoic intrusion age of the East Pelagonian granitoids (based on an unspecified K/Ar age of around 600 to 1000 Ma (Deleon, 1966) as well as an Proterozoic sedimentation age of the recent East Pelagonian marbles.

The West Pelagonian Zone in Albania and NW Greece consists of granites, orthogneisses and micaschists and is superimposed by Jurassic ophiolites and unmetamorphosed Ordovician to Devonian carbonates (Dumurdzanov, 1988). Hoxha (2001) supposes that the ophiolites were originally situated in the Vardar Zone and thrusted during Early Cretaceous times onto the WPZ, whereas Robertson and Shallo (2000) as well as Bortolotti et al. (2002) assume that the ophiolites were originated in the Pindos Zone. Three metamorphic events during pre-Alpine and Alpine times were proven by the investigations of Mposkos et al. (2001). According to them, the crystalline basement was affected by an amphibolite facies metamorphism (P = 3.5-6 kbar and T = 640-700° C) as well as a low pressure / high temperature event (P ~ 2.5 kbar and T = 600-610° C) during pre-Alpine times. Conditions of the upper greenschist facies were reached during the Alpine orogeny. However, these investigations were not accompanied by geochronological analyses. The timing of the events therefore remains uncertain.

Especially the southern part of the Pelagonian Zone was subject to numerous recent geochronological and structural geological studies, which investigates predominantly the Alpine orogenic history. For detailed informations the reader is referred to the literature cited below Fig. 1.2.
In contrast to this only limited modern structural geological, petrological and geochronological data are available from the northern Pelagonian Zone, whereas these data practically do not exist for the Yugoslavian part of the Pelagonian Zone. Detailed petrological investigations are missing for the entire Greek mainland. A comprehensive compilation of the previous studies is given in Fig. 1.2.

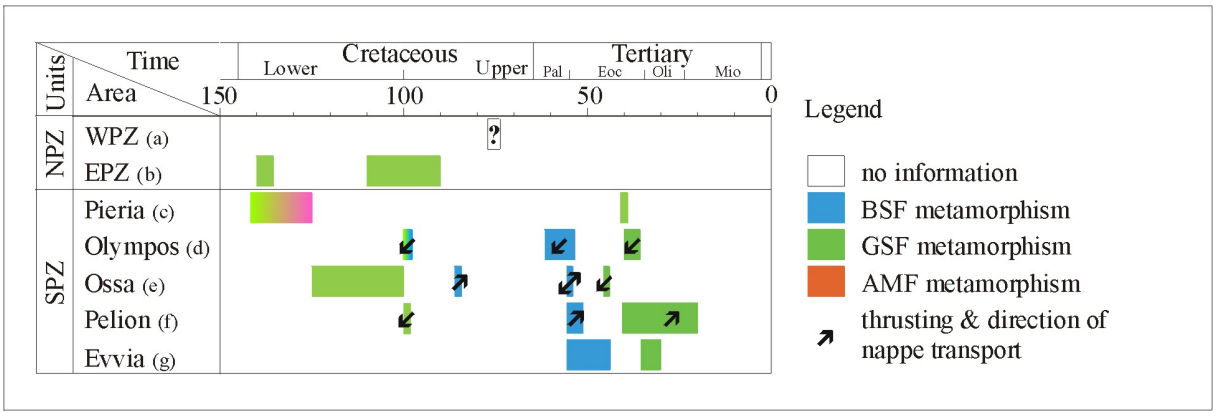

Fig. 1.2: Comprehensive and generalised comparison of previous structural geological, petrographical and geochronological studies form the entire Pelagonian Zone. The pre-Alpine evolution is not considered. Indexes: (a) Koroneos et al. (1993) and Mposkos et al. (2001); (b) Borsi and Ferrara in: Mercier (1973); (c) Barton (1976); (d) Schermer et al. (1990); (e) Lips et al. (1998); (f) Lips et al. (1999); (g) Faupl et al. (2002). Shaded areas = transition between two metamorphic grades; AFM = amphibolite facies, BSF = blueschist facies and GSF = greenschist facies.

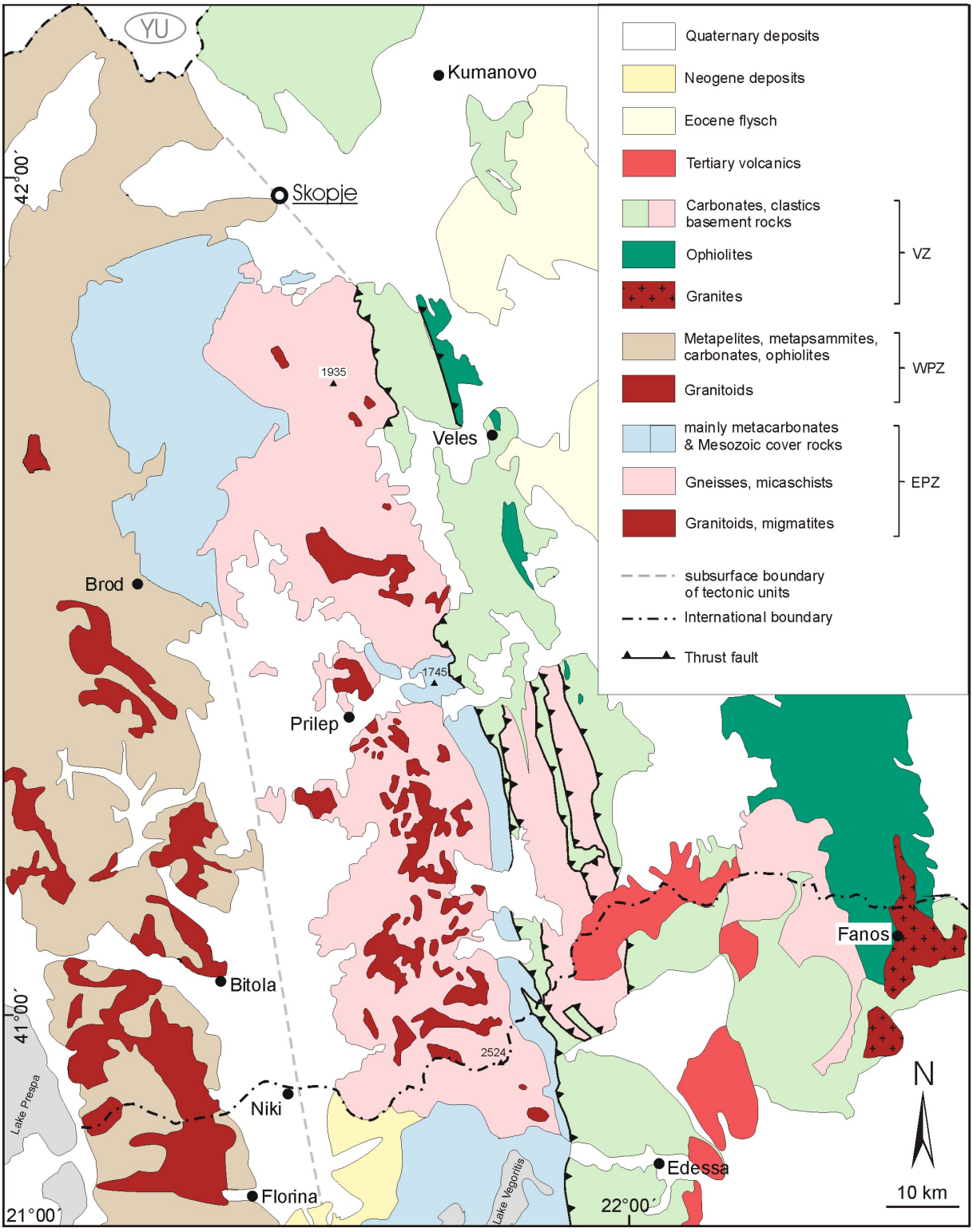

Fig. 1.3: Simplified geological sketch map of study area in northern Greece and the Republic of Macedonia. Compiled from the geological map of Greece (1:500.000) and the geological map of the Republic of Macedonia (1:500.000). Abbreviations: EPZ = East Pelagonian Zone, WPZ = West Pelagonian Zone, VZ = Vardar Zone.

2.3 The Vardar Zone

The term Vardar Zone was also established by Kossmat (1924), named by the river Vardar. Based on differences in their Cretaceous sedimentation history, Mercier (1973) subdivided the Vardar Zone into three NNW-SSE trending units (Almopias, Paikon and Peonias), whereas the investigations of Kockel et al. (1977) led to the present division of the Vardar Zone into the following five units (from W to E):

(I) The Almopias Unit (AU) comprises mainly ophiolites overlain by conglomerates and Late Cretaceous shallow water carbonates. Crystalline basement rocks superimposed by calcschists, serpentinites, marbles and metaporphyrites occur only in the Ano Peternik Unit (APU), which is subunit of the Almopias Unit (Fig. 1.1A) in NW Greece and the Republic of Macedonia. North of Kavardarci, the AU consists of only Late Cretaceous sediments. Two different metamorphic events are known in the AU. The first, pre Maastrichtian event yielded greenschist facies to blueschist facies conditions, while upper greenschist facies conditions represent the second event at around 63 Ma (Mercier, 1973). A relatively steep E dipping thrust fault marks the boundary between the Almopias unit and the adjacent East Pelagonian Zone. The boundary itself is a up to 4 km broad sinistral strike-slip fault, the so called 'zone de broyage longitudinal' (Mercier, 1973), which is also thought to be responsible for the earthquake flattened Skopje in 1962.

(II) The Paikon Unit (PU) comprises crystalline basement rocks overlain by marbles, calc schists, a metavolcanic sedimentary sequence (rhyolite, spilite, basalt), Late Jurassic to Early Cretaceous shallow water carbonates as well as terrestic sediments of a continental molasse. The latter are transgressively overlain by Late Cretaceous shallow water carbonates and clastic sediments. During Late Jurassic to Early Cretaceous times the volcanics of the PU were affected by a blueschist metamorphic event (T = 330-450° C, P = 3-7 kbar; Baroz et al., 1987), related to subduction. Upper greenschist facies conditions represent a second post Maastrichtian metamorphism.

Both, the Almopias and Paikon Unit are overlaid by an Late Maastrichtian to Eocene flysch and were affected by a Pliocene volcanism.

(III) Early to Middle-Jurassic ophiolites (gabbros, dolerites and pillow lavas) build up the Guevguelije Unit (GU). During Tithonian times the ophiolite complex was intruded by the Fanos granite (Borsi et al., 1966) and covered by shallow water carbonates. The GU underwent only contact metamorphism.

(IV) The Stip Axios Massif (SAM) comprises pre-Alpine basement rocks intruded by Late Jurassic granites (167-142 Ma, Rb/Sr-biotite Borsi et al., 1966). Intensive mylonitisation of the SAM rocks under GSF conditions at around 156 Ma (Rb/Sr) is reported by Borsi et al. (1966).

(V) The Circum Rhodope Belt (CRB) comprises basement rocks and ophiolites, which covered by Mesozoic sediments.

2.4 Location of study areas

The main study area is located in NW-Greece and the Republic of Macedonia. This study is focused on the East Pelagonian Zone, whereas additional investigations were carried out in the adjacent West Pelagonian Zone and Almopias Unit (VZ). Samples for geochronological, thermochronological and structural investigations were taken along E-W trending profiles covering each of the zones named above. For petrological investigations, samples were only taken from the EPZ.

Additional samples for fission track thermochronology were obtained from the Olympos – Kranea (Fig. 1.1A) region to compare the latest geodynamic evolution and cooling histories of the southern and northern Pelagonian Zones.

Field work was carried out in 1998, 1999 and 2001. Unfortunately the field campaign in the Republic of Macedonia was limited to the autumn of 1998, because of the unstable political situation and the civil war in the Kosovo area. Thus it was not possible to collect further samples to intensify the investigations.

3 Geothermochronology

3.1 Sample preparation

3-6 kg of unaltered rock material were crushed in a jaw crusher. For whole rock age determinations a sample split was powdered in a tungsten carbide mill. The samples were washed and sieved in several intervals. A Wilfley shaking table was used for separation if only apatite and zircon concentrates were required. Carbonates were dissolved using 5% acetic acid. Quartz and feldspar were removed during an initial density separation with sodium-polytungstate (ρ=2.9 g/cm³). White mica, biotite, apatite and zircon were separated by hand magnet and a Franz Magnetic separator. Methylene iodide (ρ=3.3 g/cm³) was used to separate apatite from zircon.
Hand picking under the binocular microscope was performed to gain pure mineral concentrates. A detailed description of geochronological sample preparation is for instance given in Geyh and Schleicher (1990).

3.2 Principle of radiometric dating

The determination of radiometric ages, geological events and their duration is based on the decay of long-lived radionuclides. Rutherford (1906) noted at first that the decay of a radioactive mother nuclide to its stable daughter nuclide and therefore the ratio of radioactive mother isotopes and stable daughter isotopes depends only on the time since the isotope system had closed, expressed by equation 3.1 below.

$$N_D = N_P\left(e^{\lambda t} - 1\right) \qquad (3.1)$$

N_D = number of daughter atoms
N_P = number of parent atoms
λ = decay constant
t = time elapsed since the system was closed

3.3 U/Pb dating in zircons

Minerals containing natural uranium (e.g. zircon, monazite, apatite) can be dated by the conventional uranium / lead method (Faure, 1986). Uranium has three unstable isotopes ^{238}U, ^{235}U and ^{234}U, which decay to ^{206}Pb, ^{207}Pb and ^{208}Pb. The current concentrations of the parent isotopes and those of the lead daughter isotopes accumulated since radioactive equilibrium was established in a closed system lead to three independent possibilities for dating described by the equations 3.2–3.2.2 below.

The data is generally evaluated in concordia or discordia diagrams. The U/Pb ages are concordant if the same age is obtained from all three independent systems (^{238}U/^{206}Pb, ^{235}U/^{207}Pb and ^{207}Pb/^{206}Pb).

The U/Pb concordia ages were calculated using the software program Pb-Dat (Ludwig, 1988). For further informations on U/Pb geochronology and age calculations see Faure (1986), Geyh and Schleicher (1990) and Wendt (1986).

$$t = \frac{1}{\lambda_{238}} \ln\left(\frac{^{206}Pb^*}{^{238}U} + 1\right) \qquad (3.2)$$

where:

t = time elapsed since the system was closed

λ = decay constant

$$t = \frac{1}{\lambda_{235}} \ln\left(\frac{^{207}Pb^*}{^{235}U} + 1\right) \qquad (3.2.1)$$

$$\left(\frac{^{207}Pb}{^{206}Pb}\right)^* = \left[\frac{\left(^{207}Pb/^{204}Pb\right) - \left(^{207}Pb/^{204}Pb\right)_0}{\left(^{206}Pb/^{204}Pb\right) - \left(^{206}Pb/^{204}Pb\right)_0}\right] \qquad (3.2.2)$$

3.3.1 Analytical method

Prior to the U/Pb analyses the internal structure of the zircons were analysed by cathodoluminescence (CL) using a JEOL JXA 8900 Superprobe electron microprobe analyser equipped with a CL detector unit (Institute of Geosciences, University of Tübingen).

From each sample four zircon fractions differing in morphology and colour were separated by hand picking and washed in hot 6N HCl and hot 7N HNO_3 to remove surface contaminations before starting the dissolution process. A mixed $^{205}Pb/^{235}U$ tracer solution was added to the grains. The dissolution of grains was performed in PTFE vessels mounted in a 1900 psig Parr acid digestion bomb (Parrish, 1987) using the vapour digestion method of Wendt (1991). The bomb was stored in a heat cupboard at 200° C for seven days in 22N HF and for one day in 6N HCl to assure re-dissolution of the fluorides into chloride salts and to avoid U-Pb fractionation according to Mattinson (1994). U and Pb were separated and purificated in Teflon columns with a 40 µl bed of Bio-Rad AG1-X8 (100-200 mesh) anion exchange resin (Poller et al., 1997). Further details on U-Pb analytical techniques are described by Chen et al. (2000).

The U/Pb measurements were carried out on a Finnigan MAT 262 mass spectrometer at the Institute of Geosciences of the University of Tübingen, using Thermal Ionisation Mass Spectrometry (TIMS). Pb was measured at around 1300° C in single-filament mode and was loaded with a Si-gel (Cameron et al., 1969) onto a pre-conditioned Re filament. U was loaded with 1N HNO_3 onto a pre-conditioned Re filament and was measured in double-filament configuration. Total procedural blanks were <15 pg for Pb and <5 pg for U. A factor of 1‰ per mass unit for instrumental mass fractionation was applied to all Pb analyses, using NBS SRM 981 standard as reference material. Initial common Pb remaining after correction for tracer and blank was corrected using values from the Stacey and Kramers (1975) model. The U/Pb ages were calculated using the decay constants for U published by Jaffrey et al. (1973).

3.3.2 Results

In order to determine the intrusion age of the granitoids, three samples derived from the East Pelagonian Zone were analysed using the conventional U/Pb technique. Samples 8-4 and M98/17 are derived from massive intrusion bodies, whereas sample M99/12 was taken from a small elongated intrusion body. A classification of the granites of the East Pelagonian Zone is given in Fig 3.1.

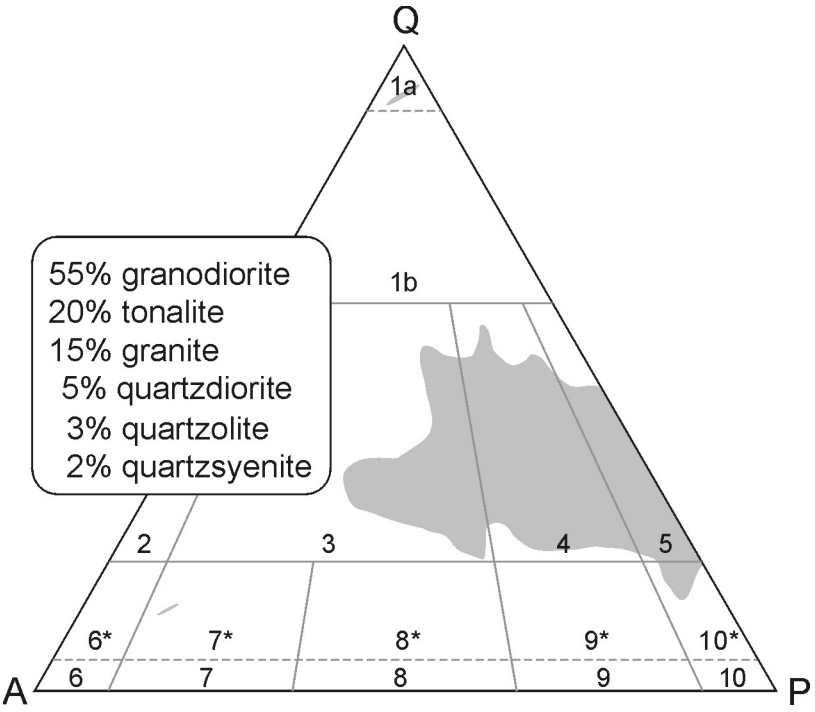

Fig. 3.1: Classification of intrusive rocks of the Selecka mountains, CPZ based on 200 modal analyses (grey areas). Data adapted from Dumurdzanov (1986). 1a) quartzolite, 1b) granitoides rich by quartz, 2) alkaline feldspar granite, 3) granite, 4) granodiorite, 5) tonalite, 6*) alkaline-feldspar quartzsyenite, 7*) quartzsyenite, 8*) quartzmonzonite, 9*) quartzmonodiorite, 10*) quartzdiorite, 6) alkaline-feldspar syenite, 7) syenite, 8) monzonite, 9) monzodiorite, 10) diorite or gabbro.

3.3.2.1 Internal structure of dated zircons

Cathodoluminescence studies on zircon obtained from the dated granites show that all zircons have an euhedral shape and show a concentric, commonly fine oscillatory zoning partially interrupted by dissolution surfaces (see appendix D1, plate a-c). Most of the grains contain inclusions and embayments. Only few grains include inherited cores. Additional features are truncations, dissolved cores, sector zoning and multiple discrete cores. A difference in the internal structure of the zircons from different fractions was not found.

According to Hanchar et al. (1993) and Hanchar et.al (1995) the euhedral shape of crystals, fine oscillatory zoning, the presence of multiple discrete cores and sector zoning indicates (rapid) igneous growth of zircons. Dissolution surfaces can be developed during partial resorption in melt (igneous) or by abrasion and metamorphic growth. Embayments mostly indicate resorbed inclusions or an arrested stage of rapid growth (probably igneous).

Considering the features mentioned above the internal structure of the zircons derived from EPZ granitoids indicate magmatic growth without subsequent metamorphic overgrow.

3.3.2.2 U/Pb dating on zircons

The results of the U/Pb measurements are presented in Fig 3.2. The complete analytical data set is given in Tab. 3.1.

Three fractions (3,4,5) of colourless, euhedral prismatic crystals of sample M99/12 plot on a concordia line with an age of 299±1 Ma (MSWD=0.01). Fraction number two (pink, euhedral prismatic) plots slightly below the concordia line at ~ 273 Ma, which is interpreted as Pb-loss after zircon crystallisation. The latter is not considered in the age calculation.

From granite 8-4 three fractions of colourless, euhedral, short prismatic grains (2,3,4) plot on a concordia line representing an age of 244±1 Ma (MSWD=6.9). Fraction number five (short prismatic, yellow) plots significantly below the concordia line and gives an upper intercept age of 1715±56 Ma. The 244±1 Ma age is interpreted as the granite emplacement age, whereas the 1715±56 Ma age may represent an older inherited component.

Granite sample M98/17 contains three fractions (1,2,4) of yellow, euhedral crystals plotting on the concordia at 246±7 Ma, which is considered as the age of granite emplacement. The pink, euhedral crystals of fraction number 3 plot also on the concordia but around 253 Ma. The slight increased MSWD value of 17 is based on the higher $^{206}Pb/^{207}Pb$ (0.05099±1.75) error of fraction number four (Tab. 3.1).

Sample (fraction)	$^{206}Pb^*$ [mol/g]	$^{207}Pb^*$ [mol/g]	$^{208}Pb^*$ [mol/g]	Σ Pb [ppm]	U [ppm]	$\frac{206}{238}$ ± σ	$\frac{207}{235}$ ± σ	$\frac{207}{206}$ ± σ	apparent ages [Ma] $\frac{206}{238}$	$\frac{207}{235}$	$\frac{207}{206}$ ± σ
8-4											
(2)	2.482x10-8	1.270x10-9	3.665x10-9	6.2	151.7	0.0392 ± 0.53	0.2768 ± 0.60	0.0512 ± 0.28	248.1	248.1	248.3 ± 6.4
(3)	5.629x10-8	2.876x10-9	7.931x10-9	13.9	349.3	0.0386 ± 0.64	0.2723 ± 0.88	0.0511 ± 0.57	244.4	244.5	245.1 ± 13.0
(4)	2.951x10-8	1.515x10-9	4.722x10-9	7.4	185.9	0.0381 ± 0.65	0.2695 ± 0.74	0.0514 ± 0.35	240.8	242.3	257.0 ± 8.0
(5)	1.959x10-7	1.135x10-8	2.197x10-8	48.4	1082.4	0.0434 ± 0.53	0.3465 ± 0.53	0.0579 ± 0.06	273.8	302.1	526.8 ± 1.2
M99/12											
(1)	3.978x10-9	2.075x10-10	6.165x10-10	1.5	20.1	0.0474 ± 1.57	0.3411 ± 4.63	0.0522 ± 4.27	298.7	298.0	292.1 ± 98.0
(2)	3.093x10-7	1.617x10-8	1.913x10-8	72.0	1723.6	0.0430 ± 0.58	0.3102 ± 0.58	0.0523 ± 0.06	271.6	274.4	298.2 ± 1.4
(3)	5.162x10-8	2.700x10-9	5.766x10-9	13.2	260.6	0.0475 ± 0.54	0.3427 ± 0.87	0.0523 ± 0.68	299.2	299.2	299.4 ± 16.0
(4)	4.6453 x 10-8	2.432x10-9	4.139x10-9	12.1	233.1	0.0478 ± 0.58	0.3450 ± 1.13	0.0524 ± 0.95	301.0	301.0	301.0 ± 22.0
(5)	1.6204 x 10-8	8.478x10-10	1.925x10-9	4.6	81.9	0.0474 ± 0.56	0.3421 ± 1.56	0.0523 ± 1.43	298.7	298.8	299.4 ± 33.0
M98/17											
(1)	4.711x10-7	2.413x10-8	4.958x10-8	113.1	2938.1	0.0384 ± 0.54	0.2715 ± 0.55	0.0512 ± 0.06	243.2	243.9	251.0 ± 1.3
(2)	2.231x10-7	1.140x10-8	3.150x10-8	55.6	1393.1	0.0384 ± 0.52	0.2705 ± 0.54	0.0511 ± 0.13	242.9	243.1	245.2 ± 3.0
(3)	1.019x10-7	5.223x10-9	1.310x10-8	25.3	611.2	0.0400 ± 0.54	0.2825 ± 0.61	0.0513 ± 0.27	252.6	252.7	253.2 ± 6.2
(4)	3.510x10-7	1.790x10-8	3.208x10-8	100.2	2164.8	0.0389 ± 0.58	0.2733 ± 1.94	0.0510 ± 1.75	245.8	245.3	240.3 ± 40.0

Tab. 3.1: U/Pb analytical data. All errors refer to 2σ and are given in %.

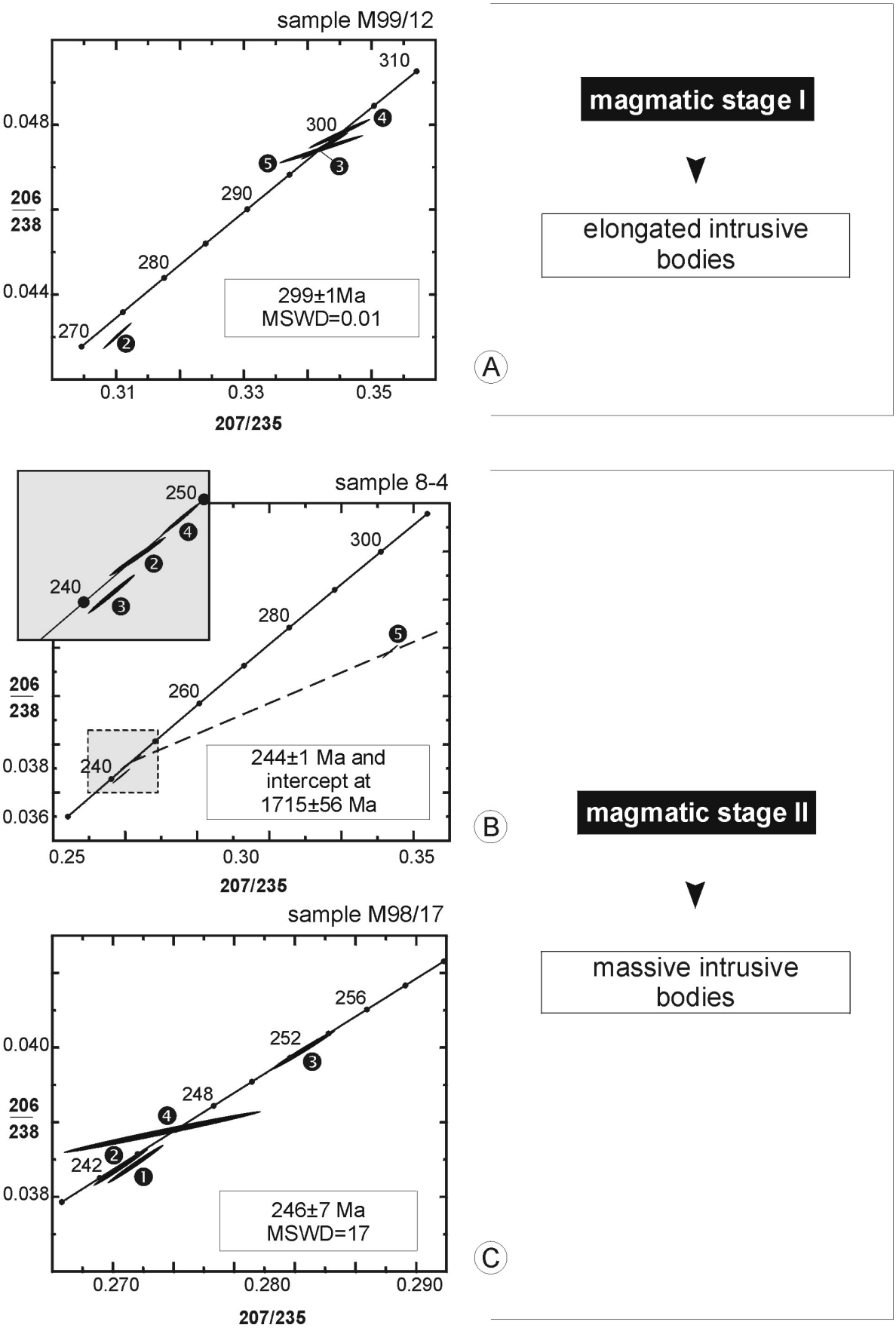

Fig. 3.2: U/Pb concordia plots. Numbers in circles are related to different analysed zircon fractions.

3.4 $^{87}Sr/^{86}Sr$ isotopy

The $^{87}Sr/^{86}Sr$ ratio of seawater is controlled by mixing Sr isotopes derived from the three following sources (Burke et al., 1982): (1) young volcanic rocks, (2) old sialic rocks of the continental crust and (3) marine carbonate rocks of Phanerozoic age (eq. 3.3, 3.3.1).

$$\left(\frac{^{87}Sr}{^{86}Sr}\right)_{sw} = \left(\frac{^{87}Sr}{^{86}Sr}\right)_{V} v + \left(\frac{^{87}Sr}{^{86}Sr}\right)_{S} s + \left(\frac{^{87}Sr}{^{86}Sr}\right)_{M} m \qquad (3.3)$$

(sw) = seawater
(V, S, M) = young volcanic, old sialic and marine carbonate rocks

$$\left(\frac{^{87}Sr}{^{86}Sr}\right)_{sw} = 0.704v + 0.720s + 0.708m \qquad (3.3.1)$$

Therefore, the $^{87}Sr/^{86}Sr$ ratio of seawater can be used as an indicator of kinds of rocks that are exposed to chemical weathering on the surface and/or in oceanic basins (Burke et al., 1982). Erosion of sialic rocks leads to higher $^{87}Sr/^{86}Sr$ ratios than input from young volcanic material. The $^{87}Sr/^{86}Sr$ ratio of marine carbonate minerals is identical to that of seawater at the time of deposition (Fig. 3.3), supposed that there had been no alteration of the $^{87}Sr/^{86}Sr$ ratio during diagenesis, dolomitization and regional metamorphism.

Uncertainties of the method arise from (a) alteration of the $^{87}Sr/^{86}Sr$ ratio during diagenesis or regional metamorphism, (b) inaccurate age assignment, and (c) variations of oceanic $^{87}Sr/^{86}Sr$ ratio at near-shore environment areas with input of young volcanics or old cratonic rocks. Starting from this it is obvious that the $^{87}Sr/^{86}Sr$ ratio does not provide an absolute age, but it is a suitable method to estimate the deposition age of the current metacarbonates.

3.4.1 Results

Measured $^{87}Sr/^{86}Sr$ ratios between 0.7077-0.7078 obtained from two East Pelagonian dolomite marbles (samples M98/42 and GR99/20) correspond with four similar periods with $^{87}Sr/^{86}Sr$ ratios of seawater during Phanerozoic time (Fig. 3.3).
The Tertiary period (case ①) is irrelevant, because it post dates the metamorphism. Structural and U/Pb geochronological data exclude cases ③ and ④, because they denote that carbonate deposition took place before granite emplacement. Thus, a mid-Triassic deposition age of the metacarbonates can be supposed (case ②).

The identical $^{87}Sr/^{86}Sr$ ratios of both samples allow the assumption that there was no intense alteration of the Sr-system during diagenesis and subsequent metamorphism.

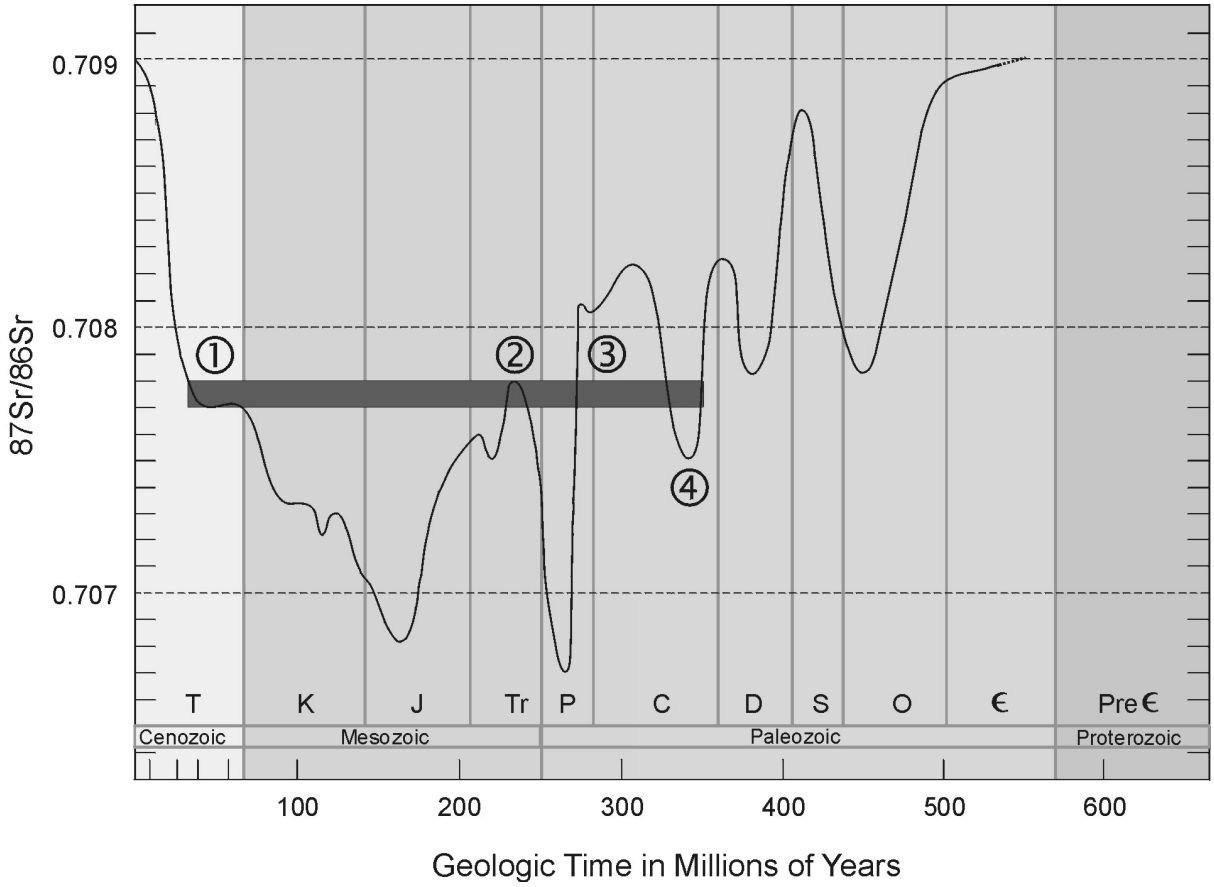

Fig. 3.3: Variation of $^{87}Sr/^{86}Sr$ ratio (curve) of marine carbonates in Phanerozoic time. Based on Faure (1986), data by Burke (1982) using the time scale of Palmer (1983). Grey beam = area of $^{87}Sr/^{86}Sr$ ratio of analysed samples. For numbers in circles, see text explanations.

3.5 K/Ar, $^{40}Ar/^{39}Ar$ dating

The K/Ar method is a widely used tool for geochronological purposes and it is based on the radioactive decay of ^{40}K to ^{40}Ca (90%) and ^{40}Ar (10%). The method requires sample splitting for separate determination of K and $^{40}Ar^*$. ^{40}K can be directly calculated from the K concentration of a sample (measured by flame-photometry, isotope dilution method etc), because the composition of K in terrestrial samples in generally constant. $^{40}Ar^*$ is measured in a mass spectrometer after removing atmospheric argon by heating and adding an isotope spike for the determination of the Ar concentration. The K/Ar age can be calculated from equation 3.4.

$$t_s = \frac{1}{\lambda}\left[\frac{^{40}Ar^*}{^{40}K}\left(\frac{\lambda}{\lambda_e}\right)+1\right] \qquad (3.4)$$

t_s = age of the sample
λ = decay constant
$(^{40}Ar^*/^{40}K)$ = measured ratio of the sample
$(\lambda/\lambda_e)_m$ = measured ratio of the standard

If co-genetic minerals or different grain sizes of the same mineral were analysed from a sample, the data can also be evaluated in $^{40}Ar^*$ / K-diagrams (Harper, 1970). The K/Ar age obtained from such an isochron diagram, is the ^{40}K retention age and is identified as the age of metamorphic recrystallisation. Additionally the diagram provides information about the K/Ar system, whereas the system is undisturbed if the isochron intersect the origin of the co-ordinate system. The quantity of loss or gain of $^{40}Ar^*$ can be obtained from negative or positive intercepts of the isochron with the $^{40}Ar^*$ axis.

In contrast to the conventional K/Ar method the $^{40}Ar/^{39}Ar$ method does not require sample splitting, because the age can be directly determined by the measurement of the $^{40}Ar/^{39}Ar$ ratio (eq. 3.5). ^{39}Ar is produced by irradiation of ^{39}K in a reactor, while the irradiation parameters (e.g. neutron flux) are monitored by age standards of known age irradiated along with the samples.
The Ar is released by step heating and the $^{40}Ar/^{39}Ar$ ratio of each heating step is analysed by mass spectrometry. The irradiation factor J (eq. 3.5.1) is determined by the measurement of the age standards. Advantages of this method in respect to the conventional K/Ar total fusion method arise from (a) homogeneous, not splitted samples, (b) the possibility to detect disturbances of the K/Ar system (anomalous domains with Ar-loss or inherited / excess Ar) by step heating and (c) to exclude those domains from the age calculation. Additional informations, like degassing of intergrowth, the presence of multiple mica generations etc., can be obtained from the Ca/K and Cl/K ratios (McDougall and Harrison, 1988; Villa et al., 1997).

$$t_s = \frac{1}{\lambda}\ln\left(\frac{^{40}Ar^*}{^{39}Ar}J+1\right) \qquad (3.5)$$

t_s = age of the sample
λ = decay constant
$(^{40}Ar^*/^{39}Ar)$ = measured ratio of the sample
$(^{40}Ar^*/^{39}Ar)_m$ = measured ratio of the standard
tm = age of the standard

$$J = \frac{\left(e^{\lambda_{tm}}-1\right)}{\left(^{40}Ar^*/^{39}Ar\right)_m} \qquad (3.5.1)$$

Plateau ages were defined and calculated using the criteria of Fleck et al. (1977), Lee et al. (1989) and Snee et al. (1988). Because of possible experimental fractionation (Dalrymple and Lanphere, 1974), steps containing less than 3% of total ^{39}Ar release are generally not considered in the plateau age calculation. The ages were calculated with the program Isoplot/Ex rev. 2.49 of Ludwig (2001). The assumption that non-atmospheric argon is of atmospheric composition is tested by the use of $^{39}Ar/^{40}Ar$ vs. $^{36}Ar/^{40}Ar$ correlation plots (Roddick et al., 1980). Increments which have a similar composition of extraneous (non-radiogenic) argon should lie on a mixing line between non-radiogenic argon of $^{36}Ar/^{40}Ar$ ratio given by the y-intercept and radiogenic $^{40}Ar^*$ given by the x-intercept at a $^{39}Ar/^{40}Ar$ ratio corresponding to the age of the increments. If non-radiogenic component or components do not appear to have atmospheric composition, an intercept age was calculated and the quality of fit of the regression is expressed by the MSWD (mean weighted squared deviation)-value (York, 1969). According to Elias (1998), MSWD-values > 10.0 indicate that data scattering is greater than expected from the experimental error.
For further details on the K/Ar and $^{40}Ar/^{39}Ar$ dating method, see Dalrymple and Lanphere (1969), Faure (1986) and McDougall and Harrison (1988).

3.5.1 Analytical methods

The conventional K/Ar age determinations on biotite and white mica concentrates were carried out at the Institute of Nuclear Research (Drebrecen, Hungary).
The samples are degassed by high frequency induction heating. SAES St 707 ion collector pumps equipped with a titanium sponge are separating Ar from emanating volatiles. The concentration of radiogenic Ar ($^{40}Ar^*$) is determined using the isotope dilution method combined with an ^{38}Ar spike. The isotope compositions are measured by mass spectrometry. The average error of a single age analysis dated by this method is about 3.5 % (2σ).

Additionally to the conventional K/Ar method five samples were analysed using the $^{40}Ar/^{39}Ar$ method at the Institute of Mineralogy of the University of Bern (Switzerland).
100 mg of biotite or muscovite sample material were wrapped together with a Fish Canyon biotite age standard into aluminium foil, stored in plastic tube and sent to the irradiation. The sample and the reference material were step heated (8 to 13 steps) and degassed in a double –vacuum resistance oven connected to a MAP 215-50 gas mass spectrometer.

3.5.2 Results of K/Ar dating

39 white mica and 10 biotite concentrates derived from 36 samples of the West and East Pelagonian Zone and the adjacent Vardar Zone were analysed by the conventional K/Ar method. The complete analytical data set is given in Tab. 3.2 - Tab. 3.4, the distribution of the K/Ar-ages is displayed in Fig. 3.5, and the results are described for each zone separately below.

3.5.2.1 West Pelagonian Zone (WPZ)

Three white mica concentrates derived from two samples were analysed from the West Pelagonian Zone.

Sample 8-25 is from a paragneiss near Florina (Fig. 3.5). The micas are oriented parallel to a well developed NE-SW trending stretching lineation with top to NE sense of shear. The 200-355µm fraction yields an age of 76±3 Ma, whereas an age of 40±2 Ma is determined on the fraction <10µm. The latter age is considered as geological meaningless because there is no evidence for a younger mica generation within the thin section.
White micas of sample 8-24 are derived from a W-E trending mylonitic fault with a top to the W sense of shear near Brod yielded a K/Ar age of 36±1 Ma.

Sample code	Rock type	Dated mineral	Grain size [µm]	K [%]	40Ar* [cc STP/g]	$^{40}Ar^*/\overline{^{40}Ar_{(tot)}}$	Age ± σ [Ma]
8-24	myl	wm	<2	6.72	9.393x10E-6	61.6	35.6±1.4
8-25	pg	wm	200-355	8.24	2.473x10E-5	89.5	75.6±3.0
			<10	5.33	8.345x10E-6	62.9	39.9±2.0

Tab. 3.2: K/Ar analytical data of the West Pelagonian Zone. Abbreviations: myl = mylonite; pg = paragneiss; wm = white mica; STP = standard temperature and pressure, * = radiogenic. Errors refer to 1σ confidential level.

3.5.2.2 East Pelagonian Zone (EPZ)

Altogether 26 white mica and 10 biotite concentrates separated from 28 samples (paragneisses, orthogneisses, amphibolites and granitoids) were dated from the EPZ, whereby three age groups can be distinguished.

(1) Hercynian group

A K/Ar white mica age of 294±11 Ma and a K/Ar biotite age of 334±13 Ma are obtained from amphibolite sample M98/16. Both micas are orientated parallel to a well developed foliation and are synkinematic. The higher age of the biotite is related to chloritisation. K/Ar biotite ages of 312±12 to 447±17 Ma are obtained from granitic rocks of the EPZ (8-4, M98/14, M98/17).

(2) Early Eohellenic group (Tithonian – Barremian)

Most of the determined ages belong to the second Eohellenic group. The ages scatter between 118±5 and 148±6 Ma with a clear maximum around 130-140 Ma (Fig. 3.13). From some samples (8-7, M98/13, M98/46 and M99/13) white mica as well as biotite were analysed. Samples M99/13 and M98/46 show no significant difference of the white mica and biotite ages. This indicates contemporaneous crystallisation as also shown by the Ar/K-correlation plots (Fig. 3.4a,b).

The younger K/Ar biotite age of 62±3 Ma (sample M98/13, K/Ar white mica age 132±5 Ma) is related to weathering, while the older K/Ar biotite age of 267±10 Ma (sample 8-7; K/Ar white mica age 144±5 Ma) is related to chloritisation and K loss. Thus, these biotite ages are geologically meaningless.

Furthermore there is no difference between the ages derived from different grain sizes (GR01/20, GR01/21; Fig 3.4c,d).

(3) Late Eohellenic group (Albian – Turonian)

Significantly younger ages are only obtained from the eastern margin of the EPZ and from the Kaimakzalan area (Fig. 3.5). The K/Ar white mica age of 111±4 Ma (sample 8-23) is related to a WSW sense of shear, while the 99±4 Ma K/Ar biotite age of sample GR99/38 is related to SE directed movements. An K/Ar white mica age of 94±4 Ma is obtained from sample 8-28.

Sample code	Rock type	Dated mineral	Grain size [µm]	K [%]	40Ar* [cc STP/g]	$^{40}Ar^*/\overline{^{40}Ar_{(tot)}}$	Age ± σ [Ma]
8-9$^{(BSF)}$	bs	wm	200-355	8.03	4.411x10E-5	87.5	136±5.1
8-2	mc	wm	125-200	4.27	2.277x10E-5	60.3	132.2±5.3
8-3	gn	wm	80-200	9.14	4.331x10E-5	80.0	118.0±4.5
M98/27	mc	wm	63-125	7.11	3.985x10E-5	82.7	135.7±5.2
8-21	am	wm	200-355	8.42	4.644x10E-5	85.7	136.6±5.1
8-22	gn	wm	200-355	9.07	4.931x10E-5	81.6	134.7±5.1
8-23	mc	wm	<10	4.76	2.124x10E-5	80.6	111.3±4.2
8-6	mc	wm	200-355	7.08	3.691x10E-5	84.4	129.4±4.9
8-7	pr	fu	200-355	7.53	4.393x10E-5	91.2	144.2±5.4
		bt	200-355	5.04	5.460x10E-5	80.7	267.1±10.1
M98/5	gn	wm	200-315	8.67	5.190x10E-5	85.2	147.8±5.7
M98/7	gn	wm	200-355	9.22	5.240x10E-5	82.0	140.6±5.3
M98/13	gn	wm	200-315	9.28	4.948x10E-5	74.1	132.2±5.1
		bt	200-315	5.53	1.355x10E-5	43.8	62.0±2.7
M98/16	am	bt	80-160	4.76	6.789x10E-5	89.1	334.0±12.7
		wm	80-160	3.67	4.560x10E-5	82.8	294.3±11.2

Tab. 3.3: K/Ar analytical data of the East Pelagonian Zone. Abbreviations: am = amphibolite; bs = blueschist; bt = biotite; fu = fuchsite; gn = gneiss; mc = micaschist; pr = prasinite; STP = standard temperature and pressure; wm = white mica; * = radiogenic. Errors refer to 1σ confidential level. $^{(BSF)}$ = blueschist facies rock. Continues.

Sample code	Rock type	Dated mineral	Grain size [µm]	K [%]	40Ar* [cc STP/g]	$^{40}Ar^*/^{40}Ar_{(tot)}$	Age ± σ [Ma]
M98/46.2	gn	wm	200-355	9.05	5.011*10E-5	78.4	137.1±5.3
		bt	200-355	8.26	4.519x10E-5	92.0	137.1±5.2
M98/35	mc	wm	200-355	9.22	5.051x10E-5	78.1	135.7±5.3
8-5$^{(AMF)}$	gn	wm	355-500	7.41	4.034x10E-5	87.6	134.9±5.1
M99/13	mc	wm	200-355	8.93	4.527x10E-5	85.0	125.9±4.8
		bt	200-355	7.57	3.696x10E-5	85.9	121.4±4.6
M99/8	gn	wm	200-355	8.39	4.731x10E-5	87.1	139.5±5.3
M99/5.1	mc	wm	200-355	9.08	4.986x10E-5	89.9	135.5±5.1
GR99/21	mc	wm	200-355	8.93	5.262x10E-5	82.0	145.6±5.5
			80-160	7.24	4.340x10E-5	82.6	148.0±5.6
8-28	mc	wm	<10	3.59	1.344x10E-5	73.0	93.8±3.6
GR99/38	mc	bt	80-160	7.61	2.997x10E-5	91.6	98.6±3.7
GR01/20	mc	wm	80-160	8.89	4.613x10E-5	47.5	128.8±5.4
GR01/21	mc	wm	250-355	8.94	4.515x10E-5	88.8	125.5±4.8
			80-160	8.69	4.612x10E-5	92.8	131.6±5.0
8-4	g	bt	200-355	7.73	1.022x10E-4	95.6	311.6±11.6
M98/14	g	bt	200-315	8.17	1.467x10E-4	95.1	411.0±16.0
M98/17	g	bt	80-200	7.55	1.487x10E-4	93.8	446.5±16.8
M99/12	g	bt	200-355	7.464	3.855x10E-5	78.8	128.2±4.9

Tab. 3.3: K/Ar analytical data of the East Pelagonian Zone. Abbreviations: bt = biotite; g = granite; gn = gneiss; mc = micaschist; STP = standard temperature and pressure; wm = white mica; * = radiogenic. Errors refer to 1σ confidential level. $^{(AMF)}$ = amphibolite facies rock. Continued.

3.5.2.3 Vardar Zone

In the Vardar Zone white mica concentrates were derived from the basement rocks of the Almopias Unit (8-33, GR99/33), an Upper Cretaceous limestone (M98/40) and metaflysch (M98/39) as well as from crystalline pebbles from a conglomerate (8.32-1, 8.32-2). The results gave three age groups.

(1) Early Eohellenic group

White micas derived from a Cretaceous limestone (M98/40, detrital) and from crystalline pebbles of a conglomerate S Megaplatanos (8-32.1, 8-32.2) yield ages between 144±6 and 133±5 Ma, which are significantly older than the expected deposition age (probably Late Cretaceous).

(2) Late Eohellenic group

An Upper Eohellenic K/Ar white mica age of 102±4 Ma is obtained from a micaschist (GR99/33) of the Almopias Unit (Fig. 3.5).

(3) Latest Cretaceous

Three fine grained white mica fractions were dated from a the metaflysch (sedimentation age is probably Maastrichtian (Jacobshagen, 1986), sample M98/39). The fractions between 2.0-0.6 and <0.6 µm yield an age of 66±3, while an age of 76±3 Ma is obtained from the fraction >2µm (Tab. 3.4). The latter probably represents a mixed age of an older detrital component with newly grown white mica, which corresponds well with thin section observations and the Ar*/K-correlation plot (Fig. 3.4f). An age of 66±3 Ma (Fig. 3.5) is also obtained from a micaschist (8-33) of the Ano Peternik Unit.

Sample code	Rock type	Dated mineral	Grain size [µm]	K [%]	40Ar* [cc STP/g]	$\frac{^{40}Ar^*}{^{40}Ar_{(tot)}}$	Age ± σ [Ma]
M98/40	lm	wm	80-160	8.15	4.568x10E-5	90.0	138.7±5.3
			2-6	5.013	1.504x10E-5	84.1	75.6±2.9
M98/39	myl	wm	2-0.6	6.276	1.642x10E-5	81.2	66.1±2.5
			<0.6	6.288	1.635x10E-5	76.9	65.7±2.5
8-33	mc	wm	<10	2.22	5.819x10E-6	62.2	66.2±2.6
GR99/33	mc	wm	200-355	8.7	3.557x10E-5	82.7	102.3±3.9
		wm	<2	4.57	1.571x10E-5	81.5	86.3±3.3
8-29B	fl	wm	0.6-2.0	4.39	1.568x10E-5	80.5	89.6±3.4
		wm	<0.6	4.88	1.264x10E-5	73.3	64.6±2.5
8-30B	lm	wm	<2	4.56	1.155x10E-5	80.1	64.0±2.4
8-32.1	lm	wm	160-250	9.01	4.828x10E-5	91.4	132.8±5.0
8-32.2	lm	wm	160-250	8.80	5.144x10E-5	91.4	144.4±5.5

Tab. 3.4: K/Ar analytical data of the Vardar Zone. Abbreviations: fl = flysch; lm = limestone; mc = micaschist; myl = mylonite; STP = standard temperature and pressure; wm = white mica; * = radiogenic. Errors refer to 1σ confidential level.

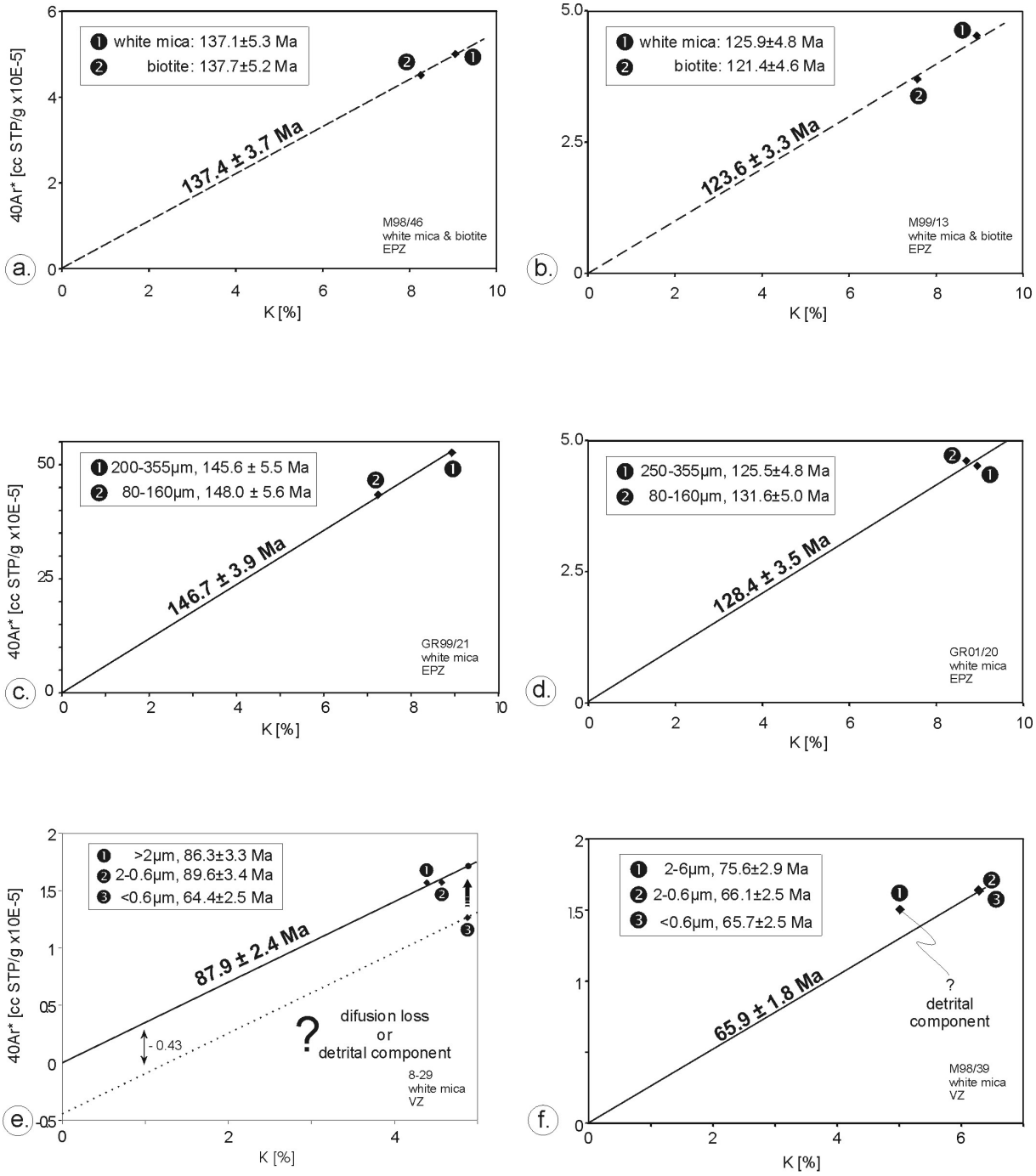

Fig. 3.4: K vs. ^{40}Ar* diagrams after Harper (1970). Intercepts with (a) negative ^{40}Ar* axis indicate ^{40}Ar* loss and (b) positive ^{40}Ar* axis = gain of ^{40}Ar*. Solid line: isochron defined by different grain sizes of the same mineral; dashed line: isochron defined by co-genetic minerals; doted line = uncertain. For explanations see text.

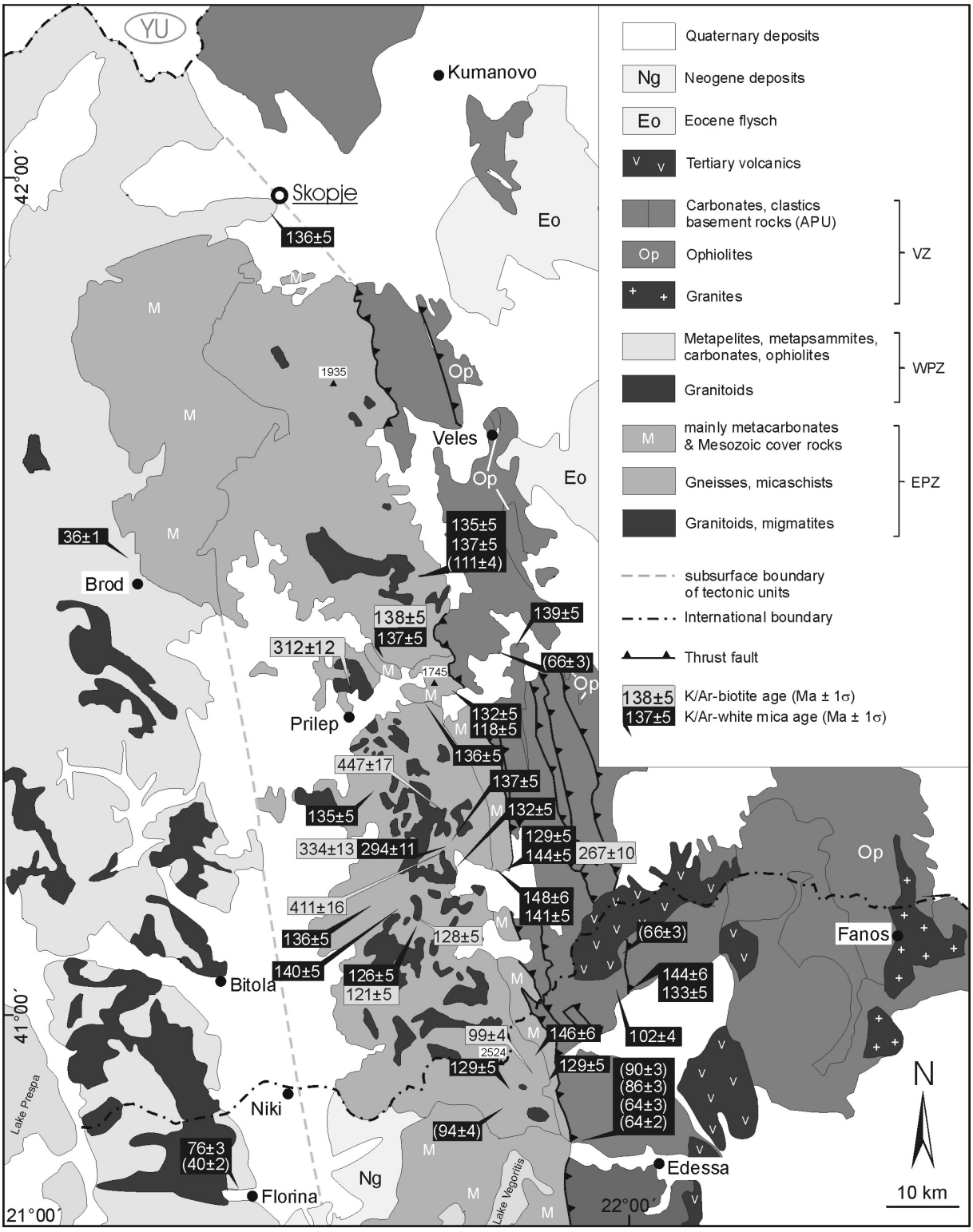

Fig. 3.5: Distribution of K/Ar ages obtained from the northern Pelagonian Zone and the adjacent Vardar Zone in the Republic of Macedonia and NE Greece. Ages in parenthesis indicate analysed fraction < 63µm. Abbreviations: APU = Ano Peternik Unit; EPZ = East Pelagonian Zone; VZ = Vardar Zone; WPZ = West Pelagonian Zone.

3.5.3 Results of $^{40}Ar/^{39}Ar$ dating

The K/Ar data do not provide any information about disturbances of the K/Ar system. Therefore, five samples were additionally analysed using the $^{40}Ar/^{39}Ar$ technique. The analytical results are listed in Tab. 3.5. A comparison of the K/Ar and $^{40}Ar/^{39}Ar$ data is given in Tab. 3.16. The complete $^{40}Ar/^{39}Ar$ step heating data set is given in appendix D3.

Sample	Mineral [µm]	J	TFA ± σ [Ma]	WMPA ± σ [Ma]	Σ 39Ar [%]	IA ± σ [Ma]	MSWD
8-9	white mica	0.00104	148.8 ± 1.4	-	-	148.7±3.3	6.9
M99/13	biotite	0.00104	131.8 ± 2.7	-	-	134.0±2.7	8.3
	white mica	0.00104	132.5 ± 0.8	132.9 ± 0.1	48.0	132.5±2.6	12.0
GR99/33	white mica	0.00104	100.9 ± 2.6	-	-	101.7±2.3	11.9
GR99/38	biotite	0.00104	110.5 ± 2.1	-	-	112.5±2.5	22.0

Tab. 3.5: $^{40}Ar/^{39}Ar$ analytical data. IA = inverse isochron age, J = irradiation factor, TFA = total fusion age, WMPA = weighted mean plateau age, MSWD = mean squared weighted deviation. All errors refer to 1σ.

All incremental heating experiments on white mica (M99/13, 8-9, GR99/33) and biotite (M99/13, GR99/38) resulted in flat diffusion loss spectra with substantial Ar loss the lower temperature steps (Fig. 3.6a-e).
Except sample M99/13 (white mica) all ^{39}Ar-release spectra form only 'plateau like' age patterns, without fulfilling the criteria for 'plateau' ages (defined by a minimum of 30% of total ^{39}Ar release obtained from a minimum of three continuous steps).
On the blueschists (sample 8-9) a 'nearly plateau age' of 149±1 Ma was determined. Identical ages for biotite (132±0.1 Ma) and white mica (133±0.8 Ma) are derived from micaschist sample M99/13 (EPZ), indicating contemporaneous crystallisation of the two phases.
Younger ages between 112±1 and 103±1 Ma are obtained from the Vardar Zone (GR99/33) and from a shear zone (top to SE sense of shear) NE Panagitsa (Kaimakzalan). Inverse isochron ages were calculated for all samples. The lower temperature steps and those that are not lying on the isochron were excluded from the age calculation (Fig. 3.6a-e). MSWD values range from 6.9 to 22.
However, there are no significant differences of the weighted mean plateau and inverse isochron ages with respect to the total fusion ages (Tab. 3.5).

Intergrowths in white mica are negligible as indicated by nearly homogeneous flat Ca/K ratios (Fig. 3.6a,c,d). Higher Ca/K ratios in biotite are due to intergrowth with a Ca-rich phase (epidote, feldspar) without exert influence on the radiogenic age (Fig 3.6b,e). Nearly homogeneous Cl/K ratios in all samples denote also the presence of a second phase.

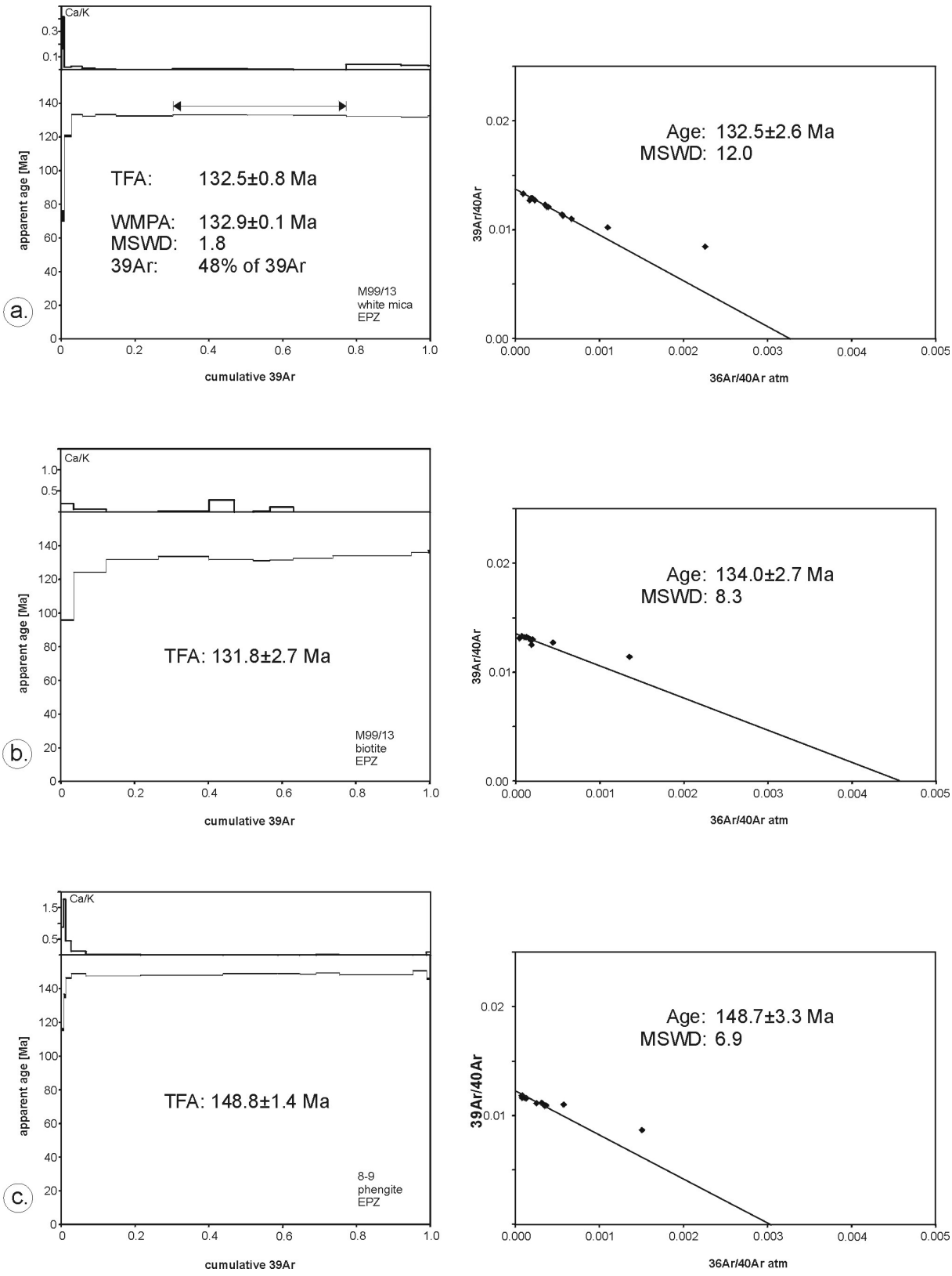

Fig. 3.6: left side: $^{40}Ar/^{39}Ar$- release spectra and K/Ca-ratio; right side: inverse isochron plots. TFA = total fusion age, MSWD = mean squared weighted deviation, WMPA = weighted mean plateau age. Continues.

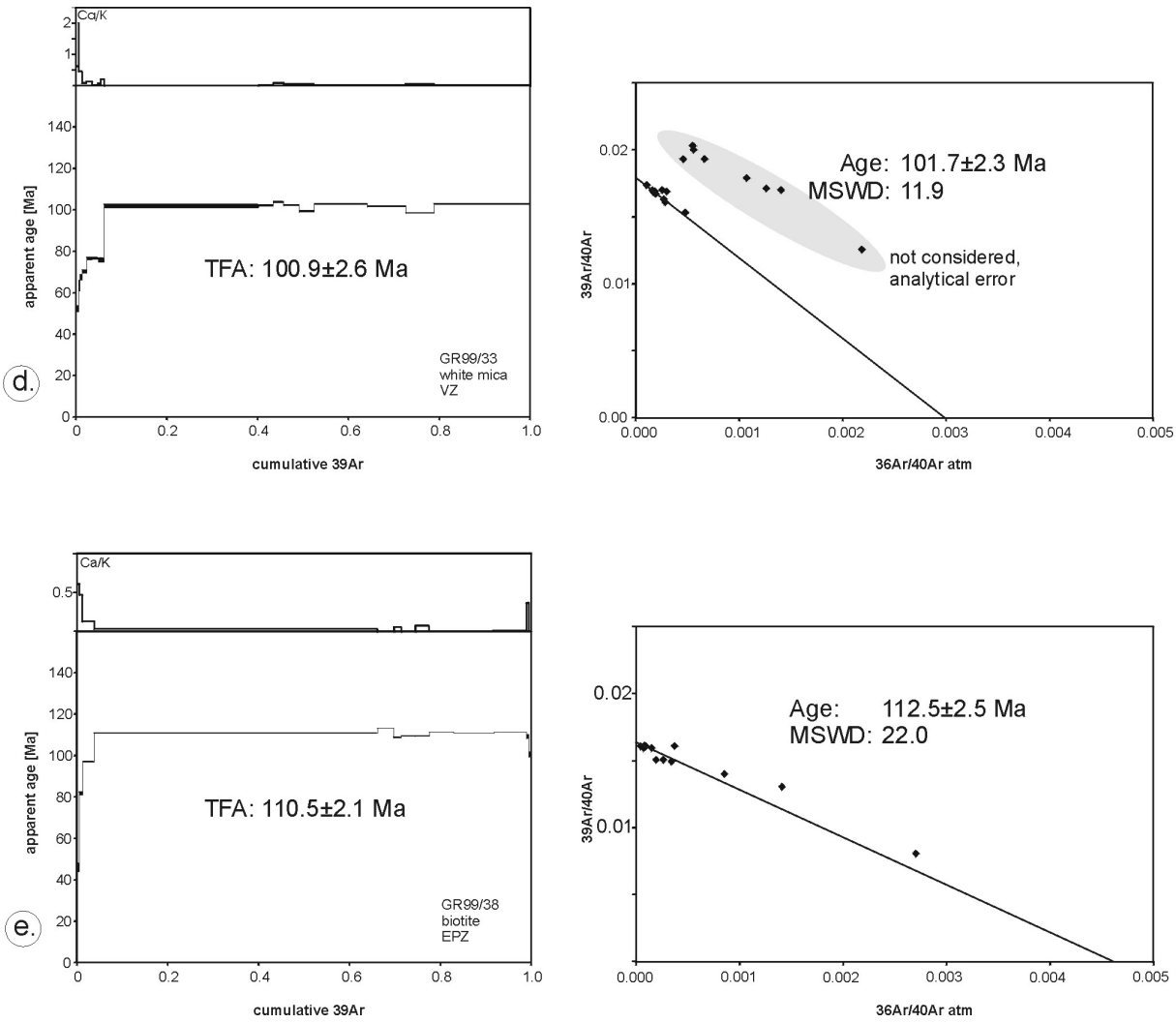

Fig. 3.6: continued.

3.6 Rb/Sr dating

Rubidium comprise the two naturally occurring isotopes ^{85}Rb and ^{87}Rb. The latter is radioactive and decays to stable ^{87}Sr. Sr has four naturally occurring isotopes (^{88}Sr, ^{87}Sr, ^{86}Sr and ^{84}Sr) which are all stable. The Rb/Sr age can be determined by using equation 3.6.1. In the case, that white mica and whole rock analyses were carried out on the same sample, the age was calculated by the slope of an isochron. For further details of the Rb/Sr method and data evaluation, see Faure (1986) and Wendt (1986).

$$\left(\frac{^{87}Sr}{^{86}Sr}\right)=\left(\frac{^{87}Sr}{^{86}Sr}\right)_i+\frac{^{87}Rb}{^{86}Sr}\left(e^{\lambda t}-1\right) \qquad (3.6)$$

$$t=\frac{1}{\lambda}\ln\left[\frac{\frac{^{87}Sr}{^{86}Sr}-\left(\frac{^{87}Sr}{^{86}Sr}\right)_i}{\frac{^{87}Rb}{^{86}Sr}}+1\right] \qquad (3.6.1)$$

t = time elapsed since the system was closed
λ = decay constant
$^{87}Sr/^{86}Sr$ = measured ratio
$(^{87}Sr/^{86}Sr)_i$ = initial ratio

3.6.1 Analytical method

Three white mica and two biotite concentrates as well as two whole rock samples were analysed by the ^{87}Rb/^{87}Sr method. The samples were spiked with a ^{84}Sr/^{87}Rb tracer solution and decomposed for three days at 100° C using a HF-$HClO_4$ (2ml HF + 20 drops of $HClO_4$) solution. Rb and Sr were isolated by conventional ion exchange chromatography using a 5 ml resin bed (Bio Rad AG, 50W-X12, 200-400 mesh) on quartz columns (see Hegner et al. 1995 for details). The measurements were made on a Finnigan MAT 262 mass spectrometer at the Geochemical Institute of the University of Tübingen, using Thermal Ionisation Mass Spectrometry (TIMS).
Sr was measured in single filament mode and was loaded with a TA-HF activator on pre-conditioned W filaments. Rb was loaded with ultra-pure H_2O on pre-conditioned Re filaments and measurements were performed in a Re double filament configuration. The ^{87}Sr/^{86}Sr isotope ratios were normalised to ^{86}Sr/^{88}Sr = 0.1194. Analyses of the NBS 987 Sr standard (240 scans) yielded a ^{87}Sr/^{86}Sr ratio of 0.710255 ± 0.000012. Total procedural blanks (chemistry and loading) were <200 pg for Sr.

The Rb/Sr ages were calculated using the program Isoplot/Ex 2.49 (Ludwig, 2001) and the decay constants for Rb given by Steiger and Jäger (1977).

3.6.2 Results

In order to verify the accuracy of the data obtained from the K/Ar system by an independently operating isotope system, Rb/Sr measurements were carried out on five selected samples. The results are presented in Tab 3.6.

Sample	rock type	Mineral	Rb [ppm]	Sr [ppm]	$^{87}Rb/^{86}Sr$	$^{87}Sr/^{86}Sr \pm \sigma$	age $\pm \sigma$ [Ma]
8-9	blueschist	white mica	372.4	458.8	2.350	0.712985 ± 7	(194.8 ± 10.0)
		whole rock	64.4	144.5	1.289	0.710046 ± 7	
8-5	micaschist	white mica	445.0	202.5	6.380	0.741925 ± 13	(139.2 ± 4.8)
		whole rock	203.8	245.8	2.405	0.734060 ± 9	
M98/7	gneiss	white mica	623.7	5.0	387.000	1.487198 ± 14	142.2 ± 1.4
M98/17	granite	biotite	672.0	26.7	73.852	0.838144 ±10	126.9 ± 1.3
M99/12	granite	biotite	386.8	9.4	122.090	0.916933 ± 15	122.1 ± 1.2

Tab. 3.6: Rb/Sr analytical data. Ages in parenthesis are isochron ages. All errors refer to 1σ

The blueschist S of Skopje (sample 8-9, white mica and whole rock) yield an isochron age of 195±10 Ma, with an initial $^{87}Sr/^{86}Sr$ ratio of 0.70648±0.00024.

Ages between 142±1 and 139±5 Ma (initial $^{87}Sr/^{86}Sr$ ratio = 0.72930±0.00022) are obtained from a greenschist facies gneiss (sample M98/7) and an amphibolite facies micaschist (sample 8-5; white mica and whole rock).

The biotite concentrates derived from granites of the EPZ, yield ages between 127±1 to 122±1 Ma. Additional whole rock analyses of the samples M98/7, M98/17 and M99/12 were not carried out. The calculations with various initial $^{87}SR/^{86}Sr$ ratios (0.705-0.715), did not show significant changes of the radiometric age, due to low Sr (5-27ppm) and high Rb (387-672ppm) contents. Furthermore, the granites were dated by the U/Pb method. Thus the additional information from the Rb/Sr system is not required for the geological interpretation.

3.7 Zircon and apatite fission-track dating

The fission-tack dating method is a widely used tool to reconstruct the low temperature history of rocks (Wagner and Van den Haute, 1992). The fission track age is a function of the spontaneous track density derived from spontaneous fission of ^{238}U and the uranium content, which can be determined by the evaluation of the fission of ^{235}U induced by the irradiation of the sample material in a reactor facility. The fission track age can be calculated after Price and Walker (1963), as modified by Naeser (1967), using the equation 3.7.

$$t = \frac{1}{\lambda_\alpha} \ln\left[\left(\frac{\lambda_\alpha}{\lambda_f}\right)\left(\frac{\rho_s}{\rho_i}\right) I\sigma\phi + 1\right] \qquad (3.7)$$

where

$\lambda\alpha$ = α-decay constant for ^{238}U (1.55125×10^{-10} a^{-1} (Jaffrey et al., 1973))

λf = decay constant for spontaneous fission of ^{238}U (8.46×10^{-17} a^{-1})

σ = cross-section for neutron fission reaction of ^{235}U (580.2×10^{-24} cm² (Hanna et al., 1969))

I = atomic ratio of $^{235}U/^{238}U$, as relative abundance of two U-isotopes

ϕ = thermal neutron fluence (n/cm²)

ρ_s = density of spontaneous tracks (tracks/cm²)

ρ_t = density of induced tracks (tracks/cm²)

3.7.1 ζ-Calibration

To avoid differences based on individual parameters for etching and counting technique (using dry or immersion objectives) and on the variables ϕ, σ, λ_f, Hurford and Green (1983) introduced the ζ-calibration approach, which avoids these problems by the determination of age standards of known age (Tab. 3.7) combined with dosimeter glasses of known uranium content (Tab. 3.8).

Standard material	Age [Ma]	References
Buluk member (zrn)	16.4 ± 0.2	Hurford and Watkins (1987)
Durango (ap)	31.4 ± 0.6	McDowell and Keizer (1977)
Fish Canyon volcanic tuff (ap, zrn)	27.8 ± 0.2	Hurford and Hammerschmidt (1985)
Tardree rhyolite (zrn)	58.7 ± 1.1	

Tab. 3.7: Age standards used in this study; ap = apatite standard, zrn = zircon standard.

Dosimeter glass	Natural uranium content	Reference
Corning CN 2 for zircon	38 ppm	Hurford and Green (1983)
Corning CN 5 for apatite	12 ppm	

Tab. 3.8: Dosimeter glasses used for ζ-calibration.

The personal ζ-factor of an irradiation is determined by the counting of included age standards and micas covering the dosimeter glasses and can be expressed by the following equation 3.8:

$$\zeta = \frac{\left(e^{\lambda_\alpha t_{std}} - 1\right)}{\lambda_\alpha \left(\frac{\rho_s}{\rho_i}\right)_{std} G \rho_d} \qquad (3.8)$$

G = geometry factor (0.5 for external detector method)

ρ_d = dosimeter track density (tracks/cm²)

t_{std} = age of the standard

$(\rho_s/\rho_i)_{std}$ = track density ratio of the standard

Including the ζ-factor, the fission track age equation (3.8) rearranges to:

$$t_s = \frac{1}{\lambda_\alpha} \ln\left[\lambda_\alpha \left(\frac{\rho_s}{\rho_i}\right)_s \rho_d G \zeta + 1\right] \qquad (3.8.1)$$

$(\rho_s/\rho_i)_s$ = track density ratio of the sample

For apatite a personal ζ-factor of 388.5±10.1 was determined on 8 apatite standards (four irradiations; Tab. 3.9). A zircon ζ-value of 120.5±2.2 is calculated on 10 zircon standards of five irradiations (Tab. 3.10).

Age Standart	Number of grains	Spontaneous		Induced		P_{χ}^2 (%)	Dosimeter		ζ ±1σ
		ρ_s	N_s	ρ_i	N_i		ρ_d	N_d	
AD	24	2.43	[301]	6.73	[833]	99.8	4.18	[4219]	417.2±29.4
AF	25	1.70	[233]	5.42	[743]	100.0	4.29	[4219]	415.1±32.7
AF	25	1.53	[205]	5.70	[764]	100.0	5.79	[5692]	360.4±29.5
AF	25	1.68	[228]	5.88	[800]	100.0	5.27	[5180]	372.3±29.2
AD	25	2.56	[411]	8.00	[1283]	99.8	5.27	[5180]	373.3±22.6
AD	25	2.29	[406]	8.43	[1495]	99.7	5.79	[5692]	399.7±23.9
AF	25	1.82	[231]	6.36	[807]	100.0	5.23	[5139]	373.9±29.2
AD	25	2.24	[379]	7.49	[1264]	100.0	5.23	[5139]	401.2±25.0
weighted mean:									**388.5±10.1**

Tab. 3.9: Determination of ζ-factors for apatite. Track densities (ρ) are as measured (x10^5 tr/cm^2); number of tracks counted (N) shown in brackets; ρs = spontaneous track density, ρi = induced track density, ρd = track density of dosimeter glass (CN5); $P\chi^2$: probability obtaining chi-square value for n degree of freedom (where n = No. Crystals -1). AD = Durango apatite, AF = Fish Canyon apatite.

Age Standart	Number of grains	Spontaneous		Induced		P_χ^2 (%)	Dosimeter		ζ ±1σ
		ρ_s	N_s	ρ_i	N_i		ρ_d	N_d	
ZF	25	56.17	[784]	88.55	[1236]	97.9	7.18	[7060]	122.9±6.2
ZF	21	51.27	[509]	60.94	[605]	99.6	5.53	[5436]	120.2±7.7
ZF	25	53.21	[999]	62.05	[1165]	100.0	5.50	[5411]	118.5±5.8
ZF	24	56.12	[855]	66.35	[1011]	99.9	5.50	[5411]	120.2±6.2
ZF	25	59.94	[931]	84.93	[1319]	90.2	6.46	[6354]	122.6±5.9
ZT	18	61.15	[535]	38.52	[337]	99.6	5.53	[5436]	134.3±9.9
ZT	25	56.89	[878]	34.02	[525]	99.9	5.50	[5411]	128.3±7.7
ZT	25	65.59	[1167]	68.68	[1222]	88.9	10.82	[10670]	116.2±5.4
ZT	24	63.40	[698]	43.51	[479]	100.0	6.46	[6354]	125.3±8.0
ZB	20	11.16	[386]	20.14	[697]	6.3	5.50	[5411]	107.8±7.2
weighted mean:									**120.5±2.2**

Tab. 3.10: Determination of ζ-factors for zircon. Track densities (ρ) are as measured (x10^5 tr/cm^2); number of tracks counted (N) shown in brackets; ρs = spontaneous track density, ρi = induced track density, ρd = track density of dosimeter glass (CN2); $P\chi^2$: probability obtaining chi-square value for n degree of freedom (where n = no. crystals -1). ZB = Buluk zircon, ZF = Fish Canyon zircon, ZT = Tardree rhyolite zircon.

3.7.2 Statistic evaluation of FT data

The precision of the fission track data is evaluated by several statistic tests. The single grain age distribution is numerically assessed using the chi-square (χ^2) test. The single grain ages are considered to represent a normal Poissonian distribution, if the χ^2 probability ($P\chi^2$) is larger than 5 %. If the χ^2 probability is less than 5 % the sample is considered to have failed the χ^2 test and the FT age is calculated as mean age. In this case the grains may belong to multiple age populations. The fission track data were evaluated using the TRACKKEY (vers. 4.1) program of Dunkl (2002). The complete evaluated FT data of this study is given in Appendix D1 and D2.

3.7.3 Sample preparation

The zircons were embedded in PFA (tetrafluoroethylene-perfluoroalkoxyethylene copolymer) teflon. The apatites were mounted on glass slides and embedded in ARALDIT-D (20 g ARALDIT-D + 4 g hardener) epoxy resin.

Grinding paper (2500 and 1200 mesh) and oil based diamond solutions (grain sizes: 9 µm, 3 µm and 1 µm) were used to produce a smooth internal surface of the zircon and apatite grains.

All zircons were etched using KOH-NaOH (46 g KOH + 32 g NaOH) eutectic liquid stored in a heat oven at 215° C (Gleadow et al., 1976) for 16 to 83 hours. 5.5N HNO_3 was used as etchant for the apatites, while the samples were exposed for 20 seconds at 21° C to the acid.

The apatite and zircon mounts were covered by a flake of muscovite (India or Goodfellow, with low U-content) and packed with parafilm, Tesa, foam and PE-foil. Together with the samples, reference material of known age (Tab. 3.7) and dosimeter glasses (Tab. 3.8) were sent to the irradiation. Due to reactor problems the samples were irradiated in different reactor facilities (RISØ, Roskilde/Denmark; ANSTO reactor, Lucas Heights (Sydney/Australia); TRIGA reactor, Oregon State University, USA) using a neutron fluence of 1.4–1.6x10^{15} n/cm² for zircon samples and 4.0x10^{15} n/cm² for apatite samples. It came out during an intralaboratory study of the Tübingen fission track working group, that the flux of the ANSTO reactor has high spatial variation. This leads to a gradient in the sample batch and therefore to a gradient of the ages depending on the sample position. The involved samples were irradiated twice using the TRIGA reactor.

The muscovite flakes were etched with 40% HF for 30 minutes (apatite detectors) or 20 minutes (zircon detectors).

3.7.4 Measurement conditions

Apatite and zircon fission track dating was carried out using the external detector method (EDM). The measurements were performed on a Zeiss optical microscope (Axioscope) equipped with a computer controlled positioning tablet operating with "FTStage" software version 3.12 (Dumitru, 1993) and a digitising tablet for apatite track-lengths measurements.
Spontaneous tracks of zircon were counted using an oil objective. Induced tracks of the external detectors as well as spontaneous and confined tracks of apatite were counted under a dry objective. All measurements were performed using 1000x magnification. Measurement conditions were equal for samples and standards.

3.7.5 Results

3.7.5.1 Northern Pelagonian Zone and Vardar Zone

From the northern Pelagonian Zone and the adjacent Vardar Zone 20 apatite and 22 zircon samples were dated by the fission track dating method. The analytical data are presented in Tab. 3.11 and Tab. 3.12, and the distribution of the FT ages is shown in Fig. 3.7.

(1) Vardar Zone

The zircon FT ages obtained from the VZ display ages between 80±4 (Fanos granite) to 58±5 Ma (Ano Peternik Unit). The latter is assessed as uncertain due to the low amount of dated grains (n=5). Unfortunately most of the zircons separated from the Late Cretaceous flysch (M98/39, M98/40) dissolved during sample preparation and etching. The few number of grains, which 'survived' the procedure, are heavily metamictimized and not suitable for FT dating.

The apatite FT ages decrease from the east (60±3 Ma) towards to the west (52±3 Ma). The relatively high error of sample GR99/33 (47±7 Ma) obtained from the Ano Peternik Unit is related to the low number of determined grains (n=17) and their low uranium content (4.6±75%).
Apatites and zircons derived from an andesite (sample GR99/32) at Mt. Kozuf yield an identical FT-age of 2.3 Ma.

(2) East Pelagonian Zone

Within the EPZ the oldest zircon FT ages (86±4 to 80±6 Ma) are obtained from the innermost part, while the zircon FT-ages systematically decreases towards the eastern (71±4 Ma) and the western margin (63±4 Ma), with slightly younger ages in the west. Due to their low amount of countable grains, some EPZ samples (M98/35, 8-4, M99/7) display relatively high errors (see Tab. 3.11). However these samples passed the χ^2-test with a χ^2-probabilty between 24.1 to 93.4% and are within the 1σ range of the zircon FT ages obtained from adjacent samples (see Fig. 3.7).

The apatite FT ages consistently decrease from the eastern (46±3 Ma) to the western margin (32±4 Ma).

(3) West Pelagonian Zone

In the WPZ the zircon FT ages decrease from the east (53±3 Ma) towards to the west (39±2 Ma). An age of 61±4 Ma is obtained from a mylonitic sample (8-24) near Brod (see Fig. 3.7).
In contrast, the apatite FT ages display a nearly homogeneous age pattern around 31±2 to 29±5 Ma.

From Fig. 3.7 It is obvious that, for the zircon FT ages there is no significant difference between Vardar Zone and the East Pelagonian Zone. There is a systematic decrease of the zircon FT ages (63±4 to 39±2 Ma) from the western margin of the East Pelagonian Zone towards to the West Pelagonian Zone.
In contrast, the apatite FT ages systematically decrease from the eastern VZ (60±3 Ma) towards to the WPZ (31±2 Ma).

All determined zircon and apatite samples passed the χ^2-test, while the χ^2-probabilty ranges between 24.1 to 100.0%. This indicates that none of the samples, including the flysch samples (M98/39 and M98/40) of the VZ, contain multiple age populations, which is also verified by the radial plots (all single grain ages are within the 2σ range; appendix D1, D2).

Sample	Alt. (m)	Number of grains	Spontaneous		Induced		P_{χ}^{2} (%)	Dosimeter		Central age (Ma) ±1s	Mean track lenght [µm]	std. dev [µm]	Number of tracks
			ρ_s	N_s	ρ_i	N_i		ρ_d	N_d				
Vardar Zone													
GR99/27	740	19	332.4	[1111]	178.0	[595]	100.0	7.18	[7060]	80.3±4.4	-	-	-
GR99/32	1230	20	24.3	[239]	459.6	[4518]	84.0	7.18	[7060]	2.3±0.2	-	-	-
GR99/33	580	5	255.9	[327]	170.6	[218]	67.9	6.46	[6354]	58.1±5.2	-	-	-
East Pelagonian Zone													
8-21	320	17	81.6	[946]	36.0	[418]	100.0	5.50	[5411]	75.0±4.7	-	-	-
M98/7	400	20	143.4	[1832]	66.3	[847]	91.5	5.50	[5411]	71.3±3.4	-	-	-
M98/14	580	16	105.3	[1004]	52.8	[503]	48.3	5.50	[5411]	65.8±4.0	-	-	-
M98/17	680	20	166.5	[1260]	92.6	[701]	80.0	6.89	[6750]	74.2±3.9	-	-	-
M98/35	995	7	206.4	[284]	95.9	[132]	99.6	5.50	[5411]	70.9±7.6	-	-	-
M98/46.2	1090	20	149.1	[1055]	59.2	[419]	99.6	5.50	[5411]	82.9±5.1	-	-	-
8-4	850	11	108.6	[715]	44.2	[291]	24.1	5.50	[5411]	80.1±6.4	-	-	-
M99/15	810	21	135.4	[1983]	107.0	[1567]	91.2	10.85	[10670]	82.2±3.3	-	-	-
M99/13	720	20	171.6	[1231]	129.5	[929]	99.9	10.85	[10670]	86.1±4.1	-	-	-
M99/8	700	17	155.8	[720]	102.0	[471]	97.0	7.18	[7060]	65.8±4.2	-	-	-
M99/7	940	5	146.4	[259]	136.8	[242]	93.4	10.85	[10670]	69.6±6.4	-	-	-
M99/5	680	13	155.5	[642]	105.6	[436]	97.6	7.18	[7060]	63.4±4.2	-	-	-
GR99/11	800	17	159.1	[1204]	103.5	[783]	93.0	7.18	[7060]	66.2±3.4	-	-	-
GR99/12	1570	11	168.2	[463]	111.9	[308]	97.7	6.87	[6750]	61.9±4.8	-	-	-
West Pelagonian Zone													
8-24	600	15	111.9	[658]	61.1	[359]	98.4	5.5	[5411]	60.5±4.2	-	-	-
M99/1	450	19	111.9	[770]	90.5	[623]	99.6	7.18	[7060]	53.3±3.1	-	-	-
M99/2	590	12	136.3	[402]	102.8	[303]	68.4	6.46	[6354]	51.4±4.1	-	-	-
GR99/5a	950	20	116.2	[1062]	116.9	[1069]	99.9	6.56	[6354]	38.6±1.9	-	-	-
GR99/6	510	20	181.2	[1140]	143.4	[902]	100	6.46	[6354]	49.0±2.4	-	-	-

Tab. 3.11: Analytical data of zircon fission track dating of samples derived from the West and East Pelagonian Zone and the Vardar Zone. Track densities (ρ) are as measured (x10^5 tr/cm^2); number of tracks counted (N) shown in brackets; ρs = spontaneous track density, ρi = induced track density, ρd = track density of dosimeter glass; zircon ages calculated using dosimeter glass: CN2 with ζ-CN2 = 122.5±2.2; Pχ^2: probability obtaining Chi-square value for n Degree of freedom (where n = no. crystals -1).

Sample	Alt. (m)	Number of grains	Spontaneous		Induced		P_{χ}^2 (%)	Dosimeter		Central age (Ma) ±1s	Mean track lenght [µm]	std. dev [µm]	Number of tracks
			ρ_s	N_s	ρ_i	N_i		ρ_d	N_d				
Vardar Zone													
GR99/27	740	31	7.0	[1116]	12.0	[1909]	100.0	5.27	[5180]	59.6±2.9	13.88±0.24	1.53	42
M98/39	520	49	4.5	[575]	9.9	[1258]	99.8	5.87	[5766]	51.9±3.0	14.01±0.44	1.59	13
M98/40	520	35	5.4	[572]	10.5	[1123]	90.7	5.27	[5180]	51.9±3.1	13.36±0.34	1.44	18
GR99/32	1230	30	0.2	[46]	10.5	[2007]	100.0	5.27	[5180]	2.3±0.4	-	-	-
GR99/33	580	17	0.8	[66]	1.9	[160]	99.7	5.87	[5766]	46.9±7.0	-	-	-
East Pelagonian Zone													
M98/7	400	21	3.5	[536]	8.6	[1307]	84.4	5.79	[5692]	46.0±2.7	13.56±0.21	1.25	36
M98/17	680	29	3.3	[263]	9.1	[722]	100.0	5.79	[5692]	40.8±3.2	12.98±0.34	1.28	14
M98/46.2	1090	24	1.2	[161]	3.4	[454]	99.9	5.79	[5692]	39.8±3.8	-	-	-
M99/15	810	28	9.2	[766]	25.8	[2149]	84.4	5.79	[5692]	40.0±2.0	13.25±0.19	1.86	100
M99/13	720	30	3.1	[469]	10.5	[1576]	93.4	5.79	[5692]	33.4±2.0	-	-	-
M99/12	670	30	3.1	[467]	10.5	[1576]	95.6	5.79	[5692]	33.2±2.0	13.60±0.39	1.85	22
M99/8	700	22	0.6	[40]	1.9	[125]	100.0	5.79	[5692]	35.9±6.6	-	-	-
M99/5	680	12	0.8	[29]	2.3	[89]	100.0	5.79	[5692]	36.5±7.9	-	-	-
M99/4	600	17	1.0	[81]	3.1	[257]	100.0	5.23	[5139]	31.9±4.2	-	-	-
GR99/11	800	29	7.4	[806]	19.5	[2132]	74.3	5.87	[5766]	43.0±2.2	14.12±0.19	1.44	60
GR99/12	1570	30	6.7	[662]	18.1	[1803]	34.6	5.87	[5766]	41.8±2.3	14.15±0.19	1.4	52
West Pelagonian Zone													
M99/1	450	14	2.733	[54]	10.6	[210]	99.8	5.79	[5692]	28.9±4.5	-	-	-
GR99/2	410	10	0.6	[41]	2.4	[168]	99.9	5.27	[5180]	24.9±4.4	-	-	-
GR99/5a	950	29	6.3	[632]	23.3	[2346]	99.9	5.87	[5766]	30.6±1.6	14.09±0.18	1.47	65
GR99/6	510	32	2.4	[394]	8.4	[1406]	97.5	5.27	[5180]	28.6±1.8	-	-	-

Tab. 3.12: Analytical data of apatite fission track dating of samples derived from the West and East Pelagonian Zone and the Vardar Zone. Track densities (ρ) are as measured (x10^5 tr/cm^2); number of tracks counted (N) shown in brackets; ρs = spontaneous track density, ρi = induced track density, ρd = track density of dosimeter glass; Apatite ages calculated using dosimeter glass: CN5 with ζ-CN5 = 388.5±10.1; $P\chi^2$: probability obtaining Chi-square value for n Degree of freedom (where n = no. crystals -1).

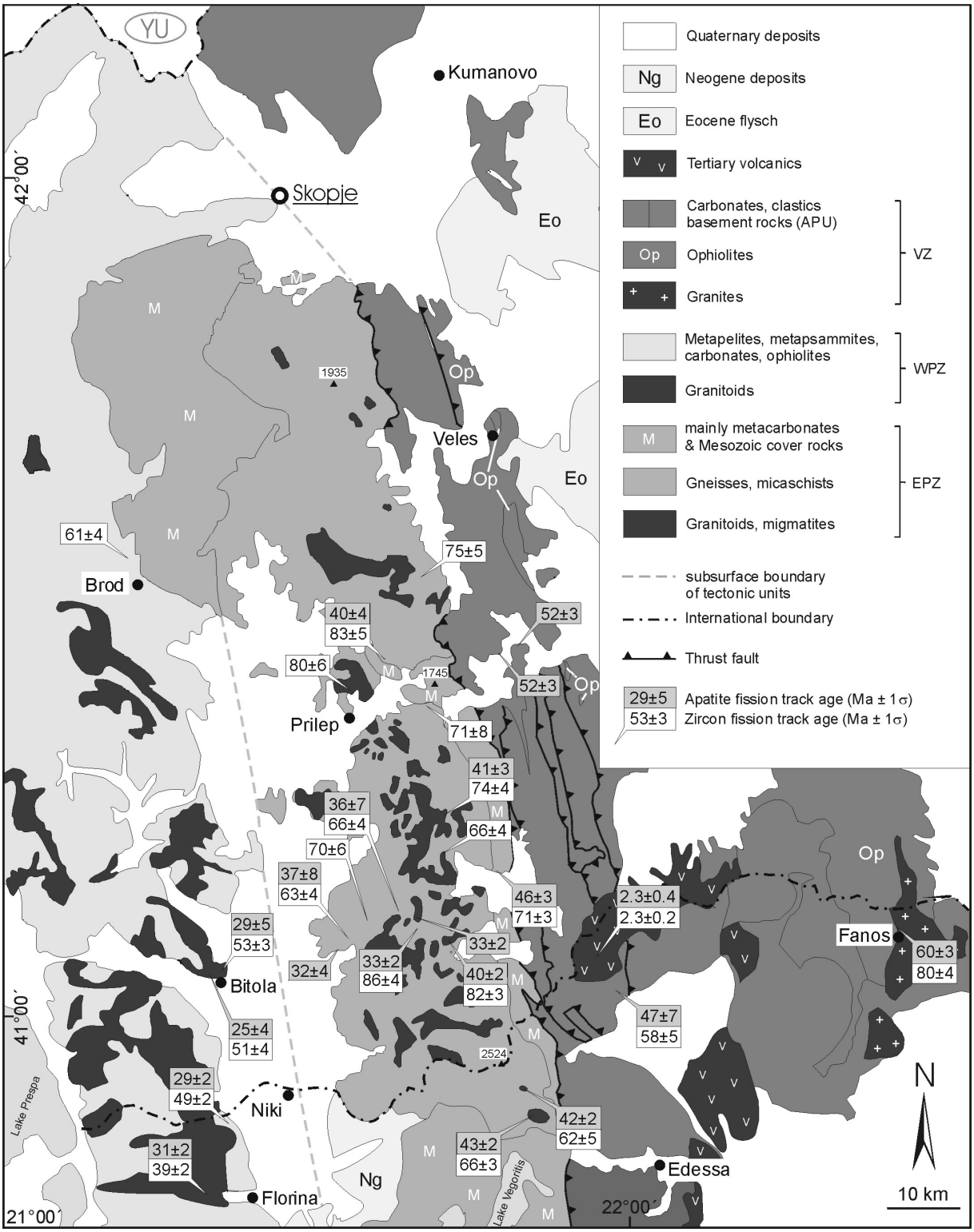

Fig. 3.7: Distribution of zircon and apatite fission track ages of the northern Pelagonian Zone and the Vardar Zone. All errors refer to 1σ confidential level. Abbreviations: EPZ = East Pelagonian Zone, VZ = Vardar Zone, WPZ = West Pelagonian Zone, YU = Serbia.

3.7.5.2 Olympos-Kranea Area

In order to compare the low temperature cooling history of the northern Pelagonian Zone with the southern parts of the Pelagonian Zone, additional samples were determined from the Olympos-Kranea region in Greece. The analytical data are given in Tab 3.13. Note that the Intrapierien Unit (cf. Fig. 3.8) was former named as Infra-pierien unit by Schermer (1992). The unit was renamed, because the Intrapierien Unit is embedded between the Lower and Upper Pierien Unit (=intra) and is not the footwall (=infra) of the Pierien unit. For didactical reasons, the Pierien unit was also subdivided into a Lower and Upper Pierien unit.

Sample	Alt. (m)	Number of grains	Spontaneous		Induced		P_{χ}^2 (%)	Dosimeter		Central age (Ma) ±1s
			ρ_s	N_s	ρ_i	N_i		ρ_d	N_d	
Zircon										
GR01/28	900	21	78.5	[926]	64.3	[758]	97.7	6.51	[6402]	47.7±2.6
GR01/29	960	18	48.8	[633]	37.4	[485]	48.1	6.51	[6402]	51.0±3.6
GR01/35	810	20	58.0	[935]	64.6	[1042]	96.8	6.51	[6402]	35.1±1.8
GR01/36.1	960	9	59.5	[269]	71.9	[325]	98.9	6.51	[6402]	32.4±2.8
GR01/38.1	800	20	109.1	[1748]	55.9	[895]	46.5	6.51	[6042]	76.3±3.7
Apatite										
GR01/28	900	24	0.994	[43]	6.867	[297]	100.0	5.23	[5139]	14.7±2.4
GR01/35	810	3	0.803	[3]	4.551	[38]	99.1	5.23	[5139]	17.9±11.2
GR01/36.1	960	6	0.649	[6]	4.221	[39]	100.0	5.23	[5139]	15.6±6.9
GR01/38.1	800	9	0.799	[23]	4.479	[129]	100.0	5.23	[5139]	18.1±4.1

Tab. 3.13: Analytical data of zircon and apatite fission track dating of samples derived from the Olympos – Kranea area. Track densities (ρ) are as measured (x10^5 tr/cm^2); number of tracks counted (N) shown in brackets; ρs = spontaneous track density, ρi = induced track density, ρd = track density of dosimeter glass; Apatite ages calculated using dosimeter glass: CN5 with ζ-CN5 = 388.5±10.1; zircon ages calculated using dosimeter glass: CN2 with ζ-CN2 = 122.5±2.2; Pχ^2: probability obtaining chi-square value for n degree of freedom (where n = no. crystals -1).

The zircon FT ages of the Olympos area display two different age groups. Ages of 35±2 and 32±3 Ma derived from the Lower Pierien Unit (LPU; GR01/35, GR01/36), whereas an age of 76±4 Ma (GR01/38) is obtained from the Intrapierien Unit situated in the northern part of the Olympos area, representing the hanging wall. From the Kranea region ages of 51±4 and 48±3 Ma are derived from the Upper Pierien Unit (UPU).

In contrast to the zircon FT ages, the apatite FT ages display a homogeneous age pattern between 18±4 and 15±2 Ma. The relatively high errors (see Tab. 3.13) are related to the low number of countable grains (n=3-9) and their low uranium content (10-17 ppm). Responsible for the low amount of countable apatite grains is the intense deformation associated with contemporaneous destruction of the apatite grains. All measured samples passed the χ^2-test with a χ^2-probability of 46.4 to 100.0% (Tab. 3.13).

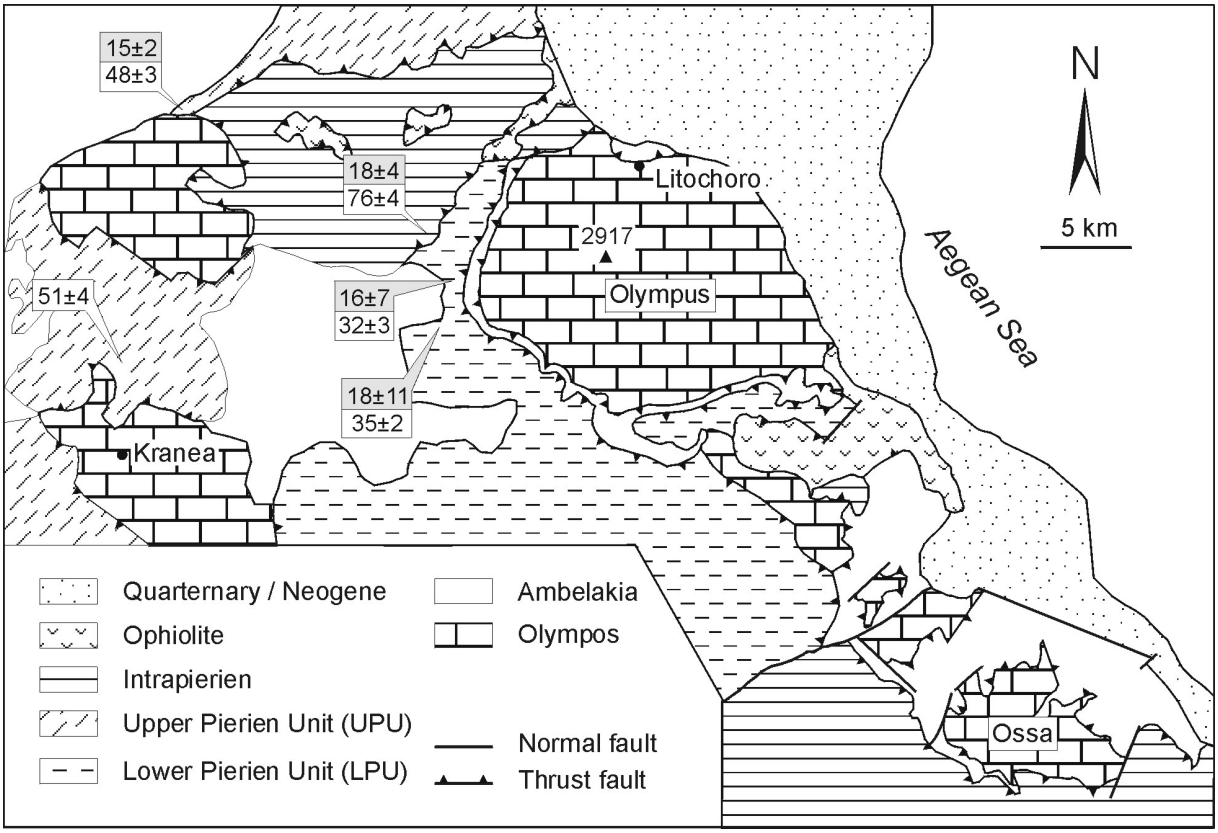

Fig. 3.8: Distribution of zircon and apatite fission track ages of the Olympos – Kranea area. All errors refer to 1σ confidential level. Map complied from Schermer (1990) and the Geological Map of Greece (1:500.000). Grey background = apatite FT age, white background = zircon FT ages.

3.8 Apatite track length measurements

Based on the annealing behaviour of fission tracks (increasing temperature leads to track shortening and contemporaneous track density reduction), the measurement of the fission track lengths provides the possibility to interpret the apparent ages in respect to their time temperature history. Generally it has to be distinguished between "projected track lengths" and "confined track lengths". Projected track lengths represent the apparent lengths of tracks, which intersect the etched surface, and are not suitable for track-length measurements (Gleadow et al., 1986). Confined tracks are fully enclosed in the crystal and are etched out through tracks (TINTs) and through the cleavage (TINCLEs). According to Donelick et al. (1999), confined tracks used for track-length measurements have to fulfil the criteria that (a) the track is defined by two clearly visible ends and (b) the track has to be parallel to the surface (± 10°).

Gleadow et al. (1986) were the first to recognise that confined tracks underwent different thermal histories displaying characteristic track length distributions, which are represented by different groups (Fig. 3.9).

a.) Mean track lengths between 14 to 15.5 µm are obtained from volcanic rocks and rapidly cooled intrusive rocks.
b.) Tracks from undisturbed basement, which underwent slow cooling or regional metamorphism have a mean track length of 12-14 µm.
c.) Bimodal and d.) mixed distributions are attributed to different kinds of thermal overprint.

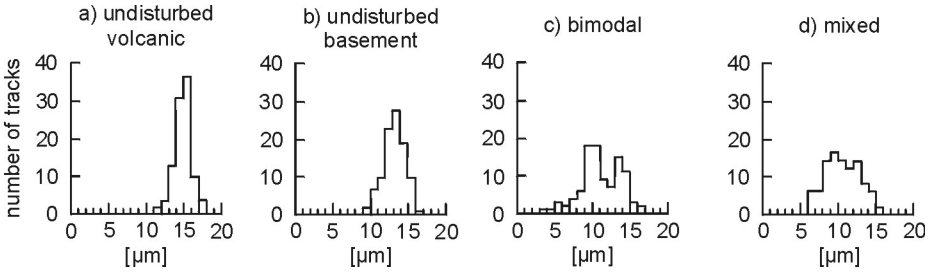

Fig. 3.9: Distributions of confined track length in apatite underwent different thermal histories. Redrawn from Gleadow et al. (1986).

Increasing temperature leads to annealing of the fission tracks by track length shortening until the entire track is annealed and disappears (Naeser and Faul, 1969; Green et al., 1986; Laslett et al., 1987). This process occurs over a wide temperature interval (Wagner and Van den Haute, 1992), the so called 'partial annealing zone' (PAZ). The lower limit of PAZ is the temperature, at which the track begins to anneal. The upper limit is represented by the temperature at which the track is completely annealed and disappears. For the zircon partial annealing zone (ZPAZ), a temperature interval between 190-260° C is given by Zaun and Wagner (1985), whereas the apatite partial annealing zone (APAZ) ranges between 70-125° C (Gleadow et al., 1983).

The annealing behaviour of apatite (generalised formula [$Ca_5(PO_4)_3(F,Cl,OH)$]) is also coupled to its chemical composition. Chlorapatite is much more resistant to annealing than flourapatite (Green et al., 1986; Green et al., 1989). Therefore the chemical composition of apatite has to be determined for a reliable interpretation of the apatite fission track data.

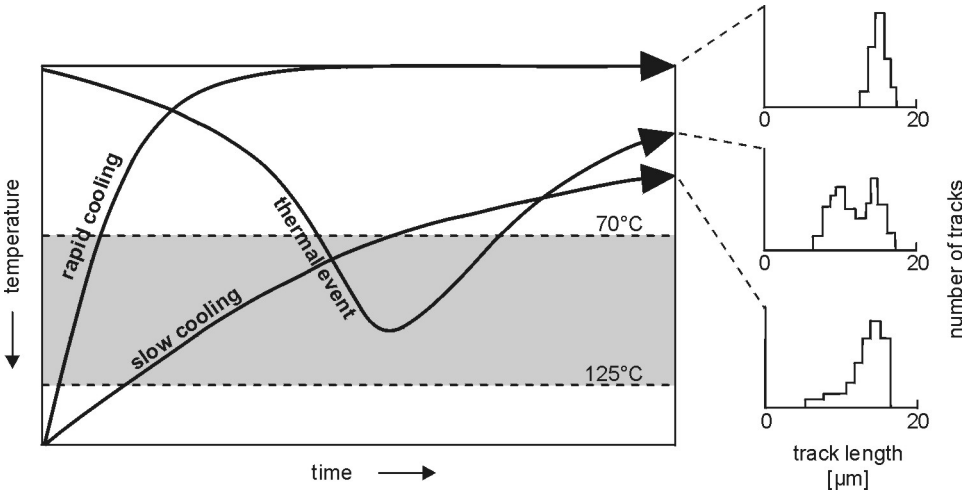

Fig. 3.10: Diagram depicting the apatite partial annealing zone concept. After Seward (1993)

3.8.1 Chemical composition of apatites

The chemical composition of apatites, was measured using a JEOL 8900 Superprobe electron microprobe (Institute of Mineralogy, University of Tübingen). A MAC 4570 "apatite S" (apatite A: P, Ca and F) as well as AS-TIMEX standards (sanidine: Si; tugtupite: Cl; fluorite: F and rhodonite: Mn) were used for the calibration of measured elements. Measurement conditions were: 15 kV accelerating voltage, 20 nA probe current using a beam diameter of 20 µm. Data reduction was performed using a ZAF correction.

Calibration problems arise from the quality of the MAC 4570 "apatite S" standard used for the P, Ca and F calibration, because the reference standard analysis is only based on a microprobe analyse and not verified by wet chemical analysis and does not yield the ideal cation distribution (appendix B). This means, that the determined P_2O_5 content is probably too high, what leads to inaccuracies of the measurements. According to Stormer (1993), fluorine and chlorine may diffuse irregularly under increasing duration of exposure to the electron beam.

Another problem leading to inaccuracies of the microprobe measurements is the uneven surface of the apatite grains, based on the etching of the apatite mounts. This methodical error can not be avoided, because for a meaningful geological interpretation fission track lengths measurements and chemical analyses would have to be performed on the same mount.

Taken into account these problems, it is obvious that the results shown in chapter 3.9.1 have to be regarded as qualitative and not as absolute values. However, the data quality is sufficient to differentiate between Cl- and F-apatite.

3.8.2 Results

From the West Pelagonian Zone only sample GR99/5 contains sufficient amounts of confined tracks with a mean track length of 14.09±0.18 µm (σ = 1.47 µm). The absence of confined tracks in the rest of the West Pelagonian samples is due to their low uranium content (appendix D1 l.-o.).

All samples from the East Pelagonian Zone (M99/12, M99/15, M98/17, M98/7) have mean track lengths between 12.98±0.34 to 13.56±0.21 µm. Slightly longer tracks of 14.12±0.19 and 14.19±0.19 µm are obtained from the Kaimakzalan area (samples GR99/11 and GR99/12). The standard deviation for all samples range between 1.25 to 1.86 µm.

Mean track lengths between 13.36±0.34 and 14.01±0.44 µm (σ = 1.44 to 1.59 µm) are obtained from the samples of the Vardar Zone (GR99/27, M98/39, M98/40).

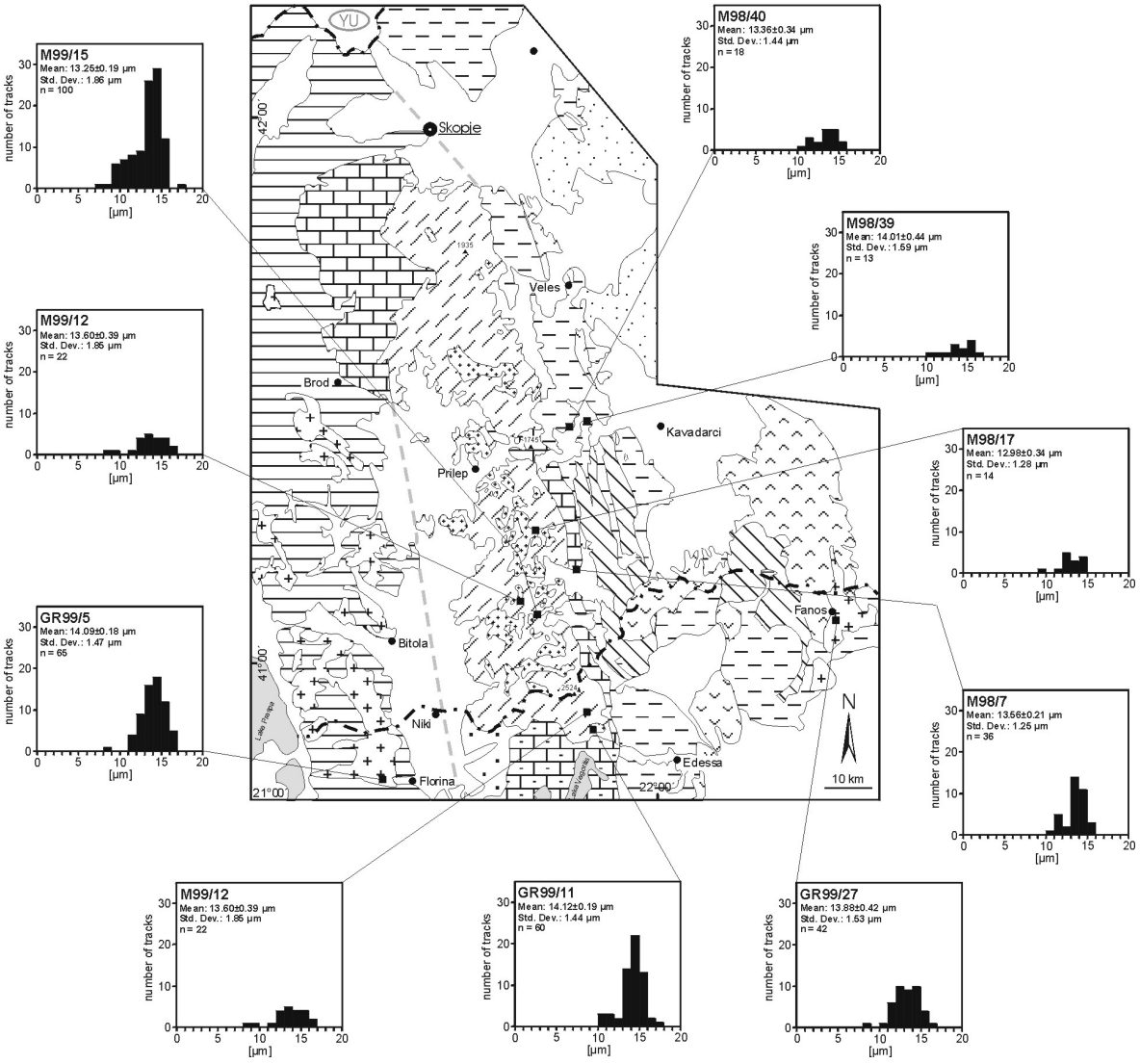

Fig. 3.11: Track-lenghts distributions of apatite samples from the northern Pelagonian Zone and Vardar Zone. For explations, see text.

All measured track-lengths distributions refer to an undisturbed basement, which underwent slow cooling or regional metamorphism (Gleadow et al., 1986).
Related to their young apatite fission track ages of around 18 Ma (see Tab. 3.13) and their very low uranium content (appendix D1 u.-x.), the apatites derived from the Olympos-Kranea area do not contain confined tracks.

3.9 Thermal modelling

The fission track length distribution in apatite is a function of the time-temperature evolution and can be used to reveal the latest cooling history. The thermal history was modelled with the computer program 'AFTSolve' (vers. 1.2.2) of Ketcham et al. (2000) using the measured track length distribution and the apparent apatite fission-track age. The program models the annealing behaviour for apatite with different chemical compositions and describes the way of the sample through the PAZ.
Input parameters are the apparent apatite fission track age, the fission track length distribution, chlorine contents and additional time temperature constraints (e.g. sedimentation age, geochronological data of other minerals). Limiting boundary conditions are a surface temperature of 20° C and a maximum temperature of 325° C. The operator can choose between several single and multi-kinetic annealing models (Laslett et al., 1987; Crowley et al., 1991; Ketcham et al., 1999).
'AFTSolve' uses a Monte Carlo algorithm to simulate a best fit thermal evolution path for an apatite sample. The conformity of the measured and modelled data is evaluated by the Kolmogorov-Smirnov (K-S) test and the age-goodness of fit (AgeGOF). A self-consistence of 100 % between measured and modelled data is indicated by a value of 1.0 (solid black line, cf. Fig. 3.12). The model reaches good values if the result of both tests is ≥ 0.5 (dark grey area, cf. Fig. 3.12). Acceptable values (light grey area, cf. Fig. 3.12) are indicated by values ≥ 0.05.

3.9.1 Results

The electron microprobe analyses of apatite carried out on seven selected samples (see appendix B) of the West and East Pelagonian Zone and Vardar Zone indicate that most of the apatites are nearly of pure fluorine end-member (F = 2.5-4.3 wt%) composition, partly with negligible contents of chlorine (0.1 wt%). Only the samples M99/15 and GR99/5 contain minor amounts of chlorine (0.2-0.5 wt%).

The 'AFTSolve' (vers. 1.2.2) modelling were performed using the following parameters: For F-apatite the single kinematic annealing model of Crowley et al. (1991) (F-apatite) was chosen, whereas the Durango model of Crowley et al. (1991) was applied for Cl-apatite. Boundary conditions are the zircon FT retention temperature (240±50° C) and the APAZ (125-70° C).

For the West Pelagonian Zone the model (Fig. 3.12a) displays relative fast cooling between 220 and 85° C, stagnation and remaining of the sample in the APAZ between 30 and 23 Ma at around 80° C, followed by slow decreasing cooling (2.5° C/Ma).

All East Pelagonian models display slow continuous cooling for the time between ~80 and 50 Ma followed by remarkably faster cooling recorded in all samples (Fig. 3.12b-g.). At around 40 Ma the models suggests the beginning of a slow cooling period, whereas some samples remained in the APAZ (Fig. 3.12c,d,e). The latter is also indicated by the track length distribution and the presence of some shortened tracks. Except models (Fig. 3.12b,g) all models for the EPZ (Fig. 3.12c-f) indicate onset of final increased cooling around 10 Ma.

In the Vardar Zone the thermal modelling was applied on one sample derived from the Fanos granite (GR99/27, Fig 3.12h) and on two samples of a metaflysch (M98/39, M98/40; Fig. 3.12i-j). The model for the Fanos granite indicates continuous cooling between 80 and 56 Ma, stagnation of the sample in the APAZ (60-30 Ma) at around 80° C, and slow final cooling (2.1° C/Ma).
The probably Maastrichtian deposition of the flysch (Jacobshagen, 1986) is followed by rapid burial of the rocks beyond the APAZ and total track annealing, as indicated by the track length and single grain age distributions.

Evidence for conformity of measured data and calculated models is given by the statistical evaluation of the data. Both, K-S test and Age GOF, generally reach values between 0.8-1.0. Only the models (Fig. 3.12f,i,j) display lower values (0.5-0.7), but are also above the suggested lower limit of acceptance (0.5).

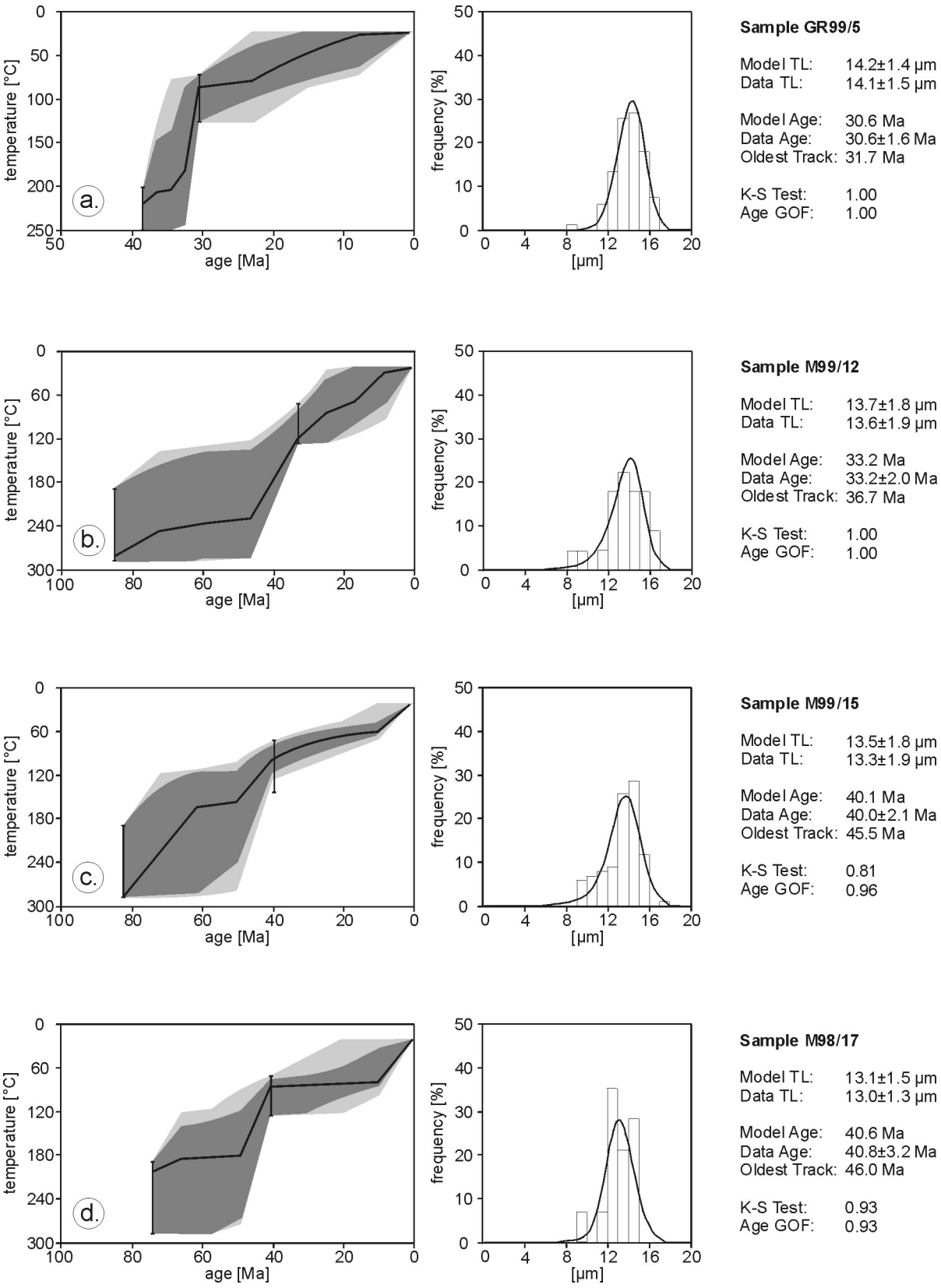

Fig. 3.12: Time–temperature paths modelled by AFTSolve. a.: West Pelagonian Zone, b.-g.: East Pelagonian Zone, h.-j.: Vardar Zone. Track lenght distributions (histogram on the right side) are normalized to n=100. The fit between the observed and modeled data (T-t paths left side) is indicateed as follows: solid black line = best fit; dark grey area = good fit; light grey area = acceptable fit. Abbreviations: GOF = goodness of fit between modeled and caculated age; K-S = Kolmogorov-Smirnov statistical test; TL = track lenght. Continues.

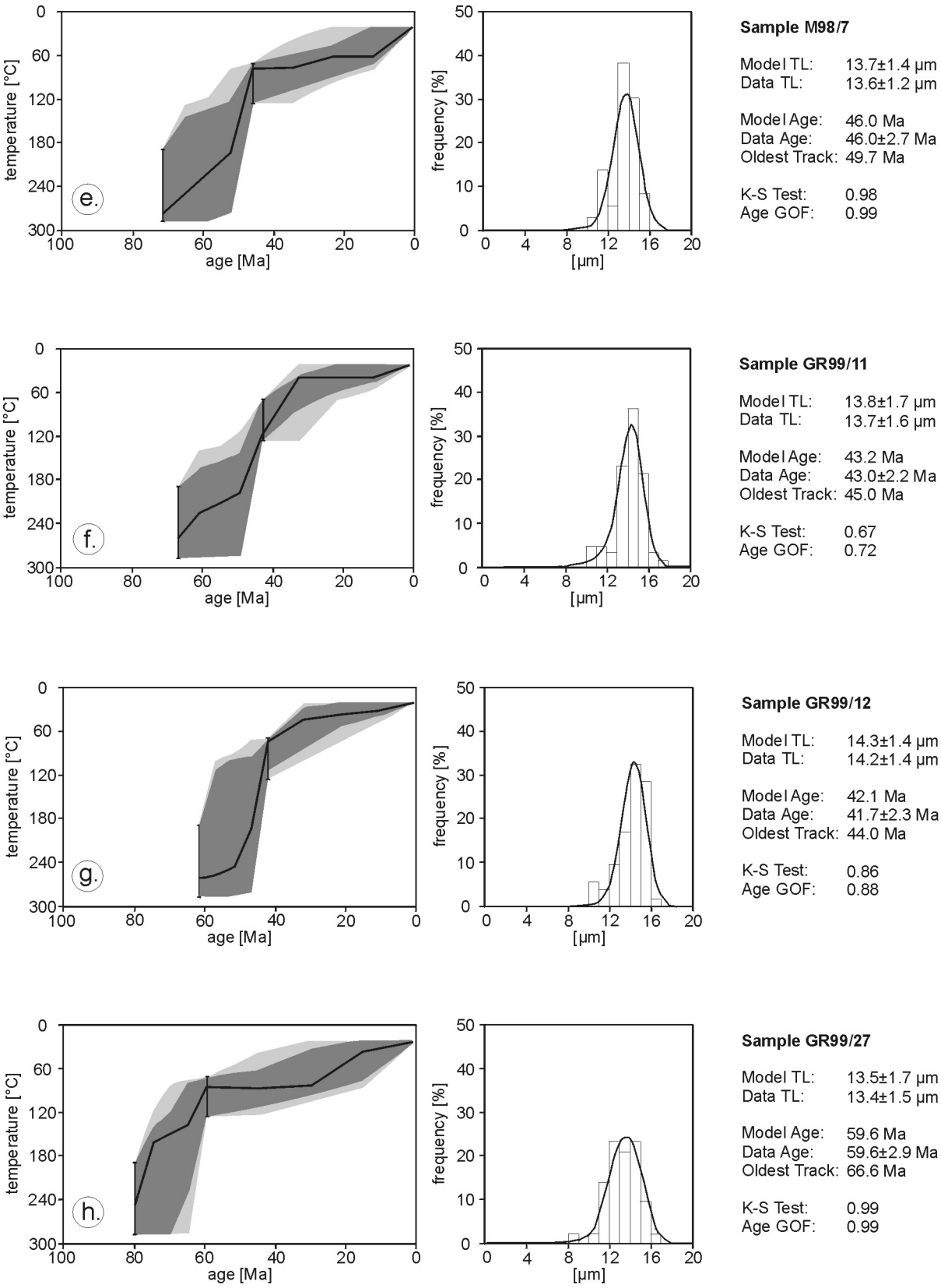

Fig. 3.12: Time–temperature paths modelled by AFTSolve; a.: West Pelagonian Zone, b.-g.: East Pelagonian Zone, h.-j.: Vardar Zone. Continues.

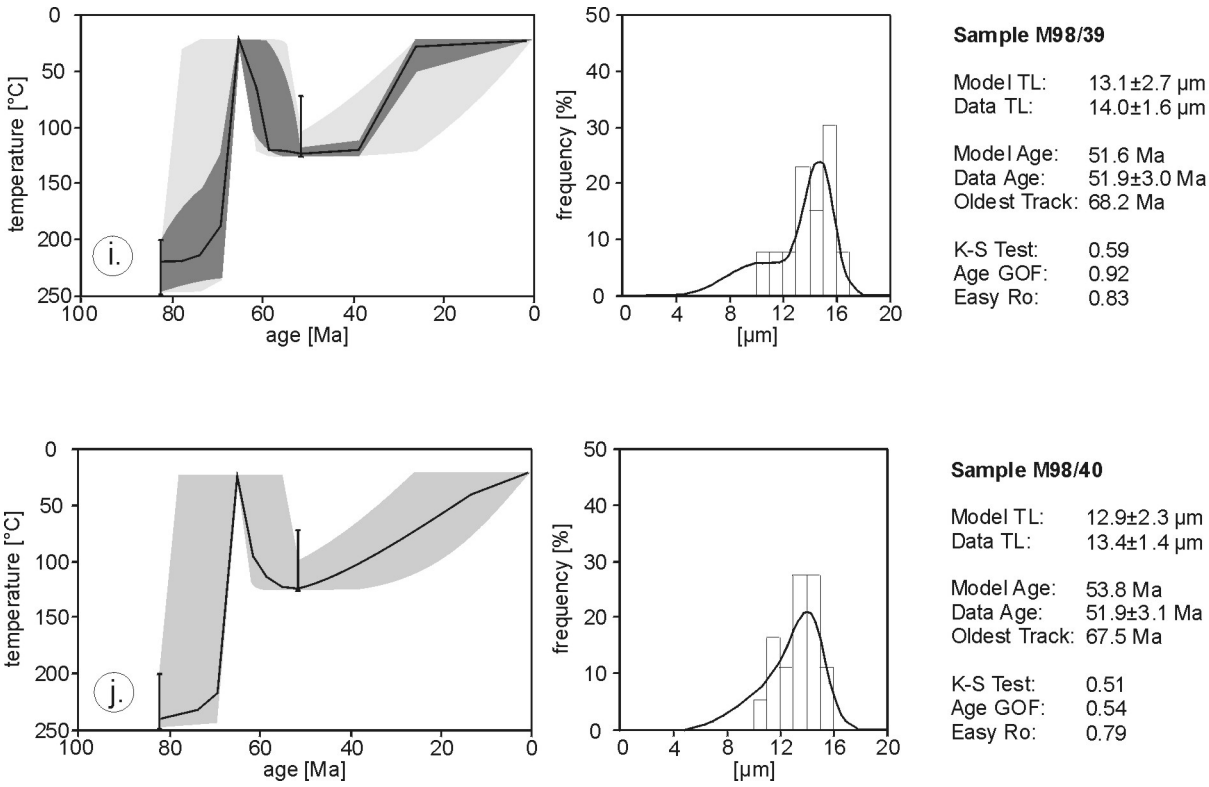

Fig. 3.12: Time–temperature paths modelled by AFTSolve; a.: West Pelagonian Zone, b.-g.: East Pelagonian Zone, h.-j.: Vardar Zone. Continues.

3.10 Interpretation of geothermochronological data

3.10.1 The concept of isotopic closure

During the last three decades, the concept of 'blocking temperatures' (Jäger, 1973) or 'closure temperatures' (Dodson, 1973) had been widely applied in Earth sciences. In essence the model is based on the assumption that the isotopic composition of a mineral is not modified if the ambient temperature drops below a mineral specific temperature. A selection of published closure temperatures (T_c) is given in Tab. 3.14.
The method was originally developed for the Central Alps and was later attributed to universal validity and has been used for interpretation of numerous geochronological studies without assessing their basis (Villa, 1998).

Mineral	Decay	Tc[° C]	References
biotite	$^{40}Ar/^{39}Ar$	320-350	Kirschner et al. (1996)
	K/Ar	~100	Hurley et al. (1962)
		<180	Dunlap (2000)
		300±50	Dodson (1973)
		450	Villa and Puxeddu (1994)
	$^{87}Rb/^{87}Sr$	300±50	Jäger et al. (1967)
white mica	$^{40}Ar/^{39}Ar$	>400	Kirschner et al. (1996)
	K/Ar	350±50	Purdy and Jäger (1967)
		500±50	Hammerschmidt and Frank (1991)
	$^{87}Rb/^{87}Sr$	500±50	Jäger et al. (1967)
		600-650	Steck and Hunziker (1994)

Tab. 3.14: Selection of published 'closure temperatures'.

There is numerous evidence that isotopic closure is not only related to defined temperature interval. It is also controlled by parameters described below.

Dunlap (2000) found out that $^{40}Ar^*$ diffusion in biotite from ancient orogens reset by long isothermal periods (>10 Ma) occur as low as 180° C. A biotite closure temperature of around 100° C is described by Hurley et al. (1962). The interdependence of T_c in biotite and XFe-ratio (higher XFe = higher T_c) is specified by Harrison et al. (1985), whereas the content of halogenides (F^-, Cl^-) will have a more significant effect on T_c (Grove and Harrison, 1996). The investigations of Kramar et al. (2001) indicate that $^{40}Ar^*$ diffusion is also related to deformation processes and seriously influences the radiometric age.

In case of the Rb/Sr-system the isotopic exchange during cooling of rocks depends on the mineral grain size, tracer ^{87}Sr diffusion coefficients and the modal proportions of each mineral and their ^{87}Sr content. The parameters listed above control also the chemical exchange between the different phases, whereas the Rb/Sr partitioning data controls the chemical exchange among the phases during cooling (Jenkin et al., 1995; Jenkin et al., 2001).

Different modal compositions of rocks, which underwent the same cooling history, can also yield different ages (e.g. >100 Ma).

Contrary to the 'isotopic closure' temperatures the effective retention temperature of fission tracks is defined as the temperature at which 50 % of the original number of fission tracks are preserved. For the apatite chronometer a widely accepted T_c = 100±20° C is given by Wagner (1968), Naeser and Faul (1969) and Hurford (1986)

Hurford et al. (1989) propose a T_c for zircon fission tracks of 225±25° C for faster cooling rates (>10° C/Ma) and a T_c of 240±50° C (Hurford, 1986) for systems with slower cooling rates. A zircon FT retention temperature of 350° C is proposed by Carpéna (1992).

3.10.2 Summary of geochronological data

Clear evidence for two magmatic stages (I: Late Carboniferous (~300 Ma), II: Late Permian – Early Triassic (~245 Ma)) in the East Pelagonian Zone during the Variscan orogeny is supported by U/Pb dating of zircon and accompanying CL-studies of their internal structure. In contrast to this, K/Ar biotite ages obtained from three granite samples display higher ages (between 311.6±11.6 and 446.5±16.8 Ma; Tab. 3.16). This is interpreted in terms of excess $^{40}Ar^*$ as consequence of metasomatic alteration processes during the Eohellenic orogeny. The younger K/Ar biotite age of 128.2±4.9 Ma (sample M99/12) means total reset of the K/Ar system and is related to a more intense greenschist facies metamorphic overprint of the margins of the intrusive body. Contrary to the K/Ar ages both biotite concentrates analysed by the Rb/Sr method yield ages of 126.9±1.3 and 122.1±1.2 Ma (Tab. 3.16), what indicates homogenisation of the Rb/Sr system during the Eohellenic orogeny.

Based on the K/Ar age determinations on different rocks of the East and West Pelagonian Zone and the Vardar Zone, at least 7 different tectonometamorphic events were dated (see Fig. 3.13). The results focus especially on the Lower to Upper Cretaceous evolution of the Eastern Pelagonian Zone.

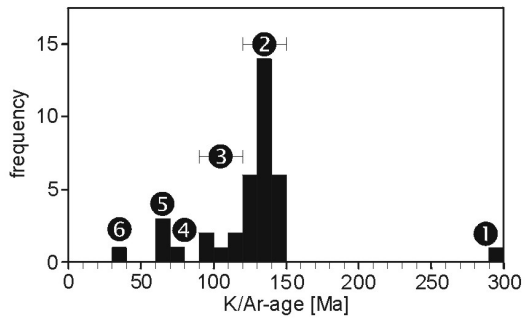

	Affected units	Metamorphic grade	MNTD	Event
1	EPZ	GSF to (?) AMF	?	D0
2	EPZ, VZ*)	(BSF); upper GSF to AMF	⇗	D1+D2
3	EPZ + VZ	GSF	⇖	D3
4	WPZ	GSF	⇗	D4
5	VZ	lower GSF	⇦	D5
6	WPZ	lower GSF	⇦	D6

Fig. 3.13: Statistical distribution of K/Ar ages obtained from the northern Pelagonian Zone and the adjacent Vardar Zone. Only ages of geological significance are considered. Abbreviations: AMF = amphibolite facies metamorphism; BSF = blueschist facies metamorphism; EPZ = East Pelagonian Zone; GSF = greenschist facies metamorphism; MNTD = main nappe transport direction; VZ = Vardar Zone; WPZ = West Pelagonian Zone; number in circles = age groups; *) detrital white mica. For detailed description of the events (D_0-D_6) see chapter 4 and 5.

The evaluation of the K/Ar data in $^{40}Ar^*/K$ correlation plots (cf. Fig. 3.4) clearly demonstrate that none of the analysed samples experienced loss or gain of radiogenic argon. None of the samples displays differences in the radiometric age, with respect to different metamorphic grades, grain sizes and chemical compositions.

Except for sample GR99/33, the $^{40}Ar/^{39}Ar$ ages are higher than the K/Ar ages of the same sample (Tab. 3.16). The K and $^{40}Ar^*$ contents obtained from the $^{40}Ar/^{39}Ar$ measurements are systematically higher than those contents measured by the conventional K/Ar technique (Tab. 3.15). The potassium content was calculated from the ^{39}Ar content (conversion factor 7.73 x 10^{-9} cm^3/ppm K).

Thus the differing ages are probably related to handpicking (heterogenisation) of the $^{40}Ar/^{39}Ar$ samples and/or to different analytical techniques. However the ages are within the 2σ-error range and thus do not exert influence on the geological interpretation.

Sample	K%	$^{40}Ar^*$ /ccm	K/Ar-age	K%	$^{40}Ar^*$ /ccm	$^{40}Ar/^{39}Ar$-age
8-9wm	8.03	4.44	136±5	9.1	5.79	149±1
M99/13wm	8.93	4.53	126±5	9.5	5.37	133±1
M99/13bt	7.57	3.70	121±5	8.11	4.53	132±3
GR99/38	7.61	3.00	99±4	7.49	3.50	111±2

Tab. 3.15: Comparison between conventional K/Ar and $^{40}Ar/^{39}Ar$ total degassing data. All errors refer to 1σ. $^{40}Ar^*$ concentrations $x10^{-5}$.

In most cases, where K/Ar, $^{40}Ar/^{39}Ar$ and Rb/Sr age determinations were carried out on the same sample, the obtained ages are nearly identical (Tab. 3.16). Therefore these ages are interpreted as crystallisation ages. Neither the 'closure temperature' concept of Dodson (1973) is applicable to them, nor exhumation rates can be calculated from these ages. As a possible reason fast cooling of the rocks after the Lower Eohellenic orogeny is suggested.

Problematic are the ages obtained from different geochronological systems on sample 8-9 (blueschist). The different K/Ar and $^{40}Ar/^{39}Ar$ ages (Tab. 3.16) are probably related to handpicking of the $^{40}Ar/^{39}Ar$ sample aliquot (see above). The interpretation of the significant higher Rb/Sr age of 195±10 Ma (Tab. 3.16) is uncertain. Possible reasons are for example the later disturbing of the Rb/Sr system caused by fluids or loss of non radiogenic Sr.

Sample	rock type	Mineral	K/Ar age	$^{40}Ar/^{39}Ar$ age*)	Rb/Sr age	U/Pb-zircon age
8-9	blueschist	white mica	136±5	149±0.2	195±10	(-)
8-5	micaschist	white mica	135±5	(-)	139±7	(-)
M98/7	gneiss	white mica	141±5	(-)	142±1	(-)
M99/13	micaschist	white mica	126±5	133±1	(-)	(-)
		biotite	121±5	132±3	(-)	(-)
GR99/33	micaschist	white mica	102±4	101±3	(-)	(-)
GR99/38	micaschist	biotite	99±4	111±2	(-)	(-)
8-4	granite	biotite	312±12	(-)	(-)	244±1
M98/14	granite	biotite	411±16	(-)	(-)	(-)
M98/17	granite	biotite	447±17	(-)	127±1	246±7
M99/12	granite	biotite	128±5	(-)	122±1	299±1

Tab. 3.16: Age data comparison of samples analysed by different geochronological systems. (-) = not measured; *) total fusion age. Ages in Ma, all errors refer to 1σ confidential level.

Zircon and apatite fission track age determinations were carried out on samples derived from the West and East Pelagonian Zone and the Vardar Zone. Zircon FT ages of 85-60 Ma obtained from the East Pelagonian Zone and the Vardar Zone display contemporaneous cooling of both units below the 240° C isotherm, while the cooling of the West Pelagonian rocks was significantly later at around 50 Ma. In the East Pelagonian Zone the oldest ages were obtained from the lower unit, whereas the youngest ages were derived from samples of the upper unit. This inverse age distribution is interpreted to be related to the re-heating of the upper unit caused by north-eastward thrusting of the West Pelagonian Zone onto the East Pelagonian Zone during Campanian time.
The zircon FT ages are systematically younger that than the K/Ar, $^{40}Ar/^{39}Ar$ and Rb/Sr ages, except sample 8-24 which derived from a mylonite (lower greenschist facies conditions) near Brod. The K/Ar white mica age of 36±1 Ma is significantly younger than the zircon FT-age of 61±4 Ma. An explanation might be, that (a) the temperature during mica growth was not high enough to reset the zircon FT-age or (b) that the duration of the tectonic event was too short to complete track annealing.

The apatite FT ages continuously decrease from the eastern Vardar Zone (60 Ma) towards to the West Pelagonian Zone (around 30 Ma), which indicates progressive exhumation and cooling of rocks in westward direction.

Especially the distribution of the zircon FT ages obtained from the northern Pelagonian Zone clearly denies the existence of a metamorphic core complex. In the case of a metamorphic core complex the youngest ages are located in the centre (cf. Tauern window, Eastern Alps) and not as in this study, at the margins.

Complementary to the $^{40}Ar/^{39}Ar$ age determinations carried out by Lips et al., (1999, 1998) and (Schermer et al., 1990) in the Olympos-Ossa and Pelion region, zircon and apatite fission track age determinations were performed to complete the low temperature part of the cooling path.
Zircon FT ages around 50 Ma are obtained from the Upper Pierien unit, whereas ages of 35 Ma are derived from the Lower Pierien unit. From the Infrapierien unit, which is located between the Upper and Lower Pierien Unit, an age of 76 Ma is determined. The latter is similar to the ages obtained from the East Pelagonian Zone. Schermer et al. (1990) also obtained higher $^{40}Ar/^{39}Ar$ ages of around 100 Ma from the Intrapierien Unit. Two different and significantly younger tectonometamorphic events occurred within the Lower and Upper Pierien Unit. The first around 60-56 Ma is associated with blueschist facies metamorphism and the second between 40 and 36 Ma is accompanied by greenschist facies conditions.
The preservation of the older ages of the Intrapierien Unit indicates that the duration of the tectonometarphic event was too short for total thermal re-equilibration of the Intrapierien Unit. Thus neither the isotope system ($^{40}Ar/^{39}Ar$) was reset, nor the zircon fission tracks were annealed.

Contrary to the zircon FT ages the apatite FT ages cluster around 15-18 Ma, which indicates contemporaneous cooling of all units in the Olympos-Kranea region below 100° C.

None of the analysed zircon and apatite FT samples contains multiple age populations or displays mixed track length distributions.

4 Tectonometamorphic evolution

4.1 Introduction

Modern structural geological data are only limited available for the Greek part of the northern Pelagonian Zone and does practically not exist for the part which is exposed in the Republic of Macedonia. Detailed structural geological investigations in the Greek part of the East Pelagonian Zone (Kaimakzalan, Mount Voras) are currently carried out by Avgerinas (Institute of Geology, Aristotele University of Thessaloniki, Greece). For first results the reader is referred to Avgerinas et al. (2001)

Structural analyses were carried out additionally to the geochronological investigations presented in chapter 3. Due to the problems which were already mentioned in chapter 1, it was not possible to conduct more detailed structural analyses in the Republic of Macedonia as planed at the beginning of the project. A summary of the tectonometamorphic evolution of the study area is given below.

The northern Pelagonian Zone is separated by a NNW-SSE trending shear zone from the Vardar Zone (Fig. 4.1).

The boundary between the West and East Pelagonian Zone is not exposed at the surface. According to the lithological and petrological differences between the two units (cf. chapter 2), the occurrence of the thrust zone is necessary. It is supposed, that the fault is situated below the Quaternary deposits of the plain between Bitola and Prilep, as also supposed by Mountrakis (1984). In the north, the assumed fault is covered by allochtonous Mesozoic marble. The supposed subsurface progression of the fault is marked by the hatched line in Fig. 4.1.

The boundary between the Vardar Zone and the East Pelagonian Zone is marked by an eastward dipping thrust zone, which is also known as 'zone de broyage longitudinal' Mercier (1973). The thrust zone comprises different rock types (limestones, marbles, serpentinites, clastics), which are intensely imbricated.

4.2 Results

In the study area the following tectonometamorphic events can be distinguished. If available, additional informations from other authors, are also presented. The timing of the different tectonometamorphic events is based on the geochronological investigations carried out in this study (cf. chapter 3). All structures which yield the same age are regarded to belong to same event.

1. D_0 Relics of the Variscan orogeny (Late Carboniferous – Early Permian)

   D_0 structures were only recognised in an amphibolite sample (M98/16) of the central part of the East Pelagonian Zone. Hornblende and micas are orientated parallel to a well developed foliation (S_0). The assemblage of hornblende + quartz + plagioclase + garnet + biotite and white mica indicates upper greenschist facies to lower amphibolite facies conditions.

   Mposkos et al. (2001), also describe an amphibolite facies metamorphic event for Late Carboniferous to Early Permian times in the West Pelagonian Zone. However, structural geological data for this event are not available.

2. D_1 Late Jurassic (~150 Ma)

   Structures of the Late Jurassic event D_1 are only preserved at the bottom of the marble covering the northern part of the northern Pelagonian Zone in the Republic of Macedonia. D_1 is classified by the development of a first Alpine foliation (S_{A1}) and as well as an approximately E-W trending stretching lineation (L_{str1}). The deformation is accompanied by metamorphism (M_{A1}) under blueschist facies conditions.
   Despite of the same radiometric age, this event was separated from D_2. Because it is thought to belong to an Late Jurassic event within the Vardar Zone.

3. D_2 Early Eohellenic event (Tithonian - Barremian; 148-130 Ma)

   During D_2, SW-NE directed compression leads to the development of NNW-SSE trending tight to isoclinal folds. The resulting fold axial plane foliation (S_{A2}) is the dominating fabric element in the East Pelagonian Zone. In general the S_{A2} foliation strikes NNW-SSE and dips westward at the western margin of the EPZ and to eastward directions at the eastern margin (Fig. 4.1). Parallel to the fold axis a stretching lineation is developed. The S_{A2} foliation is re-folded by NW-SE or NNW-SSE trending wide open folds, while phyllosilicate rich layers are crenulated. Most of the observed D_2 folds in the East Pelagonian Zone are E vergent.
   The development of a NE-SW trending stretching lineation is related to top to NE sense of shear (Fig. 4.2; appendix A, plate 1a), determined on porphyroclasts. Also during D_2 porphyroblast and clasts orientated parallel to a NW-NNW / SE-SSE trending stretching lineation were developed. They indicate opposite transport of the East Pelagonian rocks to both NW and SE directions. The movements are interpreted as contemporaneous strike-slip movements during compression and probably indicate a transpressional deformation regime.

   Problems arise, according to the age determinations (cf. 3.5), from the contemporaneous occurrence of two different stretching lineations during D_2. Neither they were observed to exist parallel in the same sample nor differences in their radiometric ages were detected. Therefore it is not possible to clarify if these structures were developed at the same time or alternately. The coexistence of both lineations can also indicate that the deformation was locally concentrated and did not affect the whole ‘rock-package’. The latter can be explained by strain partitioning. However, the resolution of the K/Ar data as well as the structural data does

not provide a final interpretation. Maybe more detailed $^{40}Ar/^{39}Ar$ investigations and structural mapping can solve this problem in the future.

The original mylonitic fabric of the D_2 shear zones was either overprinted 1) by a later thermal event or 2) subsequently to the deformation event, as indicated by the static recrystallisation of quartz.

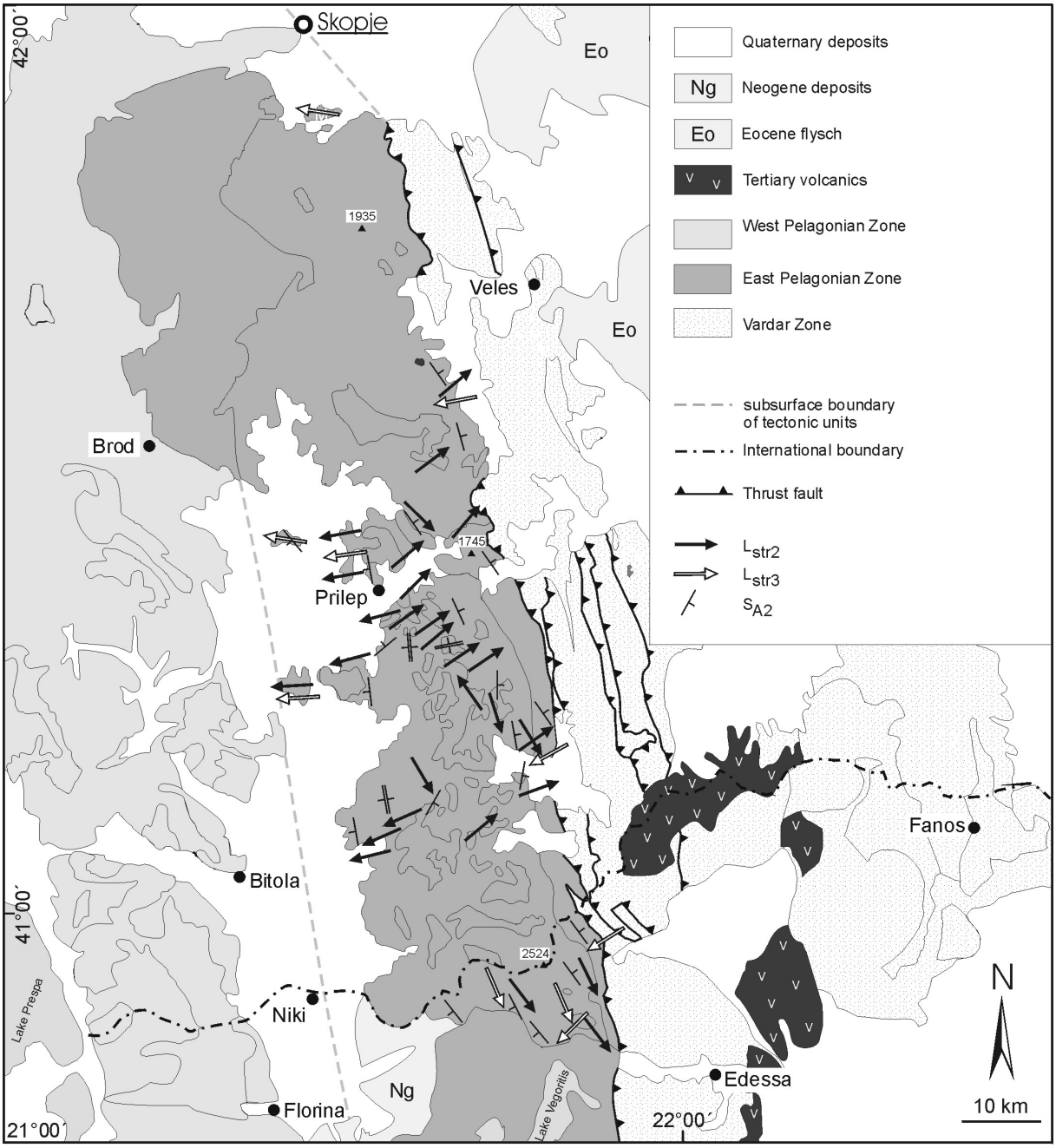

Fig. 4.1: Simplified geological sketch map of the study area including major thrust zones and the orientation of the S_{A2} foliation as well as D_2 and D_3 stretching lineations.

During D_2 the metamorphism (M_{A2}) reached upper greenschist facies to amphibolite facies conditions. The metamorphic grade increases from the margins (upper unit) towards to the centre (lower unit) of the East Pelagonian Zone. The granites of the East Pelagonian Zone were only affected at their outer margins. In the central part of the intrusion bodies the original granoblastic texture is well preserved. For the results of the geothermobarometric calculations see chapter 5.3.

4. D_3 Late Eohellenic event (Middle Cretaceous; 110-90 Ma)

The second Eohellenic event is limited to the uppermost parts of the upper unit of the East Pelagonian Zone and to the Almopias Unit. In the East Pelagonian Zone the rocks were not penetrative affected by D_3. In contrast to this, the crystalline basement and the Mesozoic cover rocks of the Ano Peternik Unit (Vardar Zone) underwent intensive diapthorism and deformation. Shear sense indicators in the East Pelagonian Zone, which are developed parallel to a WSW-ENE trending stretching lineation, display westward thrusting of the Vardar nappes onto the Pelagonian crystalline (Fig. 4.2; appendix A, plate 1b-c). During D_3 a foliation (S_{A3}) and crenulation cleavage were developed. The S_{A3} crenulation cleveage differs from the S_{A2} crenulation on smaller micas which were developed under lower PT conditions. S_{A3} is developed subparallel to S_{A2}. The westward movements are accompanied by compensatory extensional movements, which are directed to SE (Fig 4.1; appendix A, plate 1d). They indicate the continuation of the transpressional deformation regime. The attribution of NW-SW trending folds to D_3 is uncertain. Because some of these folds formed under semi-ductile to brittle conditions, they are regarded to represent the latest D_3 structures.

The accompanied metamorphism (M_{A3}) did not exceed middle greenschist facies conditions (cf. Avgerinas et al., 2001). The rocks of the Almopias Zone underwent intense diaphtorism under middle greenschist facies conditions.

5. D_4 Late Cretaceous event (~ 80-70 Ma)

Both, the West and East Pelagonian Zone, were affected by the fourth event (D_4). In the West Pelagonian Zone a new foliation S_{A4} as well as a stretching lineation L_{str4} was developed. Porphyroclasts orientated parallel to L_{str4} indicate top to NE sense of shear (Fig. 4.2; appendix A, plate 1e). In the East Pelagonian Zone shear bands and cataclastic shear zones (Fig. 4.2; appendix A, plate 1f) display also top to NE sense of shear. The structures described above are linked to north-eastward thrusting. They probably represent the final emplacement of the western Pelagonian margin onto the Pelagonian basement.

The accompanied metamorphism (M_{A4}) yielded middle greenschist facies conditions in the West Pelagonian Zone. The maximum temperature must have been below 450° C, as indicated by the brittle rheological behaviour of feldspar (appendix A, plate 1e). In contrast to this, in the East Pelagonian Zone the temperature did not exceed ~300° C, displayed by the semi-brittle to brittle deformation of quartz.

6. D_5 Late Cretaceous – Early Tertiary event

This event was only recognised in the Almopias Unit (Vardar Zone). Discrete shear zones indicate top to WSW thrusting (Fig. 4.2; appendix A, plate 1g). During D_5 the metamorphism (M_{A5}) did not exceed lower greenschist facies conditions.

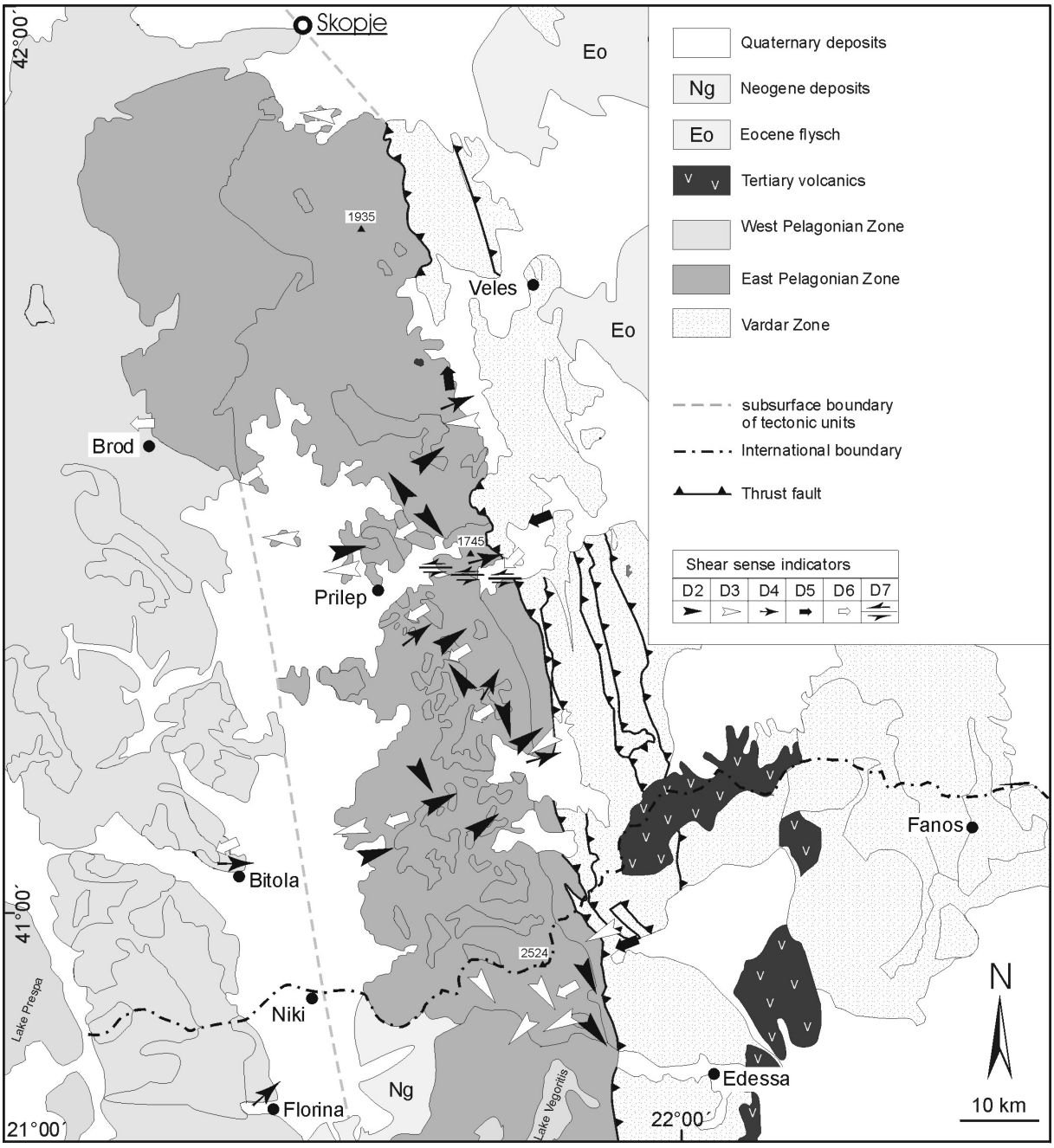

Fig. 4.2: Simplified geological sketch map including shear sense indicators which display different transport directions during the alpine tectonometamorphic events D_2 to D_7.

7. D_6 Shear zones (Paleocene – Middle Oligocene)

   D_6 is mainly marked by the development of slickensides, as well as cataclastic and pseudotachylitic shear zones (appendix A, plate1h-j), which indicate top to W-SW (Fig. 4.2) thrusting. The cataclastic shear zones strike NW-SE in average and dip gently to NE. The thickness varies between several cm and up to 2 meters. The best out crops are situated along the road from Vitoliste to Prilep.

   Porphyroclasts (appendix A, plate 1k) as well as quartz c-axis orientations indicate westward movements along a mylonitic shear zone occur N Brod (WPZ). The mylonitic foliation trends WSW-ENE and dips gently (~60°) to NNW. The stretching lineation dips flat (~5°) to the W. The movements are regarded as contemporaneous normal faulting during uplift of the West Pelagonian Zone.

8. D_7 Shear zones (post Middle Oligocene)

   Movements along E-W trending cataclastic strike-slip faults occur in the East Pelagonian Zone. They are very well exposed along the road from Kavardarci to Prilep. They transect the D_6 shear zones. High angle normal faults, which indicate top to NE transport were also developed during D_7.

4.3 Summary

The results of the structural investigations indicate, that the rocks of the West Pelagonian Zone, the East Pelagonian Zone and the Vardar Zone underwent a polyphase deformation history during the Alpine orogeny. Relict structures of the Variscan orogeny are rarely preserved.

During Cretaceous times the tectonometamorphic evolution was accompanied by alternating nappe transport directions towards the NE and to the W to SW and back to NE (Tab. 4.1). In contrast, nappe transport during the Tertiary occurred only to W and SW directions (Tab. 4.1). The tectonometamorphic events are the result of progressive convergence between the Apulian and European plate, which took place from Late Jurassic to Late Tertiary.

Event	Affected unit	PT conditions	Mineral assemblage	Thrusting top to	Age [Ma]
D_0	WPZ	AMF (a)		no data	~ 300
	EPZ	upper GSF to ? AMF	hbl + bt + msc + qtz + grt ± chl		
D_1	VZ	BSF	cc + ab + ep + crossite + phe	no data	~ 150
D_2	EPZ	upper unit: upper GSF	qtz + plag + bt + phe + cld + grt + ep + chl	NE	148-130
		lower unit: AMF	qtz + grt + ky + stau + bt + phe		
D_3	WPZ ?		(?)	SW	110-90
	EPZ	GSF	qtz + ab + msc + bt + grt + chl + ep		
	VZ	GSF			
D_4	WPZ	GSF	qtz + msc + chl	NE	70-80
	EPZ	semi-brittle and brittle	(-)		
	VZ	brittle	(-)		
D_5	VZ	lower GSF (dyn)	qtz + msc + chl	WSW	~ 65
D_6	WPZ	brittle	(-)	SW	~ 55-30
	EPZ	brittle	(-)		
	VZ	brittle	(-)		
D_7	WPZ	lower GSF (dyn)	qtz + msc + ep	W and NE	≤ 30
	EPZ	brittle	(-)		
	VZ	brittle	(-)		

Tab. 4.1: Summary of tectonometamorphic events of the northern Pelagonian Zone and the Vardar Zone in northern Greece and the Republic of Macedonia. Abbreviations: AMF = amphibolite facies, BSF = blueschist facies, EPZ = East Pelagonian Zone, GSF = greenschist facies, VZ = Vardar Zone, WPZ = West Pelagonian Zone, (a) Mpokos et al. (2001), (dyn) = dynamo-metamorphism. Mineral abbreviations after Kretz (1983).

Further detailed structural geological investigations as well as detailed mapping of the northern Pelagonian Zone and the Vardar Zone are required in the future.

5 Mineral chemistry

5.1 Introduction

Due to the lack of information on the metamorphic history of the East Pelagonian Zone, some minerals (garnet, biotite, white mica, ilmenite and chlorite) were analysed for geothermobarometric calculations. The aim is to provide additional informations about the metamorphic evolution of this unit. Also the chemical composition of white micas used for geochronological investigations was analysed on a few selected samples (8-21, M98/43, M99/13 and M98/8).

The mineral assemblage of those rocks of the EPZ that were used for geothermobarometric investigations is given below.

5.1.1 Lower unit

Three micaschist samples (M98/19, M98/22 and 8-5), derived from the innermost part of the East Pelagonian Zone (Selecka Mountains, Rep. of Macedonia) were investigated from the lower unit of the East Pelagonian Zone. The mineral assemblages are given in Tab. 5.1.

Sample(s)	Rock type	Paragenesis
M98/19	micaschist	garnet + biotite + muscovite + quartz ± sphene ± chlorite
M98/22, 8-5	micaschist	garnet + muscovite + kyanite + (staurolite) + (chlorite) ± sphene

Tab. 5.1: Mineral assemblages of samples of the lower unit investigated by microprobe analyses and used for geothermobarometric calculations. Minerals in parenthesis are not present in all quoted samples.

In sample M98/19 biotite is partly alterated to chlorite at the margins. Therefore only unalterated biotite grains were analysed. The assemblage of garnet + muscovite + kyanite + staurolite + quartz in sample M98/22 is over-grown by large chlorite blasts, which grew during a later event. The duration of the later must have been very short, because neither the garnet nor the kyanite show any alteration within the thin sections.

5.1.2 Upper unit

Altogether 7 samples of the upper unit of the East Pelagonian Zone were used for microprobe analyses. The mineral assemblage of those samples that were used for geothermobarometric investigation is given in Tab. 5.2.

Samples	Rock type	Paragenesis
GR99/26, GR99/40	micaschist	garnet + muscovite + chlorite + chloritoid + quartz + ilmenite ± (rutile)

Tab. 5.2: Mineral assemblages of samples of the upper unit investigated by microprobe analyses and used for geothermobarometric calculations. Minerals in parenthesis are not present in all quoted samples.

5.2 Analytical method

Mineral chemical analyses were carried out using a JEOL 8900 Superprobe electron microprobe (Institute of Geosciences, Tübingen). Astimex standards (F-phlogopite: F; albite: Na; ilmenite: Ti; bustamite: Ca; periclase: Mg; rhodonite: Mn; sanidine: K, Si; plagioclase: Al; hematite: Fe and tugtupite: Cl) were used for the calibration of the measured elements. Measurement conditions used: 15 kV accelerating voltage, 20 nA probe current using a beam diameter between 1 and 5 µm (depending on the measured mineral). Data reduction was performed using a ZAF correction. For further details and analytical procedures, see Reed (1993, 1996). The complete analytical data set is given in Appendix B.

5.2.1 Garnet

The mineral formula (general: $X_3Y_2[ZO_3]_4$) was calculated on the basis of 12 oxygen atoms. The Fe^{3+} content, which is not directly determinable by microprobe analyses, was estimated on the cation translation of the *X*-position. For the case that $X \leq 3$, all iron had been regarded as Fe^{2+}. If $X > 3$, excessive Fe^{2+} was converted to Fe^{3+} according to Ryburn et al. (1976). The end-members of the garnet mixed-crystals were calculated in the order: andradite ($Ca_3(Fe^{3+},Ti)_2[SiO_4]_3$), pyrope ($Mg_3Al_2[SiO_4]_3$), spessartine ($Mn_3Al_2[SiO_4]_3$), grossular ($Ca_3Al_2[SiO_4]_3$) and almandine ($Fe_3Al_2[SiO_4]_3$).

Rim-core-rim zoning profiles of garnets can be used to determine the metamorphic evolution from the chemical composition. Numerous models were developed to explain the compositional zoning in garnet, among them element fractionation models (e.g. Hollister, 1966; Tracy et al., 1976; Crawford, 1977; Thompson et al., 1977) and diffusion models (e.g. Anderson and Buckley, 1973; Woodsworth, 1977; Yardley, 1977; Dempster, 1985). Some schematical garnet zoning profiles are given in Fig. 5.1.

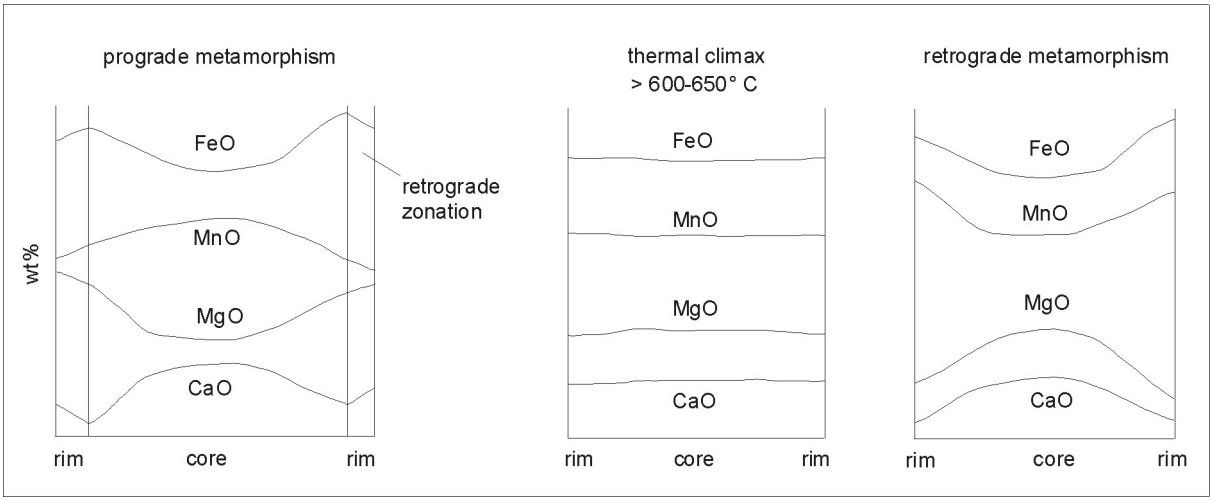

Fig. 5.1: Schematic garnet zoning profiles after Hollister (1966); Tracy (1976); Thompson et al. (1977); Woodsworth (1977); Yardley (1977); Tracy (1982) and Dempster (1985).

Garnet zoning profiles were measured on 6 samples from the East Pelagonian Zone. Samples GR99/26 and GR99/40 derived from the highest structural levels (Kaimakzalan area, NW-Greece), whereas the samples M98/19, M98/22 and 8-5 are derived from the structural deepest levels of the East Pelagonian Zone (Selecka Mountains, Rep. of Macedonia). Sample M98/5 is obtained from the eastern margin of the East Pelagonian Zone (W Vitoliste). Representative rim-core-rim zoning profiles of FeO, MgO, CaO and MnO in the investigated garnets are given in Fig. 5.2.

Most of the analysed garnets of the lower and upper unit are almandine rich end-members (63.12-80.81 mol%). Only garnets of sample M98/5 (UU) contain less almandine (29.97-47.41 mol%). The garnets of the lower unit contain more pyrope (11.51-28.91 mol%) than those of the upper unit (0.55-10.15 mol%). Contrary to this the garnets of the upper unit have a significantly higher grossular content (6.23-26.02 mol% in samples GR99/26 and GR99/40; 45.58-56.24 mol% in sample M98/5; cf. Tab. 5.3). All analysed garnets contain negligible amounts of andradite (0.00-3.40 mol%). The spessartine content varies between 0.98 and 13.24 mol%. A comprehensive summary of the end-member composition of all examined garnets is given in Tab. 5.3.

Rim-core-rim microprobe analyses from garnets of the upper unit indicate a prograde zoning of the garnet crystals (Fig. 5a-d). There is no evidence for a later retrograde overprint in the investigated garnets.
The profiles obtained from garnets of the lower unit display either prograde zoning (sample M98/22 and 8-5; Fig 5e-l) or flat horizontal lines. A retrograde growth of garnet indicated by decreasing Fe contents at the rims occurs by some of the investigated garnets. The horizontal flat zoning profiles could be either related to thermal equilibration of the garnet or may indicate that these garnets are grown under constant temperatures.

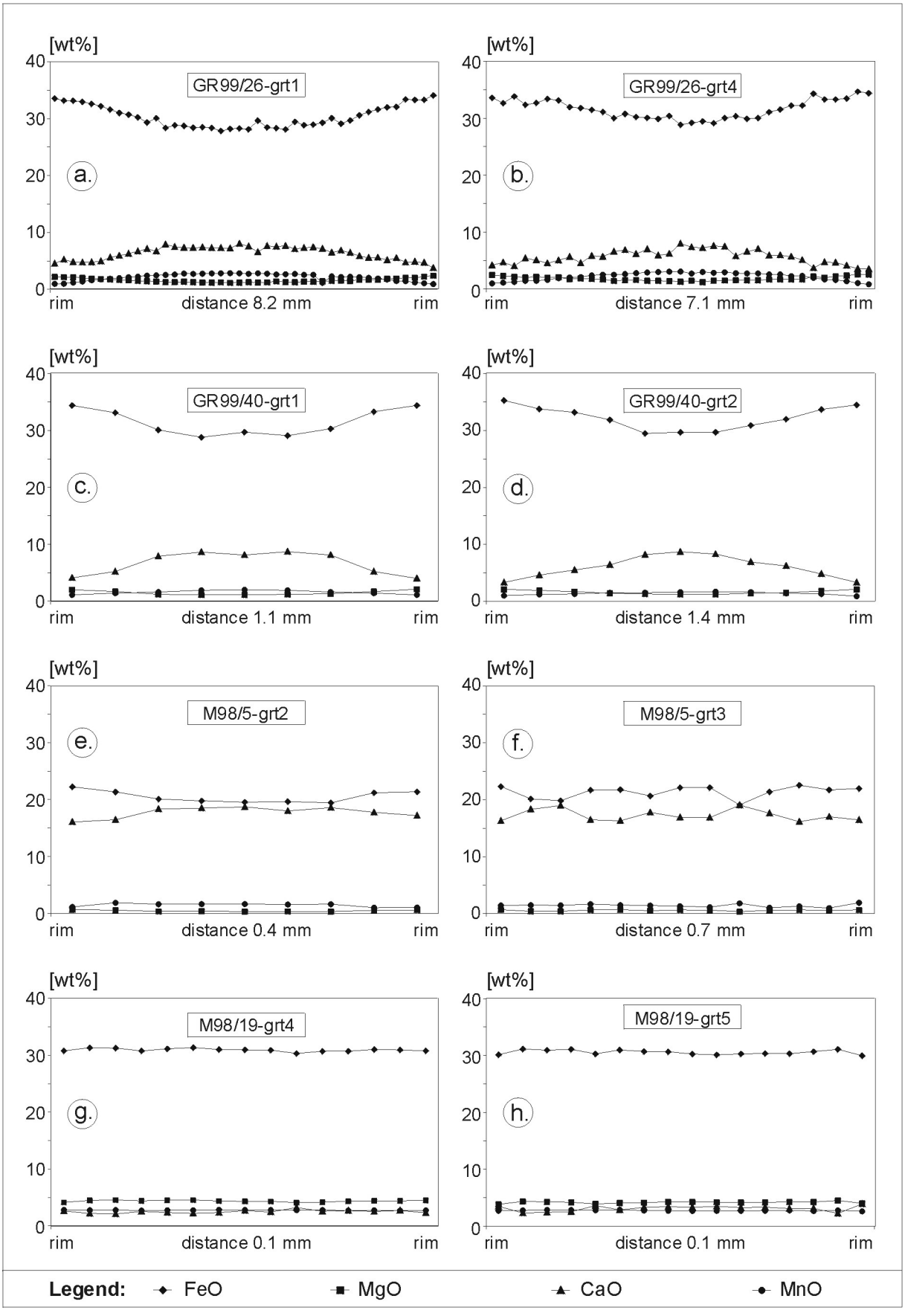

Fig. 5.2: Representative rim-core-rim zoning profiles of FeO, MgO, CaO and MnO in garnets from different structural levels of the East Pelagonian Zone (continues).

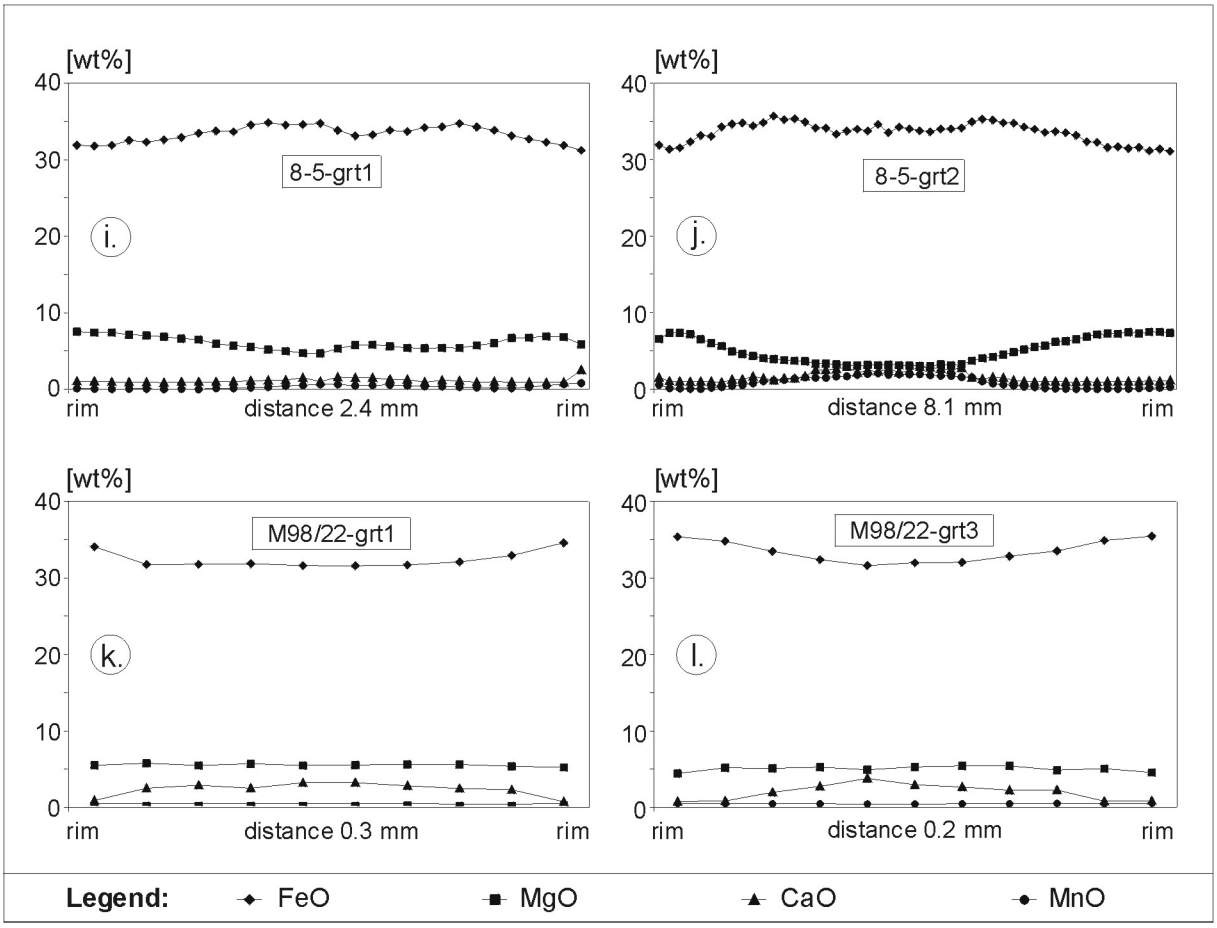

Fig. 5.2: continued.

	sample	andradite		pyrope		spessartine		grossular		almandine	
		core	rim	core	rim	core	rim	core	rim	core	rim
upper unit	**M98/5**	0.00-0.00	0.00-0.00	0.55-2.96	1.74-2.74	3.42-13.24	2.37-4.41	45.58-56.24	47.24-51.97	29.97-47.11	42.94-47.41
	GR99/26	0.00-0.00	0.00-0.40	4.80-5.30	5.07-10.15	6.79-7.63	1.9-7.68	21.6-24.24	6.23-22.41	63.12-66.58	65.04-77.69
	GR99/40	0.00-0.05	0.00-0.90	4.45-6.51	6.01-8.63	1.36-4.83	0.83-3.08	17.67-26.02	11.55-19.59	64.10-67.40	70.41-79.71
lower unit	**8-5**	0.00-1.01	0.00-2.86	12.33-18.71	23.18-28.91	1.49-4.39	0.23-1.83	2.87-6.95	0.00-7.03	74.22-76.93	67.62-70.08
	M98/19	0.00-0.02	0.00-1.58	12.87-19.55	11.51-18.70	6.03-6.39	5.49-6.71	5.88-10.52	6.12-18.70	67.42-69.86	63.8-69.38
	M98/22	1.36-3.40	0.00-0.00	17.22-21.43	15.44-21.68	0.98-1.17	1.03-1.30	0.00-9.02	0.00-6.70	68.47-75.25	74.76-80.81

Tab. 5.3: Compilation of rim – core garnet endmembers. Endmembers were calculated after Rickwood (1968) in mol.%.

5.2.2 Biotite

Biotite belongs to the group of trioctahedral micas (general formula: $K_2R^+_6[Al_2Si_6O_{22}/(OH)_4]$. The formula was normalised on 11 anhydrous oxygens.

Because of the absence of biotite and coexisting garnet in the investigated microprobe samples from the upper unit, biotite analyses were only carried out on two samples of the lower unit (samples M98/19 and M99/13). Rim-core-rim analyses display a nearly homogeneous distribution of Ti (0.00-0.10 pfu), Mg (1.42-1.55 pfu) and Fe^{2+} (0.86-1.03 pfu) without any zoning caused by biotite growth. Both measured samples plot in the meroxene field (Fig. 5.3) of the classification diagram for biotite of Foster (1960).

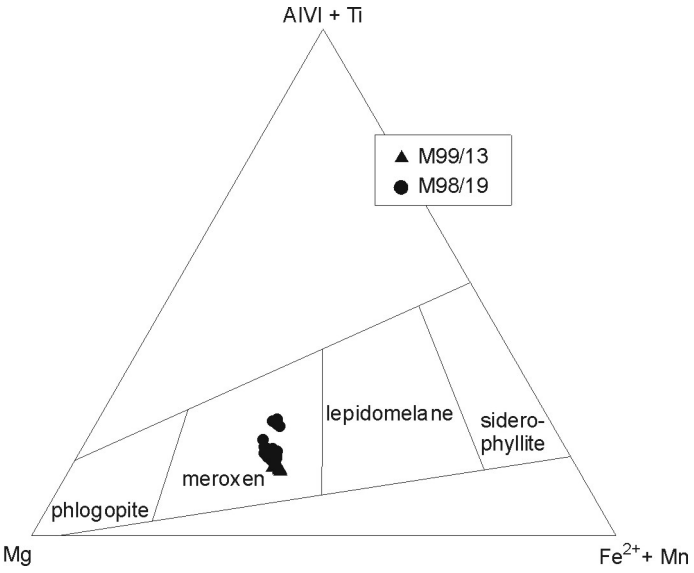

Fig. 5.3: Variation diagram of biotites of the lower unit after Foster (1960).

5.2.3 White mica

White mica belongs to the dioctahedral mica group (general formula: $KAl_2[AlSi_3O_{10}/(OH)_2]$). The formula was normalised on 11 anhydrous oxygens.

The occurrence of different white mica varieties is related to various substitution possibilities. According to Massonne and Schreyer (1987), increasing pressure leads to higher Si contents, as described in equation 5.1.

$$Al^{IV}+Al^{VI} \rightleftharpoons Si^{IV}+(Mg,Fe)^{VI} \qquad (5.1)$$

Phengites are intermediate members of the mixing line between muscovite and celadonite. The end-members were calculated according to Schliestedt (1980) using equations 5.2a,b,c.

paragonite (pg) = Na/(Na*K)*100 (5.2a)

celadonite (cel) = (Si-3)*100 (5.2b)

muscovite (msc)= 100-(paragonite+celadonite) (5.2c)

Microprobe analyses of white micas were carried out on micaschists of the lower unit (samples M98/19, M98/22 and 8-5) as well as on micaschists (samples M98/8, M99/13, GR99/26 and GR99/40), blueschists (M98/43) and amphibolites (8-21) of the upper unit of the East Pelagonian Zone.

All analysed white micas are muscovite end-members (47.13-77.01 mol%; Fig 5.4). The celadonite component varies between 2.08 and 49.94 mol%. The paragonite content of white micas from micaschists of the lower unit scatters between 15.02 and 23.60 mol%. With exception of the garnet-chlorite-chloritoid micaschists from the Kaimakzalan area (GR99/26 and GR99/40; pg = 11.35-21.27 mol%), all samples of the upper unit contain only minor amounts of paragonite (0.81-15.75 mol%).

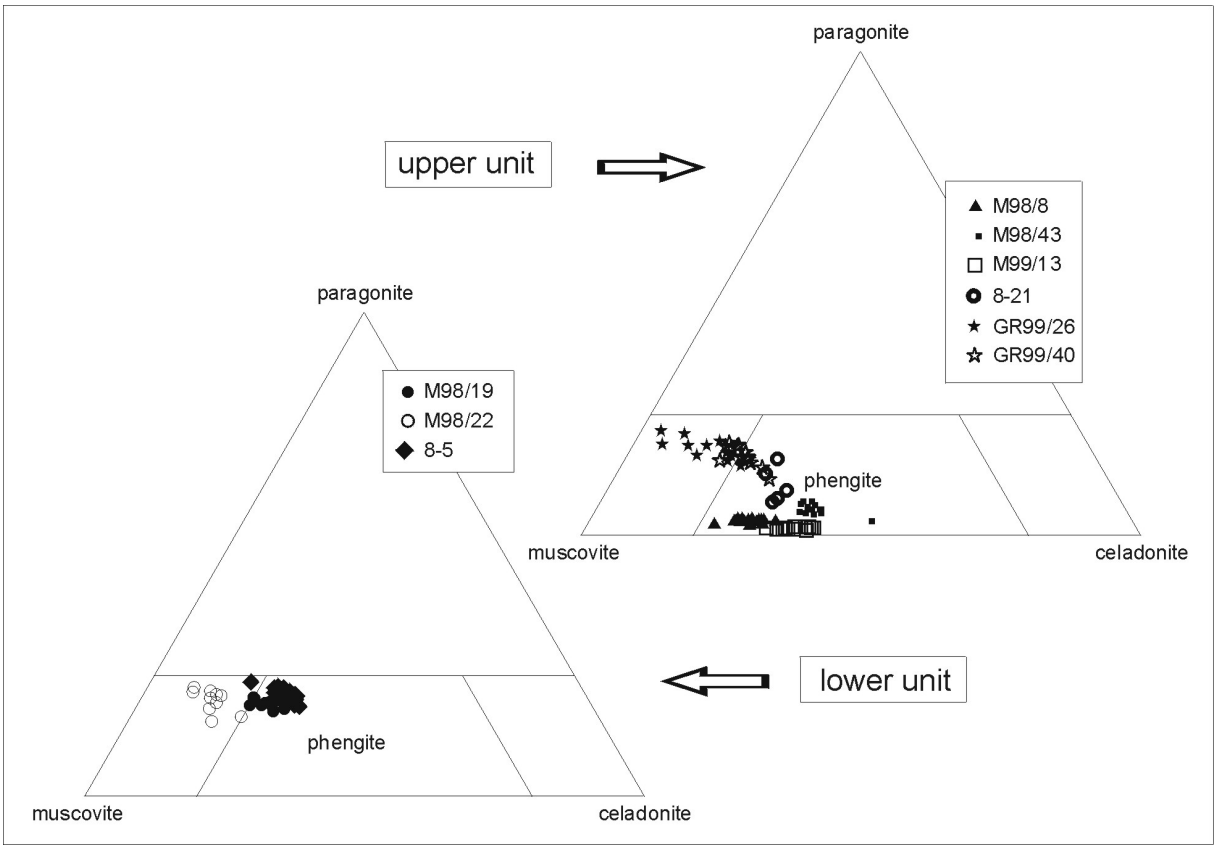

Fig. 5.4: Classification of white micas from the lower and upper unit of the East Pelagonian Zone, after Schliestedt (1980).

5.2.4 Chlorite

The basic structure of chlorite (generalised formula: (Mg, Al, Fe)$_{12}$[(Si,Al)$_8$O$_{20}$](OH)$_{16}$) consists of regularly alternating talc like ($Y_3Z_4O_{10}$) and brucite-like ($Y_3(OH)_6$) sheets. The chlorite analyses were normalised to 14 anhydrous oxygens, assuming all iron is ferrous (Laird, 1988). Wet chemical analyses compiled by Foster (1962) show, that Mg-rich chlorite contains up to 4 wt% Fe_2O_3, whereas Fe-rich chlorite contains up to 20 wt% Fe_2O_3. According to Foster (1962), any chlorite analysis that contain ≥ 0.5 wt% Na_2O, K_2O or CaO has to be excluded from the evaluated data.

Microprobe analyses of chlorite were carried out on two garnet-chlorite-chloritoid micaschists (samples GR99/26 and GR99/40) from the upper unit of the East Pelagonian Zone (Kaimakzalan area).

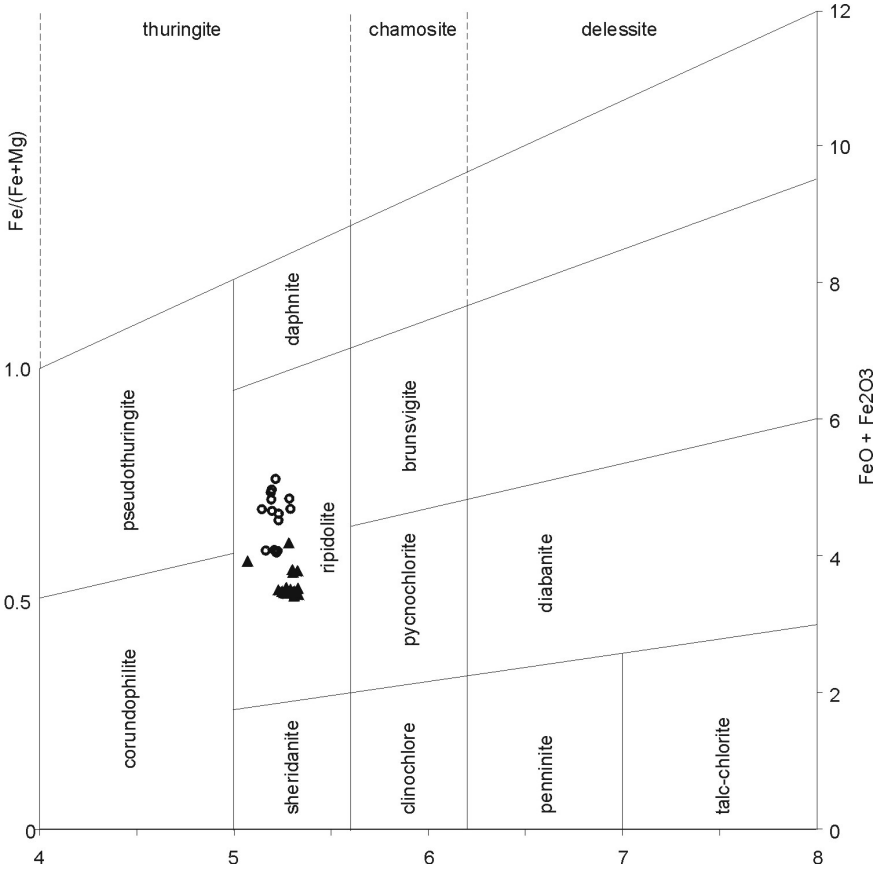

Fig. 5.5: Nomenclature of chlorites after Hey (1954). Symbols refer to samples: ○ = GR99/40; ▲ = GR99/26

None of the analysed chlorites contain more than 0.06 wt% Na_2O, K_2O or CaO. The Fe^{2+} content ranges from 2.25 to 2.67 pfu in sample GR99/26 and from 2.62 to 3.19 in sample GR99/40, whereas the Mg content scatters between 1.01 and 1.77 pfu in sample GR99/40 and ranges from 1.95 to 2.20 pfu in sample GR99/26 respectively. All analysed chlorites plot in the ripidolite field (Fig. 5.5). Zoning of Fe^{2+} and Mg is not developed in the investigated samples.

5.2.5 Ilmenite

Ilmenite microprobe analysis were carried out on ilmenite inclusions of garnet (sample GR99/26). The general formula (ABO_3) was calculated on the basis of 6 oxygens. The Fe^{3+} content was estimated according to Carmichael (1967). The investigated ilmenites contain between 0.07 and 0.18 Fe^{3+} pfu. The proportions of the geikielite ($MgTiO_3$) and the pyrophanite ($MnTiO_3$) component of < 0.1 pfu are negligible.

5.3 Geothermobarometry

Exchange and net transfer reactions provide multitude possibilities to calculate pressure and temperature depending metamorphic reactions. Numerous experimentally and empirically calibrated geothermometers and barometers had been developed for different mineral parageneses in the past. For an overview the reader is referred to Spear (1995). Those that are used in this study, are described below.
According to the goal of this study (cf. chapter 1), not all available geothermobarometers were used. This might be the target and task of detailed petrological investigations in the future.

5.3.1 Geothermometry

5.3.1.1 Garnet-biotite geothermometers

The Fe/Mg distribution between coexisting garnet and biotite depends on the temperature and is related to the Fe/Mg exchange reaction (eq. 5.3), whereas increasing temperature leads to higher Mg-contents in garnet and higher Fe-contents in biotite. According to Ferry and Spear (1978), the pressure dependence (volume change max. 0.057 cal/bar) of the reaction is negligible.

$$Fe_3Al_2[SiO_4]_3 + KMg_3[AlSi_3O_{10}/(OH)_2] \rightleftharpoons Mg_3Al_2[SiO_4]_3 + KFe_3[AlSi_3O_{10}/(OH)_2] \qquad (5.3)$$

almandine + phlogopite ⇌ pyrope + annite

(a) Ferry and Spear (1978)

The garnet-biotite geothermometer by Ferry and Spear (1978) was experimentally calibrated on synthetic garnet and biotite. Furthermore the Fe/Mg exchange between garnet and biotite depends also on the Ca/Mn-content of garnet and the Ti- and Al^{VI} concentrations of biotite. The geothermometer is only valid for garnets containing less than 20 mol% grossular and spessartine, whereas the $(Al^{VI}+Ti)/(Al^{VI}+Ti+Fe+Mg)$ ratio should not exceed 0.15 and the (Ca+Mn)/(Ca+Mn+Mg+Fe) ratio is ≤ 0.2. The temperature can be calculated from equation 5.4.

$$T[°C] = \frac{\left(12454 + 0.057 * P_{[bars]}\right)}{\left(4.662 - 3R * \ln K_D\right)} - 273 \quad (5.4)$$

$$K_D = \left(\left(Mg / Fe\right)_{grt} / \left(Mg / Fe\right)_{bt}\right) \quad (5.4.1)$$

$$R = 1.987 cal / molK$$

(b) Perchuk and Lavrent'eva (1983)

The calibration of Perchuk and Lavrent'eva (1983) is based on the experimental reactions of Mg-, Fe- and Al-oxalates using amorphous SiO_2. The temperature can be calculated from equation 5.5.

$$T[°C] = \frac{\left(7843.7 + \Delta V * \left(P_{[bars]} - 6000\right)\right)}{\left(R * \ln K_D + 5.699\right)} - 273 \quad (5.5)$$

$$K_D = \left(\left(Mg / Fe\right)_{grt} / \left(Mg / Fe\right)_{bt}\right) \quad (5.5.1)$$

$$R = 1.987 cal / molK$$

(c) Indares and Martignole (1985)

Hodges and Spear (1982) improved the garnet-biotite geothermometer of Ferry and Spear (1978), by the consideration of Ca in the temperature calculation. Based on this, Indares and Martignole (1985) suggested a garnet-biotite geothermometer, which also considers the Ti- and Al^{VI} content of biotite. The geothermometer was calibrated on geothermodynamic and empirical data, whereas the temperature can be calculated from equation 5.6.

$$T[°C] = \frac{\left(12454 + \left(0.057 * P[bar]\right) - \left(22353 * XTi_{(bt)}\right) + \left(9000 * \left(XCa_{(grt)} + Mn_{(grt)}\right)\right)\right)}{\left(4.662 - 3R * \ln K_D\right)} - 273 \quad (5.6)$$

$$K_D = \left(\left(Fe / Mg\right)_{grt} / \left(Fe / Mg\right)_{bt}\right) \quad (5.6.1)$$

$$R = 1.987 cal / molK$$

$$XAL^{VI}{}_{(bt)} = Al^{VI} / (AL^{VI} + Ti + Fe + Mg + Mn) \quad (5.6.2)$$

$$XTi_{(bt)} = Ti / (AL^{VI} + Ti + Fe + Mg + Mn) \quad (5.6.3)$$

$$XCa_{(grt)} = Ca / (Ca + Fe + Mg + Mn) \quad (5.6.4)$$

$$XMn_{(grt)} = Mn / (Ca + Fe + Mg + Mn) \quad (5.6.5)$$

(d) Hoinkes (1986)

Because small grossular concentrations (below 10 mol%) lead to significant temperature variations the garnet-biotite geothermometer was recalibrated by Hoinkes (1986), taking into account that increasing Ca-contents of garnet decrease the distribution coefficient K_D. The temperature can be calculated from equation 5.7.

$$T[°C] = \frac{\left(2089 + 0.00956 * P_{[bars]}\right)}{\left(0.7821 - \ln K_D - 2.978 * X(Ca) + 5.906 * \left(X(Ca)_{grt}\right)^2\right)} - 273 \qquad (5.7)$$

$$X(Ca) = Ca/(Fe + Mg + Ca + Mn) \qquad (5.7.1)$$

$$K_D = \left((Mg/Fe)_{grt}/(Mg/Fe)_{bt}\right)$$

5.3.1.1.1 Results

The garnet-biotite geothermometers were only applied to one sample from the lower unit (M98/19), because none of the other microprobe samples contain garnet and biotite. All temperatures were calculated at given pressures of 5, 7 and 10 kbar, with the exception of the geothermometer of Perchuk and Lavrent'eva (1983) which was calculated at 6 kbar. The results are given in Tab. 5.4. The temperatures were calculated by combining garnet rims with biotite rims.

calibration	P [kbar]	sample M98/19	
		T_{min} [°C]	T_{max} [°C]
Ferry and Spear(1978)	5	506	557
	7	510	561
	10	520	572
Hoinkes (1986)	5	529	611
	7	536	618
	10	547	630
Indares and Martignole (1985)	5	502	558
	7	509	565
	10	518	576
Perchuk and Lavrent`eva (1983)	6	504	572

Tab. 5.4: Summary of temperatures calculated by various garnet-biotite geothermometers at different given pressures for sample M98/19 (lower unit, East Pelagonian Zone).

The temperatures calculated by the garnet-biotite geothermometer of Ferry and Spear (1978) yielded maximum temperatures between T ~ 560-570° C and are identical (Tab. 5.4) to the temperatures obtained by the geothermometers of Indares and Martignole (1985) and Perchuk and Lavrent'eva (1983). Slightly increased (Al^{VI}+Ti)/(Al^{VI}+Ti+Fe+Mg) ratios of around 0.17 (calibration limit = 0.15; cf. 5.3.1.1a) seems to have no significant effect on the temperatures calculated by the Ferry and Spear (1978) geothermometer.

In contrast to this, the temperatures obtained from the Ca corrected geothermometer of Hoinkes (1986) yielded the highest temperatures (T_{max} ~ 630°C).

5.3.1.2 Garnet-phengite geothermometers

The temperature dependent Mg/Fe^{2+} exchange reaction between coexisting garnet and phengite (eq. 5.8) can be used for metamorphic temperature estimations. Increasing temperature leads to higher Fe-contents in garnet and increased Mg-contents in phengites.

$$1/6\ Mg_3Al_2[SiO_4]_3 + KFe_{0.5}Al_2Si_{3.5}O_{10}(OH)_2 \rightleftharpoons 1/6\ Fe_3Al_2[SiO_4]_3 + KMg_{0.5}AlSi_{3.5}O_{10}(OH)_2 \quad (5.8)$$

1/6 pyrope + Fe-phengite ⇌ 1/6 almandine + Mg-phengite

(a) Krogh and Raheim (1978)

This geothermometer is calibrated for phengites with low Fe^{3+} contents. The presence of Fe^{3+} will lower the $K_D^{grt+phe}$ value and raise the calculated temperatures at given pressures. Hence the thermometer is calibrated on basaltic rocks, its applicability to pelitic rocks is uncertain. The temperature can be obtained from equation 5.9.

$$T[°C] = \frac{\left(3685 + 77.1 * P_{[kbar]}\right)}{\ln_{KD} + 3.52} \quad (5.9)$$

$$K_D = \left(\left(Fe/Mg\right)_{grt} / \left(Fe/Mg\right)_{phe}\right) \quad (5.9.1)$$

(b) Green and Hellman (1982)

Green and Hellmann (1982) found out that the calculated temperature between garnet and phengite is strongly related to the *mg* number (eq. 5.10.2) and the Ca-content of phengite. That means decreasing *mg* numbers move K_D to higher values. The temperatures can be obtained from equation 5.10a for low Ca-systems with *mg* ~ 67 from equation 3.10b, for low Ca-systems with *mg* ~ 20-30 and for basaltic systems with *mg* ~ 67 from equation 5.10c respectively. If the Fe^{3+} content of phengite is unknown, the temperatures have to be regarded as maximum temperatures only.

$$T[°C] = \frac{\left(5560 + 0.036 * P_{[bars]}\right)}{\ln_{KD} + 4.65} \quad (5.10a)$$

$$T[°C] = \frac{\left(5680 + 0.036 * P_{[bars]}\right)}{\ln_{KD} + 4.48} \quad (5.10b)$$

$$T[°C] = \frac{\left(5170 + 0.036 * P_{[bars]}\right)}{\ln_{KD} + 4.17} \quad (5.10c)$$

$$K_D = \left(\left(Fe/Mg\right)_{grt} / \left(Fe/Mg\right)_{phe}\right) \quad (5.10.1)$$

$$mg = (100 + Mg^{2+}) / (Mg^{2+} + Fe^{2+}) \quad (5.10.2)$$

(c) Hynes and Forest (1988)

According to Hynes and Forest (1988) the temperatures obtained from the calibration of Green and Hellman (1982) are much higher than those obtained from garnet-biotite geothermometers, if the geothermometer is applied to pelitic rocks, which underwent regional metamorphism between 3-7 kbar. In this case the temperature can be obtained from their re-calculation (5.11).

$$T[°C] = \frac{\left(4.79 * 10^3\right)}{\ln_{KD} + 4.13} \quad (5.11)$$

$$K_D = \left(\left(Fe/Mg\right)_{grt} / \left(Fe/Mg\right)_{phe}\right) \quad (5.11.1)$$

5.3.1.2.1 Results

The garnet-phengite geothermometers were applied on three samples of the lower unit (M98/19, M98/22 and 8-5) and on sample GR99/40 from the upper unit. According to the low Ca-content (~ 0.01 pfu) and *mg* numbers between 53 and 80 of the examined phengites, all temperatures which were calculated with the garnet-phengite geothermometer of Green and Hellman (1982) were using equation 5.6a. A summary of the obtained temperatures at various given pressures (5, 7, 10 kbar) is presented in Tab. 5.5.

In the lower unit the maximum temperatures calculated by the geothermometer of Green and Hellman (1982) scatter between 550-650° C (Tab. 5.5). The highest temperatures were obtained from sample M98/22, which is in good accordance with the prograde garnet zoning profiles (cf. Fig. 5.2k,l). The lowest T_{max} between 550-580° C were derived from sample M98/19. This correlates very well with a) the retrograde overprint at the garnet rims (cf. Fig. 5.2g,h) and b) the location of the sample at the upper most part of the lower unit of the east Pelagonian Zone. The sample of the upper unit (GR99/40) gave maximum temperatures between 550-570° C.

Thus, that the Fe^{3+} content is unknown all temperatures calculated by the Green and Hellman (1982) geothermometer have to be regarded as maximum temperatures.
The temperatures which were calculated by the other geothermometers are significantly lower (cf. Tab 5.5).

calibration	P	sample 8-5		sample M98/22		sample M98/19		GR99/40	
	[kbar]	T_{min}	T_{max}	T_{min}	T_{max}	T_{min}	T_{max}	T_{min}	T_{max}
Krogh & Raheim (1978)	5	453	470	450	502	394	427	382	420
	7	481	498	477	531	420	453	407	447
	10	522	540	518	575	458	493	445	486
Green & Hellman (1982)	5	579	595	576	626	521	553	509	547
	7	590	606	586	637	531	564	519	557
	10	606	623	602	654	546	579	534	573
Hynes & Forest (1988)	3-7	496	515	493	551	431	467	418	460

Tab. 5.5: Summary of temperatures calculated by various garnet-phengite geothermometers. Samples 8-5, M98/22 and M98/19 are derived from the lower unit, sample GR99/40 from the upper unit of the East Pelagonian Zone.

The best results were obtained from the garnet-phengite geothermometer of Green and Hellman (1982), because the temperatures are in the range of the T conditions which can be estimated by mineral critical assemblages. Similar results for sample M98/19 were obtained from the garnet-biotite geothermometer of Ferry and Spear (1978).
The significant lower temperatures obtained form the Krogh and Raheim (1978) and Hynes and Forest (1988) geothermometers can be explained in the following way: The geothermometer of Krogh and Raheim (1978) it is probably not applicable to rocks of pelitic composition (c.f. 5.3.1.2).

The lowest temperatures were obtained from the re-calibrated Krogh and Raheim (1978) geothermometer by Hynes and Forest (1988). They either indicate that the pressures were >7 kbar, or that re-calibration is limited to defined whole rock compositions and therefore not applicable to all rocks of pelitic composition.

5.3.1.3 Chlorite geothermometers

(a) Cathelineau (1988)

The Al^{IV} content in the tetrahedral site of chlorites increases with temperature and is related to a decrease in the molar fraction of the Si^{IV} rich end-members. The chlorite geothermometer of Cathelineau (1988) is empirically calibrated for temperatures between 150° C to 300° C, where extrapolations to higher and lower temperatures are possible. The relation between the Al^{IV} content and T is given in equation 5.12. The presence of Fe^{3+} lowers the temperatures.

$$T[°C] = -61.92 + \left(321.28 * Al^{IV}\right) \quad (5.12)$$

(b) Jowett (1991)

The Fe and Mg-content affects Al_M^{IV} independently of the temperature. Thus X(Fe) normalisation (eq. 5.13) is used to estimate the $Al^{IV} - T$ correlation. The calibration is valid for chlorites with X(Fe) < 0.6.

$$T[°C] = 319 Al_C^{IV} - 69 \quad (5.13)$$

where

$$Al_C^{IV} = Al_M^{IV} + 0.1\left(Fe / Fe + Mg\right) \quad (5.13.1)$$

5.3.1.3.1 Results

Because the calculated temperatures are only based on the chemical composition of chlorite, the values presented here have to be regarded as minimum temperatures. The temperatures calculated by the geothermometers of Jowett (1991) are consistently between 5 and 10 degrees higher, than those obtained from the calibration of Cathelineau (1988). The thermometer of Jowett (1991) is not applicable to sample GR99/40, because of its higher X(Fe) ratio (>0.6).

	Cathelineau (1988)	Jowett (1991)
T_{min} [°C]	368	375
T_{max} [°C]	384	390

Tab. 3.6: Comparison of temperatures calculated by various chlorite geothermometers for sample GR99/26.

5.3.1.4 Garnet – ilmenite geothermometer

Pownceby et al. (1987) using the Mn/Fe exchange (eq. 5.14) between garnet and ilmenite for the experimental calibration of their garnet-ilmenite geothermometer. It is calibrated for T = 600-900° C and P = 2-5 kbar and is valid for hematite (Fe_2O_3) and geikielite ($MgTiO_3$) contents up to 10 mol%. T can be estimated from equation 5.15.

$$Fe_3Al_2[SiO_4]_3 + 3\ MnTiO_3 \rightleftharpoons Mn_3Al_2[SiO_4]_3 + 3\ FeTiO_3 \quad (5.14)$$

almandine + 3 pyrophanite ⇌ spessartine + 3 ilmenite

$$T[°C] = \frac{\left(-4089 + 420 * \left(2 * X(Mn)_{ilm} - 1\right)\right) - \left(77 * \left(2 * X(Mn)_{grt} - 1\right)\right)}{\left(-R * \ln_{KD}\right) - 1.44} \quad (5.15)$$

$$K_D = \left((Mn/Fe)_{grt} / (Mn/Fe)_{ilm}\right) \quad (5.15.1)$$

$$X(Mn)_{grt} = \left(Mn/(Mn+Fe)\right) \quad (5.15.2)$$

$$X(Mn)_{ilm} = \left(Mn/(Mn+Fe)\right) \quad (5.15.3)$$

5.3.1.4.1 Results

There are no consistent temperatures calculated by the garnet-ilmenite geothermometer. The calculated temperatures scatter between 525° C and unrealistic high temperatures >1000 °C.

All measured ilmenites containing less Fe^{3+} (0-0.176 pfu) and negligible Mg-contents (0-0.014 pfu). The $XMn_{(ilm)}$ ratio ranges between 0.013 and 0.042.

According to Pownceby et al. (1987) low Mn-, increased Fe^{3+}- and Mg contents within ilmenite as well as unprecise microprobe analyses (measurement errors around 1% yielding to inaccuracies between 70-150° C) can be responsible for unrealistic temperatures.

Furthermore the sample did not underwent the required PT conditions of the calibration (c.f. 3.1.1.4 and 3.1.2.1.1), as indicated by the garnet-phengite and garnet-chlorite geothermometers. Schulze (1992) recommend to discourage from the use of this geothermometer, due to the high sensitivity to low Mn-contents in ilmenite.

5.3.2 Geobarometry

None of the investigated microprobe samples contains a paragenesis which is suitable for geobarometric calculations. Therefore the pressure was estimated by the Si content of phengite according to Massonne and Schreyer (1987).

5.3.2.1 Phengite geobarometer

Massonne and Schreyer (1987) found out that increasing pressure leads to higher Si content per formula unit in phengite, whereas increasing temperatures has only a minor effect on the Si content of phengite. The geobarometer was calibrated for the limiting assemblage of phengite + phlogopite + K-feldspar + quartz. In the past it was applied by numerous researchers without fulfilling the calibration requirements.

Natural phengites which do not coexist with the limiting assemblage described above, but with some other Mg-Fe silicates provide minimum pressures.

5.3.2.1.1 Results

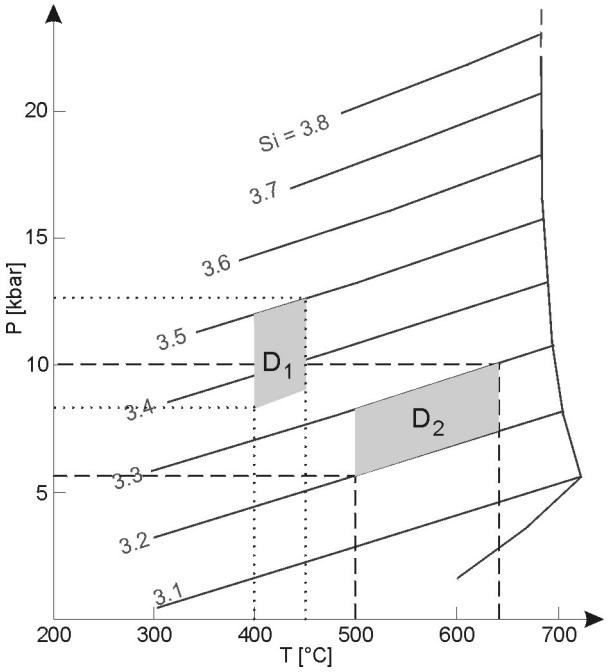

Most of the investigated white micas of the East Pelagonian Zone contain a relative homogeneous Si content between 3.2 and 3.3 pfu in average. That indicates minimum pressures between 6 and 10 kbar for the upper greenschist to amphibolite facies metamorphism during D_2 (Fig. 3.6). Maximum Si contents of 3.5 pfu are obtained from the blueschists (sample M98/43) and indicate a minimum pressure of 12.5 kbar (Fig. 3.6) for the blueschist facies event (D_1).

Fig. 3.6: Curves of constant Si content in phengites after Massonne and Schreyer (1987). Grey boxes display measured Si contents of phengites derived from the East Pelagonian Zone. D_1 = blueschist facies event; D_2 = upper greenschist to amphibolite facies event.

For D_1 maximum temperatures of ~400-450° C were assumed. This is based on investigations of Faryad and Henjes-Kunst (1997) carried out on blueschists facies rocks, which were developed contemporaneous in the Meliata unit (north of the Vardar Zone).

According to Massonne and Schreyer (1987) even vast variations of the Si content of phengite may be due to the fact that phengite often does not completely equilibrate with the matrix and retains its original composition over a long time. The presence of Fe^{2+} and Fe^{3+} as well as the exchange of Na for K lowers the Si content, whereas the presence of F tends to increase it. Based on the amount of uncertainties it is obvious that the pressure estimated by the Si content has to be treated very carefully.

5.4 Summary

Geothermobarometric investigations were only carried on samples related to the blueschist facies event (D_1) and the upper greenschist to amphibolite facies event (D_2). No suitable mineral assemblage permitting geothermobarometric investigations were found in the samples, which belong to the second Eohellenic event (D_3). This is also related to the fact, that the D_3 event did not penetrative affect the East Pelagonian zone. According to Avgerinas et al. (2001) the metamorphism during D_3 did not exceed the PT-conditions of the middle greenschist facies.

According to the geochronological, structural and petrological investigations carried out in this study the following pressure-temperature-time-deformation (PT-t-d) path (Fig. 5.7) can be drawn for the East Pelagonian Zone.

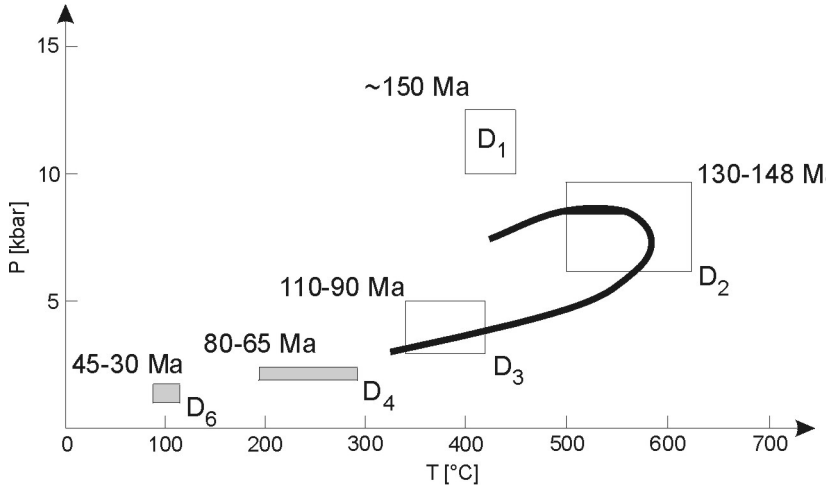

Fig. 5.7: Pressure –Temperature-time (PT-t-d) path for the East Pelagonian Zone. The timing of the different tectonometamorphic events (D_n) is based on the geochronological investigations of this study. PT conditions during D3 are from Avgerinas et al. (2001) For explanations of the path see text.

During D_1 the metamorphism reached blueschist facies conditions (T_{max} 400-450° C at P ≥ 12.5 kbar). This event is only preserved in the variegated sequence at the bottom of the allochtonous marble, which overlay the northern most part of northern Pelagonian Zone.

Upper greenschist to amphibolite facies conditions in the East Pelagonian Zone were reached during D_2. Geothermobarometric calculations gave maximum temperatures of around 550° C in the upper unit and around 600-650° C in the lower unit. However the maximum temperatures must have been below 650° C, because structures related to anatexis were not found. Minimum pressures estimated by the Si content of phengite scatter between 6 and 10 kbar.

Lower to middle greenschist facies conditions were reached during D_3. This event only affected the upper unit of the East Pelagonian Zone and the crystalline slices of the Almopias Unit (Vardar Zone).

During D_4 the deformation in the East Pelagonian Zone occurred only under brittle conditions. The temperature during D_4 must have been >190° C and <300° C, as indicated by the reseted zircon FT ages (75-65 Ma) of the upper unit (cf. 3.10.2). The zircons of the lower unit were not reseted as indicated by their higher ages between 80-86 Ma (cf. 3.7.5). In West Pelagonian Zone the metamorphism during D_4 reached middle greenschist facies conditions below 450° C (cf. 4.2).

D_5 affected only the Vardar Zone under greenschist facies conditions at the Cretaceous – Tertiary transition. Therefore D_5 is not considered in the PT-t-d path (Fig. 5.7).

Apatite FT ages between 45 and 30 Ma indicate continuos cooling below 100° C of the East Pelagonian Zone during D_6.

Especially for the metamorphic evolution during D_3 further investigations are required in the future. It is suggested to carry out these examinations in the Ano Peternik Unit (Vardar Zone), which underwent an intense tectonometamorphic overprint during D_3.

6 Interpretation and comparison of the geodynamic evolution with neighbouring regions

According to the structural, petrological and geochronological investigations carried out in this study, the following model for the geodynamic evolution of the Northern Pelagonian Zone can be drawn. Additionally, the results are compared with data that are available from other region of the Pelagonian Zone.

(1) During the Late Carboniferous (299±1 Ma, U/Pb zircon; cf. 3.2.2.2) the Pelagonian basement is intruded by granites (Fig. 6.1a and 6.2a) accompanied by compressional deformation (elongated magmatic bodies) and metamorphism of greenschist facies to (?) amphibolite facies conditions (K/Ar - white mica age 294±11 Ma).

The Late Carboniferous magmatism and metamorphism is also described from the Kaimakzalan area (Avgerinas et al., 2001) and other regions of the Pelagonian Zone: Varnountas granite, Rb/Sr-age 297±5 Ma (Koroneos et al., 1993); Kastoria granite, U/Pb zircon 302 Ma (Mountrakis et al., 1983); Pieria area, U/Pb zircon (Yardwood and Aftalion, 1976); Evia Island, U/Pb zircon 308-319 Ma (DeBono, 1998); Olympos region (Reischmann et al., 2001; Schermer et al., 1990); Ossa-Pelion area (Lips et al., 1998; Lips et al., 1999). DeBono (1998) suggests an active continental margin setting (subduction of the Paleotethyan ocean beneath Laurussia) for the emplacement of the granitoids (Fig. 6.1a). The latter is in good accordance with geochemical investigations of Anders et al. (2002)

(2) During the Late Permian and Early Triassic (~245 Ma, U/Pb zircon; cf. 3.2.2.2) the crystalline basement is again intruded by granites (Fig. 6.1b and 6.2b). They are represented by the massive intrusive bodies of the East Pelagonian Zone. Relics of accompanying metamorphism are not preserved. Despite Alpine deformation and metamorphism the cores of these bodies remained unstrained. After the granite emplacement, carbonates, clastic rocks and volcanics were deposited on the Pelagonian crystalline during Triassic to (?) Lower Jurassic time, which is indicated by $^{87}Sr/^{86}Sr$ ratios measured on Pelagonian marbles (cf. 3.4.1).

The Late Permian – Early Triassic intrusions are probably related to the final closure and subduction of the Paleo-Tethys. In the Western Pelagonian Zone the Upper Permian – Lower Triassic event is proven by Rb/Sr age determinations (248-255 Ma) on a granite by Koroneos et al. (1993).

(3) In Late Jurassic time intra-oceanic subduction (Fig. 6.1d and 6.2d) in the Vardar zone (Pamic, 2002) was accompanied by deformation (D_1) under blueschist facies conditions ($^{40}Ar/^{39}Ar$ phengite age 149±1 Ma; cf. 3.5.3). The blueschist facies assemblage is preserved at the bottom of the allochtonous marble, which superimpose the northern Pelagonian Zone (c.f. Fig. 1.3).

(4) During Late Jurassic to Early Cretaceous time (148-130 Ma; K/Ar, $^{40}Ar/^{39}Ar$ and Rb/Sr white mica and biotite ages; cf. 3.5.2, 3.5.3 and 3.6.2) oceanic crust was thrust onto the Pelagonian margins (Fig. 6.1e). This is the consequence of the closure of the oceanic basins surrounding the Pelagonian micro-continent (Vardar ocean on the eastern margin and Pindos ocean situated at the western margin; Fig. 6.1d). The progressive convergence of the Apulian and European plates resulted in the compression of the Pelagonian micro-continent (Fig. 6.1e). The accompanying metamorphism yielded upper greenschist facies to amphibolite facies conditions (T_{max} < 650° C at P_{min} 6-10 kbar; cf. 5.4). The SW-NE directed convergence of the Apulian and European plates is associated with contemporaneous movements directed to NW- NNW and SE -SSE, which is interpreted as a transpressional deformation regime. According to the structural (cf. 4.2) and geochronological data, nappe transport during Early Cretaceous occurred towards to NE.

Age determinations in the Kaimakzalan area carried out by Borsi and Ferrara (in Mercier, 1973) yielded identical Rb/Sr-muscovite and biotite ages between 140 and 134 Ma. According to Perraki et al. (2002) the PT conditions of the upper greenschist metamorphism in the Olympos-Ossa region during the Early Cretaceous orogeny reached T_{max} ~500±50° C at P ~10-11 kbar.
Eastward directed Early Eohellenic emplacement of the Pindos ophiolites onto the western Pelagonian margin is also described from the (a) Pagondas Complex ,Euboea in Eastern Greece (Robertson, 1991), (b) the Olympos area Barton (1975; 1976; 1979), (c) the Korabi Zone in W Albania (Robertson and Shallo, 2000) and (d) from the Drina-Ivanjica Zone in Serbia (Robertson and Karamata, 1994).
Contrary to this, DeBono (1998) and (Hoxha, 2001) suggest only westward emplacement of the Vardar ophiolites onto the Pelagonian micro-continent during Late Jurassic and Early Cretaceous time. Earlier westward directed emplacement of the Vardar ophiolites between 162 and 174 Ma onto the eastern most Pelagonian margin is proven by Vergely et al., (1998). The earlier closure of the Vardar basin might have triggered the westward subduction in the Pindos ocean (Robertson and Shallo, 2000). A transpressional tectonic setting is also described by Stampfli et al. (2001).

(5) A second Eohellenic event at the Early Cretaceous – Late Cretaceous transition (110-90 Ma) is related to thrusting of the Vardar ophiolites (Fig. 6.1f) in W-SW direction onto the Pelagonian Zone (K/Ar and $^{40}Ar/^{39}Ar$ white mica and biotite ages; cf. 3.5.2.2-3.5.2.3 and 3.5.3). The accompanied metamorphism did not exceed lower to middle greenschist facies conditions (cf. 4.2). This event was penetrative in the Almopias Unit, whereas the East Pelagonian Zone was only affected in the uppermost part of the upper unit. Synkinematic movements directed to SE-SSE and NW-NNW display the continuation of the transpressional regime. During this event the allochtonous Pelagonian marble was thrust onto the northern Pelagonian Zone.

Rb/Sr ages of Borsi and Ferrara (in Mercier, 1973) carried out in the Kaimakzalan area and the Almopias Unit (Vardar Zone) yield identical ages. In contrast to the northern Pelagonian Zone, the Pelagonian crystalline in the Olympos-Ossa and Pelion area was strongly affected by the Upper Eohellenic phase, eliminating most of the older structures (Schermer et al., 1990; Lips et al., 1998; Lips et al., 1999), whereas the

nappe stacking was accompanied by blueschist to greenschist facies metamorphism. According to Schermer (1990) this event marks the onset of subduction (A-type) of continental crust (Fig. 6.1f) in the Alpine orogeny.

(6) During the Campanian (~75 Ma, K/Ar white mica age; cf. 3.5.2.1) north-eastward thrusting of the West Pelagonian Zone (Fig. 6.1g and 6.2g) occurred under greenschist facies conditions. In the East Pelagonian Zone shearbands and cataclastic shear zones were developed under brittle conditions. This is also documented by the zircon FT ages (cf. 3.7.5), which indicate cooling of rocks below 240±50° C.
It is assumed that this event represents also the final emplacement of the western Pelagonian margin onto the Pelagonian crystalline. The thrusting of West Pelagonian nappes onto the east Pelagonian crystalline leads to the rejuvenation of the zircon FT ages in the upper unit of the East Pelagonian Zone.

NE directed nappe transport under blueschist to greenschist facies conditions is safely proven in the Ossa and Pelion area by (Lips et al., 1998; Lips et al., 1999). Contrary to this, Schermer (1990) suggest continuation of W to SW directed thrusting of the Vardar nappes.

Homogenous zircon FT ages around 85-70 Ma (cf. 3.7.5) obtained from the East Pelagonian Zone and the Vardar Zone in this study, strongly negate westward thrusting of Vardar nappes during Campanian time. The latter is also supported by the presence of an undisturbed clastic – carbonatic sequence (Coniac – Maastrichtian) in the Almopias unit, which overlays concordant the eastern Pelagonian continental margin (Jacobshagen, 1986).

(7) The final collision of the margin of the East Pelagonian Zone and the Vardar Zone at the Cretaceous – Tertiary transition (Fig. 6.1h) is marked by a lower greenschist facies event (K/Ar-white mica ages around 65 Ma, cf. 3.5.2.3). Nappe transport occurred towards the W to SW (cf. 4.2). The formation of the present anticlinal structure of the East Pelagonian Zone (Fig. 6.2h) was probably also developed during this time, as indicated by zircon fission track dating (cf. 3.7.5.1). Thereby the oldest zircon FT ages are obtained from the central part (lower unit), whereas the youngest ages are derived from the margins (upper unit) of the East Pelagonian Zone. This inverse zircon FT ages also clearly indicate, that the East Pelagonian Zone do not represent a metamorphic core complex. In this case the youngest ages have to be obtained from the lower unit.

In the Olympos-Ossa region this event is recorded in blueschist facies mylonites ($^{40}Ar/^{39}Ar$ white mica ages between 61 and 53 Ma (Schermer et al., 1990; Lips et al., 1998; Lips et al., 1999).

a. **Late Carboniferous - Early Permian**

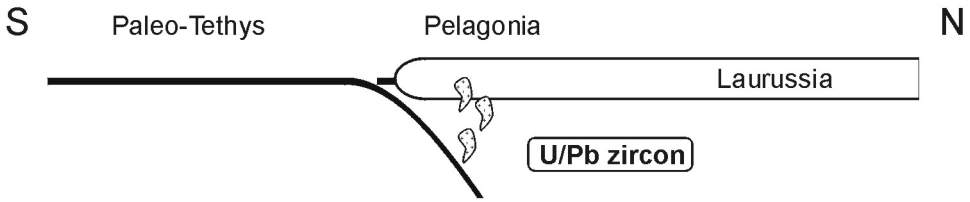

b. **Late Permian - Early Triassic**

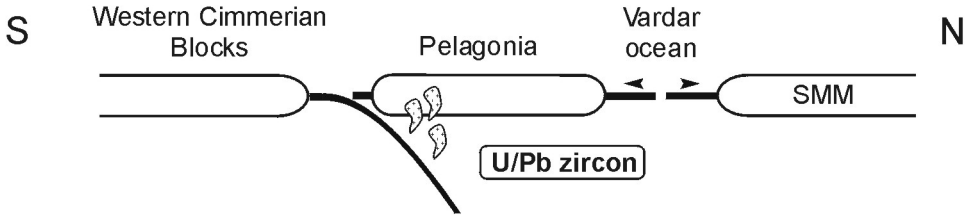

c. **Middle Jurassic**

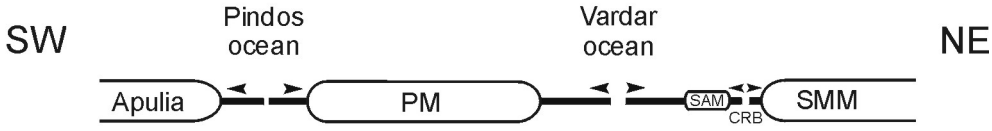

d. **Late Jurassic**

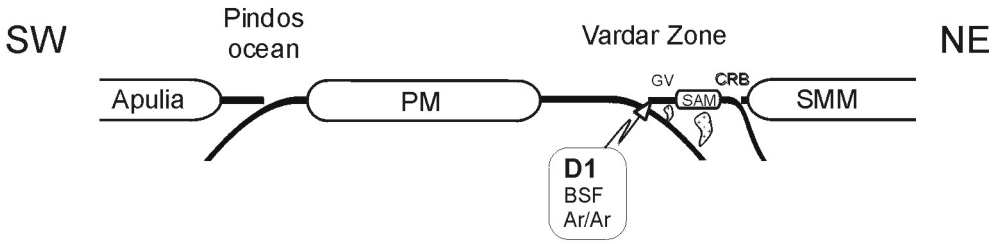

e. **Latest Jurassic - Early Cretaceous**

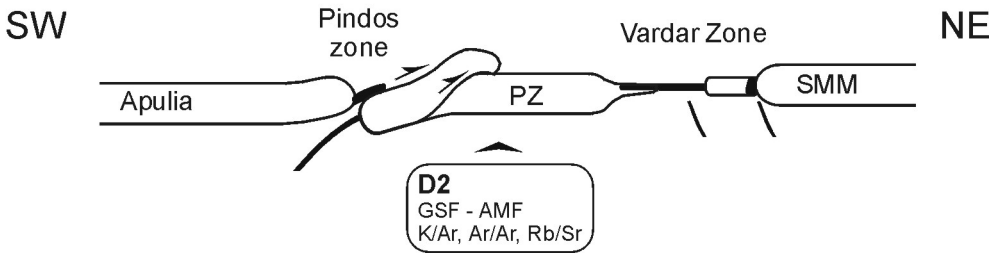

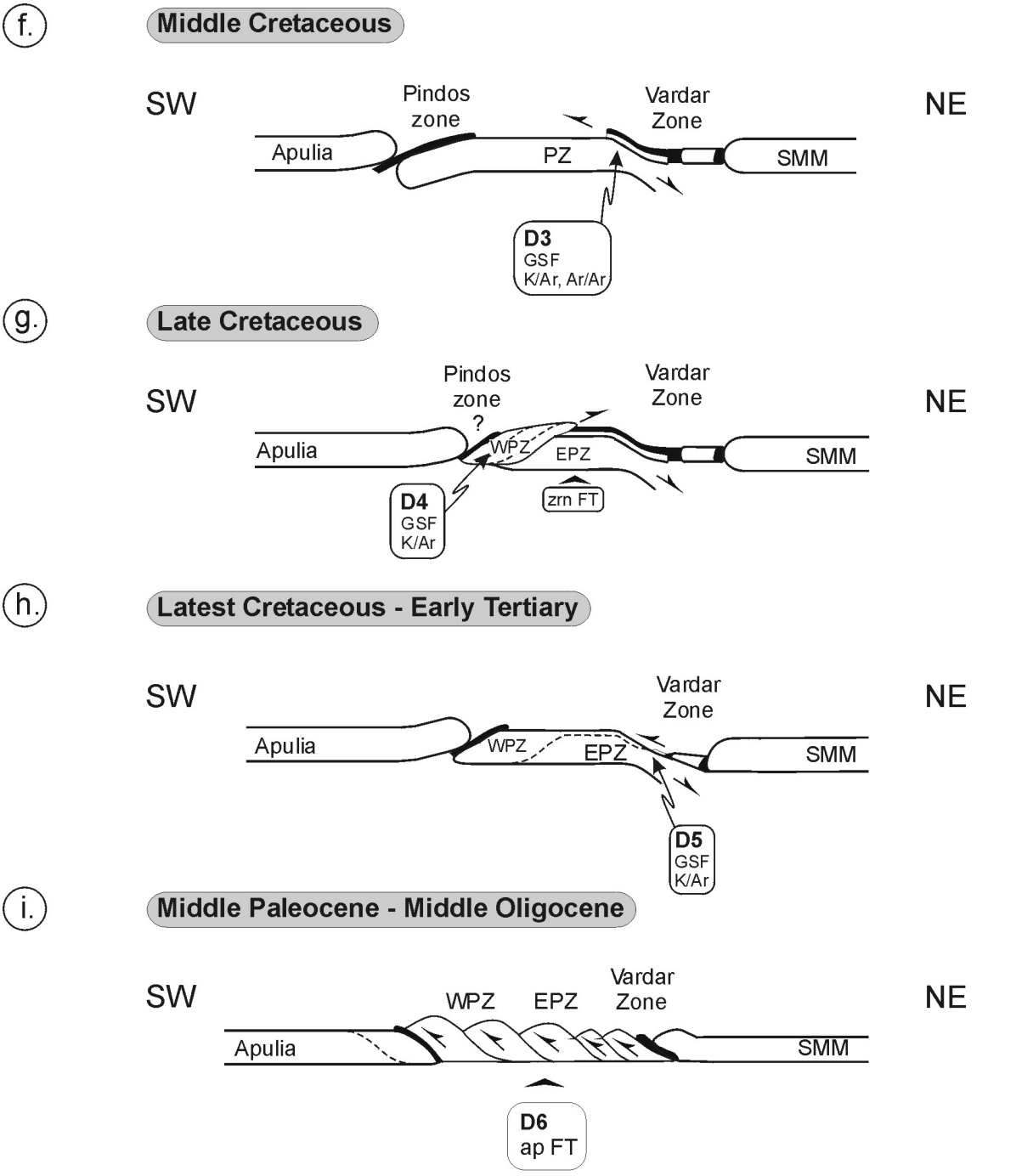

Fig. 6.1: Schematic profiles representing the geodynamic evolution of the northern Pelagonian Zone in northwestern Greece and the Republic of Macedonia in respect to the surrounding Zones. For clearness reasons the Almopias and Paikon Unit of the Vardar Zone (situated W of the Geuvguelije Unit) and Apulia was treated undifferentiated.

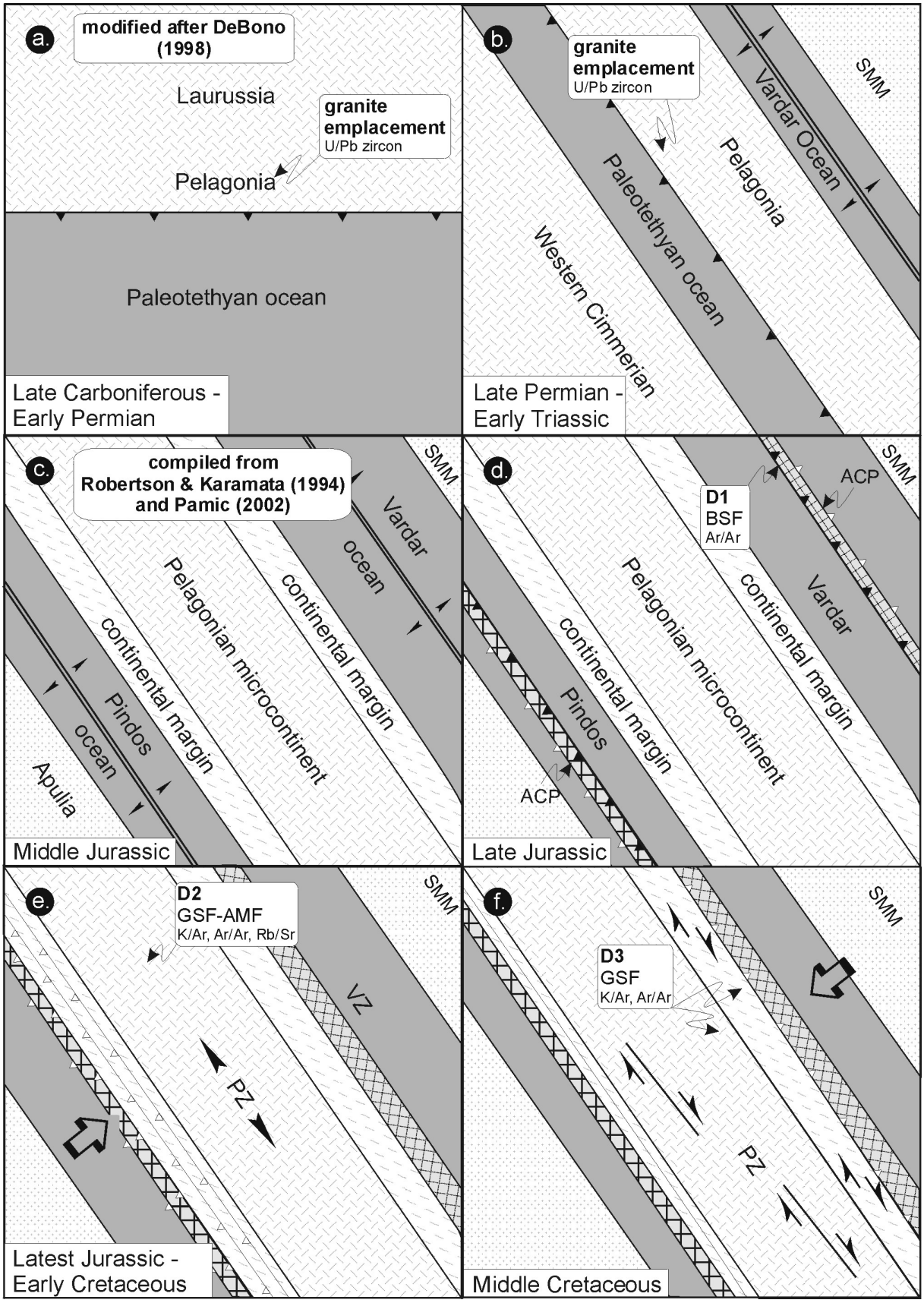
a.
modified after DeBono (1998)
Laurussia
granite emplacement
U/Pb zircon
Pelagonia
Paleotethyan ocean
Late Carboniferous - Early Permian
b.
granite emplacement
U/Pb zircon
SMM
Vardar Ocean
Pelagonia
Paleotethyan ocean
Western Cimmerian
Late Permian - Early Triassic
c.
compiled from Robertson & Karamata (1994) and Pamic (2002)
SMM
Vardar ocean
Pelagonian microcontinent
continental margin
continental margin
Pindos ocean
Apulia
Middle Jurassic
d.
D1
BSF
Ar/Ar
ACP
SMM
Vardar
Pelagonian microcontinent
continental margin
continental margin
Pindos
ACP
Late Jurassic
e.
D2
GSF-AMF
K/Ar, Ar/Ar, Rb/Sr
SMM
VZ
PZ
Latest Jurassic - Early Cretaceous
f.
D3
GSF
K/Ar, Ar/Ar
SMM
PZ
Middle Cretaceous

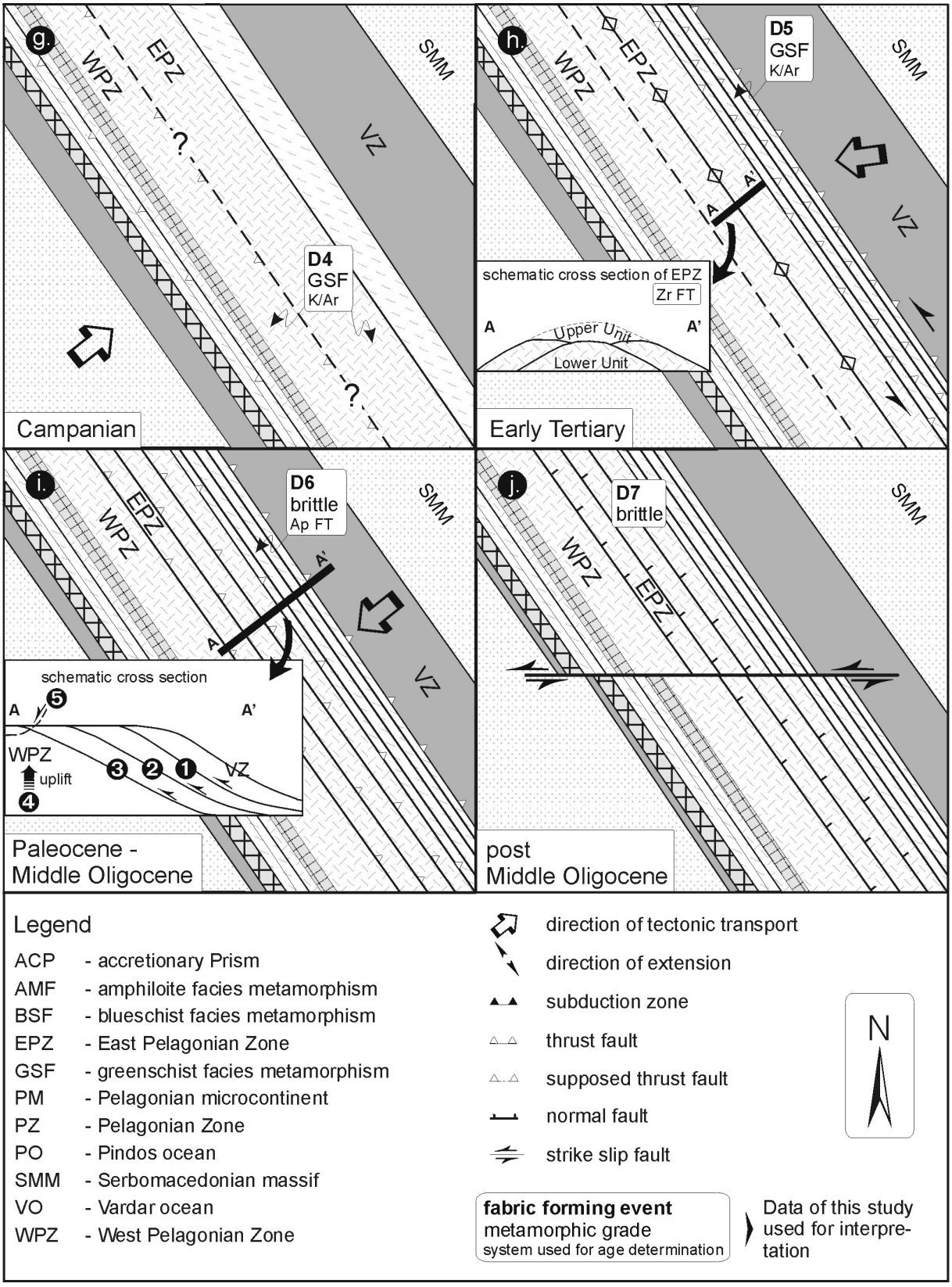

Fig. 6.2: Schematic representation of the geodynamic evolution of the northern Pelagonian Zone in north-western Greece and the Republic of Macedonia. The width as well as the orientation of the Zones are generalised schematic. For clearness reasons the Vardar Zone and Apulia was treated undifferentiated.

(8) During Late Paleocene and Middle Oligocene time the convergence between the Apulian and European plates continues. Final cooling of rocks below the 100° C isotherm (apatite FT ages; cf. 3.7.5.1) starts in the eastern Vardar Zone (Gevgeliji unit) at 60 Ma and progresses in westward direction towards to the West Pelagonian Zone (30 Ma). The structural data and apatite fission track ages indicate, that the northern Pelagonian Zone as well as the Vardar Zone represent a forward propagating thrust complex (Fig. 6.1i and 6.2i). The structure was formed as a result of a propagating master fault accompanied by piggyback transport of the hangingwall units. The exhumation of the West Pelagonian Zone during Late Eocene to Middle Oligocene time is triggered by progressive forward thrusting. As consequence the allochtonous northern Pelagonian marble was thrust westward along a low angle mylonitic detachment fault (Fig. 6.2i). The movements took place around 36 Ma (K/Ar white mica age; cf. 3.5.2.1).

In the Olympos-Ossa area westward directed nappe stacking occurred between 62 and 55 under blueschist facies and around 40 to 36 Ma under greenschist facies conditions (Lips et al., 1998; Schermer et al., 1990). Both events are also documented by the zircon FT ages of the Lower and Upper Pierien Unit of this study (cf. 3.7.5.2). In contrast to this, in the Pelion area nappe transport was directed to NE and the second event lasted until Early Miocene (Lips et al., 1999).

(9) The latest, post Middle Oligocene event is marked by the development of sinistral W-E rending strike slip faults as well as NW-SE trending normal faults, which indicate top to NE normal faulting (Fig. 6.2j). These are interpreted as being related to the exhumation of the rocks of the West Pelagonian Zone.

Apatite FT ages around 18 to 15 Ma obtained from the Olympos-Kranea area (cf. 3.7.5.2) indicate, that from Middle Miocene time on, exhumation of rocks occurred below 100° C.

7 Conclusions

Late Carboniferous to Early Permian granite emplacement in the Pelagonian basement is related to the subduction of the Paleo-Tethyan ocean. The accompanying metamorphism reached upper greenschist to lower amphibolite facies conditions. The Early Triassic opening of the Vardar ocean and formation of the Pelagonian micro-continent is associated with granite emplacements in the East Pelagonian Zone. During Triassic and Jurassic times the Pelagonian basement was overlain by a sedimentary succession (volcanics, carbonates, clastics).

The present structure of the northern Pelagonian Zone is the result of the convergence between the Apulian and European plate. During Late Jurassic to Late Tertiary times the rocks of the northern Pelagonian Zone and the adjacent Vardar Zone underwent a polyphase tectonometamorphic history (D_1-D_7).

In Cretaceous times the direction of nappe transport switches several times from NE towards the W to SW directions. The top to NE directed transport of the Pindos ophiolites onto the western Pelagonian margin during the Early Cretaceous led to intense deformation and metamorphism under upper greenschist to amphibolite facies conditions (T_{max} <650° C at P_{min} 6-10 kbars). Between 110 and 90 Ma westward thrusting of the Vardar ophiolites onto the northern Pelagonian Zone was accompanied by deformation under greenschist facies conditions. During the Late Cretaceous north-eastward nappe transport occurred under greenschist facies conditions in the West Pelagonian Zone and under semi-brittle to brittle conditions in the East Pelagonian Zone.
In contrast to this, during Tertiary times nappe transport remains stable to W-SW. The final collision of the Vardar Zone and the northern Pelagonian Zone took place in Early Paleocene. Ongoing westward thrusting led to the formation a hinterland dipping duplex during Early Eocene to Middle Oligocene time. Progressive forward thrusting is coupled with exhumation of rocks of the Vardar Zone as well as the East and West Pelagonian Zone. As a consequence, the allochtonous northern Pelagonian marble was thrust westward along a low angle detachment fault during Late Eocene. The termination of tectonically driven uplift of the Pelagonian Zone took place during the Middle Miocene.

The results of this study also point out that the northern Pelagonian Zone in north-western Greece and the Republic of Macedonia does not form a metamorphic core complex like the tectonic windows (Olympos-Ossa, Kranea, Pelion) exposed in the southern Pelagonian Zone. The present day structure is a large NNW-SSE trending anticline, established during Early Tertiary times, which is overprinted by the later westward propagating thrust complex. Also in contrast to the southern Pelagonian Zone nearly all movements during Tertiary took place under brittle conditions.

In addition the geochronological data of this study show no hint for the presence of Proterozoic rocks within the East Pelagonian Zone.

8 References

Anders, B., T. Reischmann and U. Poller (2002): Geochemistry and geochronology of basement rocks from the Pelagonian Zone, Greece. - Geochimica et Cosmochimica Acta, sepcial supplement **66/15A**: A19.

Anderson, D. E. and G. R. Buckley (1973): Zoning in garnets - diffusion models. - Contributions to Mineralogy and Petrology **40**: 87-104.

Arsovski, M. and N. Dumurdzanov (1984): Recent findings of the structure of the Pelagonian anticlinorium and its relation with the Rhodopean and Serbian - Macedonian Massif. - Geologica Macedonica **sep.**

Arsovski, M., N. Dumurdzanov, S. Hristov, T. Ivanov, V. Ivanova, P. Petkovski and R. Stojanov (1977): Correlation of the Pre-Cambrian complexes of the Pelagonian Massif, Vardar Zone and Serbo-Macedonian massif. - Proceedings of the Colloquium on the Geology of the Aegean Region **6/2**: 549-557.

Aubouin, J. (1959): Contribution à l`étude géologique de la Gréceseptentrionale: le confins de l`Epire de la Thessalie. - Annales géologiques des pays helléniques **10**: 1-484.

Aubouin, J., M. Bonneau, J. Davidson, P. Leboulenger, S. Matesco and A. Zambetakis (1976): Esquisse structurale de l`Arc égéen externe des Dinarides aux Taurides. - Bulletin de la Société Géologique de France **7/2**: 327-336.

Aubouin, J., J. H. Brunn, P. Celet, J. Dercourt, J. Godfriaux and J. Mercier (1963): Esquisse de la géologie de la Grèce. - Livre Mémoire Paul Fallot **2**: 283-610.

Avgerinas, A., A. Kilias, A. Koronaios, D. Mountrakis, W. Frisch, I. Dunkl and T. Most (2001): Cretaceous structural evolution of the Pelagonian crystalline in western Voras Mt. (Macedonia, Northern Greece). - Deltio tes Ellenikes Geologikes Etaireias = Bulletin of the Geological Society of Greece **34/1**: 129-136.

Baroz, F., J. Bebien and M. Ikenne (1987): An example of high-pressure low-temperature metamorphic rocks from an island-arc: the Paikon Series (Innermost Hellenides, Greece). - Journal of Metamorphic Geology **5/4**: 509-527.

Barton, C. M. (1975): Mount Olympos, Greece: new light on an old window. - Journal of the Geological Society of London **131**: 389-396.

Barton, C. M. (1976): The tectonic vector and emplacement age of an allochthonous basement slice in the Olympos area, N.E. Greece. - Bulletin de la Société Géologique de France **7/XVIII**: 253-258.

Barton, C. M. (1979): Structural evolution of the Vadar root zone, nothern Greece: Discussion and reply. - Geological Society of America **90/1**: 125-128.

Borsi, S., G. Ferrara, J. Mercier and E. Tongiorgi (1966): Age stratigraphique et radiometrique jurassique superieur d'un granite des zones internes des Hellenides (granite de Fanos, Macedoine, Grece)Translated Title: Stratigraphic and upper Jurassic radiometric age of a granite of the interior zones of the Hellenides. - Revue de geographie physique et de geologique **2/4**: 279-287.

Bortolotti, V., M. Marroni, L. Pandolfi, G. Principi and E. Saccani (2002): Interaction between Mid-Ocean Ridge and Subduction Magmatism in Albanian Ophiolites. - Journal of Geology **110**: 561-576.

Brunn, J. H. (1956): Contribution à l`étude géologique du Pinde septentrionale et d`une partie de la Macédoine occidentale. - Annales géologiques des pays helléniques **I/7**: 1-358.

Bucher, K. and M. Frey (1994): Petrogenesis of Metamorphic Rocks. -Springer Verlag: pp. 318

Burke, W. H., R. E. Denison, E. A. Hetherington, R. B. Koepnick, H. F. Nelson and J. B. Otto (1982): Variation of seawater $^{87}Sr/^{86}Sr$ throughout Phanerozoic time. - Geology **10**: 516-519.

Cameron, A. E., D. E. Smith and R. L. Walker (1969): Mass spectromerty of nanogram size samples of lead. - Anal. Chem. **41**: 525-526.

Carmichael, I. S. E. (1967): The iron-titanium oxides of salic volcanic rocks and their associated ferromagnesian silicates. - Contributions to Mineralogy and Petrology **14**: 36-64.

Carpéna, J. (1992): Fission track dating of zircon: zircons from Mont Blanc granite (French-Italian Alps). - Journal of Geology **100**: 411-421.
Cathelineau, M. (1988): The chlorite and illite geothermometers. - Chemical Geology **70/1-2**: 182.

Celet, P. and J. Ferriere (1978): Les Hellenides internes: Le Pelagonien. - Eclogae geologicae Helvetiae **73/467-495**.

Chen, F., E. Hegner and W. Todt (2000): Zircon ages and Nd isotopic and chemical compositions of orthogneisses from the Black forest, Germany: evidence for a Cambrian magmatic arc. - International Journal of Earth Sciences **88/88**.

Crawford, M. L. (1977): Calcium zoning in almandine garnet, Wissahickon formation, Philadelphia, Pennsilvania. - Canadian Mineralogist **15**: 243-249.

Crowley, K. D., A. E. Cameron and R. L. Schaefer (1991): Experimental studies of annealing of etched fission tracks in flourapatite. - Geochimica et Cosmochimica Acta **55**: 1449-1465.

Dalrymple, G. B. and M. A. Lanphere (1969): Potassium - argon dating. - Freeman and company: pp.259.

Dalrymple, G. B. and M. A. Lanphere (1974): $^{40}Ar/^{39}Ar$ age spectra of some undisturbed terrestrial samples. - Geochimica et Cosmochimica Acta **38**: 715-738.

DeBono, A. (1998): Pelagonian margins in central Evia island (Greece). Stratigraphy and geodynamic evolution. Doctoral Université de Lausanne: pp. 114

DeBono, A., S. Cirilli, D. Vachard, I. Vavassis and G. M. Stampfli (1999): The Liri unit: An external unit at the base of the Pelagonia terrane in Central Evia island. Evidence for a Paleotetyan suture in the hellenides. - Terra abstracts **4**: 314.

Deleon, G. (1966): translated title: Isotopic age of granitic rocks of Pelagonia and western Macedonia. - Ref. VI. Colloqium of Jugoslavian Geologists, Ohrid.

Dempster, T. J. (1985): Garnet zoning and and metamorphism of the barrovian type area, Scotland. - Contrib. Mineral. Petrol. **89**: 30-38.

Dodson, M. (1973): Closure temperature in cooling geochronological and petrological systems. - Contributions to Mineralogy and Petrology **40**: 259-274.

Donelick, R. A., R. A. Ketcham and W. D. Carlson (1999): Variabillity of apatite fission-track annealing kinetics: II. Crystallographic orientation effects. - American Mineralogist **84**: 1224-1234.

Dumitru, T. A. (1993): A new computer-automated microscope stage system for fission-track analysis. - Nucl. Tracks Radiat. Meas. **21**: 575-580.

Dumurdzanov, N. (1985): Petrogenic characteristics of the high metamorphic and magmatic rocks of the central and western part of Selecka Mountain, SR Macedonia. - Geologica Macedonica **2**: 173-220.

Dumurdzanov, N. (1988): Devonian magmatic rocks in West Macedonian Zone (SR Macedonia - Yugoslavia). - Geologica Macedonica **T3/1**: 57-78.

Dunkl, I. (2002): TRACKKEY: a windows program for calculation and graphical presentation of fission track data. - Computers and Geosciences **28/2**: 3-12.

Dunlap, W. J. (2000): Nature´s diffusion experiment: The cooling-rate cooling age correlation. - Geology **28/2**: 139-142.

Elias, J. (1998): The thermal history of the Ötztal-Stubai complex (Tyrol, Austria/Italy) in the light of the lateral extrusion model. - Tübinger Geowissenschaftliche Arbeiten, Reihe A **42**: pp. 172.

Faryad, S. W. and F. Henjes-Kunst (1997): Petrolgic and geochronologic constraints on the tectonometamorphic evolution of the Meliata unit blueschists, Western Carpathians (Slovakia). - Mineralia Slovaca: pp.145-145.

Faupl, P., K. Petrakakis, G. Migiros and A. Pavlopoulos (2002): Detrital blue amphiboles from the western Othrys Mountain and their relationship to the blueschist terrains of the Hellenides (Greece). - International Journal of Earth Sciences **91/3**: 433-444.

Faure, G. (1986): Principiles of Isotope Geology. - John Wiley & Sons: pp.589.

Ferry, J. M. and F. S. Spear (1978): Experimental calibration of the partitioning of Fe and Mg between biotite and garnet. - Contributions to Mineralogy and Petrology **66/2**: 113-117.

Fleck, R. J., J. F. Sutter and D. H. Elliot (1977): Interpretation of discordant $^{40}Ar/^{39}Ar$ age spectra of Mesozoic tholeiites from Antarctica. - Geochimica et Cosmochimica Acta **41**: 15-32.

Foster, M. D. (1960): Interpretation of the composition of trioctahedral micas. - U.S. Geological Survey, Professional paper **354-B**: 24-29.

Foster, M. D. (1962): Interpretation of the composition and a classification of the chlorites. - U.S. Geological Survey, Professional paper **414/A**: pp. 22.

Geyh, M. A. and H. Schleicher (1990): Absolute age determination. - Springer Verlag: pp.503.

Gleadow, A. J. W., I. R. Duddy, P. F. Green and J. F. Lovering (1986): Confined fission track length in apatite: a diagnostic tool for thermal history analyses. - Contributions to Mineralogy and Petrology **94**: 405-415.

Gleadow, A. J. W., I. R. Duddy and J. F. Lovering (1983): Fission track analysis: a new tool for the evaluation of thermal histories and hydrocarbon potential. - Aust. Petrol. Explor. Assoc. J. **23**: 93-102.

Gleadow, A. J. W., A. J. Hurford and R. D. Quaife (1976): Fission track dating of zircon: improved etching techniques. - Earth and Planetary Science Letters **33**: 273-276.

Godfriaux, J. (1962): Sur la présence de l` Eocène dans les calcaires supérieur de l` Olympe (Thessalie septentrionale, Grèce). - Bulletin Sociéte Geoloqique France **VII/4**: 49-54.

Green, P. F., I. R. Duddy, A. J. W. Gleadow, P. R. Tingate and G. M. Laslett (1986): Thermal annealing of fission tracks in apatite: 1. A quantitative description. - Chemical Geology **59**: 237-253.

Green, P. F., I. R. Duddy, G. M. Lasslett, K. A. Hegarty, A. J. W. Gleadow and J. F. Lovering (1989): Thermal annealing of fission tracks in apatite. - Chemical Geology **79**: 155-182.

Green, T. H. and P. L. Hellman (1982): Fe-Mg partitioning between coexisting garnet and phengite at high pressure, and comments on a garnet-phengite geothermometer. - Lithos **15/4**: 253-266.

Grove, M. and T. M. Harrison (1996): $^{40}Ar^*$ diffusion in Fe-rich biotite. - American Mineralogist **81**: 940-951.

Hammerschmidt, K. and E. Frank (1991): Relics of high pressure metamorphism in the Lepontine Alps (Switzerland) - $^{40}Ar/^{39}Ar$ and microprobe analyses on white mica. - Schweizerische Mineralogische und Petrographische Mitteilungen **71**: 261-274.

Hanchar, J. M. and C. F. Miller (1993): Zircon zonation patterns as revealed by cathodoluminescence and backsacattered electron images: Implications for interpretation of complex crustal histories. - Chemical Geology **110**: 1-13.

Hanchar, J. M. and R. L. Rudnick (1995): Revealing hidden structures: The application of cathodoluminescence and back-scattered electron imaging to dating zircons from lower crustal xenoliths. - Lithos **36**: 289-303.

Hanna, G. C., C. H. Wescott, H. D. Lemmel, B. R. Leonard, J. S. Story and P. M. Attree (1969): Revision of values for the 2200 m/s neutron constants for four fissile nuclides. - Atom. Energ. Rev. **7**: 3-92.

Harper, C. T. (1970): Graphical solutions to the problem of radiogenic Argon-40 loss from metamorphic minerals. - Eclogae geologicae Helvetiae **63/1**: 119-140.

Harrison, T. M., I. Duncan and I. McDougall (1985): Diffusion of $^{40}Ar^*$ in biotite: Temperature, pressure and compositional effects. - Geochimica et Cosmochimica Acta **49**: 2461-2468.

Hey, M. H. (1954): A new review of the chlorites. - Mineralogical Magazine **30**: 277-292.

Hodges, K. V. and F. S. Spear (1982): Geothermometry, geobarometry and the Al_2SiO_5 triple point at Mt. Moosilauke, New Hampshire. - American Mineralogist **67**: 1118-1134.

Hoinkes, G. (1986): Effect of grossular content in garnet on the partitioning of Fe and Mg between garnet and biotite. - Contributions to Mineralogy and Petrology **92**: 393-399.

Hollister, L. S. (1966): Garnet zoning: an interpretation - based on the Rayleigh fractionation model. - Science **154**: 1642-1651.

Hoxha, L. (2001): The Jurassic-Cretaceous orogenic event and its effects in the exploration of sulphide ores, Albanian ophiolites, Albania. - Eclogae geologicae Helvetiae **94**: 339-350.

Hurford, A. J. (1986): Cooling and uplift patterns in the Lepontine Alps South Central Switzerland and age of vertical movement on the Insubric fault line. - Contributions to Mineralogy and Petrology **92**: 413-427.

Hurford, A. J., M. Flisch and E. Jäger (1989): Unravelling the thermo-tectonic evolution of the Alps: a contribution from fission track analysis and mica dating. - Geological Society Special Publication **45**: 369-398.

Hurford, A. J. and P. F. Green (1983): The zeta callibration of fission-track dating. - Isotope Geoscience **1**: 285-317.

Hurford, A. J. and K. Hammerschmidt (1985): $^{40}Ar/^{39}Ar$ and K/Ar dating of the Bishop and Fish Canyon Tuffs: calibration ages for fission track standards. - Chemical Geology **58**: 23-32.

Hurford, A. J. and R. T. Watkins (1987): Fission track age of the tuffs of the Buluk Member, Bakate Formation, Northern Kenya: A suitable fission-track age standard. - Chemical Geology **66**: 209-216.

Hurley, P. M., H. Hughes, W. H. Pinson and H. W. Fairbairn (1962): Radiogenic argon and strontium diffusion parameters in biotite at low temperatures obtained from Alpine fault uplift in New Zealand. - Geochimica et Cosmochimica Acta **26**: 67-80.

Hynes, A. and R. C. Forest (1988): Empirical garnet-muscovite geothermometry in low-grade metapelites, Selwyn Range (Canadian Rockies). - Journal of Metamorphic Geology **6/3**: 297-309.

Indares, A. and J. Martignole (1985): Biotite-garnet geothermometry in the granulite facies: the influence of Ti and Al in biotite. - American Mineralogist **70**: 272-278.

Jacobshagen, V. (1986): Geologie von Griechenland. - Beiträge zur regionalen Geologie der Erde. **19**, Geb. Bornträger: pp.363.

Jacobshagen, V., S. Dürr, F. Kockel, K. O. Kopp and G. Kowalczyk, Eds. (1978): Structure and Geodynamic Evolution of the Aegean Region. Alps, Apennines, Hellenides.

Jaffrey, A. H., K. F. Flynn, L. E. Glendenin, W. C. Bentley and A. M. Essling (1973): Precision measurements of half-lives and specific activities of ^{235}U and ^{238}U. - Phys. Rev. Sect. C, Nucl. Phys. **4**: 1889-1906.

Jäger, E. (1973): Die alpine Orogenese im Lichte der radiometrischen Altersbestimmung. - Eclogae geologicae Helvetiae **66**: 11-21.

Jäger, E., E. Niggli and E. Wenk (1967): Rb/Sr Altersbestimmungen an Glimmern der Zentralaplen. - Beiträge zur geologischen Karte der Schweiz N.F. **134**: pp. 67.

Jenkin, G. R. T., R. M. Ellam, G. Rogers and F. M. Stuart (2001): An investigation of closure temperature of Rb-Sr biotite system: The importance of the cation exchange. - Geochimica et Cosmochimica Acta **65/7**: 1141-1160.

Jenkin, G. R. T., G. Rogers, A. E. Fallick and C. M. Farrow (1995): Rb-Sr closure temperatures in bi-mineralic rocks: a mode effect and test for different diffusion models. - Chemical Geology **122**: 227-240.

Jowett, E. G. (1991): Fitting iron and magnesium into the hydrothermal chlorite geothermometers. - Geological Society of Canada, Abstracts with Programs **16**: 62.

Ketcham, R. A., R. A. Donelick and W. D. Carlson (1999): Variabillity of apatite fission-track annealing kinetics: III. Extrapolation of geological time scales. - American Mineralogist **84**: 1235-1255.

Ketcham, R. A., R. A. Donelick and M. B. Donelick (2000): AFTSolve: A program for multi-kinetic modelling of apatite fission-track data. - Geological Materials Research **2/1**: 1-32.

Kilias, A., H. Fassoulas, M. Priniotakis, A. Sfeikos and W. Frisch (1991): Deformation and HP/LT metamorphic conditions at the tectonic window of Kranea (W. Thessaly, Nothern/Central Greece). - Zeitschrift deutsche Geologische Gesellschaft **142**: 87-96.

Kilias, A. and D. Mountrakis (1985): Das "Rizomata-Fenster" im nordoestlichen Pieria-Gebirge; Neue Daten zur geologischen Grenze der Pelagonischen und der Axios-Zone in Griechenland. - Neues Jahrbuch für Geologie und Palaeontologie, Monatshefte **4**: 248-256.

Kirschner, D. L., C. Hunziker and M. Cosca (1996): Closure temperatures of argon in micas; a review and reevaluation based on Alpine samples. - Geological Society of America, Abstracts with Programs **28/7**: 441.

Kockel, F., H. Mollat and H. W. Walther (1977): Erlaeuterungen zur Geologischen Karte der Chalkidhiki und angrenzender Gebiete, 1:100 000 (Nord-Griechenland). - Bundesanst. fuer Geowiss. und Rohst.. Hanover, Federal Republic of Germany: pp. 119.

Koroneos, A., G. Christofides, A. del Moro and A. Kilias (1993): Rb-Sr geochronology and geochemical aspects of the Eastern Varnountas plutonite (NW Macedonia, Greece). - Neues Jahrbuch für Mineralogie, Abhandlungen **165/3**: 297-315.

Kossmat, F. (1924): Geologie der zentralen Balkanhalbinsel. - Die Kriegschauplätze 1914-1918 geologisch dargestellt. **12**, Gebrüder Bornträger: pp.198.

Kramar, N., M. Cosca and C. Hunziker (2001): Heterogeneous $^{40}Ar^{*}$ distribution in naturally deformed muscovite: in situ UV-laser ablation evidence for microstructurally controlled intragrain diffusion. - Earth and Planetary Science Letters. **192**: 377-388.

Kretz, R. (1983): Symbols for rock forming minerals. - American Mineralogist **68**: 277-279.

Krogh, E. J. and A. Raheim (1978): Temperature and pressure dependence of Fe-Mg partitioning between garnet and phengite, with particular reference to eclogites. - Contributions to Mineralogy and Petrology **66/1**: 75-80.

Laird, J. (1988): Chlorites; metamorphic petrology. - Reviews in Mineralogy **19**: 405-453.

Laslett, G. M., P. F. Green, I. R. Duddy and A. J. W. Gleadow (1987): Thermal annealing of fission tracks in apatite. - Chemical Geology **65**: 1-13.

Le Pichon, X. and J. Angelier (1979): The Hellenic Arc and trench system: a key to the neotectonic evolution of the eastern Mediterranean. - Tectonics **60**: 1-42.

Lee, J. K. W., T. C. Onstott, K. V. Cashman, R. J. Cumbest and D. Johnson (1989): Incremental heating of hornblende in vacuo: Implications for $^{40}Ar/^{39}Ar$ geochronology and interpretation of thermal histories. - Geology **19**: 872-876.

Lips, A. L. W., S. H. White and J. R. Wijbrans (1998): $^{40}Ar/^{39}Ar$ laserprobe direct dating of discrete deformational events; a continueous record of early Alpine tectonics in the Pelagonian Zone, NW Aegean area, Greece. - Tectonophysics **298/1-3**: 133-153.

Lips, A. L. W., S. H. White and J. R. Wijbrans (1999): New insights from $^{40}Ar/^{39}Ar$ laserprobe dating of white mica fabrics from the Pelion Massif, Pelagonian Zone, Internal Hellenides, Greece: implications for the timing of metamorphic episodes and tectonic events in the Aegean region. - Geological Society of America, Special Publications **156**: 457-474.

Ludwig, K. R. (1988): Pbdat for MS-Dos - a computer program for IBM-PC compatibles for processing raw Pb-U-Th isotope data., United States Geological Survey. **88:** 37.

Ludwig, K. R. (2001): Isoplot/Ex rev. 2.49, a geochronological toolkit for Microsoft ECXEL. Berkeley Geochronology Center, Special Publications. Berkeley**:** pp. 55.

Massonne, H. J. and W. Schreyer (1987): Phengite geobarometry based on the limiting assemblage with K-feldspar, phlogopite and quartz. - Contributions to Mineralogy and Petrology **96**: 212-224.

Mattinson, J. M. (1994): A study of complex discordance in zircons using step-wise dissolution techniques. - Contributions to Mineralogy and Petrology **116**: 117-129.

McDougall, I. and T. M. Harrison (1988): Geochronology and Thermochronology by the $^{40A}r/^{39}Ar$ Method. - Oxford Monographs on Geology and Geophysics **9**, Oxford University Press: pp.212.

McDowell, F. W. and R. P. Keizer (1977): Timing of mid-Tertiary volcanism in the Sierra Madre Occidental between Durango city and Mazatlan, Mexico. - Geological Society of America Bulletin **88**: 1479-1487.

Medwenitsch, W. (1956a): Die Stellung der Pelagoniden in der Grenze von N- und -S Dinariden von Dinariden (s. str.) und Helleniden. - Bulletin L´Instute Geologie Republique Macédnonie **5**: 251-267.

Medwenitsch, W. (1956b): Die tektonische Stellung der Pelagoniden im Raume der Dinariden. - Berg und Hüttenmännischen Monatshefte **101/2**: Seperata.

Medwenitsch, W. (1956c): Zur Geologie Vardarisch-Makedoniens (Jugoslawien), zum Problem der Pelagoniden. - Österreichische Akademie der Wissenschaften, Sitzungsberichte der mathematisch naturwissenschaftlichen Klasse, Abteilung 1. **165/1-10**: 397-473.

Mercier, J. (1973): Contibution a l`étude du métamorphisme et l`évolution magmatique des zones internes des Hellénides. - Annales géologiques des pays helléniques **T. XX-1968**: 599-792.

Meulenkamp, J. E., M. J. R. Wortel, W. A. Van Wamel, W. Spakman and E. Hoogerduyn Starting (1988): On the Hellenic subduction zone and the geodynamic evolution of Crete since the late middle Miocene. - Tectonophysics **146**: 203-215.

Mountrakis, D. (1984): Structural evolution of the Pelagonian Zone in northwestern Macedonia, Greece. - Geological Society of Greece, Special Publications **17**: 581-590.

Mountrakis, D., E. S. Sapountzis, A. Kilias, G. Eleftheriadis and G. Christofides (1983): Paleogeographic conditions in the western Pelagonian margin in Greece during the initial rifting of the continental area. - Canadian Journal of Earth Sciences = Journal Canadien des Sciences de la Terre. **20/11**: 1673-1681.

Mposkos, E., D. K. Kostopoulos and A. Krohe (2001): Low-P / high-T pre-Alpine metamorphism and medium alpine overprint of the Pelagonian Zone documented in high-alumina metapelites from the Vernon massif, western Macedonia, Northern Greece. - Deltio tes Ellenikes Geologikes Etaireias = Bulletin of the Geological Society of Greece **XXXIV/3**: 949-958.

Naeser, C. W. (1967): The use of apatite and sphene for fission-track age determinations. - Bulletin Geological Society of America **78**: 1523-1526.

Naeser, C. W. and H. Faul (1969): Fission track annealing in apatite and sphene. - Journal of geophysical Research **74**: 705-710.

Pamic, J. (2002): The Sava-Vardar Zone of the Dinarides and Hellenides versus the Vardar Ocean. - Eclogae geologicae Helvetiae **95**: 99-113.

Parrish, R. P. (1987): An improved micro-capsule for zircon dissolution in U-Pb geochronology. - Chemical Geology **66**: 99-102.

Perchuk, L. L. and I. V. Lavrent'eva (1983): Experimental investigation of exchange equilibria in the system cordierite-garnet-biotite. In: Kinetics and equilibrium in mineral reactions. S. K. Saxena (Ed.). New York, Springer**:** 199-239.

Perraki, M., E. Mposkos, G. Hoinkes and A. Orfanoudaki (2002): Amphibole zonation in glaucophane schist, epidote-amphibolites and albite gneisses as a guide to the metamorphic evolution of the Pelagonian Zone, NE Thessaly, Greece. - Geologica Carpathica **53**: 164-165.

Phillipson, A. (1896): Reisen und Forschungen in N-Griechenland. - Zeitschrift für Geschichte und Erdkunde, Berlin **31**: 193-249.

Phillipson, A. (1898): La tectonique de L`Edéide. - Annual Géographie **7**: 117-141.

Poller, U., V. Liebetrau and W. Todt (1997): U-Pb single-zircon dating under cathodoluminescence control (CLC-method): application to polymetamorphic orthogneisses. - Chemical Geology **139**: 287-297.

Pownceby, M. I., V. J. Wall and H. S. C. O'Neill (1987): Fe-Mn partitioning between garnet and ilmenite: experimental calibration and applications. - Contributions to Mineralogy and Petrology **97**: 116-126.

Price, P. B. and R. M. Walker (1963): Fossil tracks of charged particles in mica and the age minerals. - Journal of Geophysical Research, B, Solid Earth and Planets **68**: 4847-4862.

Purdy, J. W. and E. Jäger (1967): K/Ar ages on rock-forming minerals from the Central Apls. - Mem. 1st. Geol. Mineral. Univ. Padova **30**: pp. 32.

Reed, S. J. B. (1993): Electron microprobe analysis. - **XVIII**, Cambridge Universal Press: pp.326.

Reed, S. J. B. (1996): Electron microprobe analysis and scanning electron microscopy in geology. - **XII**, Cambridge Universal Press: pp.201.

Reischmann, T., D. K. Kostopoulos, S. Loos, B. Anders, A. Avgerinas and S. A. Sklavounos (2001): Late Paleozoic magmatism in the basement rocks southwest of Mt. Oplympos, Central Pelagonian zone, greece: A Permo-Carboniferous magmatic arc. - Deltio tes Ellenikes Geologikes Etaireias = Bulletin of the Geological Society of Greece **34/3**: 985-993.

Renz, C. (1940): Die Tektonik der griechischen Gebirge. - Pragm. Akad. Athen. **8**: 1-171.

Robertson, A. and M. Shallo (2000): Mesozoic-Tertiary tectonic evolution of Albania in its regional Eastern Mediterranean context. - Tectonophysics **316**: 197-254.

Robertson, A. H. F. (1991): Origin and emplacement of an inferred late Jurassic subduction-accretion complex, Euboea, eastern Greece. - Geological Magazine **128/1**: 27-41.

Robertson, A. H. F. and S. Karamata (1994): The role of subduction-accretion processes in the tectonic evolution of the Mesozoic Tethys in Serbia. - Tectonophysics **234**: 73-94.

Roddick, J. C., R. A. Cliff and D. C. Rex (1980): The evolution of excess argon in alpine biotites - a $^{40}Ar/^{39}Ar$ analysis. - Earth and Planetary Science Letters **48**: 185-208.

Rutherford, E. (1906): Radioactive transformations. New York.

Ryburn, R. J., A. Raheim and D. H. Green (1976): Determination of the P, T paths of natural eclogites during metamorphism - record of subduction. - Lithos **9**: 161-164.

Schermer, E. R. (1990): Mechanisms of blueschist creation and preservation in an A-type subduction zone, Mt. Olympos region, Greece. - Geology. **18**: 1130-1133.

Schermer, E. R. (1992): Geometry and kinematics of continental basement deformation during alpine orogeny, Mt. Olympos region, Greece. - Journal of Structural Geology **15/3-5**: 571-591.

Schermer, E. R., D. R. Lux and B. C. Burchfiel (1990): Temperature-time history of subducted continental crust, Mt. Olympos region, Greece. - Tectonics. **9/5**: 1165-1195.

Schliestedt, M. (1980): Phasengleichgewichte in Hochdruckgesteinen von Sifnos, Griechenland. Unpublished Diss., TU Braunschweig: pp. 143.

Schulze, P. (1992): Petrogenese des metamorphen Grundgebirges der zentralen Heimefrontfjella (westliches Dronning Maud Land, Antarktis). - Berichte zur Polarforschung / Alfred-Wegener-Institut für Polar- und Meeresforschung. **VII/117**: 321 S.

Seward, D. (1993): Fission-track analysis with special respect to uplift/cooling histories of mountain belts. - In: R. Funiciello, C. A. Ricci and V. Trommsdorff: Radiometric age determinations in orogenic processes - potentials and limits., Sienna **1**:149-166

Sfeikos, A. (1992): Geology, analysis of Deformation and kinematics of the Pelagonian nappe system, Kamvounia mountains (North Thessaly, Greece). - Tübinger Geowissenschaftliche Arbeiten, Reihe A **12**: 110.

Smith, A. G. (1993): Tectonic significance of Hellenic-Dinaric ophiolites. - Geological Society of London, Special Publications **76**: 213-243

.

Snee, L. W., J. F. Sutter and W. C. Kelly (1988): Thermochronology of economic mineral deposits: dating the stages of mineralization at Panasquiera, Portugal, by high precision $^{40}Ar/^{39}Ar$ age spectrum techniques on muscovite. - Economic Geology **83**: 335-354.

Spakman, W., M. J. R. Wortel and N. J. Vlaar (1988): The Hellenic subduction zone: a tomographic image and its geodynamic implications. - Geophysical Research Letters **15**: 60-63.

Spear, F. S. (1995): Metamorphic phase equilibria and pressure-temperature-time paths. - Monograph Series Mineralogical Society of America: pp. 799.

Stacey, J. S. and J. D. Kramers (1975): Approximation of terrestrial lead isotope evolution by a two-stage model. - Earth and Planetary Science Letters. **26**: 207-221.

Stampfli, G. M., G. Borel, W. Cavazza, J. Mosar and P. A. Ziegler (2001): The paleotectonic atlas of the PeriTethyan Domain., European Geophysical Society.

Steck, A. and C. Hunziker (1994): The tertiary structural and thermal evolution of the Central Alps - compressional and extensional structures in an orogenic belt. - Tectonophysics **238**: 229-254.

Steiger, R. H. and E. Jäger (1977): Subcommission on Geochronology: Convention on the use of decay constants in geo- and cosmochronology. - Earth and Planetary Science Letters **36**: 359-362.

Stormer, J. C., M. L. Pierson and R. C. Tacker (1993): Variation of F and Cl X-ray intensity due to anisotropic diffusion in apatite during electron microprobe analysis. - American Mineralogist **78**: 641-648.

Taymaz, T., J. Jackson and R. Westaway (1990): Earthquake mechanics in the Hellenic trench near Crete. - International Geophysical Journal **102**: 695-731.

Thompson, A. B., R. J. Tracy, P. T. Lyttle and J. B. Thompson jr. (1977): Retrograde reaction histories deduced from compositional zonation and mineral inclusions in garnet from the Gassetts Schist, Vermont. - American Journal of Science **277**: 1152-1167.

Tracy, R. J. (1982): Compositional zoning and inclusions in metamorphic minerals. - in: FERRY, J.M. (eds.): Characterization of Metamorphism through Mineral Equilibria. Mineralogical Society of America, Reviews in Mineralogy **10**: 355-397.

Tracy, R. J., P. Robinson and A. B. Thompson (1976): Garnet composition and and zoning in the determination of temperature and pressure of metamorphism, central Massachusetts. - American Mineralogist **61**: 762-775.

Vavassis, I., A. DeBono, A. Valloton, G. M. Stampfli, M. Cosca and Y. Amelin (1999): U-Pb and Ar-Ar geochronological data from the pelagonian basement in Evvia (Greece): Geodynamic implications for the evolution of Paleothetys. - Terra abstracts. **4**: 314.

Vergely, P., A. Dimo and P. Monie (1998): Datation des semellesmetamorphiques ophiolitiques dÁlbanie par la methode $^{40}Ar/^{39}Ar$: conséquences sur le mécanisme de leur mise en place. - C.R. Acad. Sci. Paris **326**: 717-722.

Villa, I. M. (1998): Isotopic closure. - Terra Nova. **10**: 42-47.

Villa, I. M. and M. Puxeddu (1994): Geochronology of the Larderello geothermal field: new data and the 'closure temperature' issue. - Contributions to Mineralogy and Petrology **126**: 67-80.

Villa, I. M., G. Ruggieri and M. Puxeddu (1997): Petrological and geochronological discrimination of two white-mica generations in granite cored from the Larderello-Travale geothermal field (Italy). - European Journal of Mineralogy **9**: 563-568.

Wagner, G. A. (1968): Fission-track dating of apatites. - Earth and Planetary Science Letters **4**: 411-414.

Wagner, G. A. and P. Van den Haute (1992): Fission-track dating. - Enke: pp.285.

Wendt, I. (1986): Radiometrische Methoden in der Geochronologie. - Clausthaler Tektonische Hefte **23**, Pilger Verlag: pp.170.

Wendt, I. and W. Todt (1991): A vapor digestion method for dating single zircons by direct measurement of U and Pb without chemical separation. - Terra abstracts **3**: 507-508.

Woodsworth, G. J. (1977): Homogenization of zoned garnets from pelitic schists. - Can. Mineral. **15**: 230-242.

Yardley, B. W. D. (1977): An emirical study of diffusion in garnet. - American Mineralogist **62**: 793-800.

Yardwood, G. A. and M. Aftalion (1976): Field relations and U-Pb geochronology of a granite from the Pelagonian Zone of the Hellenides (High Pieira, Greece). - Bull. de la Soc. Geol. France. **18/2**: 259-264.

York, D. (1969): Least squares fitting of a straight line with correlated errors. - Earth and Planetary Science Letters **5**: 320-324.

Zaun, P. E. and G. A. Wagner (1985): Fission-track stability in zircons under geological conditions. - Nucl. Tracks **10**: 303-307.

Zimmerman, J. (1972): Emplacement of the Vourinos ophiolitic complex, Northern Greece. - Geological Society of America Memoir **132**: 225-239.

Appendix

Plate 1a.: Marginally deformed granite of the East Pelagonian Zone (W Vitoliste). Porphyroclast orientated parallel to S_{A2} foliation indicates top to NE sense of shear (S_{A2}: 100/40; L_{str2}: 056/32). Scale: Estwing hammer low left.

Plate 1b.: D_3 SC fabric indicating top to W sense of shear (sample MA6, Eastern Pelagonian margin, SW Veles; S_{A3}: 100/30; L_{str3}: 090/28). Long side of picture = 3.27 mm.

Plate 1c.: D_3 SC fabric indicating top to W sense of shear (sample M98/27, Eastern Pelagonian margin, SW Veles; S_{A3}: 040/58; L_{str3}: 088/15). Long side of picture = 3.27 mm.

Plate 1d.: Marble mylonite at the eastern Pelagonian margin (Izvor quarry). Sense of shear is top to SE (δ-clast; sample M98/30; S_{myl}: 345/31; L_{str}: 300/24). Long side of picture = 3.27 mm.

Plate 1e.: Paragneiss W Florina (WPZ). Antithetic bookshelf structure displays top to NE sense of shear (sample MA9; S_{A4}: 066/32; L_{str4}: 032/28). Long side of picture = 3.27 mm.

Plate 1f.: Cataclastic shear zone indicates top to NE sense of shear (sample M98/18 NW Vitoliste; shear zone: 113/40; L_{str4}: 040/13). Long side of picture = 3.27 mm.

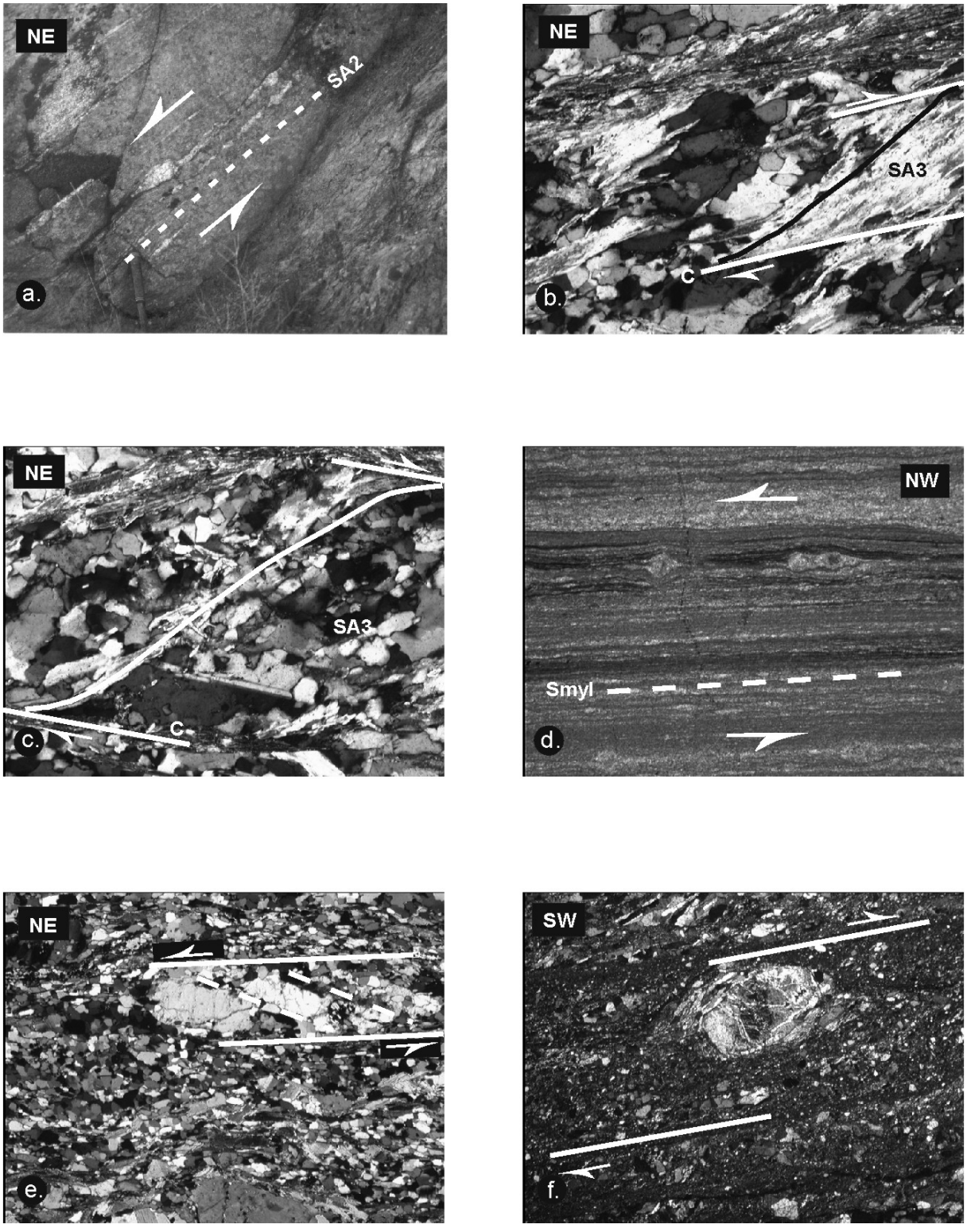

Appendix A, plate 1a-f: Representative photographs of structures belong to different tectonometamorphic events in the Northern Pelagonian Zone and the Vardar Zone in northern Greece and the Republic of Macedonia.

Plate 1g.: Shear band indicate top to E sense of shear the Almopias Unit (sample M98/39, W Kavardaci; shear zone: 083/74; L_{str5}: 103/45). Long side of picture = 3.27 mm.

Plate 1h. Thrust fault (D_6) marks the tectonic contact between the East Pelagonian Zone (gneisses in the East) and Vardar Zone (marbles and schists in the West) W Vitoliste. Direction of tectonic transport top to WSW. Scale: Geologist: 1.83 m.

Plate 1i.: Cataclastic and pseudotachylitic shear zone (D_6) of the East Pelagonian Zone SE Prilep. Shear sense not determinable. Long side of picture = 3.27 mm.

Plate 1j. Cataclastic shear zone (D6) at the margin of an East Pelagonian granite NW Vitoliste indicates top to SW thrusting (shear zone plunge to NE).

Plate 1k. Sigma clast in a mylonitic shear zone (D7) N Brod displays top to W sense of shear (sample MA8; S_{myl}: 347/37; L_{str}: 270/05). Long side of picture = 3.27 mm.

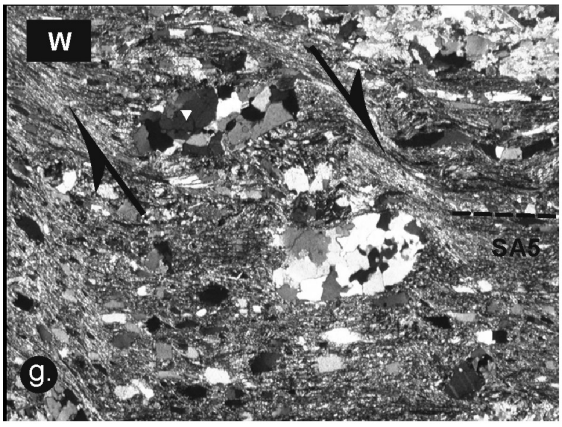

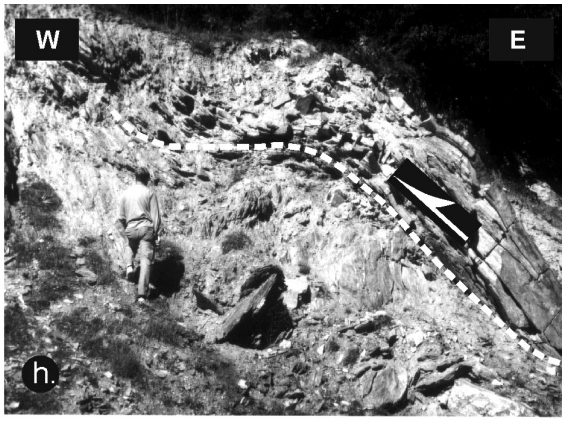

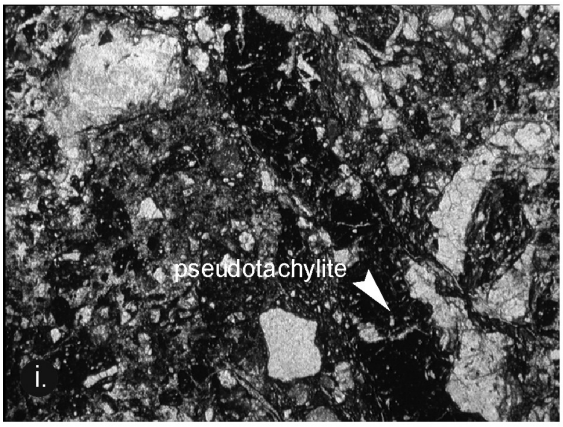

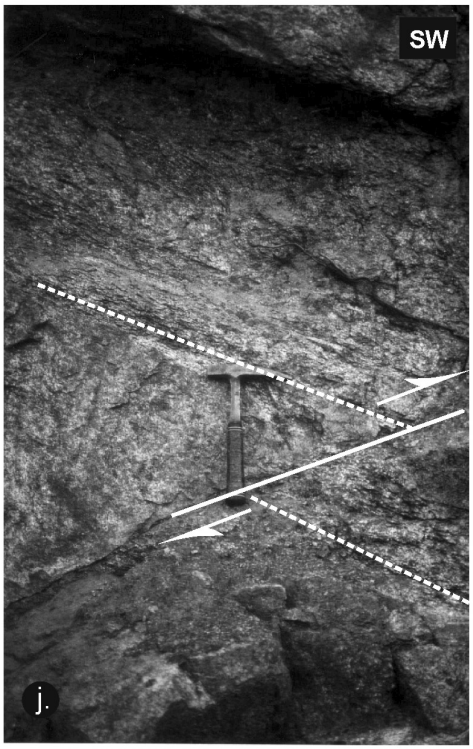

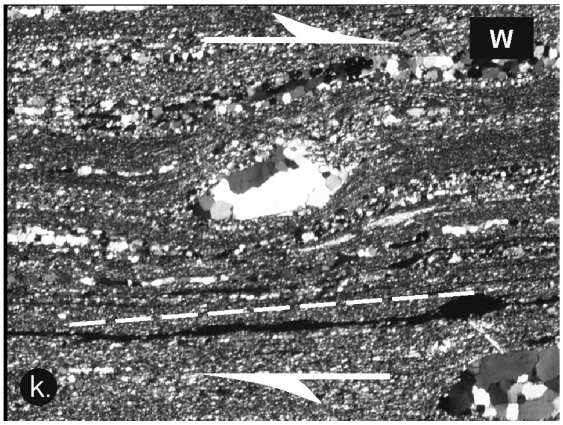

Appendix A, plate 1g-e: Representative photographs of structures belong to different tectonometamorphic events in the Northern Pelagonian Zone and the Vardar Zone in northern Greece and the Republic of Macedonia.

Appendix B: Electron microprobe analyses of apatite.

sample	Astimex	MAC	GR99/5	GR99/5	GR99/5	GR99/5	GR99/5	GR99/5	GR99/5	GR99/5	GR99/5	GR99/5	M99/12	M99/12	M99/12	M99/12	M99/12	M99/12	M99/12
analysis	standarts		1	2	3	4	5	6	7	8	9	10	1	2	3	4	5	6	7
CaO	55.81	53.30	54.14	54.17	54.51	53.78	53.18	54.51	54.76	53.67	54.66	53.93	55.36	54.24	54.54	55.55	55.91	54.95	54.85
P2O5	42.39	40.95	44.86	45.56	44.12	44.75	45.76	43.72	46.19	43.49	44.44	44.49	45.51	43.82	45.94	43.55	45.61	44.82	43.16
SrO	0.00	0.00	0.08	0.10	0.10	0.09	0.05	0.07	0.07	0.22	0.09	0.08	0.04	0.00	0.10	0.00	0.09	0.02	0.12
SiO2	0.00	0.90	0.44	0.37	0.24	0.43	0.58	0.43	0.00	0.39	0.26	0.23	0.00	0.00	0.02	0.02	0.02	0.00	0.00
MnO	0.00	0.00	0.07	0.08	0.06	0.11	0.09	0.04	0.09	0.00	0.07	0.10	0.11	0.12	0.14	0.06	0.04	0.14	0.06
Y2O3	0.00	0.00	0.07	0.08	0.09	0.00	0.05	0.03	0.00	0.03	0.05	0.08	0.00	0.04	0.04	0.02	0.01	0.01	0.01
Ce2O3	0.00	1.21	0.46	0.37	0.34	0.49	0.70	0.61	0.17	0.42	0.34	0.30	0.00	0.00	0.12	0.00	0.04	0.00	0.13
F	0.00	3.55	2.49	2.77	2.59	2.92	2.76	2.43	2.58	2.74	2.61	2.63	2.66	2.61	2.64	2.65	2.47	2.52	2.57
Cl	0.00	0.02	0.28	0.32	0.28	0.27	0.22	0.29	0.25	0.33	0.29	0.31	0.04	0.04	0.04	0.05	0.04	0.04	0.04
total	98.20	99.93	102.89	103.82	102.32	102.83	103.39	102.12	104.10	101.27	102.81	102.15	103.71	100.87	103.56	101.88	104.21	102.48	100.94
-O=F	0.00	1.49	1.05	1.17	1.09	1.23	1.16	1.02	1.09	1.15	1.10	1.11	1.12	1.10	1.11	1.12	1.04	1.06	1.08
-O=Cl	0.00	0.00	0.06	0.07	0.06	0.06	0.05	0.06	0.06	0.07	0.07	0.07	0.01	0.01	0.01	0.01	0.01	0.01	0.01
total	98.20	98.43	101.78	102.58	101.17	101.54	102.17	101.03	102.95	100.05	101.64	100.97	102.58	99.76	102.44	100.75	103.16	101.41	99.85
Kat																			
Ca	10.40	9.78	9.52	9.42	9.67	9.45	9.25	9.71	9.48	9.63	9.65	9.56	9.64	9.74	9.49	9.92	9.70	9.70	9.90
P	6.24	5.94	6.23	6.26	6.19	6.22	6.29	6.16	6.32	6.16	6.20	6.23	6.26	6.22	6.31	6.14	6.25	6.25	6.15
Sr	0.00	0.00	0.01	0.01	0.01	0.01	0.00	0.01	0.01	0.02	0.01	0.01	0.00	0.00	0.01	0.00	0.01	0.00	0.01
Si	0.00	0.15	0.07	0.06	0.04	0.07	0.09	0.07	0.00	0.06	0.04	0.04	0.00	0.00	0.00	0.00	0.00	0.00	0.00
Mn	0.00	0.00	0.01	0.01	0.01	0.02	0.01	0.01	0.01	0.00	0.01	0.01	0.01	0.02	0.02	0.01	0.01	0.02	0.01
Y	0.00	0.00	0.01	0.01	0.01	0.00	0.00	0.00	0.00	0.00	0.00	0.01	0.00	0.00	0.00	0.00	0.00	0.00	0.00
Ce	0.00	0.08	0.03	0.02	0.02	0.03	0.04	0.04	0.01	0.03	0.02	0.02	0.00	0.00	0.01	0.00	0.00	0.00	0.01
F	0.00	1.92	1.29	1.42	1.36	1.51	1.42	1.28	1.32	1.45	1.36	1.38	1.37	1.38	1.36	1.40	1.26	1.31	1.37
Cl	0.00	0.01	0.08	0.09	0.08	0.07	0.06	0.08	0.07	0.09	0.08	0.09	0.01	0.01	0.01	0.01	0.01	0.01	0.01
total (Kat)	16.64	17.87	17.25	17.29	17.38	17.38	17.18	17.35	17.21	17.45	17.37	17.34	17.30	17.37	17.21	17.48	17.25	17.29	17.46
A	6.24	6.09	6.31	6.32	6.23	6.29	6.39	6.23	6.32	6.23	6.24	6.27	6.26	6.22	6.32	6.15	6.26	6.25	6.15
B	10.40	9.85	9.57	9.47	9.72	9.51	9.32	9.77	9.51	9.68	9.69	9.60	9.66	9.76	9.52	9.93	9.72	9.72	9.92
C	0.00	1.93	1.37	1.51	1.44	1.59	1.48	1.36	1.39	1.54	1.44	1.46	1.38	1.40	1.37	1.41	1.27	1.32	1.38

Abbreviations: A (P, Si); B (Ca, Sr, Mn, Y, Ce); C (F, Cl)

Appendix B: Electron microprobe analyses of apatite.

sample	M99/12	M99/12	M99/12	M99/15	M99/15	M99/15	M99/15	M99/15	M99/15	M99/15	M99/15	M99/15	M99/15	GR99/11	GR99/11	GR99/11	GR99/11	GR99/11	GR99/11
analysis	8	9	10	1	2	3	4	5	6	7	8	9	10	1	2	3	4	5	6
CaO	55.55	54.76	56.07	53.77	54.75	54.80	55.95	55.23	55.59	54.33	55.23	55.25	54.95	53.75	53.81	54.18	54.95	54.36	53.83
P2O5	45.39	44.38	44.14	43.36	44.94	45.18	45.17	44.40	44.84	44.48	45.32	45.24	44.07	44.18	44.53	44.18	45.23	43.71	43.75
SrO	0.06	0.10	0.03	0.03	0.10	0.04	0.05	0.05	0.03	0.01	0.14	0.09	0.05	0.03	0.00	0.03	0.06	0.05	0.02
SiO2	0.00	0.01	0.02	0.48	0.05	0.07	0.05	0.02	0.02	0.00	0.09	0.02	0.08	0.47	0.43	0.45	0.08	0.44	0.53
MnO	0.12	0.10	0.09	0.10	0.05	0.07	0.11	0.09	0.05	0.07	0.00	0.05	0.07	0.10	0.10	0.01	0.11	0.09	0.03
Y2O3	0.00	0.04	0.00	0.03	0.00	0.05	0.00	0.01	0.05	0.06	0.00	0.00	0.02	0.21	0.17	0.23	0.10	0.21	0.19
Ce2O3	0.12	0.00	0.09	0.13	0.00	0.05	0.06	0.01	0.08	0.07	0.00	0.00	0.11	0.44	0.43	0.36	0.29	0.34	0.45
F	2.54	2.49	2.66	2.55	2.31	2.34	2.72	2.69	2.84	2.35	2.36	2.42	2.31	2.58	2.64	2.56	2.63	2.91	2.76
Cl	0.05	0.05	0.03	0.53	0.43	0.49	0.48	0.46	0.42	0.47	0.48	0.44	0.47	0.10	0.06	0.14	0.06	0.10	0.09
total	103.84	101.92	103.12	100.97	102.63	103.09	104.60	102.95	103.91	101.83	103.61	103.53	102.13	101.83	102.16	102.14	103.51	102.19	101.64
-O=F	1.07	1.05	1.12	1.07	0.97	0.99	1.15	1.13	1.19	0.99	0.99	1.02	0.97	1.08	1.11	1.08	1.11	1.23	1.16
-O=Cl	0.01	0.01	0.01	0.12	0.10	0.11	0.11	0.10	0.10	0.11	0.11	0.10	0.11	0.02	0.01	0.03	0.01	0.02	0.02
total	102.76	100.86	101.99	99.78	101.56	102.00	103.34	101.72	102.62	100.74	102.51	102.41	101.05	100.73	101.03	101.03	102.39	100.94	100.45
Kat																			
Ca	9.68	9.73	9.89	9.66	9.65	9.62	9.71	9.74	9.71	9.66	9.65	9.66	9.78	9.56	9.52	9.61	9.61	9.66	9.60
P	6.25	6.23	6.15	6.16	6.26	6.26	6.19	6.19	6.19	6.25	6.25	6.25	6.20	6.21	6.23	6.19	6.25	6.14	6.17
Sr	0.01	0.01	0.00	0.00	0.01	0.00	0.00	0.00	0.00	0.00	0.01	0.01	0.00	0.00	0.00	0.00	0.01	0.00	0.00
Si	0.00	0.00	0.00	0.08	0.01	0.01	0.01	0.00	0.00	0.00	0.01	0.00	0.01	0.08	0.07	0.07	0.01	0.07	0.09
Mn	0.02	0.01	0.01	0.01	0.01	0.01	0.02	0.01	0.01	0.01	0.00	0.01	0.01	0.01	0.01	0.00	0.02	0.01	0.00
Y	0.00	0.00	0.00	0.00	0.00	0.00	0.00	0.00	0.00	0.01	0.00	0.00	0.00	0.02	0.01	0.02	0.01	0.02	0.02
Ce	0.01	0.00	0.01	0.01	0.00	0.00	0.00	0.00	0.00	0.00	0.00	0.00	0.01	0.03	0.03	0.02	0.02	0.02	0.03
F	1.31	1.30	1.39	1.35	1.20	1.21	1.39	1.40	1.46	1.24	1.22	1.25	1.21	1.35	1.38	1.34	1.36	1.53	1.45
Cl	0.01	0.01	0.01	0.15	0.12	0.14	0.13	0.13	0.12	0.13	0.13	0.12	0.13	0.03	0.02	0.04	0.02	0.03	0.02
total (Kat)	17.28	17.31	17.46	17.43	17.26	17.26	17.46	17.48	17.50	17.30	17.28	17.31	17.36	17.28	17.27	17.31	17.29	17.48	17.38
A	6.25	6.23	6.16	6.24	6.27	6.28	6.20	6.19	6.19	6.25	6.27	6.26	6.21	6.28	6.30	6.27	6.26	6.21	6.25
B	9.71	9.76	9.91	9.69	9.67	9.64	9.73	9.76	9.73	9.68	9.66	9.68	9.80	9.62	9.58	9.66	9.65	9.71	9.65
C	1.32	1.32	1.39	1.50	1.32	1.35	1.53	1.53	1.58	1.37	1.35	1.37	1.35	1.38	1.40	1.38	1.37	1.55	1.48

Abbreviations: A (P, Si); B (Ca, Sr, Mn, Y, Ce); C (F, Cl)

Appendix B: Electron microprobe analyses of apatite.

sample	GR99/11	GR99/11	GR99/11	GR99/11	GR99/12	GR99/12	GR99/12	GR99/12	GR99/12	GR99/12	GR99/12	GR99/12	GR99/12	GR99/12	M98/39	M98/39	M98/39	M98/39	M98/39
analysis	7	8	9	10	1	2	3	4	5	6	7	8	9	10	1	2	3	4	5
CaO	54.13	53.66	54.20	54.39	53.86	54.11	54.17	54.54	54.56	54.47	53.40	54.33	53.99	54.04	55.20	55.36	55.92	55.80	55.45
P2O5	44.68	44.37	43.36	44.33	44.10	44.11	43.26	43.86	44.73	44.27	44.45	44.55	43.73	44.90	45.63	46.76	43.30	45.36	46.15
SrO	0.05	0.03	0.04	0.05	0.05	0.00	0.04	0.00	0.02	0.01	0.01	0.02	0.06	0.03	0.11	0.41	0.10	0.06	0.22
SiO2	0.27	0.53	0.38	0.06	0.38	0.41	0.32	0.16	0.09	0.40	0.39	0.42	0.36	0.36	0.01	0.00	0.01	0.00	0.00
MnO	0.03	0.15	0.10	0.11	0.03	0.07	0.13	0.09	0.10	0.08	0.12	0.06	0.06	0.09	0.03	0.04	0.02	0.04	0.08
Y2O3	0.14	0.15	0.16	0.00	0.22	0.15	0.10	0.06	0.16	0.19	0.26	0.20	0.17	0.15	0.00	0.01	0.05	0.00	0.02
Ce2O3	0.16	0.29	0.40	0.11	0.29	0.42	0.15	0.16	0.10	0.25	0.38	0.37	0.26	0.17	0.00	0.00	0.00	0.02	0.00
F	2.73	2.64	2.56	2.46	2.75	2.97	2.69	3.02	2.57	2.65	2.57	2.94	2.92	2.66	3.65	3.24	3.72	3.00	4.07
Cl	0.07	0.09	0.06	0.07	0.10	0.09	0.10	0.09	0.09	0.10	0.10	0.08	0.09	0.08	0.01	0.01	0.00	0.02	0.02
total	102.27	101.90	101.26	101.57	101.77	102.34	100.95	101.99	102.42	102.41	101.69	102.97	101.65	102.48	104.63	105.83	103.13	104.29	106.00
-O=F	1.15	1.11	1.08	1.04	1.16	1.25	1.13	1.27	1.08	1.12	1.08	1.24	1.23	1.12	1.54	1.37	1.57	1.26	1.71
-O=Cl	0.02	0.02	0.01	0.02	0.02	0.02	0.02	0.02	0.02	0.02	0.02	0.02	0.02	0.02	0.00	0.00	0.00	0.00	0.00
total	101.10	100.77	100.17	100.52	100.59	101.07	99.80	100.70	101.32	101.27	100.58	101.71	100.40	101.34	103.10	104.47	101.56	103.02	104.28
Kat																			
Ca	9.56	9.51	9.73	9.69	9.58	9.58	9.74	9.70	9.64	9.63	9.49	9.55	9.63	9.51	9.51	9.42	9.89	9.68	9.43
P	6.24	6.22	6.15	6.24	6.20	6.17	6.15	6.16	6.24	6.19	6.24	6.19	6.16	6.25	6.22	6.29	6.05	6.22	6.20
Sr	0.01	0.00	0.00	0.00	0.00	0.00	0.00	0.00	0.00	0.00	0.00	0.00	0.01	0.00	0.01	0.04	0.01	0.01	0.02
Si	0.04	0.09	0.06	0.01	0.06	0.07	0.05	0.03	0.01	0.07	0.06	0.07	0.06	0.06	0.00	0.00	0.00	0.00	0.00
Mn	0.00	0.02	0.01	0.02	0.00	0.01	0.02	0.01	0.01	0.01	0.02	0.01	0.01	0.01	0.00	0.01	0.00	0.01	0.01
Y	0.01	0.01	0.01	0.00	0.02	0.01	0.01	0.01	0.01	0.02	0.02	0.02	0.02	0.01	0.00	0.00	0.00	0.00	0.00
Ce	0.01	0.02	0.02	0.01	0.02	0.03	0.01	0.01	0.01	0.02	0.02	0.02	0.02	0.01	0.00	0.00	0.00	0.00	0.00
F	1.42	1.38	1.36	1.30	1.44	1.55	1.43	1.59	1.34	1.39	1.35	1.53	1.54	1.38	1.86	1.63	1.94	1.53	2.04
Cl	0.02	0.03	0.02	0.02	0.03	0.03	0.03	0.03	0.03	0.03	0.03	0.02	0.03	0.02	0.00	0.00	0.00	0.00	0.00
total (Kat)	17.31	17.28	17.38	17.28	17.36	17.45	17.44	17.53	17.30	17.34	17.24	17.41	17.46	17.26	17.60	17.38	17.90	17.44	17.72
A	6.28	6.30	6.21	6.25	6.26	6.24	6.20	6.19	6.26	6.25	6.31	6.26	6.22	6.30	6.22	6.29	6.05	6.22	6.20
B	9.59	9.57	9.79	9.72	9.63	9.63	9.79	9.73	9.67	9.68	9.55	9.60	9.68	9.55	9.53	9.47	9.90	9.69	9.47
C	1.44	1.41	1.38	1.32	1.47	1.58	1.45	1.61	1.37	1.41	1.38	1.55	1.56	1.41	1.86	1.63	1.94	1.54	2.05

Abbreviations: A (P, Si); B (Ca, Sr, Mn, Y, Ce); C (F, Cl)

Appendix B: Electron microprobe analyses of apatite.

sample	M98/39	M98/39	M98/39	M98/39	M98/39	GR99/2	GR99/2	GR99/2	GR99/2	GR99/2	GR99/2	GR99/2	GR99/2	GR99/2	GR99/2
analysis	6	7	8	9	10	1	2	3	4	5	6	7	8	9	10
CaO	56.34	55.74	54.48	55.33	55.32	54.61	54.34	54.04	54.35	53.84	54.05	53.92	54.35	54.83	53.92
P2O5	45.50	44.86	44.94	45.38	44.77	41.13	43.76	43.20	41.82	43.89	44.53	43.92	43.84	46.52	43.95
SrO	0.04	0.03	0.12	0.09	0.30	0.01	0.07	0.07	0.00	0.01	0.00	0.06	0.04	0.00	0.05
SiO2	0.00	0.00	0.25	0.01	0.03	0.50	0.49	0.52	0.54	0.41	0.52	0.42	0.45	0.19	0.51
MnO	0.01	0.03	0.00	0.05	0.00	0.26	0.18	0.14	0.18	0.16	0.27	0.27	0.32	0.23	0.27
Y2O3	0.00	0.05	0.11	0.01	0.05	0.16	0.11	0.21	0.19	0.15	0.10	0.17	0.05	0.22	0.17
Ce2O3	0.00	0.08	0.42	0.10	0.00	0.74	0.78	0.92	0.87	0.91	0.91	0.80	0.84	0.33	1.05
F	3.00	3.98	3.54	3.96	3.57	3.71	4.29	4.02	3.60	4.57	3.70	3.65	4.32	3.81	3.92
Cl	0.01	0.01	0.00	0.01	0.00	0.02	0.01	0.02	0.01	0.01	0.01	0.01	0.02	0.01	0.01
total	104.89	104.78	103.85	104.94	104.05	101.12	104.02	103.13	101.55	103.95	104.09	103.21	104.23	106.14	103.85
-O=F	1.26	1.68	1.49	1.67	1.50	1.56	1.81	1.69	1.51	1.92	1.56	1.54	1.82	1.60	1.65
-O=Cl	0.00	0.00	0.00	0.00	0.00	0.00	0.00	0.01	0.00	0.00	0.00	0.00	0.00	0.00	0.00
total	103.63	103.10	102.36	103.27	102.54	99.56	102.21	101.43	100.03	102.02	102.53	101.67	102.41	104.53	102.20
Kat															
Ca	9.72	9.64	9.49	9.53	9.63	9.93	9.50	9.55	9.81	9.41	9.42	9.50	9.49	9.30	9.45
P	6.20	6.13	6.18	6.17	6.16	5.91	6.05	6.03	5.97	6.06	6.13	6.11	6.05	6.24	6.08
Sr	0.00	0.00	0.01	0.01	0.03	0.00	0.01	0.01	0.00	0.00	0.00	0.01	0.00	0.00	0.00
Si	0.00	0.00	0.04	0.00	0.01	0.08	0.08	0.09	0.09	0.07	0.09	0.07	0.07	0.03	0.08
Mn	0.00	0.00	0.00	0.01	0.00	0.04	0.02	0.02	0.03	0.02	0.04	0.04	0.04	0.03	0.04
Y	0.00	0.00	0.01	0.00	0.00	0.01	0.01	0.02	0.02	0.01	0.01	0.02	0.00	0.02	0.01
Ce	0.00	0.00	0.02	0.01	0.00	0.05	0.05	0.06	0.05	0.05	0.05	0.05	0.05	0.02	0.06
F	1.53	2.03	1.82	2.01	1.84	1.99	2.21	2.10	1.92	2.36	1.90	1.90	2.23	1.91	2.03
Cl	0.00	0.00	0.00	0.00	0.00	0.00	0.00	0.01	0.00	0.00	0.00	0.00	0.00	0.00	0.00
total (Kat)	17.46	17.82	17.57	17.74	17.67	18.02	17.93	17.88	17.88	17.99	17.64	17.68	17.95	17.55	17.77
A	6.20	6.13	6.22	6.18	6.17	5.99	6.13	6.12	6.06	6.13	6.22	6.18	6.12	6.27	6.17
B	9.73	9.66	9.53	9.55	9.67	10.03	9.59	9.65	9.91	9.50	9.52	9.60	9.59	9.37	9.57
C	1.53	2.03	1.82	2.02	1.84	2.00	2.22	2.11	1.92	2.36	1.91	1.90	2.23	1.91	2.03

Abbreviations: A (P, Si); B (Ca, Sr, Mn, Y, Ce); C (F, Cl)

Appendix B: Electron microprobe analyses of biotite; grt-st-ky-micaschist [sample M98/19]

sample	M98-19	M98-19	M98-19	M98-19	M98-19	M98-19	M98-19	M98-19	M98-19	M98-19	M98-19	M98-19	M98-19	M98-19	M98-19	M98-19	M98-19	M98-19	M98-19	M98-19	M98-19
analysis	bt1_1	bt1_2	bt1_3	bt1_4	bt1_5	bt1_6	bt1_7	bt1_8	bt1_9	bt1_10	bt1_11	bt1_12	bt1_13	bt1_14	bt1_15	bt1_16	b2_1	b2_2	b2_3	b2_4	b2_5
SiO2	39.51	38.94	39.09	39.15	39.53	39.62	39.08	39.75	39.74	38.70	39.35	38.99	38.87	39.84	39.21	39.10	38.63	38.49	39.55	39.04	38.87
TiO2	0.71	0.74	0.76	0.72	0.69	0.76	0.72	0.74	0.70	0.76	0.78	0.79	0.80	0.78	0.81	0.84	0.73	0.70	0.73	0.72	0.70
Al2O3	18.36	18.39	18.49	18.17	17.93	18.07	17.91	17.88	17.64	18.25	17.99	18.37	17.97	18.13	18.07	18.35	18.13	18.30	18.11	18.72	18.42
Cr2O3	0.00	0.00	0.00	0.00	0.00	0.00	0.00	0.00	0.00	0.00	0.00	0.00	0.00	0.00	0.00	0.00	0.00	0.00	0.00	0.00	0.00
FeO	14.87	14.81	14.84	15.28	14.90	14.90	14.66	14.61	15.00	14.92	14.70	14.83	15.49	14.75	15.43	15.46	15.03	15.62	15.35	15.12	15.20
MnO	0.02	0.04	0.01	0.04	0.01	0.00	0.05	0.04	0.03	0.05	0.02	0.03	0.02	0.04	0.05	0.05	0.05	0.03	0.04	0.04	0.00
MgO	13.64	13.26	13.70	13.63	13.58	13.76	13.50	13.88	13.87	13.56	13.69	13.44	13.50	13.79	13.59	13.21	13.60	13.44	13.65	13.68	13.51
CaO	0.03	0.02	0.01	0.00	0.05	0.00	0.03	0.02	0.02	0.03	0.00	0.02	0.00	0.03	0.02	0.10	0.05	0.00	0.00	0.00	0.00
Na2O	0.31	0.34	0.35	0.29	0.25	0.31	0.32	0.34	0.28	0.31	0.29	0.38	0.29	0.30	0.28	0.31	0.28	0.26	0.30	0.40	0.30
K2O	8.10	8.27	8.20	8.30	8.15	8.17	8.22	8.36	8.27	8.44	8.46	8.41	8.34	8.34	8.22	8.05	8.35	8.18	8.10	8.43	8.37
total	95.81	95.01	95.73	95.88	95.41	95.91	94.81	95.95	95.80	95.38	95.62	95.64	95.61	96.35	96.03	95.80	95.19	95.40	96.18	96.47	95.74
number of cations based on 11 oxygen atoms (H2O free)																					
Si	2.88	2.87	2.86	2.87	2.90	2.89	2.89	2.90	2.90	2.85	2.88	2.86	2.86	2.89	2.87	2.87	2.85	2.84	2.88	2.84	2.85
AlIV	1.12	1.13	1.14	1.13	1.10	1.11	1.11	1.10	1.10	1.15	1.12	1.14	1.14	1.11	1.13	1.14	1.15	1.16	1.12	1.16	1.15
AlVI	0.46	0.47	0.45	0.44	0.45	0.44	0.45	0.44	0.42	0.44	0.44	0.45	0.42	0.45	0.43	0.45	0.43	0.44	0.44	0.45	0.45
Al tot.	1.58	1.60	1.59	1.57	1.55	1.55	1.56	1.54	1.52	1.59	1.55	1.59	1.56	1.55	1.56	1.59	1.58	1.59	1.56	1.61	1.59
Ti	0.04	0.04	0.04	0.04	0.04	0.04	0.04	0.04	0.04	0.04	0.04	0.04	0.04	0.04	0.05	0.05	0.04	0.04	0.04	0.04	0.04
Cr	0.00	0.00	0.00	0.00	0.00	0.00	0.00	0.00	0.00	0.00	0.00	0.00	0.00	0.00	0.00	0.00	0.00	0.00	0.00	0.00	0.00
Mg	1.48	1.46	1.49	1.49	1.49	1.50	1.49	1.51	1.51	1.49	1.50	1.47	1.48	1.49	1.48	1.44	1.50	1.48	1.48	1.49	1.48
Fe 2+	0.91	0.91	0.91	0.94	0.91	0.91	0.91	0.89	0.92	0.92	0.90	0.91	0.95	0.90	0.94	0.95	0.93	0.97	0.94	0.92	0.93
Mn	0.00	0.00	0.00	0.00	0.00	0.00	0.00	0.00	0.00	0.00	0.00	0.00	0.00	0.00	0.00	0.00	0.00	0.00	0.00	0.00	0.00
Ca	0.00	0.00	0.00	0.00	0.00	0.00	0.00	0.00	0.00	0.00	0.00	0.00	0.00	0.00	0.00	0.01	0.00	0.00	0.00	0.00	0.00
Na	0.04	0.05	0.05	0.04	0.04	0.04	0.05	0.05	0.04	0.04	0.04	0.05	0.04	0.04	0.04	0.04	0.04	0.04	0.04	0.06	0.04
K	0.75	0.78	0.77	0.78	0.76	0.76	0.78	0.78	0.77	0.79	0.79	0.79	0.78	0.77	0.77	0.75	0.79	0.77	0.75	0.78	0.78
total Kat	7.69	7.71	7.71	7.72	7.69	7.69	7.70	7.71	7.70	7.73	7.71	7.72	7.73	7.70	7.71	7.69	7.73	7.73	7.70	7.74	7.72
Fe/(Fe+Mg)	0.38	0.39	0.38	0.39	0.38	0.38	0.38	0.37	0.38	0.38	0.38	0.38	0.39	0.38	0.39	0.40	0.38	0.39	0.39	0.38	0.39
Al/(Al+Si)	0.35	0.36	0.36	0.35	0.35	0.35	0.35	0.35	0.34	0.36	0.35	0.36	0.35	0.35	0.35	0.36	0.36	0.36	0.35	0.36	0.36
Mg/(Mg+Fe)	0.62	0.61	0.62	0.61	0.62	0.62	0.62	0.63	0.62	0.62	0.62	0.62	0.61	0.62	0.61	0.60	0.62	0.61	0.61	0.62	0.61
XTi	0.01	0.01	0.01	0.01	0.01	0.01	0.01	0.01	0.01	0.01	0.01	0.02	0.02	0.01	0.02	0.02	0.01	0.01	0.01	0.01	0.01
XAlVI	0.16	0.16	0.16	0.15	0.16	0.15	0.15	0.15	0.15	0.15	0.15	0.16	0.15	0.15	0.15	0.16	0.15	0.15	0.15	0.15	0.15
XMg	0.51	0.51	0.52	0.51	0.51	0.52	0.52	0.52	0.52	0.52	0.52	0.51	0.51	0.52	0.51	0.50	0.52	0.51	0.51	0.51	0.51
XFe	0.31	0.32	0.31	0.32	0.32	0.31	0.31	0.31	0.32	0.32	0.31	0.32	0.33	0.31	0.33	0.33	0.32	0.33	0.32	0.32	0.32

Appendix B: Electron microprobe analyses of biotite; grt-st-ky-micaschist [sample M98/19]

sample	M98-19	M98-19	M98-19	M98-19	M98-19	M98-19	M98-19	M98-19	M98-19	M98-19	M98-19	M98-19	M98-19	M98-19	M98-19	M98-19	M98-19	M98-19	M98-19	M98-19	M98/19
analysis	b2_6	b2_7	b2_8	b2_9	b2_10	b2_11	b2_12	bt3_1	bt3_2	bt3_3	bt3_4	bt3_5	bt3_6	bt3_7	bt3_8	bt3_9	bt3_10	bt3_11	bt3_12	bt3_13	bt4_1
SiO2	38.93	39.43	39.36	39.63	39.39	39.28	38.67	38.48	39.17	39.28	38.79	39.31	39.51	39.30	39.04	39.57	39.44	39.62	39.84	39.37	38.05
TiO2	0.71	0.75	0.76	0.74	0.75	0.83	0.89	0.62	0.62	0.60	0.65	0.64	0.64	0.70	0.66	0.67	0.68	0.65	0.69	0.65	0.68
Al2O3	18.22	17.83	17.97	17.89	17.94	17.47	18.29	18.19	18.11	18.14	17.83	18.21	18.18	18.01	18.30	17.98	17.84	17.91	17.90	18.47	19.04
Cr2O3	0.00	0.00	0.00	0.00	0.00	0.00	0.00	0.00	0.00	0.00	0.00	0.00	0.00	0.00	0.00	0.00	0.00	0.00	0.00	0.00	0.00
FeO	15.36	15.61	14.96	15.53	15.43	15.59	15.65	14.67	15.29	15.18	15.14	14.93	15.23	15.04	14.97	14.76	14.99	14.91	14.89	14.94	15.02
MnO	0.03	0.03	0.01	0.04	0.03	0.00	0.04	0.07	0.01	0.02	0.06	0.03	0.03	0.05	0.04	0.04	0.02	0.02	0.05	0.02	0.04
MgO	13.61	13.87	13.54	13.50	13.62	13.81	13.06	13.45	13.89	13.96	13.55	13.65	13.75	13.95	13.73	13.85	13.95	13.81	13.97	13.79	13.71
CaO	0.00	0.01	0.00	0.01	0.00	0.00	0.00	0.00	0.00	0.04	0.00	0.00	0.00	0.01	0.00	0.00	0.00	0.00	0.00	0.00	0.04
Na2O	0.29	0.24	0.28	0.25	0.33	0.27	0.29	0.23	0.31	0.33	0.39	0.29	0.33	0.32	0.30	0.31	0.35	0.29	0.33	0.40	0.28
K2O	8.39	8.07	8.23	8.29	8.33	8.22	8.43	8.98	8.53	8.28	8.72	8.59	8.36	8.60	8.61	8.33	8.36	8.31	8.36	8.25	8.77
total	95.97	96.28	95.47	96.23	96.18	95.84	95.64	95.01	96.34	96.22	95.60	95.97	96.45	96.27	96.02	95.82	95.95	95.79	96.27	96.08	95.94
number of cations based on 11 oxygen atoms (H2O free)																					
Si	2.86	2.88	2.89	2.89	2.88	2.88	2.85	2.85	2.86	2.87	2.87	2.88	2.88	2.87	2.86	2.89	2.88	2.90	2.90	2.87	2.80
AlIV	1.14	1.12	1.11	1.11	1.12	1.12	1.15	1.15	1.14	1.13	1.14	1.13	1.12	1.13	1.14	1.11	1.12	1.11	1.10	1.13	1.20
AlVI	0.43	0.41	0.44	0.43	0.43	0.40	0.44	0.44	0.42	0.43	0.42	0.45	0.44	0.42	0.44	0.44	0.42	0.44	0.43	0.45	0.45
Al tot.	1.58	1.53	1.56	1.54	1.55	1.51	1.59	1.59	1.56	1.56	1.55	1.57	1.56	1.55	1.58	1.55	1.54	1.54	1.53	1.59	1.65
Ti	0.04	0.04	0.04	0.04	0.04	0.05	0.05	0.03	0.03	0.03	0.04	0.04	0.04	0.04	0.04	0.04	0.04	0.04	0.04	0.04	0.04
Cr	0.00	0.00	0.00	0.00	0.00	0.00	0.00	0.00	0.00	0.00	0.00	0.00	0.00	0.00	0.00	0.00	0.00	0.00	0.00	0.00	0.00
Mg	1.49	1.51	1.48	1.47	1.48	1.51	1.44	1.49	1.51	1.52	1.49	1.49	1.49	1.52	1.50	1.51	1.52	1.50	1.51	1.50	1.50
Fe 2+	0.94	0.95	0.92	0.95	0.94	0.96	0.96	0.91	0.93	0.93	0.94	0.91	0.93	0.92	0.92	0.90	0.92	0.91	0.91	0.91	0.92
Mn	0.00	0.00	0.00	0.00	0.00	0.00	0.00	0.00	0.00	0.00	0.00	0.00	0.00	0.00	0.00	0.00	0.00	0.00	0.00	0.00	0.00
Ca	0.00	0.00	0.00	0.00	0.00	0.00	0.00	0.00	0.00	0.00	0.00	0.00	0.00	0.00	0.00	0.00	0.00	0.00	0.00	0.00	0.00
Na	0.04	0.03	0.04	0.04	0.05	0.04	0.04	0.03	0.04	0.05	0.06	0.04	0.05	0.05	0.04	0.04	0.05	0.04	0.05	0.06	0.04
K	0.79	0.75	0.77	0.77	0.78	0.77	0.79	0.85	0.80	0.77	0.82	0.80	0.78	0.80	0.80	0.78	0.78	0.78	0.78	0.77	0.82
total Kat	7.73	7.71	7.70	7.70	7.72	7.72	7.72	7.76	7.74	7.73	7.76	7.73	7.72	7.74	7.74	7.71	7.73	7.71	7.71	7.72	7.77
Fe/(Fe+Mg)	0.39	0.39	0.38	0.39	0.39	0.39	0.40	0.38	0.38	0.38	0.39	0.38	0.38	0.38	0.38	0.37	0.38	0.38	0.37	0.38	0.38
Al/(Al+Si)	0.36	0.35	0.35	0.35	0.35	0.34	0.36	0.36	0.35	0.35	0.35	0.35	0.35	0.35	0.36	0.35	0.35	0.35	0.35	0.36	0.37
Mg/(Mg+Fe)	0.61	0.61	0.62	0.61	0.61	0.61	0.60	0.62	0.62	0.62	0.61	0.62	0.62	0.62	0.62	0.63	0.62	0.62	0.63	0.62	0.62
XTi	0.01	0.01	0.01	0.01	0.01	0.02	0.02	0.01	0.01	0.01	0.01	0.01	0.01	0.01	0.01	0.01	0.01	0.01	0.01	0.01	0.01
XAlVI	0.15	0.14	0.15	0.15	0.15	0.14	0.15	0.15	0.15	0.15	0.14	0.15	0.15	0.14	0.15	0.15	0.15	0.15	0.15	0.16	0.15
XMg	0.51	0.52	0.51	0.51	0.51	0.52	0.50	0.52	0.52	0.52	0.52	0.52	0.52	0.52	0.52	0.52	0.53	0.52	0.52	0.52	0.52
XFe	0.32	0.33	0.32	0.33	0.33	0.33	0.33	0.32	0.32	0.32	0.32	0.32	0.32	0.32	0.32	0.31	0.32	0.32	0.31	0.31	0.32

Appendix B: Electron microprobe analyses of biotite; grt-st-ky-micaschist [sample M98/19], micaschist [M99/13]

sample	M98/19	M98/19	M98/19	M98/19	M98/19	M98/19	M98/19	M98/19	M98/19	M98/19	M98/19	M98/19	M98/19	M98/19	M98/19	M98/19	M98/19	M98/19	M98/19	M99/13
analysis	bt4_2	bt4_3	bt5_1	bt5_2	bt5_3	bt6_1	bt6_2	bt6_3	bt7_1	bt7_2	bt7_3	bt8_1	bt8_2	bt8_3	bt9_1	bt9_2	bt9_3	bt10_1	bt10_2	bt1_1
SiO2	38.25	38.19	38.65	38.01	38.42	37.80	38.60	38.39	38.36	38.30	38.00	38.06	38.48	38.35	38.20	38.15	38.52	38.42	38.01	38.81
TiO2	0.78	0.64	0.70	0.67	0.61	0.88	0.78	0.73	0.82	0.76	0.79	0.79	0.79	0.73	0.83	0.86	0.82	0.84	0.78	1.39
Al2O3	18.83	19.19	19.14	18.70	18.68	18.57	18.94	18.89	19.24	18.83	18.79	18.75	19.04	19.16	19.52	19.38	19.06	18.90	18.52	16.08
Cr2O3	0.00	0.00	0.00	0.00	0.00	0.00	0.00	0.00	0.00	0.00	0.00	0.00	0.00	0.00	0.00	0.00	0.00	0.00	0.00	0.00
FeO	15.26	14.91	14.38	14.63	15.20	15.20	14.60	14.59	13.80	14.68	14.88	14.61	14.82	14.58	14.09	14.12	14.11	14.73	14.86	16.06
MnO	0.03	0.00	0.05	0.02	0.02	0.06	0.05	0.03	0.03	0.03	0.01	0.02	0.03	0.04	0.04	0.03	0.04	0.09	0.03	0.21
MgO	13.87	13.54	13.96	13.74	13.82	13.41	13.95	13.57	12.90	13.73	13.69	13.66	13.61	13.56	13.73	13.61	13.45	13.42	13.36	12.89
CaO	0.00	0.00	0.03	0.03	0.01	0.12	0.04	0.07	0.10	0.05	0.04	0.07	0.04	0.06	0.02	0.00	0.00	0.09	0.05	0.04
Na2O	0.28	0.30	0.28	0.35	0.34	0.28	0.27	0.27	0.28	0.25	0.28	0.27	0.31	0.25	0.32	0.33	0.28	0.21	0.30	0.03
K2O	8.91	9.07	8.80	8.64	8.83	8.52	8.84	8.87	8.10	8.53	8.89	8.88	8.96	8.89	9.00	9.12	8.76	8.68	8.89	9.54
total	96.52	96.10	96.17	95.07	96.24	95.13	96.31	95.71	93.85	95.48	95.67	95.33	96.33	95.85	96.05	95.86	95.31	95.61	95.13	95.07
number of cations based on 11 oxygen atoms (H2O free)																				
Si	2.80	2.80	2.82	2.81	2.82	2.80	2.82	2.82	2.85	2.82	2.80	2.81	2.81	2.81	2.79	2.92	2.96	2.95	2.95	2.90
AlIV	1.20	1.20	1.18	1.19	1.18	1.20	1.19	1.18	1.16	1.18	1.20	1.19	1.19	1.19	1.21	1.08	1.04	1.05	1.05	1.10
AlVI	0.42	0.46	0.46	0.44	0.43	0.43	0.44	0.46	0.53	0.45	0.43	0.44	0.45	0.47	0.47	0.67	0.68	0.66	0.64	0.32
Al tot.	1.62	1.66	1.64	1.63	1.61	1.62	1.63	1.64	1.68	1.63	1.63	1.63	1.64	1.66	1.68	1.75	1.73	1.71	1.69	1.42
Ti	0.04	0.04	0.04	0.04	0.03	0.05	0.04	0.04	0.05	0.04	0.04	0.04	0.04	0.04	0.05	0.05	0.05	0.05	0.05	0.08
Cr	0.00	0.00	0.00	0.00	0.00	0.00	0.00	0.00	0.00	0.00	0.00	0.00	0.00	0.00	0.00	0.00	0.00	0.00	0.00	0.00
Mg	1.51	1.48	1.52	1.52	1.51	1.48	1.52	1.49	1.43	1.51	1.50	1.50	1.48	1.48	1.50	1.55	1.54	1.54	1.54	1.44
Fe 2+	0.93	0.91	0.88	0.91	0.93	0.94	0.89	0.90	0.86	0.90	0.92	0.90	0.91	0.89	0.86	0.90	0.91	0.95	0.96	1.00
Mn	0.00	0.00	0.00	0.00	0.00	0.00	0.00	0.00	0.00	0.00	0.00	0.00	0.00	0.00	0.00	0.00	0.00	0.01	0.00	0.01
Ca	0.00	0.00	0.00	0.00	0.00	0.01	0.00	0.01	0.01	0.00	0.00	0.01	0.00	0.01	0.00	0.00	0.00	0.01	0.00	0.00
Na	0.04	0.04	0.04	0.05	0.05	0.04	0.04	0.04	0.04	0.04	0.04	0.04	0.04	0.04	0.05	0.05	0.04	0.03	0.05	0.00
K	0.83	0.85	0.82	0.82	0.83	0.81	0.82	0.83	0.77	0.80	0.84	0.84	0.84	0.83	0.84	0.89	0.86	0.85	0.88	0.91
total Kat	7.78	7.78	7.75	7.77	7.78	7.76	7.76	7.76	7.67	7.74	7.78	7.77	7.77	7.76	7.76	8.12	8.08	8.09	8.12	7.77
Fe/(Fe+Mg)	0.38	0.38	0.37	0.37	0.38	0.39	0.37	0.38	0.38	0.37	0.38	0.38	0.38	0.38	0.37	0.37	0.37	0.38	0.38	0.41
Al/(Al+Si)	0.37	0.37	0.37	0.37	0.36	0.37	0.37	0.37	0.37	0.37	0.37	0.37	0.37	0.37	0.38	0.37	0.37	0.37	0.36	0.33
Mg/(Mg+Fe)	0.62	0.62	0.63	0.63	0.62	0.61	0.63	0.62	0.62	0.63	0.62	0.62	0.62	0.62	0.63	0.63	0.63	0.62	0.62	0.59
XTi	0.01	0.01	0.01	0.01	0.01	0.02	0.01	0.01	0.02	0.01	0.02	0.02	0.01	0.01	0.02	0.02	0.01	0.02	0.01	0.03
XAlVI	0.14	0.16	0.16	0.15	0.15	0.15	0.15	0.16	0.18	0.15	0.15	0.15	0.16	0.16	0.16	0.21	0.22	0.21	0.20	0.11
XMg	0.52	0.51	0.52	0.52	0.52	0.51	0.52	0.52	0.50	0.52	0.52	0.52	0.51	0.51	0.52	0.49	0.48	0.48	0.48	0.50
XFe	0.32	0.32	0.30	0.31	0.32	0.32	0.31	0.31	0.30	0.31	0.32	0.31	0.31	0.31	0.30	0.28	0.28	0.30	0.30	0.35

Appendix B: Electron microprobe analyses of biotite; grt-st-ky-micaschist [sample M99/13]

sample	M99/13	M99/13	M99/13	M99/13	M99/13	M99/13	M99/13	M99/13	M99/13
analysis	bt1_2	bt2_1	bt2_2	bt2_3	bt3_1	bt3_2	bt4_1	bt4_2	bt5_1
SiO2	38.75	39.36	39.05	38.54	38.75	39.21	39.17	38.61	39.16
TiO2	1.57	1.57	1.67	1.61	1.67	1.68	1.55	1.56	1.72
Al2O3	15.90	15.70	15.81	15.85	16.16	15.84	15.92	16.13	15.86
Cr2O3	0.00	0.00	0.00	0.00	0.00	0.00	0.00	0.00	0.00
FeO	16.08	16.01	16.59	16.29	15.97	15.99	16.42	15.88	15.82
MnO	0.19	0.19	0.17	0.19	0.19	0.17	0.20	0.20	0.16
MgO	12.78	13.15	12.91	12.68	12.96	12.84	13.11	12.78	13.10
CaO	0.02	0.05	0.04	0.08	0.00	0.00	0.04	0.02	0.00
Na2O	0.06	0.01	0.00	0.02	0.04	0.03	0.01	0.00	0.00
K2O	9.50	9.28	9.49	9.51	9.69	9.51	9.32	9.74	9.63
total	94.89	95.34	95.76	94.77	95.44	95.28	95.75	94.95	95.47
number of cations based on 11 oxygen atoms (H2O free)									
Si	2.90	2.93	2.90	2.90	2.89	2.92	2.91	2.89	2.91
AlIV	1.10	1.07	1.10	1.10	1.11	1.08	1.09	1.11	1.09
AlVI	0.31	0.30	0.29	0.30	0.31	0.31	0.30	0.32	0.30
Al tot.	1.41	1.38	1.39	1.40	1.42	1.39	1.39	1.42	1.39
Ti	0.09	0.09	0.09	0.09	0.09	0.09	0.09	0.09	0.10
Cr	0.00	0.00	0.00	0.00	0.00	0.00	0.00	0.00	0.00
Mg	1.43	1.46	1.43	1.42	1.44	1.43	1.45	1.43	1.45
Fe 2+	1.01	1.00	1.03	1.02	1.00	1.00	1.02	1.00	0.98
Mn	0.01	0.01	0.01	0.01	0.01	0.01	0.01	0.01	0.01
Ca	0.00	0.00	0.00	0.01	0.00	0.00	0.00	0.00	0.00
Na	0.01	0.00	0.00	0.00	0.01	0.00	0.00	0.00	0.00
K	0.91	0.88	0.90	0.91	0.92	0.90	0.88	0.93	0.91
total Kat	7.76	7.74	7.76	7.77	7.77	7.75	7.75	7.77	7.76
Fe/(Fe+Mg)	0.41	0.41	0.42	0.42	0.41	0.41	0.41	0.41	0.40
Al/(Al+Si)	0.33	0.32	0.32	0.33	0.33	0.32	0.32	0.33	0.32
Mg/(Mg+Fe)	0.59	0.59	0.58	0.58	0.59	0.59	0.59	0.59	0.60
XTi	0.03	0.03	0.03	0.03	0.03	0.03	0.03	0.03	0.03
XAlVI	0.11	0.11	0.10	0.11	0.11	0.11	0.10	0.11	0.11
XMg	0.50	0.51	0.50	0.50	0.51	0.50	0.51	0.50	0.51
XFe	0.35	0.35	0.36	0.36	0.35	0.35	0.36	0.35	0.35

Appendix B: Electron microprobe analyses of chlorite; grt-cld-schist [sample GR99/26]

sample	G99/26	G99/26	G99/26	G99/26	G99/26	G99/26	G99/26	G99/26	G99/26	G99/26	GR99/26	GR99/26	GR99/26	GR99/26	GR99/26	GR99/26	GR99/26	GR99/26	GR99/26	GR99/40
analysis	chl1_1	chl2_1	chl2_2	chl2_3	chl2_4	chl2_5	chl2_6	chl2_7	chl3_1	chl4_1	chl5_1	chl5_2	chl5_3	chl5_4	chl6_1	chl6_2	chl7_1	chl7_2	chl7_3	chl1_1
Na2O	0.03	0.00	0.00	0.01	0.00	0.00	0.00	0.00	0.00	0.00	0.00	0.00	0.02	0.00	0.01	0.00	0.00	0.00	0.00	0.00
K2O	0.00	0.04	0.00	0.02	0.01	0.01	0.00	0.00	0.00	0.01	0.00	0.00	0.00	0.00	0.01	0.00	0.01	0.01	0.00	0.00
CaO	0.02	0.04	0.01	0.07	0.04	0.02	0.04	0.02	0.04	0.04	0.01	0.01	0.02	0.02	0.05	0.02	0.01	0.02	0.03	0.05
SiO2	24.89	24.80	24.79	24.82	24.48	25.30	24.85	24.96	25.23	25.00	24.77	24.55	24.38	24.86	22.86	25.09	24.62	24.90	24.68	24.28
Al2O3	22.33	22.21	22.19	22.25	22.53	22.66	22.34	22.56	22.33	22.57	22.78	22.53	22.82	22.59	21.90	22.40	22.63	22.38	22.71	22.61
TiO2	0.09	0.08	0.05	0.05	0.05	0.05	0.06	0.08	0.03	0.06	0.05	0.08	0.07	0.01	0.09	0.11	0.10	0.08	0.19	0.08
FeO	26.29	27.53	27.85	26.15	30.18	26.16	26.68	26.24	26.46	28.16	25.42	25.43	25.57	25.48	28.79	25.34	25.45	25.19	25.71	28.97
MgO	13.95	12.16	12.46	13.61	10.37	13.83	13.66	13.86	13.65	12.32	13.68	13.45	13.33	13.49	11.68	13.78	13.61	13.85	13.59	10.96
MnO	0.06	0.17	0.11	0.06	0.19	0.08	0.06	0.06	0.05	0.13	0.10	0.08	0.08	0.06	0.15	0.06	0.15	0.08	0.12	0.15
Cr2O3	0.00	0.00	0.00	0.00	0.00	0.00	0.00	0.00	0.00	0.00	0.00	0.00	0.00	0.00	0.00	0.00	0.00	0.00	0.00	0.00
total	87.66	87.02	87.46	87.03	87.85	88.12	87.68	87.78	87.79	88.28	86.81	86.12	86.29	86.51	85.53	86.80	86.57	86.51	87.03	87.10
number of cations based on 14 oxygen atoms (H2O free)																				
Na	0.01	0.00	0.00	0.00	0.00	0.00	0.00	0.00	0.00	0.00	0.00	0.00	0.00	0.00	0.00	0.00	0.00	0.00	0.00	0.00
K	0.00	0.01	0.00	0.00	0.00	0.00	0.00	0.00	0.00	0.00	0.00	0.00	0.00	0.00	0.00	0.00	0.00	0.00	0.00	0.00
Ca	0.00	0.00	0.00	0.01	0.00	0.00	0.00	0.00	0.00	0.00	0.00	0.00	0.00	0.00	0.01	0.00	0.00	0.00	0.00	0.01
Si	2.63	2.66	2.65	2.65	2.64	2.66	2.63	2.64	2.66	2.65	2.63	2.63	2.61	2.65	2.53	2.67	2.63	2.65	2.62	2.63
AlIV	1.37	1.34	1.35	1.35	1.36	1.34	1.37	1.36	1.34	1.35	1.37	1.37	1.39	1.35	1.47	1.33	1.37	1.35	1.38	1.37
AlVI	1.42	1.48	1.45	1.44	1.51	1.46	1.43	1.44	1.45	1.47	1.49	1.49	1.50	1.50	1.40	1.47	1.48	1.47	1.47	1.51
Al tot.	2.79	2.81	2.80	2.80	2.87	2.80	2.79	2.81	2.78	2.82	2.86	2.85	2.88	2.84	2.86	2.81	2.85	2.81	2.85	2.88
Ti	0.01	0.01	0.00	0.00	0.00	0.00	0.00	0.01	0.00	0.00	0.00	0.01	0.01	0.00	0.01	0.01	0.01	0.01	0.01	0.01
Cr3+	0.00	0.00	0.00	0.00	0.00	0.00	0.00	0.00	0.00	0.00	0.00	0.00	0.00	0.00	0.00	0.00	0.00	0.00	0.00	0.00
Fe 2+	2.33	2.47	2.49	2.33	2.72	2.30	2.37	2.32	2.34	2.50	2.26	2.28	2.29	2.27	2.67	2.25	2.27	2.25	2.29	2.62
Mg	2.20	1.95	1.99	2.16	1.67	2.16	2.16	2.18	2.15	1.95	2.17	2.15	2.13	2.15	1.93	2.18	2.17	2.20	2.15	1.77
Mn	0.01	0.02	0.01	0.01	0.02	0.01	0.00	0.01	0.00	0.01	0.01	0.01	0.01	0.01	0.01	0.01	0.01	0.01	0.01	0.01
Kat tot	9.97	9.93	9.94	9.96	9.92	9.94	9.96	9.95	9.94	9.94	9.93	9.93	9.94	9.92	10.03	9.92	9.94	9.93	9.94	9.93
Vac=6-SuVI	0.05	0.09	0.06	0.06	0.09	0.07	0.04	0.05	0.06	0.07	0.07	0.07	0.07	0.08	-0.01	0.09	0.07	0.08	0.08	0.09
Fe/(Fe+Mg)	0.51	0.56	0.56	0.52	0.62	0.51	0.52	0.52	0.52	0.56	0.51	0.51	0.52	0.51	0.58	0.51	0.51	0.51	0.51	0.60
Mg/(Mg+Fe)	0.49	0.44	0.44	0.48	0.38	0.49	0.48	0.48	0.48	0.44	0.49	0.49	0.48	0.49	0.42	0.49	0.49	0.49	0.49	0.40

Appendix B: Electron microprobe analyses of chlorite; grt-cld-schist [samples GR99/26, GR99/40]

sample	GR99/40	GR99/40	GR99/40	GR99/40	GR99/40	GR99/40	GR99/40	GR99/40	GR99/40	GR99/40	GR99/40	GR99/40	GR99/40	GR99/40
analysis	chl1_2	chl1_3	chl1_4	chl2_1	chl2_2	chl3_1	chl3_2	chl3_3	chl3_4	chl4_1	chl4_2	chl5_1	chl5_2	chl5_3
Na2O	0.01	0.02	0.00	0.00	0.00	0.01	0.02	0.03	0.02	0.00	0.00	0.00	0.04	0.00
K2O	0.01	0.00	0.02	0.01	0.01	0.01	0.00	0.00	0.02	0.05	0.05	0.00	0.01	0.00
CaO	0.00	0.10	0.03	0.04	0.09	0.05	0.04	0.01	0.05	0.01	0.00	0.03	0.06	0.02
SiO2	23.95	24.35	24.26	24.05	23.60	24.08	23.37	23.69	23.60	23.52	23.69	24.13	24.24	24.04
Al2O3	22.70	22.73	22.48	22.71	22.73	22.84	22.43	22.89	22.74	23.07	22.48	22.68	22.78	22.18
TiO2	0.01	0.05	0.05	0.06	0.15	0.09	0.03	0.04	0.13	0.04	0.03	0.01	0.03	0.09
FeO	28.69	29.11	29.25	29.65	33.67	32.84	32.75	33.71	34.28	32.33	31.58	31.77	32.85	32.06
MgO	10.49	10.83	10.78	10.88	6.76	8.26	7.32	6.98	6.09	7.99	8.17	8.78	7.27	7.90
MnO	0.24	0.18	0.27	0.11	0.46	0.42	0.43	0.47	0.50	0.29	0.22	0.31	0.41	0.41
Cr2O3	0.00	0.00	0.00	0.00	0.00	0.00	0.00	0.00	0.00	0.00	0.00	0.00	0.00	0.00
total	86.10	87.36	87.14	87.52	87.47	88.61	86.39	87.81	87.44	87.30	86.22	87.71	87.70	86.70
number of cations based on 14 oxygen atoms (H2O free)														
Na	0.00	0.00	0.00	0.00	0.00	0.00	0.00	0.01	0.00	0.00	0.00	0.00	0.01	0.00
K	0.00	0.00	0.00	0.00	0.00	0.00	0.00	0.00	0.00	0.01	0.01	0.00	0.00	0.00
Ca	0.00	0.01	0.00	0.01	0.01	0.01	0.00	0.00	0.01	0.00	0.00	0.00	0.01	0.00
Si	2.62	2.63	2.63	2.60	2.61	2.62	2.61	2.61	2.62	2.59	2.63	2.63	2.66	2.66
AlIV	1.38	1.37	1.37	1.40	1.39	1.38	1.39	1.39	1.38	1.41	1.37	1.37	1.34	1.34
AlVI	1.55	1.52	1.50	1.49	1.58	1.54	1.57	1.59	1.61	1.59	1.58	1.55	1.61	1.56
Al tot.	2.93	2.89	2.87	2.89	2.97	2.92	2.96	2.98	2.98	3.00	2.95	2.92	2.95	2.90
Ti	0.00	0.00	0.00	0.00	0.01	0.01	0.00	0.00	0.01	0.00	0.00	0.00	0.00	0.01
Cr3+	0.00	0.00	0.00	0.00	0.00	0.00	0.00	0.00	0.00	0.00	0.00	0.00	0.00	0.00
Fe 2+	2.63	2.63	2.65	2.68	3.12	2.98	3.06	3.11	3.19	2.98	2.94	2.90	3.01	2.97
Mg	1.71	1.74	1.74	1.75	1.12	1.34	1.22	1.15	1.01	1.31	1.35	1.43	1.19	1.30
Mn	0.02	0.02	0.03	0.01	0.04	0.04	0.04	0.04	0.05	0.03	0.02	0.03	0.04	0.04
Kat tot	9.91	9.92	9.93	9.95	9.89	9.92	9.91	9.90	9.88	9.91	9.90	9.91	9.87	9.88
Vac=6-SuVI	0.09	0.09	0.08	0.06	0.14	0.10	0.10	0.11	0.15	0.10	0.11	0.10	0.15	0.13
Fe/(Fe+Mg)	0.61	0.60	0.60	0.60	0.74	0.69	0.72	0.73	0.76	0.69	0.68	0.67	0.72	0.69
Mg/(Mg+Fe)	0.39	0.40	0.40	0.40	0.26	0.31	0.28	0.27	0.24	0.31	0.32	0.33	0.28	0.31

Appendix B: Electron microprobe analyses of garnet; micaschist [sample M98/19]

sample	M98/19	M98/19	M98/19	M98/19	M98/19	M98/19	M98/19	M98/19	M98/19	M98/19	M98/19	M98/19	M98/19	M98/19	M98/19	M98/19	M98/19	M98/19	M98/19	M98/19	M98/19
analysis	grt1_1	grt1_2	grt1_3	grt1_4	grt1_5	grt1_6	grt1_7	grt1_8	grt1_9	grt1_10	grt1_11	grt1_12	grt1_13	grt1_14	grt1_15	grt1_16	grt1_17	grt1_18	grt1_19	grt1_20	grt1_21
SiO2	37.54	37.73	37.48	37.89	37.55	37.58	37.89	37.63	37.65	37.82	37.73	37.73	37.74	38.14	37.54	37.65	37.52	37.68	37.74	37.62	37.66
Al2O3	21.3	21.36	21.34	21.27	21.45	21.25	21.42	21.39	21.16	21.49	21.55	21.67	21.47	21.32	21.38	21.43	21.62	21.31	21.57	21.35	21.34
TiO2	0.03	0.02	0.02	0.01	0.01	0.02	0.01	0.01	0.02	0.00	0.00	0.01	0.00	0.00	0.04	0.01	0.01	0.02	0.01	0.00	0.00
FeO	29.29	30.89	31.4	29.9	31.27	30.34	30.95	31	31.03	30.27	28.27	31.5	30.34	30.98	29.73	30.75	31.09	30.09	30.79	29.84	29.77
MgO	2.96	3.79	4.11	4.07	4.43	4.31	4.75	4.36	4.63	4.56	3.95	5.14	4.33	4.56	4.47	4.81	4.8	4.45	4.52	3.77	4.24
CaO	5.66	3.32	2.66	4.29	2.55	3.73	2.33	2.49	2.26	2.99	5.68	1.56	3.28	2.64	3.51	2.25	2.11	3.35	2.41	4.28	3.91
MnO	2.97	2.85	2.9	2.62	2.83	2.67	2.74	2.79	2.81	2.67	2.48	2.79	2.73	2.74	2.67	2.73	2.76	2.68	2.75	2.65	2.65
total	99.75	99.96	99.91	100.05	100.09	99.9	100.09	99.67	99.56	99.8	99.66	100.4	99.89	100.38	99.34	99.63	99.91	99.58	99.79	99.51	99.57
FeO Ox	29.29	30.89	31.24	29.90	31.01	29.97	30.95	31.00	31.03	30.27	28.27	31.26	30.34	30.98	29.73	30.75	30.91	30.09	30.79	29.84	29.77
Fe2O3 Ox	0.00	0.00	0.17	0.00	0.29	0.41	0.00	0.00	0.00	0.00	0.00	0.27	0.00	0.00	0.00	0.00	0.20	0.00	0.00	0.00	0.00
total Ox	99.75	99.96	99.93	100.05	100.12	99.94	100.09	99.67	99.56	99.80	99.66	100.43	99.89	100.38	99.34	99.63	99.93	99.58	99.79	99.51	99.57
number of cations based on 12 oxygen atoms																					
Si	3.00	3.00	2.99	3.01	2.99	2.99	3.00	3.00	3.00	3.00	2.99	2.98	3.00	3.01	2.99	3.00	2.98	3.00	3.00	3.00	3.00
Al tot.	2.01	2.00	2.01	1.99	2.01	1.99	2.00	2.01	1.99	2.01	2.02	2.02	2.01	1.99	2.01	2.01	2.03	2.00	2.02	2.01	2.00
Ti	0.00	0.00	0.00	0.00	0.00	0.00	0.00	0.00	0.00	0.00	0.00	0.00	0.00	0.00	0.00	0.00	0.00	0.00	0.00	0.00	0.00
Fe tot.	1.96	2.06	2.09	1.98	2.08	2.02	2.05	2.07	2.07	2.01	1.88	2.08	2.02	2.05	1.98	2.05	2.07	2.00	2.05	1.99	1.98
Fe3+	0.00	0.00	0.01	0.00	0.02	0.02	0.00	0.00	0.00	0.00	0.00	0.02	0.00	0.00	0.00	0.00	0.01	0.00	0.00	0.00	0.00
Fe2+	1.96	2.06	2.08	1.98	2.06	1.99	2.05	2.07	2.07	2.01	1.88	2.07	2.02	2.05	1.98	2.05	2.05	2.00	2.05	1.99	1.98
Mg	0.35	0.45	0.49	0.48	0.52	0.51	0.56	0.52	0.55	0.54	0.47	0.61	0.51	0.54	0.53	0.57	0.57	0.53	0.54	0.45	0.50
Ca	0.48	0.28	0.23	0.36	0.22	0.32	0.20	0.21	0.19	0.25	0.48	0.13	0.28	0.22	0.30	0.19	0.18	0.29	0.21	0.37	0.33
Mn	0.20	0.19	0.20	0.18	0.19	0.18	0.18	0.19	0.19	0.18	0.17	0.19	0.18	0.18	0.18	0.18	0.19	0.18	0.19	0.18	0.18
total cat	8.00	7.99	8.01	8.00	8.01	8.01	8.00	8.00	8.00	7.99	8.00	8.01	8.00	7.99	8.00	8.00	8.01	8.00	7.99	7.99	8.00
andradite	0.00	0.00	0.79	0.00	1.30	1.84	0.00	0.00	0.00	0.00	0.00	1.20	0.00	0.00	0.00	0.00	0.90	0.00	0.00	0.00	0.00
pyrope	11.77	15.08	16.34	16.13	17.58	17.09	18.74	17.35	18.44	18.09	15.61	20.30	17.14	18.03	17.75	19.06	19.07	17.61	18.01	15.02	16.78
spessartine	6.71	6.45	6.55	5.90	6.38	6.02	6.14	6.31	6.36	6.02	5.57	6.26	6.14	6.16	6.02	6.15	6.23	6.03	6.23	6.00	5.96
grossular	16.18	9.50	6.81	12.22	5.97	8.80	6.61	7.12	6.47	8.53	16.14	3.23	9.33	7.50	10.02	6.41	5.12	9.53	6.90	12.26	11.13
almandine	65.34	68.98	69.50	65.75	68.76	66.25	68.51	69.22	68.73	67.37	62.69	69.00	67.39	68.32	66.21	68.38	68.68	66.83	68.85	66.72	66.13
% rest	0.19	0.50	0.40	0.55	0.59	0.49	0.18	0.43	0.48	0.52	0.27	0.70	0.29	0.58	0.22	0.24	0.71	0.06	0.84	0.45	0.07
Xprp = XMg	0.12	0.15	0.16	0.16	0.17	0.17	0.19	0.17	0.18	0.18	0.16	0.20	0.17	0.18	0.18	0.19	0.19	0.18	0.18	0.15	0.17
Xalm = XFe	0.65	0.69	0.70	0.66	0.69	0.67	0.69	0.69	0.69	0.67	0.63	0.69	0.67	0.68	0.66	0.68	0.69	0.67	0.69	0.67	0.66
Xsps = XMn	0.07	0.06	0.07	0.06	0.06	0.06	0.06	0.06	0.06	0.06	0.06	0.06	0.06	0.06	0.06	0.06	0.06	0.06	0.06	0.06	0.06
Xgrs = XCa	0.16	0.09	0.08	0.12	0.07	0.11	0.07	0.07	0.06	0.09	0.16	0.04	0.09	0.07	0.10	0.06	0.06	0.10	0.07	0.12	0.11
XAl	1.00	1.00	1.00	1.00	1.00	1.00	1.00	1.00	1.00	1.00	1.00	1.00	1.00	1.00	1.00	1.00	1.00	1.00	1.00	1.00	1.00

Appendix B: Electron microprobe analyses of garnet; micaschist [sample M98/19]

sample	M98/19	M98/19	M98/19	M98/19	M98/19	M98/19	M98/19	M98/19	M98/19	M98/19	M98/19	M98/19	M98/19	M98/19	M98/19	M98/19	M98/19	M98/19	M98/19	M98/19	M98/19
analysis	grt2_1	grt2_2	grt2_3	grt2_4	grt2_5	grt2_6	grt2_7	grt2_8	grt2_9	grt2_10	grt2_11	grt3_1	grt3_2	grt3_3	grt3_4	grt3_5	grt3_6	grt3_7	grt3_8	grt3_9	grt3_10
SiO2	37.77	37.78	37.62	37.67	37.63	37.73	37.72	37.67	37.42	37.83	37.05	37.49	37.77	37.52	37.74	37.77	37.89	37.98	37.67	37.52	37.46
Al2O3	21.48	21.51	21.38	21.47	21.33	21.56	21.24	21.21	21.24	21.33	20.92	21.34	21.31	21.42	21.30	21.37	21.52	21.37	21.36	21.28	21.53
TiO2	0.03	0.04	0.03	0.02	0.02	0.01	0.01	0.01	0.02	0.02	0.03	0.00	0.02	0.00	0.04	0.00	0.03	0.01	0.04	0.07	0.00
FeO	29.42	29.49	30.94	29.67	30.47	31.17	30.96	29.50	30.84	30.52	29.83	31.06	30.72	31.27	30.50	31.22	30.91	31.01	31.27	29.15	29.71
MgO	3.87	4.12	4.18	3.90	3.83	3.88	3.21	2.85	3.61	3.50	3.21	4.59	4.77	4.65	4.57	4.78	4.95	4.93	4.87	3.18	3.89
CaO	3.98	3.91	2.54	4.27	3.64	2.78	3.65	5.33	3.39	3.86	4.70	2.23	2.38	2.35	2.78	2.05	2.07	2.10	2.11	5.77	4.65
MnO	2.63	2.59	2.82	2.69	2.77	2.79	3.04	2.96	2.93	2.94	2.76	2.77	2.69	2.73	2.70	2.73	2.71	2.75	2.72	2.78	2.63
total	99.18	99.44	99.51	99.69	99.69	99.92	99.83	99.53	99.45	100.00	98.50	99.48	99.66	99.94	99.63	99.92	100.08	100.15	100.04	99.75	99.87
FeO Ox	29.42	29.49	30.94	29.67	30.47	31.17	30.96	29.50	30.84	30.52	29.80	31.01	30.72	30.96	30.50	31.22	30.91	31.01	31.05	29.08	29.39
Fe2O3 Ox	0.00	0.00	0.00	0.00	0.00	0.00	0.00	0.00	0.00	0.00	0.03	0.06	0.00	0.35	0.00	0.00	0.00	0.00	0.24	0.07	0.35
total Ox	99.18	99.44	99.51	99.69	99.69	99.92	99.83	99.53	99.45	100.00	98.50	99.48	99.66	99.97	99.63	99.92	100.08	100.15	100.06	99.76	99.90
number of cations based on 12 oxygen atoms																					
Si	3.01	3.01	3.00	3.00	3.00	3.00	3.01	3.01	3.00	3.01	3.00	2.99	3.00	2.99	3.00	3.00	3.00	3.01	2.99	2.99	2.98
Al tot.	2.02	2.02	2.01	2.01	2.01	2.02	2.00	2.00	2.01	2.00	2.00	2.01	2.00	2.01	2.00	2.00	2.01	1.99	2.00	2.00	2.02
Ti	0.00	0.00	0.00	0.00	0.00	0.00	0.00	0.00	0.00	0.00	0.00	0.00	0.00	0.00	0.00	0.00	0.00	0.00	0.00	0.00	0.00
Fe tot.	1.96	1.96	2.07	1.97	2.03	2.07	2.07	1.97	2.07	2.03	2.02	2.07	2.04	2.08	2.03	2.07	2.05	2.05	2.08	1.94	1.98
Fe3+	0.00	0.00	0.00	0.00	0.00	0.00	0.00	0.00	0.00	0.00	0.00	0.00	0.00	0.02	0.00	0.00	0.00	0.00	0.01	0.00	0.02
Fe2+	1.96	1.96	2.07	1.97	2.03	2.07	2.07	1.97	2.07	2.03	2.02	2.07	2.04	2.06	2.03	2.07	2.05	2.05	2.06	1.94	1.96
Mg	0.46	0.49	0.50	0.46	0.46	0.46	0.38	0.34	0.43	0.42	0.39	0.55	0.57	0.55	0.54	0.57	0.58	0.58	0.58	0.38	0.46
Ca	0.34	0.33	0.22	0.36	0.31	0.24	0.31	0.46	0.29	0.33	0.41	0.19	0.20	0.20	0.24	0.17	0.18	0.18	0.18	0.49	0.40
Mn	0.18	0.17	0.19	0.18	0.19	0.19	0.21	0.20	0.20	0.20	0.19	0.19	0.18	0.18	0.18	0.18	0.18	0.18	0.18	0.19	0.18
total cat	7.98	7.98	7.99	7.99	7.99	7.99	7.98	7.99	8.00	7.99	8.00	8.00	8.00	8.01	8.00	8.00	8.00	8.00	8.01	8.00	8.01
andradite	0.00	0.00	0.00	0.00	0.00	0.00	0.00	0.00	0.00	0.00	0.13	0.25	0.00	1.57	0.00	0.00	0.00	0.00	1.09	0.33	1.58
pyrope	15.65	16.51	16.74	15.51	15.25	15.55	12.87	11.44	14.43	13.96	12.91	18.25	18.89	18.47	18.12	18.87	19.55	19.44	19.27	12.63	15.48
spessartine	6.04	5.90	6.42	6.08	6.27	6.35	6.93	6.75	6.66	6.66	6.31	6.26	6.06	6.16	6.09	6.13	6.08	6.16	6.12	6.28	5.95
grossular	11.57	11.27	7.31	12.21	10.42	8.01	10.52	15.38	9.74	11.07	13.46	6.12	6.78	5.14	7.93	5.82	5.88	5.95	4.91	16.15	11.72
almandine	66.74	66.32	69.53	66.21	68.07	70.09	69.67	66.43	69.17	68.31	67.18	69.12	68.28	68.66	67.87	69.18	68.49	68.44	68.61	64.61	65.28
% rest	1.68	1.19	0.82	0.53	0.39	1.16	0.83	0.79	0.33	0.71	0.06	0.23	0.19	0.63	0.24	0.06	0.38	0.26	0.40	0.26	0.80
Xprp = XMg	0.16	0.17	0.17	0.16	0.15	0.16	0.13	0.11	0.14	0.14	0.13	0.18	0.19	0.18	0.18	0.19	0.20	0.19	0.19	0.13	0.15
Xalm = XFe	0.67	0.66	0.70	0.66	0.68	0.70	0.70	0.66	0.69	0.68	0.67	0.69	0.68	0.69	0.68	0.69	0.68	0.68	0.69	0.65	0.66
Xsps = XMn	0.06	0.06	0.06	0.06	0.06	0.06	0.07	0.07	0.07	0.07	0.06	0.06	0.06	0.06	0.06	0.06	0.06	0.06	0.06	0.06	0.06
Xgrs = XCa	0.12	0.11	0.07	0.12	0.10	0.08	0.11	0.15	0.10	0.11	0.14	0.06	0.07	0.07	0.08	0.06	0.06	0.06	0.06	0.16	0.13
XAl	1.00	1.00	1.00	1.00	1.00	1.00	1.00	1.00	1.00	1.00	1.00	1.00	1.00	1.00	1.00	1.00	1.00	1.00	1.00	1.00	1.00

Appendix B: Electron microprobe analyses of garnet; micaschist [sample M98/19]

sample	M98/19	M98/19	M98/19	M98/19	M98/19	M98/19	M98/19	M98/19	M98/19	M98/19	M98/19	M98/19	M98/19	M98/19	M98/19	M98/19	M98/19	M98/19	M98/19	M98/19	M98/19
analysis	grt4_1	grt4_2	grt4_3	grt4_4	grt4_5	grt4_6	grt4_7	grt4_8	grt4_9	grt4_10	grt4_11	grt4_12	grt4_13	grt4_14	grt4_15	grt5_1	grt5_2	grt5_3	grt5_4	grt5_5	grt5_6
SiO2	38.06	37.89	37.72	37.61	37.55	37.84	37.73	37.74	37.73	37.80	37.62	37.80	37.57	37.63	37.70	37.78	38.00	37.93	37.76	37.78	37.87
Al2O3	21.24	21.42	21.59	21.48	21.63	21.59	21.53	21.47	21.50	21.55	21.39	21.14	21.50	21.33	21.43	21.23	21.50	21.51	21.47	21.44	21.61
TiO2	0.03	0.02	0.02	0.04	0.02	0.01	0.00	0.02	0.05	0.00	0.01	0.02	0.00	0.03	0.00	0.00	0.01	0.00	0.02	0.01	0.00
FeO	30.78	31.32	31.27	30.77	31.13	31.35	31.02	30.95	30.88	30.33	30.71	30.72	31.01	30.94	30.79	30.14	31.14	30.94	31.08	30.28	30.97
MgO	4.14	4.49	4.55	4.41	4.52	4.56	4.38	4.33	4.31	4.12	4.19	4.34	4.44	4.40	4.49	3.85	4.34	4.27	4.21	3.90	4.08
CaO	2.63	2.20	2.12	2.56	2.37	2.24	2.36	2.68	2.45	3.24	2.58	2.70	2.56	2.72	2.29	3.49	2.32	2.45	2.52	3.61	2.86
MnO	2.82	2.77	2.79	2.72	2.75	2.75	2.85	2.82	2.79	2.80	2.80	2.72	2.76	2.71	2.74	2.72	2.78	2.86	2.85	2.80	2.89
total	99.70	100.11	100.06	99.59	99.97	100.34	99.87	100.01	99.71	99.84	99.30	99.44	99.84	99.76	99.44	99.21	100.09	99.96	99.91	99.82	100.28
FeO Ox	30.78	31.32	31.27	30.77	31.07	31.35	31.02	30.95	30.88	30.33	30.71	30.72	30.96	30.94	30.79	30.14	31.14	30.94	31.08	30.28	30.97
Fe2O3 Ox	0.00	0.00	0.00	0.00	0.07	0.00	0.00	0.00	0.00	0.00	0.00	0.00	0.06	0.00	0.00	0.00	0.00	0.00	0.00	0.00	0.00
total Ox	99.70	100.11	100.06	99.59	99.97	100.34	99.87	100.01	99.71	99.84	99.30	99.44	99.84	99.76	99.44	99.21	100.09	99.96	99.91	99.82	100.28
number of cations based on 12 oxygen atoms																					
Si	3.03	3.01	2.99	3.00	2.98	2.99	3.00	3.00	3.00	3.00	3.01	3.02	2.99	3.00	3.01	3.02	3.01	3.01	3.00	3.01	3.00
Al tot.	1.99	2.00	2.02	2.02	2.03	2.01	2.02	2.01	2.02	2.02	2.02	1.99	2.02	2.00	2.01	2.00	2.01	2.01	2.01	2.01	2.02
Ti	0.00	0.00	0.00	0.00	0.00	0.00	0.00	0.00	0.00	0.00	0.00	0.00	0.00	0.00	0.00	0.00	0.00	0.00	0.00	0.00	0.00
Fe tot.	2.05	2.08	2.08	2.05	2.07	2.08	2.06	2.06	2.06	2.02	2.05	2.05	2.06	2.06	2.05	2.02	2.06	2.05	2.07	2.01	2.05
Fe3+	0.00	0.00	0.00	0.00	0.00	0.00	0.00	0.00	0.00	0.00	0.00	0.00	0.00	0.00	0.00	0.00	0.00	0.00	0.00	0.00	0.00
Fe2+	2.05	2.08	2.08	2.05	2.06	2.08	2.06	2.06	2.06	2.02	2.05	2.05	2.06	2.06	2.05	2.02	2.06	2.05	2.07	2.01	2.05
Mg	0.49	0.53	0.54	0.52	0.54	0.54	0.52	0.51	0.51	0.49	0.50	0.52	0.53	0.52	0.53	0.46	0.51	0.51	0.50	0.46	0.48
Ca	0.22	0.19	0.18	0.22	0.20	0.19	0.20	0.23	0.21	0.28	0.22	0.23	0.22	0.23	0.20	0.30	0.20	0.21	0.21	0.31	0.24
Mn	0.19	0.19	0.19	0.18	0.19	0.18	0.19	0.19	0.19	0.19	0.19	0.18	0.19	0.18	0.19	0.18	0.19	0.19	0.19	0.19	0.19
total cat	7.97	7.99	8.00	7.99	8.00	8.00	7.99	8.00	7.99	7.99	7.98	7.99	8.00	8.00	7.99	7.98	7.98	7.98	7.99	7.99	7.99
andradite	0.00	0.00	0.00	0.00	0.30	0.00	0.00	0.00	0.00	0.00	0.00	0.00	0.25	0.00	0.00	0.00	0.00	0.00	0.00	0.00	0.00
pyrope	16.62	17.80	18.05	17.60	17.94	18.01	17.45	17.16	17.25	16.44	16.85	17.31	17.61	17.43	17.98	15.51	17.32	17.07	16.78	15.55	16.22
spessartine	6.44	6.24	6.29	6.17	6.20	6.17	6.45	6.35	6.35	6.35	6.40	6.17	6.22	6.10	6.24	6.23	6.30	6.50	6.46	6.35	6.53
grossular	7.59	6.27	6.05	7.34	6.46	6.36	6.76	7.64	7.05	9.30	7.46	7.74	7.05	7.75	6.59	10.11	6.66	7.04	7.22	10.35	8.17
almandine	69.35	69.68	69.61	68.89	69.09	69.46	69.34	68.85	69.35	67.91	69.29	68.77	68.86	68.73	69.19	68.15	69.72	69.40	69.53	67.75	69.08
% rest	1.26	0.51	0.57	0.71	0.57	0.39	0.75	0.40	1.05	0.95	1.07	0.48	0.36	0.10	0.93	1.16	1.09	1.14	0.78	0.77	0.85
Xprp = XMg	0.17	0.18	0.18	0.18	0.18	0.18	0.17	0.17	0.17	0.16	0.17	0.17	0.18	0.17	0.18	0.16	0.17	0.17	0.17	0.16	0.16
Xalm = XFe	0.69	0.70	0.70	0.69	0.69	0.69	0.69	0.69	0.69	0.68	0.69	0.69	0.69	0.69	0.69	0.68	0.70	0.69	0.70	0.68	0.69
Xsps = XMn	0.06	0.06	0.06	0.06	0.06	0.06	0.06	0.06	0.06	0.06	0.06	0.06	0.06	0.06	0.06	0.06	0.06	0.06	0.06	0.06	0.07
Xgrs = XCa	0.08	0.06	0.06	0.07	0.07	0.06	0.07	0.08	0.07	0.09	0.07	0.08	0.07	0.08	0.07	0.10	0.07	0.07	0.07	0.10	0.08
XAl	1.00	1.00	1.00	1.00	1.00	1.00	1.00	1.00	1.00	1.00	1.00	1.00	1.00	1.00	1.00	1.00	1.00	1.00	1.00	1.00	1.00

Appendix B: Electron microprobe analyses of garnet; micaschist [sample M98/19]

sample	M98/19	M98/19	M98/19	M98/19	M98/19	M98/19	M98/19	M98/19	M98/19	M98/19	M98/19	M98/19	M98/19	M98/19	M98/19	M98/19	M98/19	M98/19	M98/19	M98/19	M98/19
analysis	grt5_7	grt5_8	grt5_9	grt5_10	grt5_11	grt5_12	grt5_13	grt5_14	grt5_15	grt5_16	grt6_1	grt6_2	grt6_3	grt6_4	grt6_5	grt6_6	grt6_7	grt6_8	grt6_9	grt6_10	grt6_11
SiO2	37.83	37.90	37.96	37.88	37.74	37.72	37.97	38.08	38.01	38.24	38.03	37.44	37.64	37.53	38.05	37.78	38.01	38.07	38.25	38.48	38.48
Al2O3	21.63	21.47	21.69	21.44	21.55	21.54	21.45	21.51	21.56	21.73	23.01	22.78	22.52	22.66	22.74	22.64	22.87	22.92	22.97	23.12	22.98
TiO2	0.02	0.05	0.01	0.01	0.04	0.02	0.00	0.01	0.01	0.02	0.02	0.00	0.03	0.06	0.00	0.00	0.01	0.00	0.02	0.03	0.00
FeO	30.70	30.66	30.27	30.12	30.29	30.34	30.33	30.68	31.07	29.96	30.01	29.78	31.47	30.87	30.21	30.93	31.35	30.45	30.32	30.31	29.46
MgO	4.13	4.28	4.26	4.23	4.15	4.19	4.27	4.25	4.52	4.02	3.55	3.50	4.21	4.39	4.22	3.56	4.22	4.34	4.62	4.75	4.39
CaO	3.30	3.42	3.30	3.50	3.25	3.34	3.10	3.12	2.24	3.91	4.06	4.20	2.54	2.47	3.71	3.13	2.60	3.18	3.07	2.99	4.37
MnO	2.75	2.72	2.67	2.69	2.69	2.71	2.78	2.67	2.78	2.62	2.77	2.70	2.75	2.71	2.61	2.95	2.72	2.63	2.63	2.63	2.46
total	100.36	100.50	100.16	99.87	99.71	99.86	99.90	100.32	100.19	100.50	101.45	100.41	101.20	100.69	101.55	101.02	101.78	101.59	101.88	102.31	102.16
FeO Ox	30.70	30.62	30.27	30.12	30.29	30.34	30.33	30.68	31.07	29.96	30.01	29.78	31.47	30.87	30.21	30.93	31.35	30.45	30.32	30.31	29.46
Fe2O3 Ox	0.00	0.05	0.00	0.00	0.00	0.00	0.00	0.00	0.00	0.00	0.00	0.00	0.00	0.00	0.00	0.00	0.00	0.00	0.00	0.00	0.00
total Ox	100.36	100.50	100.16	99.87	99.71	99.86	99.90	100.32	100.19	100.50	101.45	100.40	101.16	100.69	101.54	100.99	101.78	101.59	101.88	102.31	102.14
number of cations based on 12 oxygen atoms																					
Si	2.99	3.00	3.00	3.01	3.00	3.00	3.01	3.01	3.01	3.01	2.97	2.95	2.96	2.95	2.96	2.97	2.96	2.96	2.96	2.96	2.97
Al tot.	2.02	2.00	2.02	2.01	2.02	2.02	2.01	2.00	2.01	2.02	2.12	2.12	2.09	2.10	2.09	2.10	2.10	2.10	2.10	2.10	2.09
Ti	0.00	0.00	0.00	0.00	0.00	0.00	0.00	0.00	0.00	0.00	0.00	0.00	0.00	0.00	0.00	0.00	0.00	0.00	0.00	0.00	0.00
Fe tot.	2.03	2.03	2.00	2.00	2.01	2.02	2.01	2.03	2.06	1.97	1.96	1.97	2.07	2.03	1.97	2.03	2.04	1.98	1.96	1.95	1.90
Fe3+	0.00	0.00	0.00	0.00	0.00	0.00	0.00	0.00	0.00	0.00	0.00	0.00	0.00	0.00	0.00	0.00	0.00	0.00	0.00	0.00	0.00
Fe2+	2.03	2.02	2.00	2.00	2.01	2.02	2.01	2.03	2.06	1.97	1.96	1.97	2.07	2.03	1.97	2.03	2.04	1.98	1.96	1.95	1.90
Mg	0.49	0.50	0.50	0.50	0.49	0.50	0.50	0.50	0.53	0.47	0.41	0.41	0.49	0.51	0.49	0.42	0.49	0.50	0.53	0.55	0.50
Ca	0.28	0.29	0.28	0.30	0.28	0.28	0.26	0.26	0.19	0.33	0.34	0.36	0.21	0.21	0.31	0.26	0.22	0.27	0.25	0.25	0.36
Mn	0.18	0.18	0.18	0.18	0.18	0.18	0.19	0.18	0.19	0.17	0.18	0.18	0.18	0.18	0.17	0.20	0.18	0.17	0.17	0.17	0.16
total cat	8.00	8.00	7.99	7.99	7.99	7.99	7.99	7.99	7.99	7.98	7.98	7.99	8.00	7.99	7.99	7.98	7.99	7.99	7.99	7.98	7.99
andradite	0.00	0.20	0.00	0.00	0.00	0.00	0.00	0.00	0.00	0.00	0.00	0.00	0.00	0.00	0.00	0.00	0.00	0.00	0.00	0.00	0.00
pyrope	16.33	16.83	16.95	16.80	16.59	16.66	17.01	16.85	17.97	15.99	14.27	14.13	16.67	17.54	16.66	14.33	16.73	17.22	18.23	18.70	17.24
spessartine	6.18	6.08	6.04	6.07	6.11	6.12	6.30	6.02	6.28	5.92	6.33	6.20	6.19	6.15	5.86	6.75	6.13	5.93	5.90	5.88	5.49
grossular	9.38	9.47	9.44	9.99	9.34	9.55	8.88	8.89	6.40	11.19	11.73	12.19	7.23	7.10	10.53	9.06	7.41	9.07	8.71	8.46	12.34
almandine	68.11	67.42	67.58	67.13	67.95	67.68	67.81	68.25	69.34	66.89	67.68	67.48	69.91	69.21	66.94	69.86	69.73	67.78	67.15	66.96	64.93
% rest	0.51	0.17	1.09	0.62	1.04	0.64	0.91	0.78	0.97	1.43	3.29	2.75	1.46	2.09	1.91	2.72	2.26	2.41	2.34	2.57	2.25
Xprp = XMg	0.16	0.17	0.17	0.17	0.17	0.17	0.17	0.17	0.18	0.16	0.14	0.14	0.17	0.18	0.17	0.14	0.17	0.17	0.18	0.19	0.17
Xalm = XFe	0.68	0.67	0.68	0.67	0.68	0.68	0.68	0.68	0.69	0.67	0.68	0.67	0.70	0.69	0.67	0.70	0.70	0.68	0.67	0.67	0.65
Xsps = XMn	0.06	0.06	0.06	0.06	0.06	0.06	0.06	0.06	0.06	0.06	0.06	0.06	0.06	0.06	0.06	0.07	0.06	0.06	0.06	0.06	0.05
Xgrs = XCa	0.09	0.10	0.09	0.10	0.09	0.10	0.09	0.09	0.06	0.11	0.12	0.12	0.07	0.07	0.11	0.09	0.07	0.09	0.09	0.08	0.12
XAl	1.00	1.00	1.00	1.00	1.00	1.00	1.00	1.00	1.00	1.00	1.00	1.00	1.00	1.00	1.00	1.00	1.00	1.00	1.00	1.00	1.00

Appendix B: Electron microprobe analyses of garnet; micaschist [sample M98/19] and grt-ky-st-schist [M98/22]

sample	M98/19	M98/19	M98/19	M98/19	M98/19	M98/19	M98/19	M98/19	M98/19	M98/19	M98/19	M98/19	M98/19	M98/19	M98/19	M98/22	M98/22	M98/22	M98/22	M98/22
analysis	grt6_12	grt6_13	grt6_14	grt7_1	grt7_2	grt7_3	grt7_4	grt7_5	grt7_6	grt7_7	grt7_8	grt7_9	grt7_10	grt7_11	grt7_12	grt1_1	grt1_2	grt1_3	grt1_4	grt1_5
SiO2	38.60	38.23	38.32	37.48	38.38	38.24	38.48	38.37	38.36	38.52	38.34	38.67	38.59	38.85	36.53	37.80	37.89	38.08	37.96	38.11
Al2O3	23.11	22.84	22.91	22.37	23.11	22.98	23.12	23.19	23.18	23.14	22.93	23.09	23.15	23.32	21.72	21.44	21.17	21.44	21.24	21.52
TiO2	0.01	0.01	0.02	0.01	0.01	0.01	0.04	0.04	0.00	0.01	0.03	0.02	0.02	0.03	0.03	0.00	0.00	0.00	0.01	0.05
FeO	30.87	30.68	28.46	28.83	29.02	31.25	30.29	30.09	28.72	28.44	28.14	30.66	31.01	29.54	29.24	34.61	32.53	32.06	32.44	32.28
MgO	4.85	4.73	2.88	3.38	3.70	4.35	4.34	4.18	3.85	4.00	4.10	4.74	4.62	4.25	3.65	5.50	5.76	5.48	5.70	5.48
CaO	2.65	2.57	6.51	4.91	5.04	2.52	2.78	3.25	5.43	5.45	5.52	2.73	2.34	3.75	4.46	0.89	2.51	2.88	2.50	3.22
MnO	2.61	2.63	2.64	2.67	2.64	2.71	2.66	2.64	2.47	2.45	2.45	2.70	2.75	2.56	2.50	0.46	0.46	0.45	0.47	0.47
total	102.70	101.75	101.77	99.67	101.91	102.09	101.72	101.80	102.04	102.04	101.51	102.65	102.52	102.33	98.20	100.70	100.32	100.39	100.32	101.12
FeO Ox	30.87	30.68	28.46	28.83	29.02	31.25	30.29	30.09	28.72	28.44	28.14	30.66	31.01	29.54	29.05	34.06	31.75	31.77	31.85	31.59
Fe2O3 Ox	0.00	0.00	0.00	0.00	0.00	0.00	0.00	0.00	0.00	0.00	0.00	0.00	0.00	0.00	0.21	0.61	0.87	0.32	0.65	0.77
total Ox	102.70	101.69	101.74	99.65	101.90	102.06	101.71	101.76	102.01	102.01	101.51	102.61	102.48	102.30	98.15	100.76	100.41	100.42	100.38	101.21
number of cations based on 12 oxygen atoms																				
Si	2.97	2.97	2.98	2.97	2.97	2.97	2.98	2.97	2.96	2.97	2.97	2.97	2.97	2.98	2.96	2.98	2.99	3.00	2.99	2.98
Al tot.	2.09	2.09	2.10	2.09	2.11	2.10	2.11	2.12	2.11	2.10	2.09	2.09	2.10	2.11	2.07	2.00	1.97	1.99	1.97	1.99
Ti	0.00	0.00	0.00	0.00	0.00	0.00	0.00	0.00	0.00	0.00	0.00	0.00	0.00	0.00	0.00	0.00	0.00	0.00	0.00	0.00
Fe tot.	1.98	1.99	1.85	1.91	1.88	2.03	1.96	1.95	1.86	1.83	1.82	1.97	2.00	1.90	1.98	2.29	2.15	2.11	2.14	2.11
Fe3+	0.00	0.00	0.00	0.00	0.00	0.00	0.00	0.00	0.00	0.00	0.00	0.00	0.00	0.00	0.01	0.04	0.05	0.02	0.04	0.05
Fe2+	1.98	1.99	1.85	1.91	1.88	2.03	1.96	1.95	1.86	1.83	1.82	1.97	2.00	1.90	1.97	2.25	2.10	2.09	2.10	2.07
Mg	0.56	0.55	0.33	0.40	0.43	0.50	0.50	0.48	0.44	0.46	0.47	0.54	0.53	0.49	0.44	0.65	0.68	0.64	0.67	0.64
Ca	0.22	0.21	0.54	0.42	0.42	0.21	0.23	0.27	0.45	0.45	0.46	0.22	0.19	0.31	0.39	0.08	0.21	0.24	0.21	0.27
Mn	0.17	0.17	0.17	0.18	0.17	0.18	0.17	0.17	0.16	0.16	0.16	0.18	0.18	0.17	0.17	0.03	0.03	0.03	0.03	0.03
total cat	7.99	7.99	7.97	7.98	7.98	7.98	7.96	7.97	7.98	7.98	7.98	7.98	7.98	7.96	8.01	8.02	8.03	8.01	8.02	8.02
andradite	0.00	0.00	0.00	0.00	0.00	0.00	0.00	0.00	0.00	0.00	0.00	0.00	0.00	0.00	0.98	2.52	3.88	1.44	2.90	3.40
pyrope	18.97	18.70	11.51	13.74	14.74	17.24	17.47	16.79	15.23	15.83	16.24	18.63	18.28	17.01	14.89	21.68	22.66	21.45	22.38	21.43
spessartine	5.80	5.91	5.99	6.17	5.98	6.10	6.08	6.03	5.55	5.51	5.51	6.03	6.19	5.83	5.80	1.03	1.03	1.00	1.05	1.04
grossular	7.45	7.31	18.70	14.35	14.43	7.18	8.04	9.38	15.45	15.51	15.72	7.71	6.66	10.79	12.11	0.00	3.22	6.66	4.15	5.65
almandine	67.77	68.08	63.80	65.75	64.86	69.48	68.41	67.81	63.77	63.16	62.53	67.62	68.87	66.37	66.23	74.76	69.22	69.45	69.52	68.47
% rest	2.27	2.28	3.09	2.73	3.17	2.57	3.94	3.78	2.81	2.94	2.59	2.61	3.03	4.17	1.55	0.75	0.67	0.25	0.48	0.88
Xprp = XMg	0.19	0.19	0.12	0.14	0.15	0.17	0.17	0.17	0.15	0.16	0.16	0.19	0.18	0.17	0.15	0.21	0.22	0.21	0.22	0.21
Xalm = XFe	0.68	0.68	0.64	0.66	0.65	0.69	0.68	0.68	0.64	0.63	0.63	0.68	0.69	0.66	0.66	0.75	0.70	0.70	0.70	0.69
Xsps = XMn	0.06	0.06	0.06	0.06	0.06	0.06	0.06	0.06	0.06	0.06	0.06	0.06	0.06	0.06	0.06	0.01	0.01	0.01	0.01	0.01
Xgrs = XCa	0.07	0.07	0.19	0.14	0.14	0.07	0.08	0.09	0.15	0.16	0.16	0.08	0.07	0.11	0.13	0.02	0.07	0.08	0.07	0.09
XAl	1.00	1.00	1.00	1.00	1.00	1.00	1.00	1.00	1.00	1.00	1.00	1.00	1.00	1.00	1.00	1.00	1.00	1.00	1.00	1.00

Appendix B: Electron microprobe analyses of garnet; grt-st-ky-schist [sample M98/22]

sample	M98/22	M98/22	M98/22	M98/22	M98/22	M98/22	M98/22	M98/22	M98/22	M98/22	M98/22	M98/22	M98/22	M98/22	M98/22	M98/22	M98/22	M98/22	M98/22	M98/22	M98/22
analysis	grt1_6	grt1_7	grt1_8	grt1_9	grt1_10	grt2_1	grt2_2	grt2_3	grt2_4	grt2_5	grt2_6	grt2_7	grt2_8	grt2_9	grt2_10	grt3_1	grt3_2	grt3_3	grt3_4	grt3_5	grt3_6
SiO2	38.22	38.03	38.01	38.22	37.71	37.70	37.69	37.81	37.95	37.99	38.12	37.88	37.68	37.83	39.03	37.61	37.97	37.93	37.97	38.00	37.93
Al2O3	21.57	21.47	21.49	21.56	21.38	21.28	21.49	21.27	21.47	21.51	21.54	21.23	21.38	21.24	21.01	21.47	21.49	21.70	21.62	21.48	21.65
TiO2	0.03	0.03	0.01	0.02	0.01	0.01	0.00	0.00	0.02	0.00	0.01	0.02	0.01	0.00	0.01	0.02	0.00	0.00	0.01	0.05	0.03
FeO	32.18	32.30	32.50	33.21	35.06	35.65	35.09	32.69	33.51	33.04	32.59	33.13	34.15	33.75	36.35	35.36	35.03	33.77	32.91	31.94	32.44
MgO	5.54	5.62	5.60	5.37	5.23	4.75	5.09	4.94	5.29	5.20	4.86	4.73	4.70	4.24	3.85	4.43	5.16	5.10	5.24	4.91	5.28
CaO	3.21	2.83	2.47	2.29	0.73	0.73	0.85	3.42	2.19	2.73	3.38	3.28	2.08	3.22	0.85	0.75	0.84	1.96	2.73	3.78	2.95
MnO	0.45	0.48	0.43	0.44	0.49	0.50	0.49	0.43	0.47	0.48	0.46	0.45	0.50	0.46	0.57	0.52	0.48	0.45	0.46	0.44	0.43
total	101.20	100.77	100.51	101.11	100.61	100.62	100.70	100.56	100.90	100.95	100.97	100.72	100.50	100.74	101.67	100.16	100.97	100.91	100.94	100.60	100.71
FeO Ox	31.58	31.68	32.08	32.91	34.58	35.34	34.64	31.95	32.96	32.46	32.28	32.52	33.73	33.31	36.35	35.36	34.77	33.45	32.37	31.61	31.98
Fe2O3 Ox	0.66	0.69	0.46	0.33	0.53	0.35	0.50	0.82	0.61	0.64	0.34	0.67	0.47	0.49	0.00	0.00	0.29	0.35	0.59	0.37	0.51
total Ox	101.26	100.83	100.55	101.14	100.66	100.65	100.75	100.64	100.96	101.01	100.99	100.79	100.55	100.79	101.67	100.16	101.00	100.94	101.00	100.64	100.76
number of cations based on 12 oxygen atoms																					
Si	2.99	2.98	2.99	2.99	2.99	2.99	2.98	2.99	2.99	2.98	2.99	2.99	2.99	2.99	3.07	3.00	2.99	2.98	2.98	2.99	2.98
Al tot.	1.99	1.99	1.99	1.99	2.00	1.99	2.00	1.98	1.99	1.99	1.99	1.98	2.00	1.98	1.95	2.02	2.00	2.01	2.00	1.99	2.01
Ti	0.00	0.00	0.00	0.00	0.00	0.00	0.00	0.00	0.00	0.00	0.00	0.00	0.00	0.00	0.00	0.00	0.00	0.00	0.00	0.00	0.00
Fe tot.	2.10	2.12	2.14	2.18	2.32	2.37	2.32	2.16	2.20	2.17	2.14	2.19	2.26	2.23	2.39	2.36	2.31	2.22	2.16	2.10	2.13
Fe3+	0.04	0.04	0.03	0.02	0.03	0.02	0.03	0.05	0.04	0.04	0.02	0.04	0.03	0.03	0.00	0.00	0.02	0.02	0.04	0.02	0.03
Fe2+	2.06	2.08	2.11	2.16	2.29	2.35	2.29	2.11	2.17	2.13	2.12	2.15	2.24	2.20	2.39	2.36	2.29	2.20	2.13	2.08	2.10
Mg	0.64	0.66	0.66	0.63	0.62	0.56	0.60	0.58	0.62	0.61	0.57	0.56	0.56	0.50	0.45	0.53	0.61	0.60	0.61	0.58	0.62
Ca	0.27	0.24	0.21	0.19	0.06	0.06	0.07	0.29	0.18	0.23	0.28	0.28	0.18	0.27	0.07	0.06	0.07	0.17	0.23	0.32	0.25
Mn	0.03	0.03	0.03	0.03	0.03	0.03	0.03	0.03	0.03	0.03	0.03	0.03	0.03	0.03	0.04	0.04	0.03	0.03	0.03	0.03	0.03
total cat	8.02	8.02	8.01	8.01	8.02	8.01	8.01	8.02	8.02	8.02	8.01	8.02	8.01	8.01	7.96	7.99	8.01	8.01	8.02	8.01	8.01
andradite	2.93	3.06	2.05	1.45	2.07	1.56	2.26	3.65	2.72	2.86	1.51	3.00	2.11	2.20	0.00	0.00	1.28	1.56	2.65	1.64	2.26
pyrope	21.60	22.02	21.96	20.94	20.67	18.78	20.13	19.47	20.77	20.40	19.00	18.61	18.59	16.70	15.44	17.64	20.25	20.04	20.57	19.26	20.75
spessartine	1.00	1.07	0.96	0.98	1.10	1.12	1.10	0.96	1.05	1.07	1.02	1.01	1.12	1.03	1.30	1.18	1.07	1.00	1.03	0.98	0.96
grossular	6.07	4.92	4.91	4.97	0.00	0.51	0.15	6.04	3.46	4.84	8.00	6.28	3.81	6.92	2.45	2.15	1.09	3.98	5.06	9.02	6.07
almandine	68.40	68.93	70.12	71.67	76.16	78.02	76.36	69.87	71.99	70.83	70.48	71.11	74.37	73.15	80.81	79.03	76.31	73.42	70.70	69.10	69.96
% rest	0.72	0.76	0.52	0.33	0.67	0.36	0.77	0.78	0.72	0.74	0.37	0.55	0.62	0.37	2.23	0.57	0.34	0.68	0.84	0.47	0.84
Xprp = XMg	0.21	0.22	0.22	0.21	0.20	0.19	0.20	0.19	0.20	0.20	0.19	0.18	0.18	0.16	0.15	0.18	0.20	0.20	0.20	0.19	0.20
Xalm = XFe	0.69	0.70	0.71	0.72	0.77	0.78	0.77	0.71	0.73	0.71	0.71	0.72	0.75	0.74	0.81	0.79	0.77	0.74	0.71	0.69	0.70
Xsps = XMn	0.01	0.01	0.01	0.01	0.01	0.01	0.01	0.01	0.01	0.01	0.01	0.01	0.01	0.01	0.01	0.01	0.01	0.01	0.01	0.01	0.01
Xgrs = XCa	0.09	0.08	0.07	0.06	0.02	0.02	0.02	0.09	0.06	0.08	0.09	0.09	0.06	0.09	0.02	0.02	0.02	0.05	0.08	0.11	0.08
XAl	1.00	1.00	1.00	1.00	1.00	1.00	1.00	1.00	1.00	1.00	1.00	1.00	1.00	1.00	1.00	1.00	1.00	1.00	1.00	1.00	1.00

Appendix B: Electron microprobe analyses of garnet; grt-st-ky-schist [sample M98/22]

sample	M98/22	M98/22	M98/22	M98/22	M98/22	M98/22	M98/22	M98/22	M98/22	M98/22	M98/22	M98/22	M98/22	M98/22	M98/22	M98/22	M98/22	M98/22	M98/22	M98/22	M98/22
analysis	grt3_7	grt3_8	grt3_9	grt3_10	grt3_11	grt4_1	grt4_2	grt4_3	grt4_4	grt4_5	grt4_6	grt4_7	grt4_8	grt4_9	grt5_1	grt5_2	grt5_3	grt5_4	grt5_5	grt5_6	grt5_7
SiO2	37.80	38.09	37.93	37.83	37.73	37.77	37.94	37.88	37.83	37.67	37.84	37.74	37.64	37.42	37.76	37.22	37.51	37.57	37.27	37.66	37.37
Al2O3	21.62	21.60	21.42	21.35	21.51	21.71	21.76	21.56	21.60	21.56	21.50	21.59	21.39	21.56	21.36	21.19	21.58	21.25	21.43	21.42	21.33
TiO2	0.03	0.04	0.01	0.00	0.00	0.00	0.00	0.00	0.02	0.00	0.00	0.01	0.01	0.00	0.01	0.02	0.03	0.04	0.03	0.02	0.03
FeO	32.62	33.31	33.91	35.21	35.66	34.69	34.53	34.69	34.88	34.53	32.88	34.41	34.92	34.79	34.20	35.33	35.20	32.91	33.36	34.44	35.48
MgO	5.42	5.41	4.86	5.05	4.56	5.09	5.32	5.39	5.33	5.48	5.10	5.40	5.23	4.97	4.02	4.52	4.82	4.34	4.31	4.69	4.68
CaO	2.65	2.23	2.25	0.80	0.85	0.99	1.01	1.10	0.93	0.90	2.79	1.36	1.01	0.87	2.35	1.05	0.94	3.33	3.20	1.53	0.92
MnO	0.46	0.47	0.52	0.49	0.55	0.47	0.51	0.47	0.50	0.48	0.43	0.47	0.48	0.50	0.53	0.53	0.50	0.45	0.49	0.51	0.50
total	100.60	101.15	100.91	100.73	100.86	100.72	101.08	101.09	101.10	100.62	100.54	100.97	100.69	100.11	100.23	99.86	100.57	99.90	100.09	100.27	100.31
FeO Ox	32.01	32.84	33.50	34.88	35.45	34.46	34.22	34.10	34.33	33.93	32.39	33.66	34.25	34.44	34.20	34.83	34.78	32.64	32.66	34.29	34.95
Fe2O3 Ox	0.68	0.52	0.46	0.37	0.24	0.25	0.34	0.66	0.61	0.66	0.54	0.83	0.74	0.39	0.00	0.55	0.46	0.30	0.77	0.17	0.59
total Ox	100.67	101.20	100.94	100.77	100.88	100.74	101.10	101.15	101.15	100.68	100.59	101.06	100.75	100.15	100.23	99.91	100.62	99.92	100.17	100.28	100.37
number of cations based on 12 oxygen atoms																					
Si	2.98	2.98	2.99	2.99	2.99	2.98	2.98	2.98	2.98	2.98	2.98	2.97	2.98	2.98	3.00	2.98	2.98	2.99	2.97	2.99	2.98
Al tot.	2.01	2.00	1.99	1.99	2.01	2.02	2.02	2.00	2.00	2.01	2.00	2.00	2.00	2.02	2.00	2.00	2.02	1.99	2.01	2.01	2.00
Ti	0.00	0.00	0.00	0.00	0.00	0.00	0.00	0.00	0.00	0.00	0.00	0.00	0.00	0.00	0.00	0.00	0.00	0.00	0.00	0.00	0.00
Fe tot.	2.15	2.18	2.24	2.33	2.36	2.29	2.27	2.28	2.30	2.28	2.17	2.27	2.31	2.31	2.28	2.37	2.34	2.19	2.22	2.29	2.36
Fe3+	0.04	0.03	0.03	0.02	0.01	0.02	0.02	0.04	0.04	0.04	0.03	0.05	0.04	0.02	0.00	0.03	0.03	0.02	0.05	0.01	0.04
Fe2+	2.11	2.15	2.21	2.31	2.35	2.28	2.25	2.24	2.26	2.24	2.14	2.22	2.27	2.29	2.28	2.33	2.31	2.17	2.18	2.28	2.33
Mg	0.64	0.63	0.57	0.60	0.54	0.60	0.62	0.63	0.63	0.65	0.60	0.63	0.62	0.59	0.48	0.54	0.57	0.51	0.51	0.56	0.56
Ca	0.22	0.19	0.19	0.07	0.07	0.08	0.09	0.09	0.08	0.08	0.24	0.11	0.09	0.07	0.20	0.09	0.08	0.28	0.27	0.13	0.08
Mn	0.03	0.03	0.03	0.03	0.04	0.03	0.03	0.03	0.03	0.03	0.03	0.03	0.03	0.03	0.04	0.04	0.03	0.03	0.03	0.03	0.03
total cat	8.02	8.02	8.01	8.01	8.01	8.01	8.01	8.02	8.02	8.02	8.02	8.02	8.02	8.01	7.99	8.02	8.01	8.01	8.02	8.01	8.02
andradite	3.04	2.32	2.04	1.65	1.06	1.14	1.51	2.94	2.63	2.56	2.43	3.71	2.88	1.76	0.00	2.51	2.08	1.36	3.52	0.75	2.64
pyrope	21.37	21.17	19.10	19.89	18.01	20.08	20.90	21.21	21.00	21.68	20.09	21.32	20.71	19.79	15.95	18.10	19.15	17.22	17.23	18.56	18.66
spessartine	1.03	1.05	1.16	1.10	1.23	1.05	1.14	1.05	1.12	1.08	0.96	1.05	1.08	1.13	1.20	1.21	1.13	1.01	1.11	1.15	1.13
grossular	4.48	3.96	4.31	0.62	1.36	1.67	1.35	0.17	0.00	0.00	5.47	0.15	0.00	0.73	6.70	0.51	0.60	8.14	5.68	3.60	0.00
almandine	70.09	71.51	73.39	76.74	78.34	76.05	75.11	74.63	75.25	74.68	71.05	73.76	75.34	76.58	76.15	77.67	77.04	72.27	72.45	75.94	77.56
% rest	1.08	0.70	0.49	0.36	0.47	0.69	0.73	0.89	0.95	1.04	0.72	1.22	0.97	0.90	0.35	0.82	0.99	0.40	1.33	0.36	0.94
Xprp = XMg	0.21	0.21	0.19	0.20	0.18	0.20	0.21	0.21	0.21	0.21	0.20	0.21	0.20	0.20	0.16	0.18	0.19	0.17	0.17	0.18	0.18
Xalm = XFe	0.71	0.72	0.74	0.77	0.78	0.76	0.75	0.75	0.76	0.75	0.72	0.74	0.76	0.77	0.76	0.78	0.77	0.73	0.73	0.76	0.78
Xsps = XMn	0.01	0.01	0.01	0.01	0.01	0.01	0.01	0.01	0.01	0.01	0.01	0.01	0.01	0.01	0.01	0.01	0.01	0.01	0.01	0.01	0.01
Xgrs = XCa	0.07	0.06	0.06	0.02	0.02	0.03	0.03	0.03	0.03	0.03	0.08	0.04	0.03	0.02	0.07	0.03	0.03	0.09	0.09	0.04	0.03
XAl	1.00	1.00	1.00	1.00	1.00	1.00	1.00	1.00	1.00	1.00	1.00	1.00	1.00	1.00	1.00	1.00	1.00	1.00	1.00	1.00	1.00

Appendix B: Electron microprobe analyses of garnet; grt-st-ky-schist [sample M98/22]

sample	M98/22	M98/22	M98/22	M98/22	M98/22	M98/22	M98/22	M98/22	M98/22	M98/22	M98/22	M98/22	8-5	8-5	8-5	8-5	8-5	8-5	8-5	8-5
analysis	grt5_8	grt5_9	grt6_1	grt6_2	grt6_3	grt6_4	grt6_5	grt6_6	grt6_7	grt6_8	grt6_9	grt6_10	grt1_1	grt1_2	grt1_3	grt1_4	grt1_5	grt1_6	grt1_7	grt1_8
SiO2	37.57	37.29	37.66	37.64	37.52	37.50	37.69	37.71	37.50	37.84	37.85	37.61	38.77	38.57	38.45	38.96	38.78	38.95	39.05	38.77
Al2O3	21.47	21.44	21.41	21.61	21.23	21.44	21.33	21.25	21.45	21.52	21.49	21.55	21.58	21.75	21.42	21.26	21.33	21.28	21.24	21.38
TiO2	0.01	0.01	0.02	0.00	0.01	0.01	0.02	0.01	0.00	0.01	0.00	0.03	0.04	0.03	0.06	0.07	0.08	0.00	0.03	0.08
FeO	35.72	35.75	34.73	34.49	33.65	34.76	33.73	34.06	33.54	34.49	34.73	35.29	32.54	32.19	32.52	32.53	32.31	32.61	32.92	33.47
MgO	4.73	4.16	5.22	5.50	4.77	5.38	4.68	5.13	5.20	5.58	5.40	4.63	7.52	7.41	7.41	7.12	7.02	6.85	6.63	6.50
CaO	0.76	1.08	0.92	1.20	2.36	0.94	2.58	1.84	2.22	0.94	1.19	0.89	1.04	1.02	0.97	0.94	0.91	0.87	0.96	0.97
MnO	0.52	0.55	0.50	0.51	0.47	0.47	0.52	0.51	0.47	0.46	0.45	0.53	0.11	0.05	0.03	0.04	0.05	0.00	0.05	0.00
total	100.78	100.28	100.46	100.95	100.01	100.51	100.55	100.51	100.38	100.85	101.12	100.54	101.62	101.03	100.85	100.93	100.53	100.57	100.93	101.21
FeO Ox	35.24	35.41	34.28	33.60	33.13	33.97	33.18	33.41	32.68	33.92	34.01	35.14	31.88	31.78	31.87	32.53	32.31	32.61	32.92	33.47
Fe2O3 Ox	0.53	0.38	0.50	0.99	0.58	0.87	0.61	0.72	0.95	0.63	0.80	0.16	0.73	0.45	0.72	0.00	0.00	0.00	0.00	0.00
total Ox	100.83	100.32	100.51	101.05	100.07	100.59	100.61	100.58	100.47	100.90	101.19	100.54	101.66	101.06	100.92	100.92	100.49	100.55	100.88	101.16
number of cations based on 12 oxygen atoms																				
Si	2.98	2.98	2.98	2.97	2.99	2.97	2.98	2.99	2.97	2.98	2.98	2.99	2.99	2.99	2.99	3.03	3.02	3.04	3.04	3.02
Al tot.	2.01	2.02	2.00	2.01	1.99	2.00	1.99	1.98	2.00	2.00	1.99	2.02	1.96	1.99	1.97	1.95	1.96	1.96	1.95	1.96
Ti	0.00	0.00	0.00	0.00	0.00	0.00	0.00	0.00	0.00	0.00	0.00	0.00	0.00	0.00	0.00	0.00	0.00	0.00	0.00	0.00
Fe tot.	2.37	2.39	2.30	2.27	2.24	2.30	2.23	2.26	2.22	2.27	2.29	2.34	2.10	2.09	2.12	2.11	2.11	2.13	2.14	2.18
Fe3+	0.03	0.02	0.03	0.06	0.03	0.05	0.04	0.04	0.06	0.04	0.05	0.01	0.04	0.03	0.04	0.00	0.00	0.00	0.00	0.00
Fe2+	2.34	2.37	2.27	2.21	2.21	2.25	2.20	2.21	2.16	2.24	2.24	2.33	2.06	2.06	2.07	2.11	2.11	2.13	2.14	2.18
Mg	0.56	0.50	0.62	0.65	0.57	0.64	0.55	0.61	0.61	0.66	0.63	0.55	0.87	0.86	0.86	0.82	0.82	0.80	0.77	0.75
Ca	0.06	0.09	0.08	0.10	0.20	0.08	0.22	0.16	0.19	0.08	0.10	0.08	0.09	0.09	0.08	0.08	0.08	0.07	0.08	0.08
Mn	0.03	0.04	0.03	0.03	0.03	0.03	0.03	0.03	0.03	0.03	0.03	0.04	0.01	0.00	0.00	0.00	0.00	0.00	0.00	0.00
total cat	8.02	8.01	8.01	8.03	8.02	8.03	8.02	8.02	8.03	8.02	8.02	8.00	8.02	8.01	8.02	8.00	7.99	7.99	7.98	8.00
andradite	2.17	1.71	2.23	3.42	2.60	2.69	2.72	3.25	4.31	2.66	3.37	0.73	2.86	1.98	2.69	0.00	0.00	0.00	0.00	0.00
pyrope	18.76	16.63	20.66	21.78	18.95	21.38	18.51	20.27	20.67	21.98	21.26	18.35	28.91	28.63	28.72	28.22	27.74	27.13	26.31	25.62
spessartine	1.17	1.25	1.12	1.15	1.06	1.06	1.17	1.15	1.06	1.03	1.01	1.19	0.23	0.10	0.07	0.09	0.12	0.00	0.12	0.00
grossular	0.00	1.40	0.39	0.00	4.14	0.00	4.61	1.98	2.04	0.00	0.00	1.80	0.00	0.86	0.00	2.68	2.60	2.46	2.73	2.74
almandine	77.90	79.02	75.60	73.66	73.25	74.87	72.99	73.35	71.93	74.33	74.36	77.92	68.00	68.42	68.52	69.00	69.55	70.41	70.85	71.64
% rest	0.87	0.85	0.72	1.48	0.68	1.26	0.72	0.73	1.35	0.85	0.98	0.56	0.45	0.47	0.50	2.60	1.86	2.05	2.37	1.88
Xprp = XMg	0.18	0.16	0.20	0.21	0.19	0.21	0.18	0.20	0.20	0.22	0.21	0.18	0.28	0.28	0.28	0.27	0.27	0.27	0.26	0.25
Xalm = XFe	0.78	0.79	0.76	0.74	0.74	0.76	0.73	0.74	0.73	0.75	0.75	0.78	0.69	0.69	0.69	0.70	0.70	0.71	0.72	0.72
Xsps = XMn	0.01	0.01	0.01	0.01	0.01	0.01	0.01	0.01	0.01	0.01	0.01	0.01	0.00	0.00	0.00	0.00	0.00	0.00	0.00	0.00
Xgrs = XCa	0.02	0.03	0.03	0.03	0.07	0.03	0.07	0.05	0.06	0.03	0.03	0.03	0.03	0.03	0.03	0.03	0.03	0.02	0.03	0.03
XAl	1.00	1.00	1.00	1.00	1.00	1.00	1.00	1.00	1.00	1.00	1.00	1.00	1.00	1.00	1.00	1.00	1.00	1.00	1.00	1.00

Appendix B: Electron microprobe analyses of garnet; grt-st-ky-schist [sample 8-5]

sample	8-5	8-5	8-5	8-5	8-5	8-5	8-5	8-5	8-5	8-5	8-5	8-5	8-5	8-5	8-5	8-5	8-5	8-5	8-5	8-5	8-5
analysis	grt1_9	grt1_10	grt1_11	grt1_12	grt1_13	grt1_14	grt1_15	grt1_16	grt1_17	grt1_18	grt1_19	grt1_20	grt1_21	grt1_22	grt1_23	grt1_24	grt1_25	grt1_26	grt1_27	grt1_28	grt1_29
SiO2	38.57	38.27	38.46	38.28	38.36	37.91	38.18	38.37	38.69	38.46	38.48	38.34	38.36	38.35	38.42	38.62	38.53	38.79	38.74	38.53	38.51
Al2O3	21.26	21.39	21.33	21.14	21.18	21.30	21.08	21.17	21.26	21.24	21.26	21.07	21.07	21.16	21.16	21.20	21.21	21.50	21.47	21.52	21.21
TiO2	0.02	0.03	0.03	0.03	0.06	0.03	0.00	0.04	0.00	0.02	0.03	0.03	0.13	0.02	0.04	0.00	0.05	0.07	0.02	0.10	0.00
FeO	33.77	33.66	34.56	34.90	34.55	34.83	34.76	33.86	33.12	33.38	33.84	33.66	34.21	34.30	34.82	34.28	33.83	33.13	32.69	32.39	31.87
MgO	5.93	5.71	5.54	5.20	5.00	4.75	4.68	5.31	5.77	5.84	5.61	5.41	5.37	5.42	5.40	5.73	6.02	6.70	6.76	6.91	6.82
CaO	0.96	1.00	1.09	1.14	1.22	1.48	1.00	1.56	1.48	1.48	1.27	1.27	0.91	1.17	1.09	0.90	0.98	0.94	0.89	0.88	0.89
MnO	0.14	0.13	0.20	0.27	0.43	0.51	0.66	0.63	0.46	0.52	0.56	0.47	0.37	0.35	0.27	0.21	0.14	0.15	0.28	0.47	0.67
total	100.65	100.24	101.23	100.97	100.84	100.83	100.39	100.94	100.79	100.97	101.07	100.26	100.45	100.77	101.24	100.95	100.77	101.28	100.88	100.83	100.01
FeO Ox	33.77	33.66	34.55	34.83	34.55	34.59	34.76	33.83	33.12	33.24	33.84	33.66	34.21	34.30	34.73	34.28	33.83	33.13	32.69	32.29	31.87
Fe2O3 Ox	0.00	0.00	0.01	0.08	0.00	0.26	0.00	0.03	0.00	0.15	0.00	0.00	0.00	0.00	0.10	0.00	0.00	0.00	0.00	0.11	0.00
total Ox	100.64	100.20	101.21	100.97	100.80	100.83	100.35	100.94	100.78	100.95	101.04	100.25	100.42	100.77	101.21	100.94	100.76	101.28	100.85	100.81	99.97
number of cations based on 12 oxygen atoms																					
Si	3.03	3.02	3.01	3.01	3.02	3.00	3.03	3.02	3.03	3.01	3.02	3.03	3.03	3.02	3.02	3.03	3.02	3.01	3.02	3.00	3.02
Al tot.	1.97	1.99	1.97	1.96	1.97	1.99	1.97	1.96	1.96	1.96	1.96	1.96	1.96	1.96	1.96	1.96	1.96	1.97	1.97	1.98	1.96
Ti	0.00	0.00	0.00	0.00	0.00	0.00	0.00	0.00	0.00	0.00	0.00	0.00	0.01	0.00	0.00	0.00	0.00	0.00	0.00	0.01	0.00
Fe tot.	2.22	2.22	2.26	2.30	2.28	2.30	2.31	2.23	2.17	2.19	2.22	2.22	2.26	2.26	2.29	2.25	2.22	2.15	2.13	2.11	2.09
Fe3+	0.00	0.00	0.00	0.00	0.00	0.02	0.00	0.00	0.00	0.01	0.00	0.00	0.00	0.00	0.01	0.00	0.00	0.00	0.00	0.01	0.00
Fe2+	2.22	2.22	2.26	2.29	2.28	2.29	2.31	2.22	2.17	2.18	2.22	2.22	2.26	2.26	2.28	2.25	2.22	2.15	2.13	2.10	2.09
Mg	0.69	0.67	0.65	0.61	0.59	0.56	0.55	0.62	0.67	0.68	0.66	0.64	0.63	0.64	0.63	0.67	0.70	0.78	0.78	0.80	0.80
Ca	0.08	0.08	0.09	0.10	0.10	0.13	0.08	0.13	0.12	0.12	0.11	0.11	0.08	0.10	0.09	0.08	0.08	0.08	0.07	0.07	0.08
Mn	0.01	0.01	0.01	0.02	0.03	0.03	0.04	0.04	0.03	0.03	0.04	0.03	0.02	0.02	0.02	0.01	0.01	0.01	0.02	0.03	0.04
total cat	7.99	7.99	8.00	8.00	7.99	8.01	7.99	8.00	7.99	8.00	8.00	7.99	7.99	8.00	8.00	7.99	8.00	8.00	8.00	8.00	8.00
andradite	0.00	0.00	0.04	0.34	0.00	1.16	0.00	0.14	0.00	0.69	0.00	0.00	0.00	0.00	0.46	0.00	0.00	0.00	0.00	0.51	0.00
pyrope	23.51	22.50	21.88	20.66	19.90	18.67	18.71	21.11	22.87	23.01	22.24	21.64	21.48	21.59	21.41	22.78	23.92	26.26	26.53	26.92	27.10
spessartine	0.30	0.30	0.46	0.61	0.97	1.14	1.49	1.42	1.04	1.16	1.26	1.06	0.84	0.80	0.62	0.47	0.31	0.34	0.62	1.05	1.50
grossular	2.74	2.84	3.04	2.91	3.50	3.03	2.87	4.32	4.22	3.50	3.61	3.66	2.61	3.36	2.64	2.57	2.80	2.64	2.51	1.96	2.55
almandine	73.45	74.36	74.58	75.47	75.64	76.01	76.93	73.02	71.87	71.63	72.89	73.64	75.07	74.25	74.87	74.18	72.97	70.75	70.34	69.56	68.85
% rest	1.59	0.49	1.46	1.56	1.49	0.17	1.29	1.78	1.74	1.28	1.77	1.79	1.82	1.82	1.68	1.95	1.95	1.58	1.39	0.69	1.80
Xprp = XMg	0.23	0.22	0.21	0.20	0.20	0.19	0.19	0.21	0.22	0.23	0.22	0.21	0.21	0.21	0.21	0.22	0.23	0.26	0.26	0.27	0.27
Xalm = XFe	0.74	0.74	0.75	0.76	0.76	0.76	0.77	0.74	0.72	0.72	0.74	0.74	0.75	0.75	0.76	0.75	0.74	0.71	0.71	0.70	0.70
Xsps = XMn	0.00	0.00	0.00	0.01	0.01	0.01	0.01	0.01	0.01	0.01	0.01	0.01	0.01	0.01	0.01	0.00	0.00	0.00	0.01	0.01	0.01
Xgrs = XCa	0.03	0.03	0.03	0.03	0.03	0.04	0.03	0.04	0.04	0.04	0.04	0.04	0.03	0.03	0.03	0.03	0.03	0.03	0.02	0.02	0.02
XAl	1.00	1.00	1.00	1.00	1.00	1.00	1.00	1.00	1.00	1.00	1.00	1.00	1.00	1.00	1.00	1.00	1.00	1.00	1.00	1.00	1.00

Appendix B: Electron microprobe analyses of garnet; grt-st-ky-schist [sample 8-5]

sample	8-5	8-5	8-5	8-5	8-5	8-5	8-5	8-5	8-5	8-5	8-5	8-5	8-5	8-5	8-5	8-5	8-5	8-5	8-5	8-5	8-5
analysis	grt1_30	grt2_1	grt2_2	grt2_3	grt2_4	grt2_5	grt2_6	grt2_7	grt2_8	grt2_9	grt2_10	grt2_11	grt2_12	grt2_13	grt2_14	grt2_15	grt2_16	grt2_17	grt2_18	grt2_19	grt2_20
SiO2	38.28	38.68	38.53	38.49	38.57	38.43	38.50	38.06	38.02	38.16	38.17	37.42	37.79	37.66	37.62	37.79	37.77	37.74	37.70	37.59	37.66
Al2O3	21.38	21.49	21.55	21.69	21.54	21.38	21.08	21.05	21.22	21.06	20.89	20.94	21.16	20.90	20.84	20.89	21.08	20.98	20.84	20.95	20.77
TiO2	0.00	0.04	0.00	0.04	0.09	0.01	0.03	0.03	0.00	0.00	0.06	0.04	0.00	0.00	0.02	0.23	0.04	0.04	0.05	0.03	0.00
FeO	31.24	31.90	31.35	31.54	32.54	33.26	33.02	34.47	34.64	34.80	34.41	35.02	35.83	35.21	35.37	34.91	34.12	34.10	33.31	33.74	33.99
MgO	5.88	6.55	7.36	7.33	7.16	6.52	6.01	5.64	4.94	4.60	4.32	4.04	3.91	3.78	3.69	3.64	3.31	3.33	3.24	3.06	3.05
CaO	2.48	1.48	1.02	1.00	0.94	0.97	0.97	0.83	1.25	1.25	1.62	1.41	1.14	1.40	1.36	1.67	2.50	2.51	2.60	2.92	2.13
MnO	0.82	0.57	0.13	0.09	0.03	0.01	0.17	0.25	0.42	0.53	0.75	1.04	1.13	1.19	1.37	1.53	1.48	1.49	1.66	1.67	1.86
total	100.08	100.73	99.95	100.26	100.90	100.62	99.79	100.37	100.51	100.43	100.24	99.94	100.97	100.14	100.29	100.70	100.34	100.24	99.40	99.96	99.47
FeO Ox	31.24	31.90	31.35	31.54	32.32	33.14	33.02	34.26	34.63	34.80	34.41	34.81	35.68	35.21	35.32	34.91	34.12	34.10	33.31	33.74	33.99
Fe2O3 Ox	0.00	0.00	0.00	0.00	0.25	0.13	0.00	0.23	0.00	0.00	0.00	0.23	0.16	0.00	0.05	0.00	0.00	0.00	0.00	0.00	0.00
total Ox	100.08	100.71	99.94	100.17	100.89	100.59	99.78	100.35	100.49	100.40	100.22	99.93	100.98	100.13	100.28	100.66	100.29	100.19	99.40	99.96	99.46
number of cations based on 12 oxygen atoms																					
Si	3.01	3.02	3.01	3.00	3.00	3.01	3.04	3.01	3.01	3.03	3.03	3.00	3.00	3.02	3.01	3.01	3.02	3.02	3.03	3.02	3.04
Al tot.	1.98	1.98	1.99	1.99	1.98	1.97	1.96	1.96	1.98	1.97	1.96	1.98	1.98	1.97	1.97	1.96	1.98	1.98	1.98	1.98	1.97
Ti	0.00	0.00	0.00	0.00	0.01	0.00	0.00	0.00	0.00	0.00	0.00	0.00	0.00	0.00	0.00	0.01	0.00	0.00	0.00	0.00	0.00
Fe tot.	2.05	2.08	2.05	2.06	2.12	2.18	2.18	2.28	2.29	2.31	2.29	2.35	2.38	2.36	2.37	2.33	2.28	2.28	2.24	2.26	2.29
Fe3+	0.00	0.00	0.00	0.00	0.01	0.01	0.00	0.01	0.00	0.00	0.00	0.01	0.01	0.00	0.00	0.00	0.00	0.00	0.00	0.00	0.00
Fe2+	2.05	2.08	2.05	2.06	2.10	2.17	2.18	2.27	2.29	2.31	2.29	2.34	2.37	2.36	2.37	2.33	2.28	2.28	2.24	2.26	2.29
Mg	0.69	0.76	0.86	0.85	0.83	0.76	0.71	0.66	0.58	0.54	0.51	0.48	0.46	0.45	0.44	0.43	0.39	0.40	0.39	0.37	0.37
Ca	0.21	0.12	0.09	0.08	0.08	0.08	0.08	0.07	0.11	0.11	0.14	0.12	0.10	0.12	0.12	0.14	0.21	0.22	0.22	0.25	0.18
Mn	0.05	0.04	0.01	0.01	0.00	0.00	0.01	0.02	0.03	0.04	0.05	0.07	0.08	0.08	0.09	0.10	0.10	0.10	0.11	0.11	0.13
total cat	8.00	7.99	8.00	8.00	8.01	8.00	7.98	8.01	8.00	7.99	7.98	8.01	8.00	8.00	8.00	7.99	7.99	7.99	7.98	7.99	7.98
andradite	0.00	0.00	0.00	0.00	1.08	0.56	0.00	1.02	0.02	0.00	0.00	1.03	0.72	0.00	0.25	0.00	0.00	0.00	0.00	0.00	0.00
pyrope	23.18	25.69	28.78	28.48	27.71	25.56	24.03	22.35	19.62	18.41	17.43	16.09	15.46	15.24	14.89	14.68	13.23	13.38	13.10	12.31	12.38
spessartine	1.83	1.27	0.28	0.20	0.07	0.02	0.39	0.56	0.94	1.20	1.73	2.36	2.55	2.72	3.14	3.51	3.36	3.40	3.82	3.82	4.29
grossular	7.03	4.17	2.87	2.78	1.53	2.17	2.79	1.35	3.55	3.60	4.70	3.00	2.51	4.06	3.70	4.84	7.19	7.25	7.56	8.45	6.21
almandine	67.96	68.87	68.06	68.54	69.61	71.69	72.79	74.72	75.88	76.80	76.15	77.51	78.76	77.98	78.03	76.96	76.22	75.97	75.52	75.43	77.12
% rest	0.89	1.18	0.69	0.24	0.25	0.81	1.71	0.93	0.96	1.41	1.91	0.06	0.19	1.33	1.39	1.78	0.64	1.00	0.92	0.84	1.04
Xprp = XMg	0.23	0.25	0.29	0.28	0.27	0.25	0.24	0.22	0.19	0.18	0.17	0.16	0.15	0.15	0.15	0.14	0.13	0.13	0.13	0.12	0.12
Xalm = XFe	0.68	0.69	0.68	0.69	0.70	0.72	0.73	0.75	0.76	0.77	0.77	0.78	0.79	0.78	0.78	0.77	0.76	0.76	0.76	0.76	0.77
Xsps = XMn	0.02	0.01	0.00	0.00	0.00	0.00	0.00	0.01	0.01	0.01	0.02	0.02	0.03	0.03	0.03	0.03	0.03	0.03	0.04	0.04	0.04
Xgrs = XCa	0.07	0.04	0.03	0.03	0.03	0.03	0.03	0.02	0.04	0.04	0.05	0.04	0.03	0.04	0.04	0.05	0.07	0.07	0.08	0.08	0.06
XAl	1.00	1.00	1.00	1.00	1.00	1.00	1.00	1.00	1.00	1.00	1.00	1.00	1.00	1.00	1.00	1.00	1.00	1.00	1.00	1.00	1.00

Appendix B: Electron microprobe analyses of garnet; grt-st-ky-schist [sample 8-5]

sample	8-5	8-5	8-5	8-5	8-5	8-5	8-5	8-5	8-5	8-5	8-5	8-5	8-5	8-5	8-5	8-5	8-5	8-5	8-5	8-5	8-5
analysis	grt2_21	grt2_22	grt2_23	grt2_24	grt2_25	grt2_26	grt2_27	grt2_28	grt2_29	grt2_30	grt2_31	grt2_32	grt2_33	grt2_34	grt2_35	grt2_36	grt2_37	grt2_38	grt2_39	grt2_40	grt2_41
SiO2	37.72	37.75	37.92	37.92	37.23	37.43	37.45	37.43	37.73	37.61	37.59	37.81	37.88	37.81	38.01	37.76	37.76	37.78	38.26	38.28	38.32
Al2O3	20.82	21.02	20.92	20.95	21.08	21.00	20.99	21.02	20.83	21.00	20.98	21.19	20.88	20.99	20.99	21.18	21.03	21.17	21.31	21.34	21.42
TiO2	0.05	0.01	0.07	0.07	0.06	0.00	0.04	0.04	0.00	0.02	0.03	0.02	0.02	0.01	0.05	0.04	0.01	0.05	0.03	0.05	0.04
FeO	33.73	34.59	33.52	34.24	34.01	33.92	33.64	34.14	34.01	34.19	34.93	35.33	35.34	35.03	34.75	34.26	34.17	33.54	34.10	33.61	33.29
MgO	3.16	3.11	3.13	3.11	3.08	3.04	3.01	3.21	3.10	3.23	3.70	4.03	4.22	4.52	4.82	5.18	5.51	5.68	6.18	6.25	6.49
CaO	2.45	2.28	2.66	2.18	2.38	2.89	2.77	2.67	2.51	2.76	1.48	1.34	1.54	1.47	1.14	0.97	0.94	1.01	1.00	0.93	0.92
MnO	1.98	2.06	1.89	1.93	1.93	1.95	1.82	1.74	1.73	1.56	1.52	1.03	0.72	0.58	0.46	0.32	0.25	0.13	0.06	0.05	0.00
total	99.95	100.86	100.16	100.48	99.84	100.29	99.75	100.30	99.93	100.40	100.29	100.77	100.60	100.41	100.22	99.71	99.70	99.38	100.93	100.55	100.53
FeO Ox	33.73	34.59	33.52	34.24	34.01	33.75	33.64	33.97	34.01	34.14	34.93	35.30	35.17	34.81	34.75	34.26	33.98	33.54	33.65	33.50	33.17
Fe2O3 Ox	0.00	0.00	0.00	0.00	0.00	0.19	0.00	0.19	0.00	0.06	0.00	0.03	0.19	0.25	0.00	0.00	0.21	0.00	0.50	0.12	0.13
total Ox	99.91	100.82	100.11	100.40	99.77	100.25	99.71	100.27	99.91	100.37	100.23	100.75	100.62	100.43	100.22	99.70	99.69	99.35	100.98	100.52	100.49
number of cations based on 12 oxygen atoms																					
Si	3.03	3.01	3.03	3.03	3.00	3.00	3.01	3.00	3.03	3.01	3.01	3.01	3.01	3.01	3.02	3.01	3.01	3.01	3.00	3.01	3.00
Al tot.	1.97	1.98	1.97	1.97	2.00	1.99	1.99	1.99	1.97	1.98	1.98	1.99	1.96	1.97	1.97	1.99	1.97	1.99	1.97	1.98	1.98
Ti	0.00	0.00	0.00	0.00	0.00	0.00	0.00	0.00	0.00	0.00	0.00	0.00	0.00	0.00	0.00	0.00	0.00	0.00	0.00	0.00	0.00
Fe tot.	2.26	2.31	2.24	2.29	2.29	2.27	2.26	2.29	2.28	2.29	2.34	2.35	2.35	2.33	2.31	2.28	2.28	2.23	2.24	2.21	2.18
Fe3+	0.00	0.00	0.00	0.00	0.00	0.01	0.00	0.01	0.00	0.00	0.00	0.00	0.01	0.01	0.00	0.00	0.01	0.00	0.03	0.01	0.01
Fe2+	2.26	2.31	2.24	2.29	2.29	2.26	2.26	2.28	2.28	2.28	2.34	2.35	2.34	2.32	2.31	2.28	2.26	2.23	2.21	2.20	2.18
Mg	0.38	0.37	0.37	0.37	0.37	0.36	0.36	0.38	0.37	0.38	0.44	0.48	0.50	0.54	0.57	0.61	0.65	0.67	0.72	0.73	0.76
Ca	0.21	0.19	0.23	0.19	0.21	0.25	0.24	0.23	0.22	0.24	0.13	0.11	0.13	0.13	0.10	0.08	0.08	0.09	0.08	0.08	0.08
Mn	0.13	0.14	0.13	0.13	0.13	0.13	0.12	0.12	0.12	0.11	0.10	0.07	0.05	0.04	0.03	0.02	0.02	0.01	0.00	0.00	0.00
total cat	7.99	8.00	7.98	7.98	8.00	8.01	7.99	8.01	7.99	8.00	8.00	8.00	8.01	8.01	8.00	8.00	8.01	8.00	8.01	8.00	8.00
andradite	0.00	0.00	0.00	0.00	0.00	0.87	0.00	0.84	0.00	0.25	0.00	0.15	0.86	1.12	0.00	0.00	0.97	0.00	2.21	0.55	0.57
pyrope	12.79	12.47	12.61	12.51	12.33	12.10	12.09	12.78	12.54	12.93	14.86	16.00	16.89	17.95	19.35	20.61	21.87	22.61	24.07	24.55	25.39
spessartine	4.56	4.69	4.33	4.41	4.39	4.41	4.15	3.94	3.98	3.55	3.47	2.33	1.64	1.30	1.05	0.71	0.57	0.30	0.13	0.11	0.00
grossular	7.13	6.57	7.70	6.31	6.85	7.40	8.00	6.80	7.30	7.69	4.27	3.67	3.58	3.08	3.29	2.79	1.71	2.89	0.57	2.07	2.00
almandine	75.52	76.26	75.36	76.77	76.42	75.21	75.77	75.64	76.18	75.58	77.39	77.84	77.04	76.56	76.31	75.89	74.88	74.21	73.01	72.73	72.04
% rest	1.35	1.16	1.14	1.12	0.09	0.02	0.37	0.10	1.28	0.79	1.01	0.59	1.30	0.55	1.65	0.56	0.43	0.64	0.21	0.73	0.50
Xprp = XMg	0.13	0.12	0.13	0.12	0.12	0.12	0.12	0.13	0.12	0.13	0.15	0.16	0.17	0.18	0.19	0.20	0.22	0.22	0.24	0.24	0.25
Xalm = XFe	0.76	0.77	0.75	0.77	0.76	0.75	0.76	0.76	0.76	0.76	0.78	0.78	0.78	0.77	0.77	0.76	0.75	0.74	0.73	0.73	0.72
Xsps = XMn	0.05	0.05	0.04	0.04	0.04	0.04	0.04	0.04	0.04	0.04	0.03	0.02	0.02	0.01	0.01	0.01	0.01	0.00	0.00	0.00	0.00
Xgrs = XCa	0.07	0.06	0.08	0.06	0.07	0.08	0.08	0.08	0.07	0.08	0.04	0.04	0.04	0.04	0.03	0.03	0.03	0.03	0.03	0.03	0.03
XAl	1.00	1.00	1.00	1.00	1.00	1.00	1.00	1.00	1.00	1.00	1.00	1.00	1.00	1.00	1.00	1.00	1.00	1.00	1.00	1.00	1.00

Appendix B: Electron microprobe analyses of garnet; grt-st-ky-schist [sample 8-5]

sample	8-5	8-5	8-5	8-5	8-5	8-5	8-5	8-5	8-5	8-5	8-5	8-5	8-5	8-5	8-5	8-5	8-5	8-5	8-5	8-5	8-5
analysis	grt2_42	grt2_43	grt2_44	grt2_45	grt2_46	grt2_47	grt2_48	grt2_49	grt2_50	grt3_1	grt3_2	grt3_3	grt3_4	grt3_5	grt3_6	grt3_7	grt3_8	grt3_9	grt3_10	grt3_11	grt3_12
SiO2	38.51	38.49	38.06	38.08	38.49	38.18	38.12	38.30	38.21	38.05	38.36	38.46	38.00	38.52	38.36	38.26	38.49	38.30	38.38	38.19	37.71
Al2O3	21.49	21.40	21.58	21.56	21.77	21.58	21.79	21.72	21.64	21.43	21.51	21.66	21.66	21.50	21.30	21.44	21.39	21.25	21.58	21.36	21.47
TiO2	0.07	0.03	0.06	0.07	0.02	0.02	0.04	0.02	0.03	0.03	0.00	0.00	0.02	0.02	0.03	0.04	0.03	0.04	0.04	0.02	0.01
FeO	32.35	32.39	32.10	32.18	31.46	32.04	31.95	31.97	31.39	31.34	30.53	31.10	31.24	32.04	32.09	32.85	32.45	33.35	32.83	33.40	33.93
MgO	6.86	7.13	7.27	7.24	7.43	7.28	7.49	7.46	7.34	6.08	7.56	7.73	7.56	7.43	7.25	7.27	6.96	6.88	6.71	6.30	5.73
CaO	0.98	0.90	0.96	0.99	0.97	0.97	1.07	1.00	1.13	2.09	1.78	1.60	1.12	1.04	1.01	0.93	0.94	0.95	0.93	0.98	1.05
MnO	0.06	0.00	0.06	0.01	0.05	0.10	0.15	0.17	0.27	0.76	0.44	0.33	0.09	0.04	0.01	0.04	0.05	0.00	0.08	0.11	0.13
total	100.33	100.38	100.14	100.18	100.22	100.21	100.61	100.69	100.05	99.80	100.18	100.91	99.73	100.61	100.06	100.88	100.40	100.82	100.55	100.41	100.04
FeO Ox	32.35	32.25	31.58	31.67	31.46	31.58	31.14	31.36	31.08	31.27	29.95	30.25	30.72	31.66	31.81	32.02	32.41	32.68	32.74	33.19	33.58
Fe2O3 Ox	0.00	0.15	0.58	0.57	0.00	0.51	0.89	0.67	0.35	0.07	0.64	0.94	0.58	0.42	0.31	0.92	0.05	0.74	0.10	0.24	0.38
total Ox	100.32	100.35	100.15	100.19	100.19	100.22	100.69	100.71	100.04	99.78	100.25	100.97	99.75	100.63	100.08	100.92	100.32	100.84	100.56	100.38	100.06
number of cations based on 12 oxygen atoms																					
Si	3.01	3.01	2.98	2.98	3.00	2.99	2.97	2.98	2.99	3.00	2.99	2.98	2.98	3.00	3.01	2.98	3.01	3.00	3.00	3.00	2.99
Al tot.	1.98	1.97	1.99	1.99	2.00	1.99	2.00	1.99	2.00	1.99	1.98	1.98	2.00	1.97	1.97	1.97	1.97	1.96	1.99	1.98	2.00
Ti	0.00	0.00	0.00	0.00	0.00	0.00	0.00	0.00	0.00	0.00	0.00	0.00	0.00	0.00	0.00	0.00	0.00	0.00	0.00	0.00	0.00
Fe tot.	2.11	2.12	2.10	2.11	2.05	2.10	2.08	2.08	2.05	2.07	1.99	2.02	2.05	2.09	2.10	2.14	2.12	2.18	2.15	2.20	2.25
Fe3+	0.00	0.01	0.03	0.03	0.00	0.03	0.05	0.04	0.02	0.00	0.04	0.05	0.03	0.02	0.02	0.05	0.00	0.04	0.01	0.01	0.02
Fe2+	2.11	2.11	2.07	2.08	2.05	2.07	2.03	2.04	2.03	2.06	1.95	1.96	2.01	2.06	2.08	2.09	2.12	2.14	2.14	2.18	2.22
Mg	0.80	0.83	0.85	0.85	0.86	0.85	0.87	0.87	0.86	0.71	0.88	0.89	0.88	0.86	0.85	0.85	0.81	0.80	0.78	0.74	0.68
Ca	0.08	0.08	0.08	0.08	0.08	0.08	0.09	0.08	0.09	0.18	0.15	0.13	0.09	0.09	0.08	0.08	0.08	0.08	0.08	0.08	0.09
Mn	0.00	0.00	0.00	0.00	0.00	0.01	0.01	0.01	0.02	0.05	0.03	0.02	0.01	0.00	0.00	0.00	0.00	0.00	0.01	0.01	0.01
total cat	8.00	8.00	8.02	8.02	8.00	8.01	8.03	8.02	8.01	8.00	8.02	8.03	8.02	8.01	8.01	8.03	8.00	8.02	8.00	8.01	8.01
andradite	0.00	0.67	2.57	2.51	0.00	2.26	3.02	2.81	1.53	0.32	2.83	4.13	2.59	1.85	1.38	2.59	0.21	2.67	0.45	1.05	1.72
pyrope	26.90	27.89	28.47	28.34	28.79	28.42	29.28	29.03	28.63	23.83	29.37	29.95	29.65	28.75	28.29	28.32	27.36	26.77	26.09	24.60	22.65
spessartine	0.13	0.00	0.14	0.03	0.10	0.22	0.32	0.38	0.60	1.69	0.98	0.72	0.19	0.09	0.02	0.08	0.12	0.00	0.18	0.25	0.29
grossular	2.77	1.86	0.12	0.26	2.71	0.47	0.00	0.00	1.62	5.57	2.14	0.32	0.58	1.03	1.46	0.00	2.46	0.00	2.15	1.71	1.26
almandine	70.20	69.58	68.70	68.86	68.40	68.63	67.38	67.78	67.62	68.59	64.68	64.87	66.99	68.29	68.85	69.01	69.85	70.56	71.13	72.40	74.08
% rest	0.92	0.80	0.79	0.76	0.06	0.58	1.30	0.84	0.47	0.10	0.49	0.92	0.87	0.17	0.37	0.85	1.19	0.40	0.14	0.06	0.61
Xprp = XMg	0.27	0.27	0.28	0.28	0.29	0.28	0.29	0.28	0.28	0.24	0.29	0.29	0.29	0.28	0.28	0.28	0.27	0.26	0.26	0.24	0.22
Xalm = XFe	0.70	0.70	0.69	0.69	0.68	0.69	0.68	0.68	0.68	0.69	0.65	0.66	0.68	0.69	0.69	0.70	0.70	0.71	0.71	0.73	0.74
Xsps = XMn	0.00	0.00	0.00	0.00	0.00	0.00	0.00	0.00	0.01	0.02	0.01	0.01	0.00	0.00	0.00	0.00	0.00	0.00	0.00	0.00	0.00
Xgrs = XCa	0.03	0.02	0.03	0.03	0.03	0.03	0.03	0.03	0.03	0.06	0.05	0.04	0.03	0.03	0.03	0.03	0.03	0.03	0.03	0.03	0.03
XAl	1.00	1.00	1.00	1.00	1.00	1.00	1.00	1.00	1.00	1.00	1.00	1.00	1.00	1.00	1.00	1.00	1.00	1.00	1.00	1.00	1.00

Appendix B: Electron microprobe analyses of garnet; grt-st-ky-schist [sample 8-5]

sample	8-5	8-5	8-5	8-5	8-5	8-5	8-5	8-5	8-5	8-5	8-5	8-5	8-5	8-5	8-5	8-5	8-5	8-5	8-5	8-5	8-5
analysis	grt3_13	grt3_14	grt3_15	grt3_16	grt3_17	grt3_18	grt3_19	grt3_20	grt3_22	grt3_23	grt3_24	grt3_25	grt3_26	grt3_27	grt3_28	grt3_29	grt3_30	grt3_31	grt3_32	grt3_33	grt3_34
SiO2	37.80	37.67	37.75	37.60	37.36	37.42	37.15	37.94	37.56	37.35	37.27	37.23	37.66	37.75	37.63	37.41	37.33	37.17	37.52	37.53	37.68
Al2O3	21.28	21.19	21.40	21.30	21.10	20.78	20.81	21.23	20.97	20.85	21.01	21.16	21.05	21.06	21.08	21.01	20.87	21.28	21.25	21.41	21.08
TiO2	0.07	0.01	0.03	0.04	0.03	0.06	0.05	0.03	0.13	0.10	0.00	0.02	0.08	0.03	0.06	0.03	0.00	0.00	0.03	0.00	0.05
FeO	34.71	34.94	35.01	35.28	35.41	36.56	35.52	35.57	34.19	33.57	34.33	34.08	34.10	33.22	34.02	33.71	34.22	35.38	35.14	35.24	34.99
MgO	5.45	5.16	4.83	4.47	4.32	4.09	3.95	3.80	3.48	3.40	3.71	3.77	3.84	4.07	4.10	3.77	3.73	4.11	4.20	4.69	5.08
CaO	1.13	1.14	1.19	1.58	1.43	1.50	1.38	1.60	2.42	2.77	2.19	2.19	2.45	2.47	2.45	2.54	2.20	1.20	1.24	1.46	1.23
MnO	0.13	0.28	0.28	0.55	0.89	1.06	1.42	1.48	1.57	1.85	1.78	1.55	1.28	0.85	1.05	1.83	1.53	1.02	0.95	0.42	0.35
total	100.62	100.43	100.51	100.82	100.55	101.48	100.33	101.65	100.35	99.92	100.29	100.04	100.50	99.47	100.42	100.35	99.92	100.17	100.34	100.77	100.49
FeO Ox	34.22	34.39	34.83	34.72	34.64	35.19	34.66	35.24	34.15	33.37	33.67	33.65	33.91	33.22	33.70	33.19	33.82	34.83	34.95	34.56	34.40
Fe2O3 Ox	0.55	0.61	0.19	0.62	0.85	1.52	0.96	0.37	0.04	0.22	0.73	0.48	0.21	0.00	0.36	0.57	0.44	0.61	0.21	0.75	0.65
total Ox	100.62	100.44	100.50	100.88	100.62	101.62	100.37	101.69	100.32	99.91	100.36	100.04	100.48	99.44	100.41	100.36	99.92	100.21	100.34	100.82	100.52
number of cations based on 12 oxygen atoms																					
Si	2.99	2.99	2.99	2.98	2.98	2.98	2.98	3.00	3.00	3.00	2.99	2.98	3.00	3.02	3.00	2.99	3.00	2.98	2.99	2.98	2.99
Al tot.	1.98	1.98	2.00	1.99	1.98	1.95	1.97	1.98	1.98	1.97	1.98	2.00	1.98	1.99	1.98	1.98	1.98	2.01	2.00	2.00	1.97
Ti	0.00	0.00	0.00	0.00	0.00	0.00	0.00	0.00	0.01	0.01	0.00	0.00	0.00	0.00	0.00	0.00	0.00	0.00	0.00	0.00	0.00
Fe tot.	2.29	2.32	2.32	2.34	2.36	2.43	2.39	2.35	2.29	2.26	2.30	2.28	2.27	2.22	2.27	2.25	2.30	2.37	2.34	2.34	2.32
Fe3+	0.03	0.04	0.01	0.04	0.05	0.09	0.06	0.02	0.00	0.01	0.04	0.03	0.01	0.00	0.02	0.03	0.03	0.04	0.01	0.04	0.04
Fe2+	2.26	2.28	2.31	2.30	2.31	2.34	2.33	2.33	2.28	2.24	2.26	2.26	2.26	2.22	2.24	2.22	2.27	2.33	2.33	2.29	2.28
Mg	0.64	0.61	0.57	0.53	0.51	0.48	0.47	0.45	0.41	0.41	0.44	0.45	0.46	0.49	0.49	0.45	0.45	0.49	0.50	0.55	0.60
Ca	0.10	0.10	0.10	0.13	0.12	0.13	0.12	0.14	0.21	0.24	0.19	0.19	0.21	0.21	0.21	0.22	0.19	0.10	0.11	0.12	0.10
Mn	0.01	0.02	0.02	0.04	0.06	0.07	0.10	0.10	0.11	0.13	0.12	0.11	0.09	0.06	0.07	0.12	0.10	0.07	0.06	0.03	0.02
total cat	8.02	8.02	8.01	8.02	8.03	8.05	8.03	8.01	8.00	8.01	8.02	8.01	8.01	7.99	8.01	8.02	8.01	8.02	8.01	8.02	8.02
andradite	2.45	2.75	0.87	2.80	3.84	4.30	3.97	1.64	0.18	1.01	3.32	2.16	0.93	0.00	1.60	2.60	2.01	2.78	0.96	3.39	2.94
pyrope	21.49	20.41	19.07	17.72	17.23	16.29	15.85	14.93	13.96	13.60	14.84	15.09	15.23	16.30	16.24	15.02	14.89	16.48	16.68	18.62	20.09
spessartine	0.30	0.63	0.63	1.25	2.02	2.41	3.24	3.30	3.58	4.21	4.05	3.53	2.89	1.93	2.35	4.14	3.47	2.32	2.14	0.94	0.80
grossular	0.75	0.49	2.50	1.70	0.26	0.00	0.00	2.88	6.80	6.95	2.98	4.14	6.05	7.11	5.37	4.68	4.30	0.67	2.58	0.78	0.56
almandine	75.02	75.72	76.93	76.53	76.65	77.01	76.94	77.25	75.48	74.22	74.82	75.08	74.89	74.66	74.43	73.56	75.32	77.75	77.64	76.27	75.61
% rest	0.60	0.57	0.32	0.79	0.96	1.34	0.93	0.20	1.02	0.36	0.75	0.69	0.28	0.58	0.25	0.53	0.22	1.00	0.32	1.06	0.53
Xprp = XMg	0.21	0.20	0.19	0.17	0.17	0.16	0.15	0.15	0.14	0.13	0.15	0.15	0.15	0.16	0.16	0.15	0.15	0.16	0.17	0.18	0.20
Xalm = XFe	0.75	0.76	0.77	0.77	0.77	0.78	0.78	0.78	0.76	0.75	0.75	0.75	0.75	0.75	0.75	0.74	0.76	0.78	0.78	0.77	0.76
Xsps = XMn	0.00	0.01	0.01	0.01	0.02	0.02	0.03	0.03	0.04	0.04	0.04	0.03	0.03	0.02	0.02	0.04	0.03	0.02	0.02	0.01	0.01
Xgrs = XCa	0.03	0.03	0.03	0.04	0.04	0.04	0.04	0.04	0.07	0.08	0.06	0.06	0.07	0.07	0.07	0.07	0.06	0.03	0.04	0.04	0.03
XAl	1.00	1.00	1.00	1.00	1.00	1.00	1.00	1.00	1.00	1.00	1.00	1.00	1.00	1.00	1.00	1.00	1.00	1.00	1.00	1.00	1.00

Appendix B: Electron microprobe analyses of garnet; grt-st-ky-schist [sample 8-5] and micaschist [sample M98/5]

sample	8-5	8-5	8-5	8-5	8-5	8-5	8-5	8-5	8-5	8-5	8-5	8-5	8-5	8-5	8-5	8-5	M98/5	M98/5	M98/5	M98/5
analysis	grt3_35	grt3_36	grt3_37	grt3_38	grt3_39	grt3_40	grt3_41	grt3_42	grt3_43	grt3_44	grt3_45	grt3_46	grt3_47	grt3_48	grt3_49	grt3_50	grt1_1	grt1_2	grt1_3	grt1_4
SiO2	37.87	38.28	38.57	38.64	38.41	38.63	38.53	38.32	38.51	38.70	38.61	38.59	38.50	38.63	38.67	38.22	38.58	38.32	38.61	42.13
Al2O3	21.24	21.56	21.38	21.43	21.57	21.51	21.55	21.57	21.33	21.60	21.58	21.59	21.59	21.51	21.65	21.36	20.69	20.70	20.84	22.41
TiO2	0.09	0.06	0.04	0.07	0.00	0.03	0.00	0.06	0.07	0.01	0.05	0.03	0.03	0.03	0.04	0.01	0.00	0.05	0.07	0.07
FeO	34.98	35.04	33.28	33.06	32.44	32.39	32.31	31.83	32.32	31.81	32.21	31.47	32.01	31.25	30.50	32.27	22.41	22.65	20.60	18.72
MgO	5.50	5.88	6.35	6.82	6.80	7.21	7.31	7.41	7.42	7.36	7.49	7.51	7.56	7.49	7.47	5.98	0.66	0.73	0.39	0.40
CaO	1.05	0.98	0.97	0.95	0.92	0.93	0.90	0.94	0.96	0.98	0.96	0.92	1.01	1.55	1.84	1.88	16.13	15.57	17.97	15.75
MnO	0.14	0.12	0.08	0.06	0.03	0.12	0.00	0.02	0.03	0.13	0.06	0.20	0.19	0.23	0.23	0.51	1.15	1.88	1.61	1.55
total	100.94	101.98	100.70	101.06	100.20	100.86	100.62	100.22	100.64	100.61	100.98	100.33	100.93	100.70	100.41	100.23	99.62	99.96	100.11	101.23
FeO Ox	34.37	34.33	33.28	32.91	32.44	32.16	32.03	31.58	31.86	31.79	31.78	31.43	31.40	30.85	30.41	32.18	22.41	22.65	20.60	18.72
Fe2O3 Ox	0.67	0.78	0.00	0.17	0.00	0.26	0.31	0.28	0.51	0.02	0.47	0.05	0.67	0.44	0.09	0.10	0.00	0.00	0.00	0.00
total Ox	100.93	101.99	100.66	101.05	100.16	100.85	100.62	100.17	100.68	100.59	101.00	100.31	100.96	100.73	100.40	100.23	99.62	99.89	100.08	101.03
number of cations based on 12 oxygen atoms																				
Si	2.99	2.98	3.02	3.01	3.01	3.00	3.00	2.99	3.00	3.01	3.00	3.01	2.99	3.00	3.00	3.01	3.05	3.03	3.04	3.19
Al tot.	1.98	1.98	1.97	1.97	1.99	1.97	1.98	1.99	1.96	1.98	1.97	1.98	1.98	1.97	1.98	1.98	1.93	1.93	1.93	2.00
Ti	0.01	0.00	0.00	0.00	0.00	0.00	0.00	0.00	0.00	0.00	0.00	0.00	0.00	0.00	0.00	0.00	0.00	0.00	0.00	0.00
Fe tot.	2.31	2.28	2.18	2.15	2.12	2.11	2.10	2.08	2.11	2.07	2.09	2.05	2.08	2.03	1.98	2.12	1.48	1.50	1.35	1.19
Fe3+	0.04	0.05	0.00	0.01	0.00	0.01	0.02	0.02	0.03	0.00	0.03	0.00	0.04	0.03	0.01	0.01	0.00	0.00	0.00	0.00
Fe2+	2.27	2.24	2.18	2.14	2.12	2.09	2.09	2.06	2.08	2.07	2.06	2.05	2.04	2.00	1.98	2.12	1.48	1.50	1.35	1.19
Mg	0.65	0.68	0.74	0.79	0.79	0.84	0.85	0.86	0.86	0.85	0.87	0.87	0.88	0.87	0.86	0.70	0.08	0.09	0.05	0.05
Ca	0.09	0.08	0.08	0.08	0.08	0.08	0.07	0.08	0.08	0.08	0.08	0.08	0.08	0.13	0.15	0.16	1.37	1.32	1.51	1.28
Mn	0.01	0.01	0.01	0.00	0.00	0.01	0.00	0.00	0.00	0.01	0.00	0.01	0.01	0.01	0.01	0.03	0.08	0.13	0.11	0.10
total cat	8.02	8.02	7.99	8.00	8.00	8.01	8.01	8.01	8.01	8.00	8.01	8.00	8.02	8.01	8.00	8.00	7.98	8.00	7.99	7.80
andradite	2.97	2.73	0.00	0.73	0.00	1.13	1.35	1.22	2.25	0.10	2.08	0.21	2.81	1.92	0.41	0.46	0.00	0.00	0.00	0.00
pyrope	21.64	22.89	25.03	26.62	26.57	27.93	28.27	28.82	28.72	28.69	28.91	29.25	29.26	28.90	28.96	23.49	2.69	2.96	1.56	1.74
spessartine	0.31	0.26	0.17	0.12	0.06	0.27	0.00	0.04	0.06	0.28	0.14	0.43	0.43	0.50	0.50	1.13	2.66	4.35	3.70	3.81
grossular	0.00	0.00	2.73	1.94	2.58	1.48	1.14	1.39	0.41	2.66	0.58	2.38	0.00	2.38	4.72	4.85	47.24	45.58	52.25	48.99
almandine	75.07	74.12	72.06	70.58	70.79	69.19	69.23	68.53	68.56	68.28	68.29	67.73	67.50	66.31	65.41	70.08	47.41	47.11	42.49	45.45
% rest	0.67	0.85	1.35	1.01	0.39	0.35	0.06	0.28	0.15	0.92	0.30	0.69	0.57	0.15	0.50	0.55	3.36	3.41	3.32	10.86
Xprp = XMg	0.21	0.22	0.25	0.26	0.26	0.28	0.28	0.29	0.28	0.28	0.28	0.29	0.29	0.29	0.29	0.23	0.03	0.03	0.01	0.02
Xalm = XFe	0.76	0.75	0.72	0.71	0.71	0.70	0.70	0.69	0.69	0.69	0.69	0.68	0.68	0.67	0.66	0.70	0.49	0.49	0.45	0.45
Xsps = XMn	0.00	0.00	0.00	0.00	0.00	0.00	0.00	0.00	0.00	0.00	0.00	0.00	0.00	0.00	0.00	0.01	0.03	0.04	0.04	0.04
Xgrs = XCa	0.03	0.03	0.03	0.03	0.03	0.03	0.02	0.03	0.03	0.03	0.03	0.03	0.03	0.04	0.05	0.05	0.46	0.44	0.50	0.49
XAl	1.00	1.00	1.00	1.00	1.00	1.00	1.00	1.00	1.00	1.00	1.00	1.00	1.00	1.00	1.00	1.00	1.00	1.00	1.00	1.00

Appendix B: Electron microprobe analyses of garnet; micaschist [sample M98/5]

sample	M98/5	M98/5	M98/5	M98/5	M98/5	M98/5	M98/5	M98/5	M98/5	M98/5	M98/5	M98/5	M98/5	M98/5	M98/5	M98/5	M98/5	M98/5	M98/5	M98/5	M98/5
analysis	grt2_1	grt2_2	grt2_3	grt2_4	grt2_5	grt2_6	grt2_7	grt2_8	grt2_9	grt3_1	grt3_2	grt3_3	grt3_4	grt3_5	grt3_6	grt3_7	grt3_8	grt3_9	grt3_10	grt3_11	grt3_12
SiO2	38.35	38.70	38.47	38.34	38.68	37.99	38.62	38.49	38.64	38.58	38.79	38.52	38.39	38.60	38.43	38.70	38.59	38.59	38.70	38.26	38.61
Al2O3	20.49	20.37	20.57	20.71	20.60	19.91	20.47	20.51	20.87	20.72	20.76	20.64	20.63	20.73	20.75	20.92	20.65	20.60	20.58	20.75	20.61
TiO2	0.03	0.12	0.07	0.00	0.01	0.09	0.11	0.04	0.06	0.09	0.08	0.08	0.06	0.04	0.04	0.06	0.05	0.02	0.11	0.05	0.05
FeO	22.23	21.34	20.08	19.78	19.53	19.65	19.41	21.20	21.35	22.32	20.14	19.83	21.69	21.77	20.67	22.14	22.13	19.11	21.37	22.55	21.73
MgO	0.62	0.56	0.34	0.37	0.32	0.33	0.32	0.52	0.59	0.67	0.40	0.39	0.64	0.66	0.51	0.63	0.61	0.33	0.57	0.63	0.60
CaO	16.06	16.44	18.30	18.50	18.70	18.00	18.57	17.74	17.17	16.31	18.30	18.97	16.46	16.30	17.77	16.90	16.87	19.04	17.62	16.14	17.02
MnO	1.13	1.86	1.60	1.62	1.64	1.54	1.60	1.00	1.03	1.42	1.49	1.45	1.65	1.48	1.39	1.30	1.12	1.79	1.03	1.27	0.97
total	98.92	99.40	99.47	99.36	99.52	97.65	99.11	99.54	99.79	100.19	99.98	99.89	99.53	99.60	99.62	100.72	100.07	99.51	100.00	99.72	99.58
FeO Ox	22.23	21.34	20.08	19.78	19.53	19.65	19.41	21.20	21.35	22.32	20.14	19.72	21.69	21.77	20.67	22.14	22.13	19.11	21.37	22.55	21.73
Fe2O3 Ox	0.00	0.00	0.00	0.00	0.00	0.00	0.00	0.00	0.00	0.00	0.00	0.12	0.00	0.00	0.00	0.00	0.00	0.00	0.00	0.00	0.00
total Ox	98.91	99.39	99.43	99.31	99.48	97.50	99.10	99.50	99.72	100.11	99.97	99.89	99.52	99.59	99.56	100.65	100.02	99.47	99.97	99.65	99.58
number of cations based on 12 oxygen atoms																					
Si	3.05	3.07	3.04	3.04	3.05	3.06	3.06	3.05	3.04	3.04	3.05	3.03	3.04	3.05	3.04	3.03	3.04	3.05	3.05	3.03	3.05
Al tot.	1.92	1.90	1.92	1.93	1.92	1.89	1.91	1.91	1.94	1.92	1.92	1.92	1.93	1.93	1.93	1.93	1.92	1.92	1.91	1.94	1.92
Ti	0.00	0.01	0.00	0.00	0.00	0.01	0.01	0.00	0.00	0.01	0.00	0.00	0.00	0.00	0.00	0.00	0.00	0.00	0.01	0.00	0.00
Fe tot.	1.48	1.41	1.33	1.31	1.29	1.33	1.29	1.40	1.41	1.47	1.32	1.31	1.44	1.44	1.37	1.45	1.46	1.26	1.41	1.49	1.44
Fe3+	0.00	0.00	0.00	0.00	0.00	0.00	0.00	0.00	0.00	0.00	0.00	0.01	0.00	0.00	0.00	0.00	0.00	0.00	0.00	0.00	0.00
Fe2+	1.48	1.41	1.33	1.31	1.29	1.33	1.29	1.40	1.41	1.47	1.32	1.30	1.44	1.44	1.37	1.45	1.46	1.26	1.41	1.49	1.44
Mg	0.07	0.07	0.04	0.04	0.04	0.04	0.04	0.06	0.07	0.08	0.05	0.05	0.08	0.08	0.06	0.07	0.07	0.04	0.07	0.07	0.07
Ca	1.37	1.40	1.55	1.57	1.58	1.56	1.58	1.50	1.45	1.38	1.54	1.60	1.40	1.38	1.50	1.42	1.43	1.61	1.49	1.37	1.44
Mn	0.08	0.12	0.11	0.11	0.11	0.11	0.11	0.07	0.07	0.09	0.10	0.10	0.11	0.10	0.09	0.09	0.08	0.12	0.07	0.09	0.06
total cat	7.98	7.98	7.99	8.00	7.99	7.99	7.98	8.00	7.98	7.99	7.99	8.00	7.99	7.98	7.99	8.00	8.00	7.99	7.99	8.00	7.99
andradite	0.00	0.00	0.00	0.00	0.00	0.00	0.00	0.00	0.00	0.00	0.00	0.56	0.00	0.00	0.00	0.00	0.00	0.00	0.00	0.00	0.00
pyrope	2.55	2.31	1.39	1.49	1.32	1.38	1.31	2.12	2.40	2.74	1.64	1.57	2.61	2.70	2.08	2.54	2.50	1.35	2.33	2.56	2.44
spessartine	2.63	4.37	3.73	3.75	3.81	3.70	3.74	2.34	2.37	3.28	3.44	3.35	3.83	3.42	3.21	2.98	2.61	4.16	2.39	2.94	2.25
grossular	47.49	48.90	53.91	54.13	55.00	54.78	54.97	52.41	49.85	47.70	53.41	54.81	48.34	47.64	51.89	48.95	49.50	56.00	51.88	47.13	50.04
almandine	47.33	44.41	40.98	40.64	39.86	40.14	39.98	43.14	45.38	46.28	41.51	39.71	45.21	46.24	42.82	45.53	45.39	38.48	43.40	47.37	45.27
% rest	3.57	4.59	4.00	3.34	4.02	5.20	4.23	4.29	2.85	3.66	3.68	3.68	3.57	3.20	3.30	3.35	3.98	4.08	4.40	3.05	3.83
Xprp = XMg	0.02	0.02	0.01	0.01	0.01	0.01	0.01	0.02	0.02	0.03	0.02	0.01	0.03	0.03	0.02	0.02	0.02	0.01	0.02	0.02	0.02
Xalm = XFe	0.49	0.47	0.44	0.43	0.43	0.44	0.43	0.46	0.47	0.49	0.44	0.43	0.48	0.48	0.45	0.48	0.48	0.42	0.46	0.49	0.48
Xsps = XMn	0.03	0.04	0.04	0.04	0.04	0.03	0.04	0.02	0.02	0.03	0.03	0.03	0.04	0.03	0.03	0.03	0.02	0.04	0.02	0.03	0.02
Xgrs = XCa	0.46	0.47	0.51	0.52	0.52	0.51	0.52	0.50	0.48	0.46	0.51	0.53	0.46	0.46	0.50	0.47	0.47	0.53	0.49	0.45	0.48
XAl	1.00	1.00	1.00	1.00	1.00	1.00	1.00	1.00	1.00	1.00	1.00	1.00	1.00	1.00	1.00	1.00	1.00	1.00	1.00	1.00	1.00

Appendix B: Electron microprobe analyses of garnet; micaschist [sample M98/5]

sample	M98/5	M98/5	M98/5	M98/5	M98/5	M98/5	M98/5	M98/5	M98/5	M98/5	M98/5	M98/5	M98/5	M98/5	M98/5	M98/5	M98/5	M98/5	M98/5	M98/5	M98/5
analysis	grt3_13	grt4_1	grt4_2	grt4_3	grt4_4	grt4_5	grt4_6	grt4_7	grt4_8	grt4_9	grt4_10	grt4_11	grt4_12	grt4_13	grt4_14	grt4_15	grt5_1	grt5_2	grt5_3	grt5_4	grt5_5
SiO2	38.77	38.60	38.67	38.86	38.65	38.55	38.57	38.85	38.49	38.73	38.67	38.76	38.80	38.62	38.39	38.56	38.56	38.72	38.54	38.70	38.47
Al2O3	20.74	20.76	20.59	20.62	20.87	20.74	20.83	21.02	21.02	20.50	20.76	20.70	20.84	20.59	20.60	20.79	20.77	20.60	20.92	21.02	20.89
TiO2	0.10	0.03	0.06	0.13	0.09	0.04	0.04	0.00	0.02	0.01	0.08	0.11	0.04	0.05	0.02	0.06	0.08	0.04	0.05	0.08	0.06
FeO	21.97	22.41	21.47	21.13	19.11	21.74	19.41	15.06	20.90	21.52	19.59	19.63	19.80	22.29	21.89	20.71	22.26	21.07	19.81	19.23	21.76
MgO	0.63	0.65	0.61	0.55	0.30	0.57	0.33	0.14	0.50	0.57	0.39	0.34	0.36	0.64	0.65	0.49	0.67	0.59	0.34	0.34	0.60
CaO	16.44	16.24	16.50	17.58	18.87	17.28	18.92	19.51	17.51	17.40	18.42	18.82	18.75	16.07	16.73	17.83	16.52	17.57	18.59	18.68	16.98
MnO	1.91	1.54	1.49	1.17	1.84	0.93	1.77	5.81	1.17	1.08	1.60	1.72	1.64	1.43	1.37	1.35	1.11	0.98	1.58	1.66	1.12
total	100.58	100.31	99.43	100.07	99.79	99.90	99.90	100.42	99.64	99.81	99.54	100.13	100.31	99.76	99.68	99.81	100.00	99.60	99.90	99.75	99.89
FeO Ox	21.97	22.41	21.47	21.13	19.11	21.74	19.41	15.06	20.90	21.52	19.59	19.63	19.80	22.29	21.89	20.71	22.26	21.07	19.81	19.23	21.76
Fe2O3 Ox	0.00	0.00	0.00	0.00	0.00	0.00	0.00	0.00	0.00	0.00	0.00	0.00	0.00	0.00	0.00	0.00	0.00	0.00	0.00	0.00	0.00
total Ox	100.56	100.23	99.38	100.04	99.73	99.85	99.87	100.39	99.61	99.80	99.51	100.08	100.23	99.69	99.65	99.78	99.96	99.57	99.83	99.71	99.88
number of cations based on 12 oxygen atoms																					
Si	3.04	3.04	3.06	3.05	3.04	3.04	3.03	3.04	3.04	3.06	3.05	3.04	3.04	3.05	3.04	3.04	3.04	3.05	3.03	3.04	3.03
Al tot.	1.92	1.93	1.92	1.91	1.94	1.93	1.93	1.94	1.95	1.91	1.93	1.92	1.93	1.92	1.92	1.93	1.93	1.92	1.94	1.95	1.94
Ti	0.01	0.00	0.00	0.01	0.01	0.00	0.00	0.00	0.00	0.00	0.00	0.01	0.00	0.00	0.00	0.00	0.00	0.00	0.00	0.00	0.00
Fe tot.	1.44	1.48	1.42	1.39	1.26	1.43	1.28	0.98	1.38	1.42	1.29	1.29	1.30	1.47	1.45	1.36	1.47	1.39	1.30	1.26	1.43
Fe3+	0.00	0.00	0.00	0.00	0.00	0.00	0.00	0.00	0.00	0.00	0.00	0.00	0.00	0.00	0.00	0.00	0.00	0.00	0.00	0.00	0.00
Fe2+	1.44	1.48	1.42	1.39	1.26	1.43	1.28	0.98	1.38	1.42	1.29	1.29	1.30	1.47	1.45	1.36	1.47	1.39	1.30	1.26	1.43
Mg	0.07	0.08	0.07	0.06	0.04	0.07	0.04	0.02	0.06	0.07	0.05	0.04	0.04	0.08	0.08	0.06	0.08	0.07	0.04	0.04	0.07
Ca	1.38	1.37	1.40	1.48	1.59	1.46	1.59	1.63	1.48	1.47	1.56	1.58	1.57	1.36	1.42	1.51	1.40	1.49	1.57	1.57	1.43
Mn	0.13	0.10	0.10	0.08	0.12	0.06	0.12	0.38	0.08	0.07	0.11	0.11	0.11	0.10	0.09	0.09	0.07	0.07	0.11	0.11	0.07
total cat	7.99	7.99	7.98	7.98	7.99	7.99	8.00	7.99	7.99	7.99	7.98	7.99	7.99	7.98	8.00	7.99	7.99	7.98	7.99	7.98	7.99
andradite	0.00	0.00	0.00	0.00	0.00	0.00	0.00	0.00	0.00	0.00	0.00	0.00	0.00	0.00	0.00	0.00	0.00	0.00	0.00	0.00	0.00
pyrope	2.56	2.62	2.49	2.26	1.21	2.33	1.34	0.55	2.00	2.34	1.59	1.39	1.46	2.62	2.66	1.98	2.70	2.41	1.38	1.36	2.42
spessartine	4.41	3.55	3.47	2.71	4.22	2.14	4.07	13.24	2.66	2.52	3.69	3.98	3.77	3.33	3.19	3.11	2.57	2.29	3.62	3.78	2.57
grossular	48.03	47.40	48.56	51.66	54.79	50.48	55.04	56.24	50.47	51.43	53.76	55.09	54.52	47.29	49.21	51.97	48.19	51.68	53.84	53.85	49.25
almandine	45.00	46.43	45.49	43.37	39.78	45.04	39.56	29.97	44.87	43.72	40.95	39.54	40.26	46.76	44.95	42.94	46.54	43.62	41.16	41.01	45.75
% rest	3.96	3.56	3.67	4.28	3.07	3.52	3.37	3.06	2.11	4.58	3.32	4.11	3.63	3.82	3.87	3.32	3.36	4.01	2.88	2.39	2.83
Xprp = XMg	0.02	0.03	0.02	0.02	0.01	0.02	0.01	0.01	0.02	0.02	0.02	0.01	0.01	0.03	0.03	0.02	0.03	0.02	0.01	0.01	0.02
Xalm = XFe	0.48	0.49	0.47	0.46	0.42	0.47	0.42	0.33	0.46	0.47	0.43	0.43	0.43	0.49	0.48	0.45	0.49	0.46	0.43	0.42	0.48
Xsps = XMn	0.04	0.03	0.03	0.03	0.04	0.02	0.04	0.13	0.03	0.02	0.04	0.04	0.04	0.03	0.03	0.03	0.02	0.02	0.03	0.04	0.02
Xgrs = XCa	0.46	0.45	0.47	0.49	0.53	0.48	0.53	0.54	0.49	0.49	0.52	0.52	0.52	0.45	0.47	0.50	0.46	0.49	0.52	0.53	0.48
XAl	1.00	1.00	1.00	1.00	1.00	1.00	1.00	1.00	1.00	1.00	1.00	1.00	1.00	1.00	1.00	1.00	1.00	1.00	1.00	1.00	1.00

Appendix B: Electron microprobe analyses of garnet; micaschist [sample M98/5]; grt-cld-schist [sample GR99/26]

sample	M98/5	M98/5	M98/5	M98/5	M98/5	M98/5	M98/5	M98/5	M98/5	M98/5	M98/5	M98/5	M98/5	GR99/26	GR99/26	GR99/26	GR99/26	GR99/26	GR99/26	GR99/26
analysis	grt5_6	grt5_7	grt5_8	grt5_9	grt5_10	grt5_11	grt5_12	grt5_13	grt5_14	grt5_15	grt5_16	grt5_17	grt5_18	grt1_1	grt1_2	grt1_3	grt1_4	grt1_5	grt1_6	grt1_7
SiO2	38.48	38.54	38.52	38.50	38.53	38.44	38.48	38.13	38.54	38.29	38.65	38.29	38.62	37.81	37.94	37.66	37.68	37.66	38.09	38.27
Al2O3	20.70	20.73	20.92	20.87	21.01	20.85	20.48	20.63	20.71	20.56	20.75	20.58	20.64	20.88	20.80	20.72	20.89	20.71	20.65	20.68
TiO2	0.06	0.10	0.06	0.03	0.11	0.09	0.03	0.09	0.08	0.11	0.06	0.05	0.05	0.07	0.08	0.08	0.06	0.04	0.11	0.10
FeO	21.34	21.13	21.70	20.08	21.81	22.18	22.02	22.38	18.34	20.11	21.21	22.39	21.67	33.54	33.16	33.17	32.96	32.61	32.19	31.60
MgO	0.62	0.61	0.60	0.41	0.61	0.62	0.61	0.66	0.27	0.42	0.60	0.68	0.64	2.20	2.16	2.14	2.03	1.87	1.82	1.76
CaO	17.08	17.11	17.39	18.37	16.55	16.11	16.49	16.01	19.66	18.48	16.58	16.67	16.93	4.54	5.25	4.79	4.74	4.76	4.93	5.60
MnO	1.11	1.13	1.08	1.65	1.62	1.71	1.69	1.84	1.76	1.48	1.68	1.15	1.00	0.95	1.00	1.19	1.37	1.60	1.78	1.86
total	99.45	99.35	100.28	99.95	100.31	100.01	99.87	99.79	99.42	99.50	99.58	99.83	99.59	100.02	100.40	99.76	99.77	99.29	99.58	99.87
FeO Ox	21.34	21.13	21.68	20.08	21.81	22.18	22.02	22.21	18.34	20.01	21.21	22.20	21.67	33.54	33.16	33.17	32.96	32.61	32.19	31.60
Fe2O3 Ox	0.00	0.00	0.02	0.00	0.00	0.00	0.00	0.19	0.00	0.11	0.00	0.21	0.00	0.00	0.00	0.00	0.00	0.00	0.00	0.00
total Ox	99.39	99.34	100.27	99.91	100.24	100.00	99.81	99.76	99.36	99.46	99.53	99.83	99.55	99.99	100.38	99.74	99.73	99.24	99.56	99.87
number of cations based on 12 oxygen atoms																				
Si	3.04	3.05	3.03	3.03	3.03	3.03	3.04	3.02	3.04	3.03	3.05	3.03	3.05	3.03	3.03	3.03	3.03	3.04	3.06	3.06
Al tot.	1.93	1.93	1.94	1.94	1.95	1.94	1.91	1.93	1.93	1.92	1.93	1.92	1.92	1.97	1.96	1.97	1.98	1.97	1.96	1.95
Ti	0.00	0.01	0.00	0.00	0.01	0.01	0.00	0.01	0.00	0.01	0.00	0.00	0.00	0.00	0.00	0.00	0.00	0.00	0.01	0.01
Fe tot.	1.41	1.40	1.43	1.32	1.43	1.46	1.46	1.48	1.21	1.33	1.40	1.48	1.43	2.25	2.22	2.23	2.22	2.20	2.16	2.12
Fe3+	0.00	0.00	0.00	0.00	0.00	0.00	0.00	0.01	0.00	0.01	0.00	0.01	0.00	0.00	0.00	0.00	0.00	0.00	0.00	0.00
Fe2+	1.41	1.40	1.42	1.32	1.43	1.46	1.46	1.47	1.21	1.32	1.40	1.47	1.43	2.25	2.22	2.23	2.22	2.20	2.16	2.12
Mg	0.07	0.07	0.07	0.05	0.07	0.07	0.07	0.08	0.03	0.05	0.07	0.08	0.08	0.26	0.26	0.26	0.24	0.23	0.22	0.21
Ca	1.45	1.45	1.46	1.55	1.39	1.36	1.40	1.36	1.66	1.57	1.40	1.41	1.43	0.39	0.45	0.41	0.41	0.41	0.42	0.48
Mn	0.07	0.08	0.07	0.11	0.11	0.11	0.11	0.12	0.12	0.10	0.11	0.08	0.07	0.06	0.07	0.08	0.09	0.11	0.12	0.13
total cat	7.99	7.98	8.00	8.00	7.99	7.99	8.00	8.01	7.99	8.00	7.98	8.01	7.98	7.98	7.98	7.98	7.98	7.97	7.95	7.95
andradite	0.00	0.00	0.09	0.00	0.00	0.00	0.00	0.88	0.00	0.50	0.00	0.99	0.00	0.00	0.00	0.00	0.00	0.00	0.00	0.00
pyrope	2.51	2.48	2.40	1.64	2.46	2.51	2.53	2.68	1.10	1.70	2.45	2.74	2.62	8.88	8.75	8.70	8.21	7.63	7.45	7.17
spessartine	2.58	2.60	2.48	3.79	3.69	3.93	3.95	4.23	4.07	3.43	3.88	2.66	2.32	2.19	2.30	2.74	3.15	3.71	4.14	4.31
grossular	50.00	50.01	50.23	53.33	47.73	46.82	48.79	45.73	57.52	53.70	48.42	47.61	49.70	13.17	15.29	14.01	13.79	13.97	14.50	16.41
almandine	44.92	44.91	44.80	41.24	46.11	46.74	44.73	46.48	37.31	40.68	45.26	46.01	45.35	75.76	73.66	74.55	74.84	74.69	73.91	72.11
% rest	3.29	3.14	3.02	3.14	2.52	2.92	4.45	2.76	3.60	3.63	3.10	3.11	3.69	1.02	1.86	1.52	0.98	1.26	1.83	1.85
Xprp = XMg	0.02	0.02	0.02	0.02	0.02	0.02	0.02	0.03	0.01	0.02	0.02	0.03	0.03	0.09	0.09	0.09	0.08	0.08	0.07	0.07
Xalm = XFe	0.47	0.47	0.47	0.44	0.48	0.49	0.48	0.49	0.40	0.44	0.47	0.49	0.48	0.76	0.74	0.75	0.75	0.75	0.74	0.72
Xsps = XMn	0.02	0.03	0.02	0.04	0.04	0.04	0.04	0.04	0.04	0.03	0.04	0.03	0.02	0.02	0.02	0.03	0.03	0.04	0.04	0.04
Xgrs = XCa	0.48	0.48	0.48	0.51	0.46	0.45	0.46	0.45	0.55	0.51	0.47	0.46	0.48	0.13	0.15	0.14	0.14	0.14	0.15	0.16
XAl	1.00	1.00	1.00	1.00	1.00	1.00	1.00	1.00	1.00	1.00	1.00	1.00	1.00	1.00	1.00	1.00	1.00	1.00	1.00	1.00

Appendix B: Electron microprobe analyses of garnet; grt-cld-schist [sample GR99/26]

sample	GR99/26	GR99/26	GR99/26	GR99/26	GR99/26	GR99/26	GR99/26	GR99/26	GR99/26	GR99/26	GR99/26	GR99/26	GR99/26	GR99/26	GR99/26	GR99/26	GR99/26	GR99/26	GR99/26	GR99/26	GR99/26
analysis	grt1_8	grt1_9	grt1_10	grt1_11	grt1_12	grt1_13	grt1_14	grt1_15	grt1_16	grt1_17	grt1_18	grt1_19	grt1_20	grt1_21	grt1_22	grt1_23	grt1_24	grt1_25	grt1_26	grt1_27	grt1_28
SiO2	37.86	37.91	38.28	38.39	37.90	38.06	37.99	38.08	37.70	38.11	37.61	37.89	38.14	38.13	37.93	37.68	37.76	38.11	38.10	38.13	37.72
Al2O3	20.65	20.74	20.62	20.47	20.68	20.66	20.59	20.62	20.66	20.58	20.56	20.44	20.55	20.75	20.63	20.61	20.53	20.60	20.69	20.50	20.52
TiO2	0.09	0.08	0.06	0.13	0.11	0.09	0.15	0.09	0.09	0.10	0.05	0.09	0.04	0.11	0.07	0.01	0.11	0.10	0.12	0.11	0.09
FeO	31.01	30.72	30.24	29.35	30.07	28.39	28.84	28.74	28.42	28.50	28.37	27.84	28.21	28.29	28.14	29.66	28.47	28.34	28.11	29.44	28.86
MgO	1.68	1.61	1.48	1.42	1.38	1.30	1.28	1.33	1.26	1.21	1.17	1.22	1.14	1.17	1.26	1.22	1.23	1.39	1.28	1.25	1.36
CaO	5.91	6.27	6.69	7.11	6.69	7.91	7.46	7.31	7.30	7.38	7.28	7.28	7.22	8.00	7.56	6.55	7.63	7.52	7.64	7.08	7.29
MnO	1.99	2.15	2.23	2.42	2.46	2.53	2.62	2.78	2.72	2.75	2.79	2.83	2.84	2.83	2.74	2.83	2.76	2.61	2.67	2.71	2.55
total	99.21	99.49	99.63	99.29	99.29	98.99	98.93	98.96	98.17	98.66	97.87	97.62	98.16	99.31	98.34	98.56	98.49	98.71	98.62	99.24	98.39
FeO Ox	31.01	30.72	30.24	29.35	30.07	28.39	28.84	28.74	28.42	28.50	28.37	27.84	28.21	28.29	28.14	29.66	28.47	28.34	28.11	29.44	28.86
Fe2O3 Ox	0.00	0.00	0.00	0.00	0.00	0.00	0.00	0.00	0.00	0.00	0.00	0.00	0.00	0.00	0.00	0.00	0.00	0.00	0.00	0.00	0.00
total Ox	99.19	99.47	99.60	99.28	99.28	98.94	98.93	98.95	98.15	98.62	97.82	97.59	98.14	99.28	98.32	98.56	98.48	98.68	98.60	99.22	98.38
number of cations based on 12 oxygen atoms																					
Si	3.05	3.05	3.07	3.08	3.05	3.06	3.06	3.07	3.06	3.08	3.06	3.09	3.09	3.06	3.07	3.06	3.06	3.07	3.07	3.07	3.06
Al tot.	1.96	1.97	1.95	1.94	1.96	1.96	1.96	1.96	1.98	1.96	1.97	1.96	1.96	1.96	1.97	1.97	1.96	1.96	1.97	1.95	1.96
Ti	0.01	0.00	0.00	0.01	0.01	0.01	0.01	0.01	0.01	0.01	0.00	0.01	0.00	0.01	0.00	0.00	0.01	0.01	0.01	0.01	0.01
Fe tot.	2.09	2.07	2.03	1.97	2.03	1.91	1.94	1.94	1.93	1.92	1.93	1.90	1.91	1.90	1.90	2.01	1.93	1.91	1.90	1.98	1.96
Fe3+	0.00	0.00	0.00	0.00	0.00	0.00	0.00	0.00	0.00	0.00	0.00	0.00	0.00	0.00	0.00	0.00	0.00	0.00	0.00	0.00	0.00
Fe2+	2.09	2.07	2.03	1.97	2.03	1.91	1.94	1.94	1.93	1.92	1.93	1.90	1.91	1.90	1.90	2.01	1.93	1.91	1.90	1.98	1.96
Mg	0.20	0.19	0.18	0.17	0.17	0.16	0.15	0.16	0.15	0.15	0.14	0.15	0.14	0.14	0.15	0.15	0.15	0.17	0.15	0.15	0.16
Ca	0.51	0.54	0.57	0.61	0.58	0.68	0.64	0.63	0.63	0.64	0.64	0.64	0.63	0.69	0.66	0.57	0.66	0.65	0.66	0.61	0.63
Mn	0.14	0.15	0.15	0.16	0.17	0.17	0.18	0.19	0.19	0.19	0.19	0.20	0.19	0.19	0.19	0.19	0.19	0.18	0.18	0.18	0.18
total cat	7.96	7.96	7.95	7.94	7.96	7.95	7.95	7.95	7.95	7.94	7.95	7.93	7.93	7.95	7.94	7.96	7.95	7.94	7.94	7.95	7.96
andradite	0.00	0.00	0.00	0.00	0.00	0.00	0.00	0.00	0.00	0.00	0.00	0.00	0.00	0.00	0.00	0.00	0.00	0.00	0.00	0.00	0.00
pyrope	6.87	6.54	6.07	5.85	5.62	5.35	5.26	5.49	5.25	5.02	4.88	5.16	4.80	4.80	5.22	5.05	5.05	5.76	5.30	5.15	5.59
spessartine	4.62	4.97	5.18	5.66	5.72	5.90	6.12	6.50	6.44	6.49	6.63	6.79	6.79	6.59	6.48	6.65	6.47	6.13	6.31	6.33	5.98
grossular	17.37	18.34	19.66	21.05	19.67	23.35	22.06	21.63	21.87	22.04	21.89	22.10	21.83	23.57	22.61	19.47	22.62	22.35	22.83	20.93	21.62
almandine	71.14	70.14	69.10	67.45	68.99	65.40	66.56	66.38	66.44	66.44	66.59	65.95	66.58	65.05	65.69	68.82	65.86	65.75	65.56	67.59	66.81
% rest	1.53	1.38	1.97	2.44	1.63	2.01	2.01	2.13	2.56	2.70	2.56	3.30	3.41	2.07	2.64	1.95	1.82	2.43	2.86	2.11	1.80
Xprp = XMg	0.07	0.07	0.06	0.06	0.06	0.05	0.05	0.05	0.05	0.05	0.05	0.05	0.05	0.05	0.05	0.05	0.05	0.06	0.05	0.05	0.06
Xalm = XFe	0.71	0.70	0.69	0.68	0.69	0.65	0.67	0.66	0.66	0.66	0.67	0.66	0.67	0.65	0.66	0.69	0.66	0.66	0.66	0.68	0.67
Xsps = XMn	0.05	0.05	0.05	0.06	0.06	0.06	0.06	0.07	0.06	0.06	0.07	0.07	0.07	0.07	0.06	0.07	0.06	0.06	0.06	0.06	0.06
Xgrs = XCa	0.17	0.18	0.20	0.21	0.20	0.23	0.22	0.22	0.22	0.22	0.22	0.22	0.22	0.24	0.23	0.19	0.23	0.22	0.23	0.21	0.22
XAl	1.00	1.00	1.00	1.00	1.00	1.00	1.00	1.00	1.00	1.00	1.00	1.00	1.00	1.00	1.00	1.00	1.00	1.00	1.00	1.00	1.00

Appendix B: Electron microprobe analyses of garnet; grt-cld-schist [sample GR99/26]

sample	GR99/26	GR99/26	GR99/26	GR99/26	GR99/26	GR99/26	GR99/26	GR99/26	GR99/26	GR99/26	GR99/26	GR99/26	GR99/26	GR99/26	GR99/26	GR99/26	GR99/26	GR99/26	GR99/26	GR99/26	GR99/26
analysis	grt1_29	grt1_30	grt1_31	grt1_32	grt1_33	grt1_34	grt1_35	grt1_36	grt1_37	grt1_38	grt1_39	grt1_40	grt1_41	grt1_42	grt2_1	grt2_2	grt2_3	grt2_4	grt2_5	grt2_6	grt2_7
SiO2	38.16	37.96	37.45	38.06	38.19	37.23	37.85	37.54	37.55	37.50	37.47	37.82	37.28	37.54	37.08	37.30	37.48	37.22	37.41	37.38	37.16
Al2O3	20.52	20.63	20.53	20.47	20.42	20.49	20.86	20.51	20.68	20.85	20.64	20.79	20.73	20.64	20.67	20.70	20.80	20.49	20.82	20.98	20.77
TiO2	0.12	0.07	0.11	0.09	0.08	0.10	0.10	0.09	0.06	0.06	0.05	0.05	0.04	0.01	0.04	0.06	0.05	0.09	0.04	0.07	0.07
FeO	28.96	29.29	30.10	29.13	29.70	30.60	31.19	31.65	31.99	32.08	33.39	33.31	33.33	34.09	28.11	28.59	29.70	28.57	33.17	33.42	31.83
MgO	1.35	1.42	1.51	1.52	1.47	1.69	1.70	1.71	1.88	1.89	2.04	2.07	2.24	2.40	1.23	1.22	1.29	1.20	2.12	1.98	1.79
CaO	7.39	7.13	6.47	6.83	6.44	5.83	5.55	5.57	5.15	5.50	4.75	4.84	4.68	3.74	7.56	7.54	6.45	7.87	4.73	4.51	5.47
MnO	2.56	1.18	2.28	2.17	2.22	2.16	2.03	1.90	1.74	1.47	1.44	1.21	1.06	0.94	3.19	3.35	3.43	3.18	1.57	1.88	2.17
total	99.06	97.69	98.45	98.27	98.52	98.11	99.29	98.98	99.06	99.35	99.79	100.09	99.39	99.36	97.88	98.76	99.20	98.62	99.86	100.22	99.26
FeO Ox	28.96	29.29	30.10	29.13	29.70	30.60	31.19	31.65	31.99	32.08	33.39	33.31	33.33	34.09	28.11	28.59	29.70	28.57	33.17	33.42	31.83
Fe2O3 Ox	0.00	0.00	0.00	0.00	0.00	0.00	0.00	0.00	0.00	0.00	0.00	0.00	0.00	0.00	0.00	0.00	0.00	0.00	0.00	0.00	0.00
total Ox	99.05	97.67	98.45	98.27	98.52	98.10	99.28	98.97	99.05	99.35	99.78	100.09	99.36	99.35	97.88	98.76	99.20	98.62	99.86	100.22	99.26
number of cations based on 12 oxygen atoms																					
Si	3.08	3.07	3.04	3.08	3.09	3.04	3.05	3.04	3.04	3.03	3.02	3.03	3.01	3.03	3.03	3.03	3.03	3.03	3.01	3.00	3.01
Al tot.	1.95	1.98	1.97	1.95	1.95	1.97	1.98	1.96	1.97	1.98	1.96	1.97	1.98	1.97	1.99	1.98	1.98	1.96	1.98	1.99	1.98
Ti	0.01	0.00	0.01	0.01	0.01	0.01	0.01	0.01	0.00	0.00	0.00	0.00	0.00	0.00	0.00	0.00	0.00	0.01	0.00	0.00	0.00
Fe tot.	1.95	1.99	2.05	1.97	2.01	2.09	2.10	2.14	2.16	2.16	2.25	2.23	2.25	2.30	1.92	1.94	2.01	1.94	2.23	2.25	2.16
Fe3+	0.00	0.00	0.00	0.00	0.00	0.00	0.00	0.00	0.00	0.00	0.00	0.00	0.00	0.00	0.00	0.00	0.00	0.00	0.00	0.00	0.00
Fe2+	1.95	1.99	2.05	1.97	2.01	2.09	2.10	2.14	2.16	2.16	2.25	2.23	2.25	2.30	1.92	1.94	2.01	1.94	2.23	2.25	2.16
Mg	0.16	0.17	0.18	0.18	0.18	0.21	0.20	0.21	0.23	0.23	0.25	0.25	0.27	0.29	0.15	0.15	0.16	0.15	0.25	0.24	0.22
Ca	0.64	0.62	0.56	0.59	0.56	0.51	0.48	0.48	0.45	0.48	0.41	0.42	0.41	0.32	0.66	0.66	0.56	0.69	0.41	0.39	0.47
Mn	0.17	0.08	0.16	0.15	0.15	0.15	0.14	0.13	0.12	0.10	0.10	0.08	0.07	0.06	0.22	0.23	0.23	0.22	0.11	0.13	0.15
total cat	7.95	7.92	7.97	7.94	7.93	7.97	7.96	7.97	7.97	7.98	7.99	7.98	7.99	7.98	7.97	7.98	7.97	7.99	8.00	8.00	7.99
andradite	0.00	0.00	0.00	0.00	0.00	0.00	0.00	0.00	0.00	0.00	0.00	0.00	0.00	0.00	0.00	0.00	0.00	0.00	0.00	0.00	0.00
pyrope	5.53	5.99	6.21	6.35	6.11	6.96	6.98	7.03	7.67	7.66	8.33	8.39	9.11	9.80	5.07	4.97	5.26	4.94	8.58	7.95	7.26
spessartine	5.98	2.82	5.32	5.14	5.25	5.06	4.74	4.44	4.03	3.39	3.34	2.79	2.45	2.17	7.48	7.75	7.94	7.43	3.61	4.29	5.00
grossular	21.82	21.68	19.10	20.45	19.27	17.26	16.39	16.46	15.10	16.02	13.94	14.11	13.68	10.98	22.41	22.07	18.89	23.27	13.77	13.03	15.96
almandine	66.67	69.51	69.36	68.07	69.37	70.72	71.89	72.08	73.20	72.94	74.38	74.72	74.77	77.05	65.04	65.21	67.91	64.36	74.04	74.73	71.77
% rest	2.01	3.69	1.28	2.66	2.70	1.18	2.07	1.69	1.08	0.83	1.80	1.49	1.13	1.45	1.27	0.79	1.09	1.66	1.11	0.56	0.75
Xprp = XMg	0.06	0.06	0.06	0.06	0.06	0.07	0.07	0.07	0.08	0.08	0.08	0.08	0.09	0.10	0.05	0.05	0.05	0.05	0.08	0.08	0.07
Xalm = XFe	0.67	0.70	0.69	0.68	0.69	0.71	0.72	0.72	0.73	0.73	0.75	0.75	0.75	0.77	0.65	0.65	0.68	0.65	0.74	0.75	0.72
Xsps = XMn	0.06	0.03	0.05	0.05	0.05	0.05	0.05	0.04	0.04	0.03	0.03	0.03	0.02	0.02	0.07	0.08	0.08	0.07	0.04	0.04	0.05
Xgrs = XCa	0.22	0.22	0.19	0.20	0.19	0.17	0.16	0.16	0.15	0.16	0.14	0.14	0.14	0.11	0.22	0.22	0.19	0.23	0.14	0.13	0.16
XAl	1.00	1.00	1.00	1.00	1.00	1.00	1.00	1.00	1.00	1.00	1.00	1.00	1.00	1.00	1.00	1.00	1.00	1.00	1.00	1.00	1.00

Appendix B: Electron microprobe analyses of garnet; grt-cld-schist [sample GR99/26]

sample	GR99/26	GR99/26	GR99/26	GR99/26	GR99/26	GR99/26	GR99/26	GR99/26	GR99/26	GR99/26	GR99/26	GR99/26	GR99/26	GR99/26	GR99/26	GR99/26	GR99/26	GR99/26	GR99/26	GR99/26	GR99/26
analysis	grt2_8	grt3_1	grt3_2	grt3_3	grt3_4	grt3_5	grt3_6	grt3_7	grt3_8	grt3_9	grt3_10	grt4_1	grt4_2	grt4_3	grt4_4	grt4_5	grt4_6	grt4_7	grt4_8	grt4_9	grt4_10
SiO2	37.40	37.30	37.34	37.29	37.44	37.22	37.26	37.35	37.40	37.35	37.04	36.83	36.85	36.64	37.34	36.85	37.11	37.43	36.86	36.90	36.92
Al2O3	20.71	20.89	20.93	20.94	20.91	20.88	20.94	20.80	20.75	20.80	20.77	20.07	20.07	20.15	20.46	20.25	20.34	20.47	19.88	20.06	20.37
TiO2	0.04	0.02	0.04	0.05	0.07	0.08	0.07	0.04	0.05	0.07	0.05	0.09	0.00	0.18	0.05	0.10	0.00	0.13	0.15	0.22	0.20
FeO	32.02	28.07	28.23	28.84	28.86	29.03	28.80	29.00	28.80	28.70	28.79	33.78	32.66	33.90	32.36	33.16	33.40	33.62	32.05	31.79	31.63
MgO	1.85	1.18	1.23	1.22	1.21	1.22	1.23	1.18	1.23	1.18	1.28	2.44	2.25	2.14	2.02	2.14	1.98	2.05	1.71	1.84	1.74
CaO	5.40	7.35	7.24	7.32	7.39	7.42	7.36	7.49	7.18	7.37	7.50	4.13	4.65	3.99	5.37	5.04	4.52	5.02	5.63	4.53	5.80
MnO	2.14	3.25	3.26	3.32	3.30	3.30	3.29	3.30	3.20	3.27	3.26	0.96	1.12	1.22	1.42	1.42	1.59	1.89	2.00	2.07	2.36
total	99.56	98.07	98.27	98.98	99.18	99.15	98.95	99.16	98.61	98.74	98.68	98.30	97.60	98.21	99.02	98.96	98.94	100.61	98.28	97.41	99.02
FeO Ox	32.02	28.07	28.23	28.84	28.86	29.03	28.80	29.00	28.80	28.70	28.79	33.59	32.66	33.84	32.36	32.68	33.40	33.12	31.96	31.79	31.48
Fe2O3 Ox	0.00	0.00	0.00	0.00	0.00	0.00	0.00	0.00	0.00	0.00	0.00	0.20	0.00	0.06	0.00	0.53	0.00	0.55	0.09	0.00	0.17
total Ox	99.56	98.06	98.27	98.98	99.18	99.15	98.95	99.16	98.61	98.74	98.69	98.32	97.60	98.22	99.01	99.01	98.94	100.67	98.29	97.41	99.03
number of cations based on 12 oxygen atoms																					
Si	3.02	3.04	3.03	3.02	3.02	3.01	3.02	3.02	3.03	3.03	3.01	3.02	3.03	3.01	3.03	3.00	3.02	3.01	3.03	3.04	3.01
Al tot.	1.97	2.00	2.00	2.00	1.99	1.99	2.00	1.98	1.98	1.99	1.99	1.94	1.95	1.95	1.96	1.95	1.95	1.94	1.92	1.95	1.95
Ti	0.00	0.00	0.00	0.00	0.00	0.00	0.00	0.00	0.00	0.00	0.00	0.01	0.00	0.01	0.00	0.01	0.00	0.01	0.01	0.01	0.01
Fe tot.	2.16	1.91	1.92	1.95	1.95	1.96	1.95	1.96	1.95	1.95	1.96	2.32	2.25	2.33	2.19	2.26	2.28	2.26	2.20	2.19	2.15
Fe3+	0.00	0.00	0.00	0.00	0.00	0.00	0.00	0.00	0.00	0.00	0.00	0.01	0.00	0.00	0.00	0.03	0.00	0.03	0.01	0.00	0.01
Fe2+	2.16	1.91	1.92	1.95	1.95	1.96	1.95	1.96	1.95	1.95	1.96	2.30	2.25	2.33	2.19	2.23	2.28	2.22	2.19	2.19	2.14
Mg	0.22	0.14	0.15	0.15	0.15	0.15	0.15	0.14	0.15	0.14	0.16	0.30	0.28	0.26	0.24	0.26	0.24	0.25	0.21	0.23	0.21
Ca	0.47	0.64	0.63	0.63	0.64	0.64	0.64	0.65	0.62	0.64	0.65	0.36	0.41	0.35	0.47	0.44	0.39	0.43	0.50	0.40	0.51
Mn	0.15	0.22	0.22	0.23	0.23	0.23	0.23	0.23	0.22	0.22	0.22	0.07	0.08	0.08	0.10	0.10	0.11	0.13	0.14	0.14	0.16
total cat	7.99	7.96	7.96	7.98	7.98	7.99	7.98	7.99	7.97	7.97	7.99	8.01	7.99	8.00	7.99	8.02	8.00	8.02	8.00	7.97	8.01
andradite	0.00	0.00	0.00	0.00	0.00	0.00	0.00	0.00	0.00	0.00	0.00	0.97	0.00	0.30	0.00	2.46	0.00	2.51	0.45	0.00	0.79
pyrope	7.53	4.90	5.10	4.97	4.92	4.94	5.01	4.78	5.05	4.83	5.19	10.15	9.45	8.92	8.32	8.69	8.20	8.23	7.22	7.73	7.14
spessartine	4.95	7.68	7.68	7.69	7.63	7.59	7.62	7.60	7.46	7.60	7.52	2.27	2.67	2.88	3.32	3.28	3.74	4.31	4.80	4.94	5.51
grossular	15.80	21.96	21.57	21.43	21.60	21.58	21.55	21.82	21.18	21.68	21.88	11.38	14.04	11.66	15.90	12.25	13.46	11.98	16.64	13.68	16.32
almandine	71.72	65.46	65.65	65.91	65.85	65.90	65.82	65.80	66.31	65.89	65.41	75.23	73.85	76.23	72.45	73.33	74.59	72.97	70.90	73.64	70.24
% rest	1.33	2.22	2.15	1.04	1.07	0.50	1.03	0.66	1.39	1.23	0.41	2.17	2.54	2.12	2.07	0.43	2.29	0.80	3.41	2.13	1.54
Xprp = XMg	0.07	0.05	0.05	0.05	0.05	0.05	0.05	0.05	0.05	0.05	0.05	0.10	0.09	0.09	0.08	0.08	0.08	0.08	0.07	0.08	0.07
Xalm = XFe	0.72	0.65	0.66	0.66	0.66	0.66	0.66	0.66	0.66	0.66	0.65	0.76	0.75	0.77	0.73	0.74	0.75	0.74	0.72	0.74	0.71
Xsps = XMn	0.05	0.08	0.08	0.08	0.08	0.08	0.08	0.08	0.07	0.08	0.08	0.02	0.03	0.03	0.03	0.03	0.04	0.04	0.05	0.05	0.05
Xgrs = XCa	0.16	0.22	0.22	0.21	0.22	0.22	0.22	0.22	0.21	0.22	0.22	0.12	0.14	0.12	0.16	0.14	0.13	0.14	0.16	0.14	0.17
XAl	1.00	1.00	1.00	1.00	1.00	1.00	1.00	1.00	1.00	1.00	1.00	1.00	1.00	1.00	1.00	1.00	1.00	1.00	1.00	1.00	1.00

Appendix B: Electron microprobe analyses of garnet; grt-cld-schist [sample GR99/26]

sample	GR99/26	GR99/26	GR99/26	GR99/26	GR99/26	GR99/26	GR99/26	GR99/26	GR99/26	GR99/26	GR99/26	GR99/26	GR99/26	GR99/26	GR99/26	GR99/26	GR99/26	GR99/26	GR99/26	GR99/26	GR99/26
analysis	grt4_11	grt4_12	grt4_13	grt4_14	grt4_15	grt4_16	grt4_17	grt4_18	grt4_19	grt4_20	grt4_21	grt4_22	grt4_23	grt4_24	grt4_25	grt4_26	grt4_27	grt4_28	grt4_29	grt4_30	grt4_31
SiO2	37.10	37.04	37.33	37.37	36.93	37.27	36.44	37.08	36.67	37.69	37.19	37.47	37.06	37.31	36.82	37.93	37.10	37.33	36.96	37.39	37.09
Al2O3	20.31	20.23	19.97	19.94	19.69	20.48	19.95	19.92	19.78	19.84	19.67	20.12	20.37	20.46	20.38	20.10	20.62	20.08	19.97	19.99	20.03
TiO2	0.07	0.08	0.14	0.02	0.03	0.03	0.16	0.15	0.03	0.22	0.18	0.28	0.11	0.22	0.15	0.20	0.13	0.11	0.05	0.00	0.12
FeO	31.09	30.02	31.06	30.22	30.61	29.89	30.69	28.84	29.25	29.44	29.15	30.26	30.37	29.91	30.60	31.07	31.96	32.22	32.24	34.65	33.55
MgO	1.67	1.39	1.54	1.57	1.41	1.42	1.38	1.25	1.44	1.18	1.44	1.48	1.52	1.50	1.51	1.66	1.67	1.64	1.68	2.18	1.98
CaO	5.65	6.57	6.84	6.14	6.96	5.90	6.17	7.97	7.33	7.18	7.55	7.45	5.74	6.54	7.01	5.88	5.92	5.67	5.08	3.67	4.71
MnO	2.50	2.48	2.61	2.77	2.89	2.97	3.04	3.05	2.70	2.97	2.82	2.93	2.76	2.71	2.71	2.54	2.55	2.25	2.30	1.94	1.67
total	98.39	97.81	99.50	98.03	98.52	97.96	97.84	98.27	97.20	98.51	98.00	99.99	97.93	98.65	99.18	99.38	99.95	99.30	98.28	99.82	99.15
FeO Ox	31.09	30.02	30.76	30.22	30.08	29.89	30.41	28.84	29.20	29.44	29.15	30.03	30.37	29.91	30.03	31.07	31.54	32.22	32.24	34.32	33.31
Fe2O3 Ox	0.00	0.00	0.33	0.00	0.58	0.00	0.31	0.00	0.06	0.00	0.00	0.26	0.00	0.00	0.63	0.00	0.46	0.00	0.00	0.37	0.26
total Ox	98.39	97.81	99.53	98.02	98.58	97.96	97.86	98.26	97.20	98.51	97.99	100.01	97.93	98.65	99.24	99.37	100.00	99.30	98.28	99.85	99.17
number of cations based on 12 oxygen atoms																					
Si	3.03	3.04	3.03	3.06	3.03	3.05	3.01	3.03	3.03	3.07	3.05	3.02	3.04	3.03	2.99	3.06	3.00	3.03	3.03	3.03	3.02
Al tot.	1.96	1.96	1.91	1.92	1.90	1.97	1.94	1.92	1.93	1.90	1.90	1.91	1.97	1.96	1.95	1.91	1.96	1.92	1.93	1.91	1.92
Ti	0.00	0.00	0.01	0.00	0.00	0.00	0.01	0.01	0.00	0.01	0.01	0.02	0.01	0.01	0.01	0.01	0.01	0.01	0.00	0.00	0.01
Fe tot.	2.12	2.06	2.11	2.07	2.10	2.04	2.12	1.97	2.02	2.00	2.00	2.04	2.08	2.03	2.08	2.10	2.16	2.19	2.21	2.35	2.29
Fe3+	0.00	0.00	0.02	0.00	0.04	0.00	0.02	0.00	0.00	0.00	0.00	0.02	0.00	0.00	0.04	0.00	0.03	0.00	0.00	0.02	0.02
Fe2+	2.12	2.06	2.09	2.07	2.06	2.04	2.10	1.97	2.02	2.00	2.00	2.02	2.08	2.03	2.04	2.10	2.13	2.19	2.21	2.33	2.27
Mg	0.20	0.17	0.19	0.19	0.17	0.17	0.17	0.15	0.18	0.14	0.18	0.18	0.19	0.18	0.18	0.20	0.20	0.20	0.21	0.26	0.24
Ca	0.49	0.58	0.59	0.54	0.61	0.52	0.55	0.70	0.65	0.63	0.66	0.64	0.50	0.57	0.61	0.51	0.51	0.49	0.45	0.32	0.41
Mn	0.17	0.17	0.18	0.19	0.20	0.21	0.21	0.21	0.19	0.20	0.20	0.20	0.19	0.19	0.19	0.17	0.17	0.15	0.16	0.13	0.12
total cat	7.99	7.98	8.01	7.98	8.02	7.96	8.01	8.00	8.00	7.97	7.99	8.01	7.97	7.98	8.02	7.97	8.01	8.00	8.00	8.01	8.01
andradite	0.00	0.00	1.57	0.00	2.76	0.00	1.48	0.00	0.27	0.00	0.00	1.21	0.00	0.00	2.91	0.00	2.10	0.00	0.00	1.72	1.23
pyrope	6.93	5.80	6.40	6.62	5.88	5.89	5.76	5.30	6.13	5.00	6.15	6.11	6.30	6.20	6.11	6.95	6.71	6.89	7.09	9.03	8.23
spessartine	5.90	5.87	6.16	6.65	6.84	7.00	7.19	7.33	6.52	7.17	6.87	6.89	6.49	6.34	6.23	6.05	5.82	5.37	5.52	4.57	3.94
grossular	16.86	19.68	18.86	18.66	18.06	17.58	16.98	24.24	22.13	21.93	23.26	20.95	17.07	19.37	17.49	17.73	14.99	17.11	15.41	9.21	12.84
almandine	70.32	68.65	67.01	68.07	66.46	69.53	68.59	63.12	64.96	65.91	63.72	64.84	70.13	68.09	67.25	69.27	70.37	70.63	71.98	75.47	73.75
% rest	2.03	1.93	3.16	3.48	2.33	1.55	1.55	3.94	3.34	4.36	4.88	3.35	1.29	1.70	0.43	3.95	0.30	3.83	3.32	2.88	2.68
Xprp = XMg	0.07	0.06	0.06	0.06	0.06	0.06	0.06	0.05	0.06	0.05	0.06	0.06	0.06	0.06	0.06	0.07	0.07	0.07	0.07	0.09	0.08
Xalm = XFe	0.71	0.69	0.69	0.69	0.68	0.70	0.70	0.65	0.67	0.67	0.66	0.67	0.70	0.68	0.68	0.70	0.71	0.72	0.73	0.77	0.75
Xsps = XMn	0.06	0.06	0.06	0.06	0.07	0.07	0.07	0.07	0.06	0.07	0.06	0.07	0.06	0.06	0.06	0.06	0.06	0.05	0.05	0.04	0.04
Xgrs = XCa	0.17	0.19	0.19	0.18	0.20	0.18	0.18	0.23	0.21	0.21	0.22	0.21	0.17	0.19	0.20	0.17	0.17	0.16	0.15	0.10	0.13
XAl	1.00	1.00	1.00	1.00	1.00	1.00	1.00	1.00	1.00	1.00	1.00	1.00	1.00	1.00	1.00	1.00	1.00	1.00	1.00	1.00	1.00

Appendix B: Electron microprobe analyses of garnet; grt-cld-schist [sample GR99/26, GR99/40]

sample	GR99/26	GR99/26	GR99/26	GR99/26	GR99/40	GR99/40	GR99/40	GR99/40	GR99/40	GR99/40	GR99/40	GR99/40	GR99/40	GR99/40	GR99/40	GR99/40	GR99/40	GR99/40	GR99/40
analysis	grt4_32	grt4_33	grt4_34	grt4_35	grt1_1	grt1_2	grt1_3	grt1_4	grt1_5	grt1_6	grt1_7	grt1_8	grt1_9	grt2_1	grt2_2	grt2_3	grt2_4	grt2_5	grt2_6	grt2_7
SiO2	37.67	36.74	36.80	36.61	38.00	38.30	38.20	38.20	38.30	38.00	38.10	37.60	38.10	37.90	38.10	37.90	38.10	38.10	37.90	37.70
Al2O3	20.17	20.13	20.14	20.03	22.60	22.90	22.60	22.40	22.50	22.60	22.60	22.70	22.90	22.80	22.70	22.80	22.60	22.60	22.60	22.60
TiO2	0.20	0.10	0.07	0.00	0.00	0.00	0.10	0.10	0.00	0.00	0.00	0.00	0.00	0.00	0.00	0.00	0.00	0.10	0.10	0.10
FeO	33.30	33.88	36.05	35.19	34.40	33.10	30.10	28.80	29.70	29.10	30.30	33.30	34.40	35.30	33.80	33.20	31.90	29.50	29.70	29.70
MgO	2.21	2.35	2.52	2.49	2.00	1.70	1.20	1.10	1.10	1.20	1.30	1.70	2.10	2.10	1.90	1.70	1.40	1.30	1.20	1.20
CaO	4.64	4.07	3.55	3.51	4.10	5.20	7.90	8.60	8.10	8.70	8.10	5.20	4.00	3.30	4.60	5.50	6.40	8.20	8.70	8.30
MnO	1.57	1.36	1.03	0.82	1.10	1.40	1.60	1.90	2.00	1.90	1.60	1.40	1.10	1.00	1.20	1.30	1.50	1.50	1.60	1.70
total	99.76	98.63	100.16	98.65	102.30	102.60	101.70	101.00	101.70	101.50	102.20	101.80	102.50	102.40	102.20	102.40	101.90	101.30	101.70	101.20
FeO Ox	33.30	33.45	34.67	34.40	34.40	33.10	30.10	28.80	29.70	29.10	30.30	33.30	34.40	35.30	33.80	33.20	31.90	29.50	29.70	29.70
Fe2O3 Ox	0.00	0.48	1.53	0.87	0.00	0.00	0.00	0.00	0.00	0.00	0.00	0.00	0.00	0.00	0.00	0.00	0.00	0.00	0.00	0.00
total Ox	99.76	98.67	100.31	98.74	102.20	102.60	101.70	101.10	101.70	101.50	102.00	101.90	102.60	102.40	102.30	102.40	101.90	101.30	101.80	101.30
number of cations based on 12 oxygen atoms																				
Si	3.04	3.01	2.99	3.00	2.98	2.98	2.99	3.00	3.00	2.98	2.98	2.96	2.97	2.97	2.98	2.96	2.99	2.99	2.97	2.97
Al tot.	1.92	1.94	1.93	1.94	2.09	2.10	2.09	2.08	2.08	2.09	2.08	2.11	2.11	2.11	2.09	2.10	2.09	2.09	2.09	2.10
Ti	0.01	0.01	0.00	0.00	0.00	0.00	0.01	0.01	0.00	0.00	0.00	0.00	0.00	0.00	0.00	0.00	0.00	0.01	0.01	0.01
Fe tot.	2.25	2.32	2.45	2.41	2.26	2.16	1.97	1.89	1.95	1.91	1.98	2.19	2.24	2.31	2.21	2.17	2.09	1.94	1.95	1.95
Fe3+	0.00	0.03	0.09	0.05	0.00	0.00	0.00	0.00	0.00	0.00	0.00	0.00	0.00	0.00	0.00	0.00	0.00	0.00	0.00	0.00
Fe2+	2.25	2.29	2.35	2.36	2.26	2.16	1.97	1.89	1.95	1.91	1.98	2.19	2.24	2.31	2.21	2.17	2.09	1.94	1.95	1.95
Mg	0.27	0.29	0.30	0.30	0.23	0.20	0.14	0.13	0.13	0.14	0.15	0.20	0.24	0.25	0.22	0.20	0.16	0.15	0.14	0.14
Ca	0.40	0.36	0.31	0.31	0.34	0.43	0.66	0.72	0.68	0.73	0.68	0.44	0.33	0.28	0.39	0.46	0.54	0.69	0.73	0.70
Mn	0.11	0.09	0.07	0.06	0.07	0.09	0.11	0.13	0.13	0.13	0.11	0.09	0.07	0.07	0.08	0.09	0.10	0.10	0.11	0.11
total cat	7.99	8.01	8.05	8.03	7.98	7.97	7.96	7.95	7.96	7.98	7.98	7.99	7.97	7.98	7.97	7.98	7.97	7.96	7.98	7.98
andradite	0.00	2.21	7.04	4.04	0.00	0.00	0.00	0.00	0.00	0.00	0.00	0.00	0.00	0.00	0.00	0.00	0.00	0.00	0.00	0.00
pyrope	9.23	9.62	10.21	10.14	8.04	6.85	4.86	4.49	4.45	4.83	5.19	6.82	8.43	8.45	7.64	6.79	5.66	5.28	4.79	4.84
spessartine	3.73	3.16	2.37	1.90	2.51	3.21	3.68	4.40	4.60	4.34	3.63	3.19	2.51	2.29	2.74	2.95	3.44	3.47	3.63	3.90
grossular	13.94	9.77	3.29	6.23	11.85	15.07	23.01	25.21	23.55	25.16	23.26	15.00	11.55	9.55	13.31	15.80	18.59	23.96	24.99	24.06
almandine	73.10	75.23	77.09	77.69	77.60	74.87	68.44	65.90	67.40	65.67	67.91	74.98	77.51	79.71	76.31	74.45	72.31	67.29	66.58	67.20
% rest	3.96	0.84	1.05	0.20	2.80	3.59	3.56	3.72	3.35	2.83	2.50	2.42	3.17	3.00	3.06	2.57	3.20	3.65	2.40	2.78
Xprp = XMg	0.09	0.09	0.10	0.10	0.08	0.07	0.05	0.04	0.04	0.05	0.05	0.07	0.08	0.08	0.08	0.07	0.06	0.05	0.05	0.05
Xalm = XFe	0.74	0.76	0.78	0.78	0.78	0.75	0.68	0.66	0.67	0.66	0.68	0.75	0.78	0.80	0.76	0.74	0.72	0.67	0.67	0.67
Xsps = XMn	0.04	0.03	0.02	0.02	0.03	0.03	0.04	0.04	0.05	0.04	0.04	0.03	0.03	0.02	0.03	0.03	0.03	0.03	0.04	0.04
Xgrs = XCa	0.13	0.12	0.10	0.10	0.12	0.15	0.23	0.25	0.24	0.25	0.23	0.15	0.12	0.10	0.13	0.16	0.19	0.24	0.25	0.24
XAl	1.00	1.00	1.00	1.00	1.00	1.00	1.00	1.00	1.00	1.00	1.00	1.00	1.00	1.00	1.00	1.00	1.00	1.00	1.00	1.00

Appendix B: Electron microprobe analyses of garnet; grt-cld-schist [sample GR99/40]

sample	GR99/40	GR99/40	GR99/40	GR99/40	GR99/40	GR99/40	GR99/40	GR99/40	GR99/40	GR99/40	GR99/40	GR99/40	GR99/40	GR99/40	GR99/40	GR99/40	GR99/40	GR99/40	GR99/40	GR99/40	GR99/40
analysis	grt2_8	grt2_9	grt2_10	grt2_11	grt3_1	grt3_2	grt3_3	grt3_4	grt3_5	grt3_6	grt4_1	grt4_2	grt4_3	grt4_4	grt4_5	grt4_6	grt4_7	grt4_8	grt4_9	grt4_10	grt4_11
SiO2	38.10	38.10	37.80	37.50	37.05	37.45	37.19	37.35	37.86	37.22	36.95	37.11	37.29	37.42	37.61	37.31	37.01	36.90	37.20	37.07	37.38
Al2O3	22.60	22.50	22.70	22.60	20.01	20.76	20.74	20.21	20.09	20.75	20.58	20.66	20.61	20.53	20.79	20.73	20.79	20.52	20.56	20.55	20.54
TiO2	0.00	0.00	0.00	0.00	0.05	0.00	0.11	0.13	0.07	0.49	0.03	0.03	0.05	0.03	0.04	0.02	0.02	0.00	0.03	0.01	0.01
FeO	30.90	32.00	33.70	34.50	31.97	30.79	30.96	29.44	28.38	33.03	34.57	33.25	33.83	32.55	32.55	32.10	32.73	32.68	33.01	33.73	34.19
MgO	1.40	1.50	1.80	2.10	1.44	1.61	1.36	1.20	1.12	1.85	2.05	1.90	1.88	1.80	1.59	1.59	1.60	1.67	1.74	1.91	1.97
CaO	6.90	6.20	4.80	3.30	6.83	7.09	7.01	8.70	8.74	4.59	3.65	4.53	3.93	4.84	5.47	5.95	5.65	5.28	4.78	4.26	4.02
MnO	1.60	1.40	1.30	0.90	1.30	1.56	1.57	2.04	2.26	1.18	0.94	0.41	0.50	0.51	0.49	0.58	0.50	0.44	0.48	0.44	0.42
total	101.40	101.80	102.00	100.90	98.65	99.26	98.94	99.06	98.52	99.11	98.77	97.88	98.09	97.68	98.54	98.28	98.31	97.49	97.80	97.97	98.53
FeO Ox	30.90	32.00	33.70	34.50	31.80	30.79	30.96	29.43	28.38	33.03	34.57	33.25	33.83	32.55	32.55	32.10	32.73	32.68	33.01	33.73	34.19
Fe2O3 Ox	0.00	0.00	0.00	0.00	0.19	0.00	0.00	0.01	0.00	0.00	0.00	0.00	0.00	0.00	0.00	0.00	0.00	0.00	0.00	0.00	0.00
total Ox	101.50	101.70	102.10	100.90	98.67	99.26	98.94	99.07	98.52	99.11	98.77	97.89	98.09	97.68	98.54	98.28	98.30	97.49	97.80	97.97	98.53
number of cations based on 12 oxygen atoms																					
Si	2.99	2.99	2.97	2.98	3.03	3.02	3.02	3.03	3.07	3.01	3.02	3.04	3.05	3.06	3.05	3.04	3.02	3.03	3.05	3.04	3.05
Al tot.	2.09	2.08	2.10	2.11	1.93	1.98	1.98	1.93	1.92	1.98	1.98	1.99	1.99	1.98	1.99	1.99	2.00	1.99	1.98	1.98	1.97
Ti	0.00	0.00	0.00	0.00	0.00	0.00	0.01	0.01	0.00	0.03	0.00	0.00	0.00	0.00	0.00	0.00	0.00	0.00	0.00	0.00	0.00
Fe tot.	2.03	2.10	2.21	2.29	2.18	2.08	2.10	2.00	1.92	2.24	2.36	2.28	2.31	2.23	2.21	2.19	2.23	2.25	2.26	2.31	2.33
Fe3+	0.00	0.00	0.00	0.00	0.01	0.00	0.00	0.00	0.00	0.00	0.00	0.00	0.00	0.00	0.00	0.00	0.00	0.00	0.00	0.00	0.00
Fe2+	2.03	2.10	2.21	2.29	2.17	2.08	2.10	1.99	1.92	2.24	2.36	2.28	2.31	2.23	2.21	2.19	2.23	2.25	2.26	2.31	2.33
Mg	0.16	0.18	0.21	0.25	0.18	0.19	0.16	0.14	0.14	0.22	0.25	0.23	0.23	0.22	0.19	0.19	0.19	0.20	0.21	0.23	0.24
Ca	0.58	0.52	0.40	0.28	0.60	0.61	0.61	0.76	0.76	0.40	0.32	0.40	0.34	0.42	0.48	0.52	0.49	0.47	0.42	0.37	0.35
Mn	0.11	0.09	0.09	0.06	0.09	0.11	0.11	0.14	0.16	0.08	0.06	0.03	0.03	0.04	0.03	0.04	0.03	0.03	0.03	0.03	0.03
total cat	7.96	7.97	7.98	7.97	8.01	7.99	7.99	8.00	7.97	7.97	7.99	7.96	7.96	7.95	7.95	7.97	7.98	7.97	7.96	7.97	7.97
andradite	0.00	0.00	0.00	0.00	0.90	0.00	0.00	0.05	0.00	0.00	0.00	0.00	0.00	0.00	0.00	0.00	0.00	0.00	0.00	0.00	0.00
pyrope	5.69	6.07	7.23	8.63	6.01	6.54	5.53	5.00	4.70	7.60	8.39	7.90	7.84	7.55	6.61	6.57	6.58	6.94	7.26	7.91	8.11
spessartine	3.70	3.22	2.97	2.10	3.08	3.60	3.63	4.83	5.39	2.75	2.19	0.97	1.19	1.22	1.16	1.36	1.17	1.04	1.14	1.04	0.98
grossular	20.16	18.04	13.86	9.75	19.59	20.69	20.48	26.02	26.36	13.55	10.75	13.54	11.79	14.60	16.34	17.67	16.71	15.78	14.34	12.68	11.90
almandine	70.46	72.67	75.95	79.53	70.41	69.17	70.37	64.10	63.55	76.10	78.67	77.59	79.19	76.63	75.90	74.40	75.54	76.24	77.27	78.37	79.00
% rest	3.56	3.20	2.67	3.66	2.81	1.11	0.69	3.42	3.60	1.58	0.88	1.80	2.13	2.51	2.42	1.66	1.17	1.38	1.97	1.35	1.31
Xprp = XMg	0.06	0.06	0.07	0.09	0.06	0.06	0.06	0.05	0.05	0.08	0.08	0.08	0.08	0.08	0.07	0.07	0.07	0.07	0.07	0.08	0.08
Xalm = XFe	0.70	0.73	0.76	0.80	0.72	0.69	0.70	0.66	0.65	0.76	0.79	0.78	0.79	0.77	0.76	0.74	0.76	0.76	0.77	0.78	0.79
Xsps = XMn	0.04	0.03	0.03	0.02	0.03	0.04	0.04	0.05	0.05	0.03	0.02	0.01	0.01	0.01	0.01	0.01	0.01	0.01	0.01	0.01	0.01
Xgrs = XCa	0.20	0.18	0.14	0.10	0.20	0.20	0.20	0.25	0.26	0.14	0.11	0.14	0.12	0.15	0.16	0.18	0.17	0.16	0.14	0.13	0.12
XAl	1.00	1.00	1.00	1.00	1.00	1.00	1.00	1.00	1.00	1.00	1.00	1.00	1.00	1.00	1.00	1.00	1.00	1.00	1.00	1.00	1.00

Appendix B: Electron microprobe analyses of garnet; grt-cld-schist [sample GR99/40]

sample	GR99/40	GR99/40	GR99/40	GR99/40	GR99/40	GR99/40	GR99/40	GR99/40	GR99/40	GR99/40	GR99/40	GR99/40	GR99/40	GR99/40	GR99/40	GR99/40	GR99/40	GR99/40	GR99/40	GR99/40	GR99/40
analysis	grt4_12	grt4_13	grt4_14	grt5_1	grt5_2	grt5_3	grt5_4	grt5_5	grt5_6	grt5_7	grt5_8	grt5_9	grt5_10	grt5_11	grt5_12	grt5_13	grt5_14	grt5_15	grt5_16	grt5_17	grt5_18
SiO2	37.33	37.51	37.49	37.09	37.35	37.35	37.52	37.22	37.40	37.47	37.39	37.41	37.18	37.52	37.29	37.54	37.18	37.31	37.32	37.11	37.78
Al2O3	20.46	20.87	20.97	20.63	20.51	20.72	20.63	20.63	20.72	20.47	20.78	20.57	20.60	20.58	20.52	20.43	20.50	20.49	20.48	20.53	20.40
TiO2	0.01	0.00	0.00	0.00	0.06	0.08	0.05	0.04	0.09	0.10	0.11	0.10	0.03	0.00	0.14	0.08	0.08	0.09	0.00	0.07	0.11
FeO	34.17	35.05	34.77	33.88	32.86	31.77	31.00	30.49	29.77	29.27	29.56	29.10	29.11	29.01	28.75	28.79	28.78	28.71	28.56	28.95	28.53
MgO	2.10	2.08	2.10	1.97	1.70	1.55	1.40	1.31	1.25	1.20	1.14	1.11	1.13	1.12	1.08	1.07	1.08	1.08	0.99	1.18	1.09
CaO	3.72	3.76	3.84	4.00	5.46	6.25	6.52	7.77	8.14	8.49	8.94	8.45	8.19	8.26	8.55	8.42	8.75	8.77	8.76	8.38	8.93
MnO	0.38	0.47	0.36	0.94	1.10	1.23	1.36	0.65	1.40	1.41	1.52	1.55	0.70	1.77	1.91	1.95	1.79	1.80	0.69	1.73	1.62
total	98.17	99.74	99.53	98.51	99.04	98.94	98.48	98.11	98.77	98.41	99.43	98.29	96.95	98.26	98.24	98.28	98.16	98.26	96.80	97.95	98.45
FeO Ox	34.17	35.05	34.77	33.88	32.86	31.77	31.00	30.49	29.77	29.27	29.56	29.10	29.11	29.01	28.75	28.79	28.78	28.71	28.56	28.95	28.53
Fe2O3 Ox	0.00	0.00	0.00	0.00	0.00	0.00	0.00	0.00	0.00	0.00	0.00	0.00	0.00	0.00	0.00	0.00	0.00	0.00	0.00	0.00	0.00
total Ox	98.17	99.74	99.53	98.51	99.04	98.95	98.48	98.11	98.77	98.41	99.44	98.29	96.94	98.26	98.24	98.28	98.16	98.25	96.80	97.95	98.46
number of cations based on 12 oxygen atoms																					
Si	3.05	3.03	3.03	3.03	3.03	3.03	3.05	3.03	3.03	3.04	3.01	3.04	3.05	3.05	3.03	3.05	3.03	3.03	3.06	3.03	3.06
Al tot.	1.97	1.98	2.00	1.99	1.96	1.98	1.98	1.98	1.98	1.96	1.97	1.97	1.99	1.97	1.97	1.96	1.97	1.96	1.98	1.98	1.95
Ti	0.00	0.00	0.00	0.00	0.00	0.00	0.00	0.00	0.01	0.01	0.01	0.01	0.00	0.00	0.01	0.00	0.00	0.01	0.00	0.00	0.01
Fe tot.	2.33	2.36	2.35	2.31	2.23	2.15	2.11	2.08	2.02	1.99	1.99	1.98	2.00	1.97	1.96	1.96	1.96	1.95	1.96	1.98	1.93
Fe3+	0.00	0.00	0.00	0.00	0.00	0.00	0.00	0.00	0.00	0.00	0.00	0.00	0.00	0.00	0.00	0.00	0.00	0.00	0.00	0.00	0.00
Fe2+	2.33	2.36	2.35	2.31	2.23	2.15	2.11	2.08	2.02	1.99	1.99	1.98	2.00	1.97	1.96	1.96	1.96	1.95	1.96	1.98	1.93
Mg	0.26	0.25	0.25	0.24	0.21	0.19	0.17	0.16	0.15	0.15	0.14	0.13	0.14	0.14	0.13	0.13	0.13	0.13	0.12	0.14	0.13
Ca	0.33	0.32	0.33	0.35	0.47	0.54	0.57	0.68	0.71	0.74	0.77	0.74	0.72	0.72	0.75	0.73	0.76	0.76	0.77	0.73	0.77
Mn	0.03	0.03	0.02	0.06	0.08	0.08	0.09	0.04	0.10	0.10	0.10	0.11	0.05	0.12	0.13	0.13	0.12	0.12	0.05	0.12	0.11
total cat	7.96	7.98	7.98	7.98	7.98	7.98	7.96	7.97	7.98	7.97	8.00	7.97	7.95	7.97	7.97	7.97	7.98	7.98	7.95	7.98	7.96
andradite	0.00	0.00	0.00	0.00	0.00	0.00	0.00	0.00	0.00	0.00	0.00	0.00	0.00	0.00	0.00	0.00	0.00	0.00	0.00	0.00	0.00
pyrope	8.69	8.41	8.54	8.08	6.99	6.31	5.77	5.37	5.08	4.94	4.62	4.55	4.76	4.60	4.44	4.41	4.44	4.44	4.18	4.84	4.50
spessartine	0.89	1.08	0.83	2.19	2.57	2.85	3.19	1.52	3.24	3.30	3.50	3.61	1.68	4.13	4.46	4.57	4.18	4.21	1.65	4.04	3.80
grossular	11.07	10.94	11.23	11.79	16.13	18.29	19.33	22.92	23.80	25.13	26.07	24.90	24.79	24.39	25.25	24.97	25.86	25.93	26.57	24.73	26.52
almandine	79.35	79.57	79.39	77.94	74.32	72.56	71.72	70.19	67.88	66.63	65.80	66.94	68.78	66.87	65.86	66.04	65.52	65.42	67.60	66.39	65.17
% rest	1.47	0.72	1.18	0.84	1.68	0.82	1.66	1.05	0.87	1.74	1.28	1.16	2.57	1.34	1.28	1.72	1.33	1.48	2.66	0.99	2.17
Xprp = XMg	0.09	0.08	0.09	0.08	0.07	0.06	0.06	0.05	0.05	0.05	0.05	0.05	0.05	0.05	0.04	0.04	0.04	0.04	0.04	0.05	0.04
Xalm = XFe	0.79	0.80	0.79	0.78	0.75	0.73	0.72	0.70	0.68	0.67	0.66	0.67	0.69	0.67	0.66	0.66	0.66	0.66	0.68	0.66	0.66
Xsps = XMn	0.01	0.01	0.01	0.02	0.03	0.03	0.03	0.02	0.03	0.03	0.03	0.04	0.02	0.04	0.04	0.05	0.04	0.04	0.02	0.04	0.04
Xgrs = XCa	0.11	0.11	0.11	0.12	0.16	0.18	0.19	0.23	0.24	0.25	0.26	0.25	0.25	0.24	0.25	0.25	0.26	0.26	0.27	0.25	0.26
XAl	1.00	1.00	1.00	1.00	1.00	1.00	1.00	1.00	1.00	1.00	1.00	1.00	1.00	1.00	1.00	1.00	1.00	1.00	1.00	1.00	1.00

Appendix B: Electron microprobe analyses of garnet; grt-cld-schist [sample GR99/40]

sample	GR99/40	GR99/40	GR99/40	GR99/40	GR99/40	GR99/40	GR99/40	GR99/40	GR99/40	GR99/40	GR99/40	GR99/40	GR99/40	GR99/40	GR99/40	GR99/40	GR99/40
analysis	grt5_19	grt5_20	grt5_21	grt5_22	grt5_23	grt5_24	grt5_25	grt5_26	grt5_27	grt5_28	grt5_29	grt5_30	grt5_31	grt5_32	grt5_33	grt5_34	grt5_35
SiO2	37.45	37.44	37.71	37.54	37.91	37.51	37.83	37.38	37.63	37.45	37.18	37.18	37.39	37.43	37.33	37.44	37.42
Al2O3	20.46	20.64	20.56	20.52	20.46	20.77	20.53	20.72	20.70	20.54	20.48	20.65	20.67	20.74	20.72	20.61	20.63
TiO2	0.05	0.03	0.04	0.08	0.02	0.04	0.05	0.02	0.00	0.06	0.00	0.00	0.01	0.05	0.00	0.03	0.00
FeO	28.89	29.65	29.31	29.54	29.22	29.48	28.79	29.70	30.10	32.19	31.35	32.03	31.54	32.31	33.81	33.00	33.42
MgO	1.11	1.13	1.21	1.21	1.16	1.26	1.17	1.30	1.25	1.46	1.44	1.52	1.53	1.70	1.72	1.79	1.87
CaO	8.56	8.52	8.65	8.19	8.38	8.33	9.54	8.19	8.12	6.17	6.44	5.51	6.06	5.69	4.62	4.73	4.67
MnO	0.83	0.80	0.75	0.65	0.61	0.64	0.64	0.63	0.61	1.35	0.63	0.68	0.55	0.48	0.51	0.47	1.12
total	97.35	98.21	98.23	97.74	97.77	98.03	98.55	97.94	98.41	99.21	97.52	97.56	97.75	98.40	98.71	98.06	99.13
FeO Ox	28.89	29.65	29.31	29.54	29.22	29.48	28.79	29.70	30.10	32.19	31.35	32.03	31.54	32.31	33.81	33.00	33.42
Fe2O3 Ox	0.00	0.00	0.00	0.00	0.00	0.00	0.00	0.00	0.00	0.00	0.00	0.00	0.00	0.00	0.00	0.00	0.00
total Ox	97.35	98.21	98.23	97.73	97.76	98.03	98.55	97.94	98.41	99.22	97.52	97.57	97.75	98.40	98.71	98.07	99.13
number of cations based on 12 oxygen atoms																	
Si	3.06	3.04	3.06	3.06	3.08	3.05	3.05	3.04	3.05	3.03	3.05	3.05	3.05	3.04	3.04	3.05	3.03
Al tot.	1.97	1.98	1.96	1.97	1.96	1.99	1.95	1.99	1.98	1.96	1.98	2.00	1.99	1.99	1.99	1.98	1.97
Ti	0.00	0.00	0.00	0.00	0.00	0.00	0.00	0.00	0.00	0.00	0.00	0.00	0.00	0.00	0.00	0.00	0.00
Fe tot.	1.97	2.01	1.99	2.01	1.99	2.00	1.94	2.02	2.04	2.18	2.15	2.20	2.15	2.20	2.30	2.25	2.27
Fe3+	0.00	0.00	0.00	0.00	0.00	0.00	0.00	0.00	0.00	0.00	0.00	0.00	0.00	0.00	0.00	0.00	0.00
Fe2+	1.97	2.01	1.99	2.01	1.99	2.00	1.94	2.02	2.04	2.18	2.15	2.20	2.15	2.20	2.30	2.25	2.27
Mg	0.14	0.14	0.15	0.15	0.14	0.15	0.14	0.16	0.15	0.18	0.18	0.19	0.19	0.21	0.21	0.22	0.23
Ca	0.75	0.74	0.75	0.71	0.73	0.72	0.83	0.71	0.70	0.54	0.57	0.48	0.53	0.50	0.40	0.41	0.41
Mn	0.06	0.06	0.05	0.04	0.04	0.04	0.04	0.04	0.04	0.09	0.04	0.05	0.04	0.03	0.04	0.03	0.08
total cat	7.95	7.97	7.96	7.95	7.94	7.96	7.97	7.96	7.96	7.98	7.96	7.95	7.95	7.96	7.97	7.95	7.98
andradite	0.00	0.00	0.00	0.00	0.00	0.00	0.00	0.00	0.00	0.00	0.00	0.00	0.00	0.00	0.00	0.00	0.00
pyrope	4.63	4.64	4.98	5.03	4.85	5.22	4.80	5.37	5.14	5.99	5.99	6.38	6.40	7.03	7.08	7.47	7.64
spessartine	1.97	1.87	1.75	1.54	1.45	1.51	1.49	1.48	1.43	3.15	1.49	1.62	1.31	1.13	1.19	1.11	2.60
grossular	25.70	25.16	25.59	24.49	25.18	24.79	28.16	24.32	24.00	18.20	19.28	16.62	18.23	16.91	13.67	14.18	13.72
almandine	67.70	68.33	67.68	68.94	68.52	68.48	65.55	68.83	69.44	72.66	73.24	75.39	74.06	74.94	78.06	77.24	76.04
% rest	2.18	1.34	1.64	2.12	2.67	2.07	1.87	1.72	1.64	1.73	1.71	2.37	2.47	1.86	1.42	2.26	1.16
Xprp = XMg	0.05	0.05	0.05	0.05	0.05	0.05	0.05	0.05	0.05	0.06	0.06	0.06	0.06	0.07	0.07	0.07	0.08
Xalm = XFe	0.68	0.68	0.68	0.69	0.69	0.68	0.66	0.69	0.69	0.73	0.73	0.75	0.74	0.75	0.78	0.77	0.76
Xsps = XMn	0.02	0.02	0.02	0.02	0.01	0.02	0.01	0.01	0.01	0.03	0.01	0.02	0.01	0.01	0.01	0.01	0.03
Xgrs = XCa	0.26	0.25	0.26	0.24	0.25	0.25	0.28	0.24	0.24	0.18	0.19	0.17	0.18	0.17	0.14	0.14	0.14
XAl	1.00	1.00	1.00	1.00	1.00	1.00	1.00	1.00	1.00	1.00	1.00	1.00	1.00	1.00	1.00	1.00	1.00

Appendix B: Electron microprobe analyses of ilmenite; garnet-chloritoid-schist [samples GR99-26]

sample	G99/26	G99/26	G99/26	G99/26	G99/26	G99/26	G99/26
analysis	ilm1_1	ilm1_2	ilm1_3	ilm1_4	ilm2_1	ilm3_1	ilm3_2
SiO2	0.03	0.01	0.14	0.00	0.08	0.03	0.00
TiO2	49.95	49.19	48.54	49.81	50.19	48.82	50.22
Cr2O3	0.00	0.00	0.00	0.00	0.00	0.00	0.00
Fe2O3	0.00	0.00	0.00	0.00	0.00	0.00	0.00
MnO	1.86	1.71	1.92	1.30	1.30	0.63	0.67
MgO	0.05	0.04	0.03	0.08	0.08	0.18	0.03
FeO	44.98	44.12	44.40	44.81	45.27	46.95	47.33
total	97.03	95.19	95.30	96.00	97.10	96.72	98.36
number of cations based on 6 oxygen atoms							
Si	0.002	0.001	0.008	0.000	0.004	0.001	0.000
Ti	1.951	1.959	1.928	1.967	1.958	1.909	1.934
Cr	0.000	0.000	0.000	0.000	0.000	0.000	0.000
Fe3+	0.093	0.078	0.126	0.065	0.071	0.176	0.126
total	2.045	2.037	2.062	2.033	2.033	2.086	2.061
Mn	0.082	0.077	0.086	0.058	0.057	0.028	0.029
Mg	0.004	0.003	0.002	0.006	0.006	0.014	0.003
Fe2+	1.860	1.876	1.835	1.903	1.893	1.865	1.901
total	1.946	1.956	1.923	1.967	1.957	1.907	1.933
total	3.99	3.99	3.98	4.00	3.99	3.99	3.99
ilm (XFe)	0.958	0.961	0.957	0.968	0.969	0.980	0.985
gei (XMg)	0.002	0.002	0.001	0.003	0.003	0.007	0.001
pyro (XMn)	0.040	0.038	0.042	0.028	0.028	0.013	0.014

Appendix B: Electron microprobe analyses of white mica; blueschist [sample M98/43], amphibolite [sample 8-21], micaschist [sample M98/8]

sample	M98/43	M98/43	M98/43	M98/43	M98/43	M98/43	M98/43	M98/43	M98/43	M98/43	M98/43	M98/43	M98/43	8-21	8-21	8-21	8-21	8-21	M98/8
analysis	wm1_1	wm1_2	wm1_3	wm1_4	wm2_1	wm2_2	wm2_3	wm3	wm4	wm5	wm6	wm7	wm8	wm1	wm2	wm3	wm4	wm5	wm1_1
Na2O	0.36	0.42	0.33	0.30	0.46	0.32	0.33	0.50	0.51	0.37	0.42	0.35	0.08	0.68	0.93	0.57	0.50	1.18	0.29
K2O	9.66	9.37	10.27	10.31	9.86	9.89	9.09	10.25	10.41	9.99	10.35	10.47	4.03	10.28	9.77	10.54	10.44	9.59	10.74
CaO	0.13	0.18	0.04	0.02	0.00	0.01	0.02	0.00	0.01	0.00	0.01	0.02	0.04	0.00	0.06	0.00	0.00	0.00	0.00
SiO2	50.18	49.94	50.75	50.77	49.63	50.39	50.11	51.56	51.48	51.65	51.48	50.20	53.65	49.22	49.65	49.77	49.48	49.43	48.10
Al2O3	27.52	27.45	27.88	27.52	27.60	26.92	27.53	28.47	28.11	28.07	28.28	27.82	28.12	28.10	30.18	28.61	28.61	29.86	27.51
TiO2	0.05	0.07	0.07	0.06	0.09	0.03	0.05	0.12	0.07	0.04	0.05	0.06	0.03	0.34	0.32	0.37	0.31	0.30	0.37
FeO	3.01	2.84	3.23	2.89	3.81	3.63	2.72	4.05	3.84	3.16	3.87	3.14	3.82	3.37	3.51	3.44	3.52	3.36	5.80
MgO	3.37	3.32	3.30	3.48	3.11	3.29	3.32	3.25	3.22	3.29	3.17	3.28	3.81	3.15	2.87	3.21	3.19	2.96	2.45
MnO	0.03	0.04	0.05	0.04	0.02	0.04	0.05	0.05	0.03	0.03	0.05	0.03	0.01	0.02	0.02	0.01	0.00	0.00	0.05
Cr2O3	0.00	0.00	0.00	0.00	0.00	0.00	0.00	0.00	0.00	0.00	0.00	0.00	0.00	0.00	0.00	0.00	0.00	0.00	0.00
total	94.33	93.63	95.92	95.39	94.63	94.51	93.23	98.26	97.68	96.60	97.68	95.37	93.60	95.16	97.33	96.52	96.06	96.68	95.33
number of cations based on 11 oxygen atoms (H2O free)																			
Na	0.05	0.06	0.04	0.04	0.06	0.04	0.04	0.06	0.06	0.05	0.05	0.05	0.01	0.09	0.12	0.07	0.06	0.15	0.04
K	0.83	0.81	0.87	0.88	0.85	0.85	0.79	0.85	0.87	0.84	0.86	0.89	0.34	0.88	0.82	0.89	0.89	0.81	0.94
Ca	0.01	0.01	0.00	0.00	0.00	0.00	0.00	0.00	0.00	0.00	0.00	0.00	0.00	0.00	0.00	0.00	0.00	0.00	0.00
total	0.89	0.88	0.92	0.92	0.91	0.89	0.83	0.91	0.94	0.89	0.92	0.94	0.35	0.97	0.94	0.97	0.95	0.96	0.97
Si	3.38	3.38	3.37	3.39	3.35	3.40	3.39	3.36	3.37	3.40	3.37	3.36	3.50	3.31	3.26	3.31	3.30	3.26	3.28
AlIV	0.62	0.62	0.63	0.61	0.65	0.60	0.61	0.64	0.63	0.60	0.63	0.64	0.50	0.69	0.74	0.69	0.70	0.74	0.72
AlVI	1.57	1.57	1.56	1.55	1.55	1.54	1.59	1.54	1.54	1.57	1.55	1.56	1.66	1.54	1.59	1.55	1.55	1.59	1.50
Al tot.	2.19	2.19	2.18	2.17	2.20	2.14	2.20	2.19	2.17	2.18	2.18	2.20	2.16	2.23	2.34	2.24	2.25	2.32	2.21
Ti	0.00	0.00	0.00	0.00	0.00	0.00	0.00	0.01	0.00	0.00	0.00	0.00	0.00	0.02	0.02	0.02	0.02	0.01	0.02
Cr3+	0.00	0.00	0.00	0.00	0.00	0.00	0.00	0.00	0.00	0.00	0.00	0.00	0.00	0.00	0.00	0.00	0.00	0.00	0.00
Fe2+	0.17	0.16	0.18	0.16	0.22	0.20	0.15	0.22	0.21	0.17	0.21	0.18	0.21	0.19	0.19	0.19	0.20	0.19	0.33
Mg	0.34	0.34	0.33	0.35	0.31	0.33	0.34	0.32	0.31	0.32	0.31	0.33	0.37	0.31	0.28	0.32	0.32	0.29	0.25
Mn	0.00	0.00	0.00	0.00	0.00	0.00	0.00	0.00	0.00	0.00	0.00	0.00	0.00	0.00	0.00	0.00	0.00	0.00	0.00
Fe + Mg	0.51	0.50	0.51	0.51	0.53	0.54	0.49	0.54	0.52	0.50	0.52	0.50	0.58	0.50	0.47	0.51	0.51	0.48	0.58
various cation ratios																			
mg number	66.61	67.57	64.55	68.21	59.26	61.76	68.50	58.85	59.91	64.98	59.34	65.05	63.99	62.03	59.30	62.45	61.76	61.09	42.95
Fe/(Fe+Mg)	0.33	0.32	0.35	0.32	0.41	0.38	0.31	0.41	0.40	0.35	0.41	0.35	0.36	0.38	0.41	0.38	0.38	0.39	0.57
Mg/(Mg+Fe)	0.67	0.68	0.65	0.68	0.59	0.62	0.69	0.59	0.60	0.65	0.59	0.65	0.64	0.62	0.59	0.62	0.62	0.61	0.43
muscovite cat	0.94	0.92	0.95	0.96	0.93	0.95	0.95	0.93	0.93	0.95	0.94	0.95	0.96	0.91	0.87	0.92	0.93	0.84	0.96
paragonite	0.05	0.06	0.05	0.04	0.07	0.05	0.05	0.07	0.07	0.05	0.06	0.05	0.03	0.09	0.13	0.08	0.07	0.16	0.04
margarite	0.01	0.01	0.00	0.00	0.00	0.00	0.00	0.00	0.00	0.00	0.00	0.00	0.01	0.00	0.00	0.00	0.00	0.00	0.00
paragonite	5.36	6.38	4.66	4.24	6.62	4.69	5.23	6.90	6.93	5.33	5.81	4.83	2.93	9.13	12.64	7.59	6.78	15.75	3.94
celadonite	37.98	38.13	37.34	38.83	35.39	39.99	39.45	35.71	37.16	39.60	36.93	36.16	49.94	31.37	25.91	30.53	30.14	26.37	28.47
muskovite	56.66	55.49	58.00	56.93	57.99	55.33	55.32	57.39	55.91	55.07	57.26	59.00	47.13	59.50	61.46	61.88	63.07	57.87	67.59

Appendix B: Electron microprobe analyses of white mica; micaschist [sample M98/8]

sample	M98/8	M98/8	M98/8	M98/8	M98/8	M98/8	M98/8	M98/8	M98/8	M98/8	M98/8	M98/8	M98/8	M98/8	M98/8	M98/8	M98/8	M98/8	M98/8
analysis	wm2_1	wm2_2	wm2_3	wm3_1	wm3_2	wm3_3	wm3_4	wm3_5	wm3_6	wm3_7	wm4-1	wm4-2	wm4-3	wm4-4	wm5_1	wm5_2	wm5_3	wm6_3	wm6_4
Na2O	0.23	0.22	0.18	0.19	0.26	0.23	0.23	0.22	0.27	0.18	0.19	0.24	0.29	0.25	0.25	0.23	0.27	0.22	0.26
K2O	10.28	10.42	10.38	10.49	10.52	10.88	10.74	10.71	10.71	10.75	10.63	10.72	10.70	10.78	10.43	10.65	10.37	10.36	10.52
CaO	0.00	0.00	0.01	0.04	0.01	0.00	0.00	0.00	0.00	0.00	0.00	0.00	0.00	0.00	0.00	0.00	0.01	0.01	0.00
SiO2	47.92	47.01	48.00	47.07	48.47	46.86	48.51	48.47	48.58	48.67	46.57	47.34	47.34	47.07	47.15	47.41	46.99	48.12	48.32
Al2O3	26.15	26.95	27.00	27.09	27.08	26.78	27.13	27.70	27.44	27.88	28.42	27.60	27.49	27.57	27.01	26.41	27.22	27.40	26.90
TiO2	0.31	0.33	0.29	0.30	0.37	0.38	0.37	0.28	0.33	0.28	0.30	0.33	0.31	0.32	0.32	0.36	0.29	0.31	0.34
FeO	5.88	6.12	5.69	5.36	6.25	6.09	6.00	5.98	6.01	6.04	6.04	6.07	6.28	6.02	6.03	6.08	5.98	6.03	6.14
MgO	2.64	2.43	2.44	2.35	2.50	2.50	2.47	2.37	2.39	2.40	2.01	2.39	2.39	2.31	2.40	2.62	2.41	2.50	2.59
MnO	0.08	0.05	0.03	0.04	0.05	0.02	0.05	0.04	0.06	0.04	0.05	0.05	0.03	0.06	0.05	0.04	0.05	0.04	0.04
Cr2O3	0.00	0.00	0.00	0.00	0.00	0.00	0.00	0.00	0.00	0.00	0.00	0.00	0.00	0.00	0.00	0.00	0.00	0.00	0.00
total	93.49	93.53	94.01	92.94	95.52	93.76	95.51	95.77	95.80	96.24	94.22	94.74	94.83	94.39	93.65	93.81	93.58	95.00	95.11
number of cations based on 11 oxygen atoms (H2O free)																			
Na	0.03	0.03	0.02	0.03	0.03	0.03	0.03	0.03	0.04	0.02	0.03	0.03	0.04	0.03	0.03	0.03	0.04	0.03	0.03
K	0.91	0.93	0.91	0.94	0.91	0.97	0.93	0.93	0.93	0.93	0.94	0.94	0.94	0.95	0.93	0.95	0.92	0.90	0.92
Ca	0.00	0.00	0.00	0.00	0.00	0.00	0.00	0.00	0.00	0.00	0.00	0.00	0.00	0.00	0.00	0.00	0.00	0.00	0.00
total	0.94	0.96	0.94	0.96	0.95	1.00	0.96	0.96	0.96	0.95	0.96	0.97	0.98	0.98	0.96	0.98	0.96	0.93	0.95
Si	3.33	3.28	3.31	3.29	3.30	3.27	3.31	3.29	3.30	3.29	3.22	3.26	3.26	3.26	3.28	3.30	3.27	3.29	3.31
AlIV	0.67	0.72	0.69	0.71	0.70	0.73	0.69	0.71	0.70	0.71	0.78	0.74	0.74	0.74	0.72	0.70	0.73	0.71	0.69
AlVI	1.47	1.49	1.51	1.52	1.48	1.47	1.49	1.51	1.50	1.51	1.54	1.50	1.49	1.50	1.50	1.46	1.50	1.50	1.48
Al tot.	2.14	2.21	2.20	2.23	2.18	2.20	2.18	2.22	2.20	2.22	2.32	2.24	2.23	2.25	2.22	2.17	2.23	2.21	2.17
Ti	0.02	0.02	0.02	0.02	0.02	0.02	0.02	0.01	0.02	0.01	0.02	0.02	0.02	0.02	0.02	0.02	0.02	0.02	0.02
Cr3+	0.00	0.00	0.00	0.00	0.00	0.00	0.00	0.00	0.00	0.00	0.00	0.00	0.00	0.00	0.00	0.00	0.00	0.00	0.00
Fe2+	0.34	0.36	0.33	0.31	0.36	0.36	0.34	0.34	0.34	0.34	0.35	0.35	0.36	0.35	0.35	0.35	0.35	0.34	0.35
Mg	0.27	0.25	0.25	0.24	0.25	0.26	0.25	0.24	0.24	0.24	0.21	0.25	0.25	0.24	0.25	0.27	0.25	0.25	0.26
Mn	0.00	0.00	0.00	0.00	0.00	0.00	0.00	0.00	0.00	0.00	0.00	0.00	0.00	0.00	0.00	0.00	0.00	0.00	0.00
Fe + Mg	0.62	0.61	0.58	0.56	0.61	0.62	0.59	0.58	0.58	0.58	0.56	0.59	0.61	0.59	0.60	0.63	0.60	0.60	0.62
various cation ratios																			
mg number	44.45	41.44	43.32	43.86	41.62	42.25	42.32	41.39	41.47	41.45	37.23	41.23	40.41	40.61	41.49	43.44	41.80	42.49	42.91
Fe/(Fe+Mg)	0.56	0.59	0.57	0.56	0.58	0.58	0.58	0.59	0.59	0.59	0.63	0.59	0.60	0.59	0.59	0.57	0.58	0.58	0.57
Mg/(Mg+Fe)	0.44	0.41	0.43	0.44	0.42	0.42	0.42	0.41	0.41	0.41	0.37	0.41	0.40	0.41	0.41	0.43	0.42	0.42	0.43
muscovite cat	0.97	0.97	0.97	0.97	0.96	0.97	0.97	0.97	0.96	0.98	0.97	0.97	0.96	0.97	0.96	0.97	0.96	0.97	0.96
paragonite	0.03	0.03	0.03	0.03	0.04	0.03	0.03	0.03	0.04	0.02	0.03	0.03	0.04	0.03	0.04	0.03	0.04	0.03	0.04
margarite	0.00	0.00	0.00	0.00	0.00	0.00	0.00	0.00	0.00	0.00	0.00	0.00	0.00	0.00	0.00	0.00	0.00	0.00	0.00
paragonite	3.29	3.11	2.57	2.68	3.62	3.11	3.15	3.03	3.69	2.48	2.64	3.29	3.96	3.40	3.51	3.18	3.81	3.13	3.62
celadonite	33.09	27.66	31.22	28.88	30.44	26.97	30.68	29.20	30.04	28.94	22.38	26.00	26.06	25.59	28.04	29.85	26.99	29.19	30.73
muskovite	63.62	69.23	66.21	68.44	65.94	69.92	66.17	67.77	66.27	68.58	74.98	70.71	69.98	71.00	68.44	66.97	69.20	67.69	65.65

Appendix B: Electron microprobe analyses of white mica; micaschist [samples M98/19, M98/22]

sample	M98/19	M98/19	M98/19	M98/19	M98/19	M98/19	M98/19	M98/19	M98/19	M98/19	M98/22	M98/22	M98/22	M98/22	M98/22	M98/22	M98/22	M98/22	M98/22	M98/22
analysis	wm1	wm2	wm3	wm4	wm5	wm6	wm7	wm8	wm9	wm10	wm1_1	wm1_2	wm1_3	wm1_4	wm1_5	wm2_1	wm2_2	wm2_3	wm2_4	wm2_5
Na2O	1.24	1.47	1.35	1.46	1.40	1.39	1.25	0.83	1.32	1.33	1.52	1.39	1.47	1.26	1.47	1.50	1.64	1.13	1.30	0.85
K2O	8.95	8.85	9.07	8.94	8.97	9.12	8.76	6.10	9.01	8.99	8.53	8.57	8.62	8.96	8.71	8.57	8.79	9.01	8.53	7.31
CaO	0.00	0.00	0.00	0.02	0.01	0.00	0.00	0.00	0.00	0.00	0.00	0.02	0.00	0.00	0.02	0.02	0.00	0.00	0.04	0.03
SiO2	50.92	49.58	49.72	49.64	50.42	50.16	51.69	52.05	50.14	49.97	47.79	48.12	48.28	48.09	48.24	47.34	47.72	49.21	48.13	48.88
Al2O3	33.18	33.73	33.01	33.64	33.17	33.14	33.34	35.41	32.63	34.20	35.54	35.54	35.51	35.36	35.03	36.29	36.68	33.70	35.24	36.15
TiO2	0.36	0.37	0.37	0.36	0.35	0.33	0.37	0.36	0.38	0.35	0.23	0.21	0.22	0.26	0.27	0.23	0.20	0.19	0.21	0.22
FeO	1.50	1.39	1.44	1.40	1.45	1.39	1.40	1.40	1.45	1.25	1.01	1.33	1.06	1.13	1.02	1.27	1.03	1.49	1.39	1.45
MgO	2.42	2.16	2.32	2.19	2.38	2.43	2.45	2.27	2.44	2.07	1.56	1.51	1.58	1.37	1.68	1.18	1.18	2.10	1.35	1.47
MnO	0.01	0.02	0.02	0.00	0.01	0.02	0.01	0.00	0.01	0.00	0.01	0.00	0.01	0.00	0.01	0.02	0.00	0.01	0.02	0.00
Cr2O3	0.00	0.00	0.00	0.00	0.00	0.00	0.00	0.00	0.00	0.00	0.00	0.00	0.00	0.00	0.00	0.00	0.00	0.00	0.00	0.00
total	98.59	97.58	97.29	97.66	98.15	97.99	99.28	98.42	97.38	98.16	96.18	96.72	96.77	96.44	96.45	96.44	97.24	96.85	96.24	96.40
number of cations based on 11 oxygen atoms (H2O free)																				
Na	0.15	0.18	0.17	0.18	0.17	0.17	0.15	0.10	0.17	0.16	0.19	0.17	0.18	0.16	0.19	0.19	0.21	0.14	0.16	0.11
K	0.73	0.73	0.75	0.73	0.73	0.75	0.70	0.48	0.74	0.73	0.71	0.71	0.71	0.74	0.72	0.71	0.72	0.75	0.71	0.60
Ca	0.00	0.00	0.00	0.00	0.00	0.00	0.00	0.00	0.00	0.00	0.00	0.00	0.00	0.00	0.00	0.00	0.00	0.00	0.00	0.00
total	0.88	0.91	0.92	0.92	0.91	0.92	0.86	0.59	0.91	0.90	0.90	0.89	0.90	0.90	0.91	0.90	0.93	0.89	0.88	0.71
Si	3.24	3.19	3.21	3.20	3.23	3.22	3.26	3.24	3.24	3.19	3.11	3.12	3.13	3.13	3.14	3.08	3.08	3.19	3.14	3.15
AlIV	0.76	0.81	0.79	0.80	0.77	0.78	0.74	0.76	0.76	0.81	0.89	0.88	0.87	0.87	0.86	0.92	0.92	0.81	0.86	0.85
AlVI	1.73	1.75	1.73	1.75	1.73	1.73	1.74	1.85	1.72	1.77	1.84	1.84	1.84	1.84	1.82	1.87	1.87	1.77	1.84	1.89
Al tot.	2.49	2.56	2.52	2.55	2.50	2.51	2.48	2.60	2.48	2.58	2.73	2.72	2.71	2.71	2.68	2.79	2.79	2.58	2.71	2.74
Ti	0.02	0.02	0.02	0.02	0.02	0.02	0.02	0.02	0.02	0.02	0.01	0.01	0.01	0.01	0.01	0.01	0.01	0.01	0.01	0.01
Cr3+	0.00	0.00	0.00	0.00	0.00	0.00	0.00	0.00	0.00	0.00	0.00	0.00	0.00	0.00	0.00	0.00	0.00	0.00	0.00	0.00
Fe2+	0.08	0.07	0.08	0.08	0.08	0.07	0.07	0.07	0.08	0.07	0.06	0.07	0.06	0.06	0.06	0.07	0.06	0.08	0.08	0.08
Mg	0.23	0.21	0.22	0.21	0.23	0.23	0.23	0.21	0.23	0.20	0.15	0.15	0.15	0.13	0.16	0.11	0.11	0.20	0.13	0.14
Mn	0.00	0.00	0.00	0.00	0.00	0.00	0.00	0.00	0.00	0.00	0.00	0.00	0.00	0.00	0.00	0.00	0.00	0.00	0.00	0.00
Fe + Mg	0.31	0.28	0.30	0.29	0.30	0.31	0.30	0.28	0.31	0.26	0.21	0.22	0.21	0.19	0.22	0.18	0.17	0.28	0.21	0.22
various cation ratios																				
mg number	74.19	73.47	74.17	73.60	74.52	75.70	75.72	74.29	74.99	74.69	73.35	66.92	72.65	68.36	74.59	62.35	67.12	71.52	63.38	64.37
Fe/(Fe+Mg)	0.26	0.27	0.26	0.26	0.25	0.24	0.24	0.26	0.25	0.25	0.27	0.33	0.27	0.32	0.25	0.38	0.33	0.28	0.37	0.36
Mg/(Mg+Fe)	0.74	0.73	0.74	0.74	0.75	0.76	0.76	0.74	0.75	0.75	0.73	0.67	0.73	0.68	0.75	0.62	0.67	0.72	0.63	0.64
muscovite cat	0.83	0.80	0.82	0.80	0.81	0.81	0.82	0.83	0.82	0.82	0.79	0.80	0.79	0.82	0.79	0.79	0.78	0.84	0.81	0.85
paragonite	0.17	0.20	0.18	0.20	0.19	0.19	0.18	0.17	0.18	0.18	0.21	0.20	0.21	0.18	0.20	0.21	0.22	0.16	0.19	0.15
margarite	0.00	0.00	0.00	0.00	0.00	0.00	0.00	0.00	0.00	0.00	0.00	0.00	0.00	0.00	0.00	0.00	0.00	0.00	0.00	0.00
paragonite	17.39	20.16	18.45	19.88	19.17	18.81	17.82	17.14	18.21	18.36	21.31	19.78	20.58	17.61	20.41	21.01	22.09	16.01	18.81	15.02
celadonite	24.07	19.25	21.44	19.54	22.67	21.94	25.79	24.37	23.60	19.39	11.30	12.09	12.66	12.96	13.62	8.16	8.01	19.30	13.59	14.54
muskovite	58.53	60.60	60.11	60.58	58.15	59.25	56.39	58.49	58.19	62.25	67.39	68.13	66.76	69.43	65.97	70.82	69.90	64.69	67.61	70.44

Appendix B: Electron microprobe analyses of white mica; micaschist [sample 8-5]

sample	8-5	8-5	8-5	8-5	8-5	8-5	8-5	8-5	8-5	8-5	8-5	8-5	8-5	8-5	8-5	8-5	8-5	8-5	8-5	8-5	8-5
analysis	wm1_1	wm1_2	wm1_3	wm2_1	wm2_2	wm2_3	wm3_1	wm3_2	wm3_3	wm4_1	wm4_2	wm4_3	wm5_1	wm5_2	wm5_3	wm5_4	wm6_1	wm6_2	wm7_1	wm7_2	wm8_1
Na2O	1.50	1.39	1.74	1.63	1.49	1.43	1.61	1.52	1.57	1.42	1.34	1.43	1.37	1.31	1.58	1.60	1.37	1.45	1.33	1.59	1.54
K2O	8.80	8.93	8.56	8.47	8.60	8.92	8.52	8.68	8.65	8.64	8.81	8.82	8.71	8.80	8.49	8.55	8.84	8.85	8.38	8.36	8.55
CaO	0.00	0.01	0.01	0.07	0.08	0.05	0.01	0.00	0.00	0.01	0.02	0.02	0.00	0.00	0.00	0.00	0.00	0.00	0.00	0.01	0.03
SiO2	49.76	49.59	48.59	49.48	49.95	49.88	49.21	49.07	49.90	48.27	50.18	49.63	49.83	50.10	48.83	49.09	49.86	50.24	49.54	48.37	48.76
Al2O3	31.78	32.33	34.63	32.99	32.63	32.50	32.96	32.33	32.63	31.69	31.93	32.00	31.89	31.72	32.61	32.36	31.92	32.10	32.10	31.89	32.03
TiO2	0.38	0.37	0.35	0.45	0.44	0.36	0.46	0.39	0.41	0.47	0.39	0.35	0.42	0.34	0.42	0.42	0.39	0.38	0.42	0.46	0.41
FeO	1.00	1.05	0.84	1.01	1.02	1.14	0.99	0.94	1.00	0.94	1.09	0.98	0.90	0.98	0.93	0.91	1.23	1.00	1.07	0.94	0.87
MgO	2.14	1.89	1.12	1.87	1.98	1.93	1.90	1.96	1.90	1.85	2.19	2.05	2.18	2.21	1.88	1.93	2.03	2.14	1.98	1.90	1.88
MnO	0.02	0.03	0.00	0.01	0.00	0.06	0.00	0.00	0.00	0.01	0.00	0.02	0.00	0.03	0.03	0.02	0.01	0.05	0.00	0.00	0.01
Cr2O3	0.00	0.00	0.00	0.00	0.00	0.00	0.00	0.00	0.00	0.00	0.00	0.00	0.00	0.00	0.00	0.00	0.00	0.00	0.00	0.00	0.00
total	95.38	95.59	95.84	95.98	96.19	96.27	95.66	94.89	96.06	93.30	95.95	95.30	95.30	95.49	94.77	94.88	95.65	96.21	94.82	93.52	94.08
number of cations based on 11 oxygen atoms (H2O free)																					
Na	0.19	0.18	0.22	0.21	0.19	0.18	0.20	0.19	0.20	0.18	0.17	0.18	0.17	0.17	0.20	0.20	0.17	0.18	0.17	0.21	0.20
K	0.74	0.75	0.71	0.70	0.71	0.74	0.71	0.73	0.72	0.74	0.73	0.74	0.73	0.74	0.72	0.72	0.74	0.74	0.70	0.71	0.73
Ca	0.00	0.00	0.00	0.00	0.01	0.00	0.00	0.00	0.00	0.00	0.00	0.00	0.00	0.00	0.00	0.00	0.00	0.00	0.00	0.00	0.00
total	0.93	0.92	0.93	0.92	0.91	0.93	0.92	0.93	0.92	0.93	0.90	0.92	0.90	0.90	0.92	0.92	0.91	0.92	0.87	0.92	0.93
Si	3.27	3.25	3.17	3.23	3.25	3.25	3.22	3.24	3.25	3.24	3.28	3.26	3.27	3.28	3.23	3.24	3.27	3.27	3.26	3.24	3.24
AlIV	0.73	0.75	0.83	0.77	0.75	0.75	0.78	0.76	0.75	0.76	0.72	0.74	0.73	0.72	0.77	0.76	0.73	0.73	0.74	0.76	0.76
AlVI	1.73	1.75	1.84	1.76	1.75	1.75	1.76	1.76	1.76	1.75	1.73	1.74	1.74	1.73	1.77	1.76	1.74	1.74	1.76	1.75	1.76
Al tot.	2.46	2.50	2.67	2.54	2.50	2.50	2.54	2.52	2.51	2.51	2.46	2.48	2.47	2.45	2.54	2.52	2.47	2.46	2.49	2.52	2.51
Ti	0.02	0.02	0.02	0.02	0.02	0.02	0.02	0.02	0.02	0.02	0.02	0.02	0.02	0.02	0.02	0.02	0.02	0.02	0.02	0.02	0.02
Cr3+	0.00	0.00	0.00	0.00	0.00	0.00	0.00	0.00	0.00	0.00	0.00	0.00	0.00	0.00	0.00	0.00	0.00	0.00	0.00	0.00	0.00
Fe2+	0.05	0.06	0.05	0.06	0.06	0.06	0.05	0.05	0.05	0.05	0.06	0.05	0.05	0.05	0.05	0.05	0.07	0.05	0.06	0.05	0.05
Mg	0.21	0.18	0.11	0.18	0.19	0.19	0.19	0.19	0.18	0.19	0.21	0.20	0.21	0.22	0.19	0.19	0.20	0.21	0.19	0.19	0.19
Mn	0.00	0.00	0.00	0.00	0.00	0.00	0.00	0.00	0.00	0.00	0.00	0.00	0.00	0.00	0.00	0.00	0.00	0.00	0.00	0.00	0.00
Fe + Mg	0.26	0.24	0.15	0.24	0.25	0.25	0.24	0.24	0.24	0.24	0.27	0.25	0.26	0.27	0.24	0.24	0.27	0.26	0.25	0.24	0.23
various cation ratios																					
mg number	79.26	76.23	70.38	76.74	77.57	75.11	77.38	78.79	77.20	77.81	78.17	78.85	81.19	80.07	78.27	79.08	74.63	79.22	76.73	78.27	79.38
Fe/(Fe+Mg)	0.21	0.24	0.30	0.23	0.22	0.25	0.23	0.21	0.23	0.22	0.22	0.21	0.19	0.20	0.22	0.21	0.25	0.21	0.23	0.22	0.21
Mg/(Mg+Fe)	0.79	0.76	0.70	0.77	0.78	0.75	0.77	0.79	0.77	0.78	0.78	0.79	0.81	0.80	0.78	0.79	0.75	0.79	0.77	0.78	0.79
muscovite cat	0.79	0.81	0.76	0.77	0.79	0.80	0.78	0.79	0.78	0.80	0.81	0.80	0.81	0.82	0.78	0.78	0.81	0.80	0.81	0.78	0.78
paragonite	0.21	0.19	0.24	0.23	0.21	0.20	0.22	0.21	0.22	0.20	0.19	0.20	0.19	0.18	0.22	0.22	0.19	0.20	0.19	0.22	0.21
margarite	0.00	0.00	0.00	0.01	0.01	0.00	0.00	0.00	0.00	0.00	0.00	0.00	0.00	0.00	0.00	0.00	0.00	0.00	0.00	0.00	0.00
paragonite	20.58	19.13	23.60	22.63	20.84	19.59	22.31	21.02	21.62	19.99	18.78	19.77	19.29	18.45	22.05	22.14	19.06	19.94	19.43	22.42	21.49
celadonite	26.97	25.31	17.25	22.68	24.96	25.08	22.09	23.96	25.13	24.28	27.53	26.32	27.10	28.37	22.58	23.94	26.89	27.13	26.39	23.78	24.49
muskovite	52.45	55.56	59.15	54.69	54.20	55.33	55.60	55.02	53.25	55.73	53.69	53.91	53.61	53.18	55.37	53.92	54.05	52.93	54.17	53.79	54.02

Appendix B: Electron microprobe analyses of white mica; micaschist [sample 8-5], grt-cld-chl-micaschist [sample GR99/26]

sample	8-5	8-5	8-5	8-5	8-5	8-5	8-5	8-5	8-5	8-5	GR99/26	GR99/26	GR99/26	GR99/26	GR99/26	GR99/26	GR99/26	GR99/26	GR99/26	GR99/26
analysis	wm8_2	wm8_3	wm9_1	wm9_2	wm10_1	wm10_2	wm10_3	wm11_1	wm11_2	wm11_3	wm1_1	wm1_2	wm1_3	wm1_4	wm1_5	wm1_6	wm4_1	wm4_2	wm4_3	wm5_1
Na2O	1.56	1.52	1.47	1.41	1.57	1.61	1.62	1.53	1.49	1.52	1.48	1.39	1.21	1.32	1.63	0.92	1.32	1.35	1.18	1.23
K2O	8.68	8.49	8.39	8.12	8.70	8.72	8.63	8.75	8.91	8.76	8.71	9.28	9.44	9.01	9.17	8.53	9.08	8.67	9.36	9.31
CaO	0.04	0.03	0.00	0.02	0.01	0.00	0.00	0.00	0.00	0.00	0.04	0.00	0.00	0.00	0.00	0.04	0.02	0.07	0.00	0.01
SiO2	49.30	47.86	49.17	50.17	48.96	49.38	49.50	49.77	49.76	50.00	47.70	46.87	47.95	47.70	46.91	49.88	47.00	46.89	48.12	47.76
Al2O3	32.14	32.00	32.76	32.56	32.50	32.35	33.06	32.57	31.98	32.21	37.12	37.48	35.37	36.33	37.94	34.18	34.31	34.00	33.56	33.79
TiO2	0.42	0.37	0.44	0.41	0.41	0.45	0.44	0.42	0.40	0.42	0.20	0.10	0.19	0.16	0.12	0.18	0.36	0.28	0.31	0.32
FeO	0.98	0.96	1.17	1.03	0.83	0.99	1.01	0.79	1.08	0.92	1.29	1.26	1.71	1.47	1.30	1.83	2.14	1.46	1.75	1.43
MgO	2.01	1.75	1.82	1.97	1.86	1.98	1.98	2.00	2.12	2.07	0.80	0.57	1.25	0.98	0.54	1.82	0.81	1.03	1.20	1.11
MnO	0.00	0.02	0.00	0.04	0.00	0.01	0.00	0.02	0.00	0.03	0.00	0.01	0.00	0.04	0.00	0.02	0.00	0.00	0.02	0.00
Cr2O3	0.00	0.00	0.00	0.00	0.00	0.00	0.00	0.00	0.00	0.00	0.00	0.00	0.00	0.00	0.00	0.00	0.00	0.00	0.00	0.00
total	95.13	93.00	95.22	95.73	94.84	95.49	96.24	95.85	95.74	95.93	97.33	96.97	97.12	97.02	97.61	97.41	95.05	93.76	95.51	94.96
number of cations based on 11 oxygen atoms (H2O free)																				
Na	0.20	0.20	0.19	0.18	0.20	0.20	0.20	0.19	0.19	0.19	0.18	0.18	0.15	0.17	0.20	0.11	0.17	0.18	0.15	0.16
K	0.73	0.73	0.70	0.67	0.73	0.73	0.72	0.73	0.74	0.73	0.72	0.77	0.78	0.75	0.76	0.70	0.77	0.74	0.79	0.79
Ca	0.00	0.00	0.00	0.00	0.00	0.00	0.00	0.00	0.00	0.00	0.00	0.00	0.00	0.00	0.00	0.00	0.00	0.00	0.00	0.00
total	0.93	0.93	0.89	0.85	0.93	0.94	0.92	0.92	0.93	0.92	0.90	0.94	0.94	0.91	0.96	0.82	0.94	0.92	0.94	0.95
Si	3.25	3.23	3.23	3.27	3.23	3.24	3.22	3.25	3.26	3.26	3.07	3.04	3.12	3.09	3.03	3.21	3.13	3.15	3.18	3.17
AlIV	0.75	0.77	0.77	0.73	0.77	0.76	0.78	0.75	0.74	0.74	0.93	0.96	0.88	0.91	0.97	0.79	0.87	0.85	0.82	0.83
AlVI	1.74	1.77	1.77	1.77	1.76	1.75	1.76	1.76	1.73	1.74	1.90	1.91	1.83	1.87	1.92	1.80	1.82	1.83	1.79	1.81
Al tot.	2.50	2.54	2.54	2.50	2.53	2.50	2.54	2.51	2.47	2.48	2.82	2.87	2.71	2.78	2.89	2.59	2.69	2.69	2.61	2.64
Ti	0.02	0.02	0.02	0.02	0.02	0.02	0.02	0.02	0.02	0.02	0.01	0.00	0.01	0.01	0.01	0.01	0.02	0.01	0.02	0.02
Cr3+	0.00	0.00	0.00	0.00	0.00	0.00	0.00	0.00	0.00	0.00	0.00	0.00	0.00	0.00	0.00	0.00	0.00	0.00	0.00	0.00
Fe2+	0.05	0.05	0.06	0.06	0.05	0.05	0.05	0.04	0.06	0.05	0.07	0.07	0.09	0.08	0.07	0.10	0.12	0.08	0.10	0.08
Mg	0.20	0.18	0.18	0.19	0.18	0.19	0.19	0.19	0.21	0.20	0.08	0.06	0.12	0.09	0.05	0.17	0.08	0.10	0.12	0.11
Mn	0.00	0.00	0.00	0.00	0.00	0.00	0.00	0.00	0.00	0.00	0.00	0.00	0.00	0.00	0.00	0.00	0.00	0.00	0.00	0.00
Fe + Mg	0.25	0.23	0.24	0.25	0.23	0.25	0.25	0.24	0.27	0.25	0.15	0.12	0.21	0.17	0.12	0.27	0.20	0.18	0.22	0.19
various cation ratios																				
mg number	78.52	76.46	73.49	77.32	79.97	78.09	77.75	81.86	77.77	80.04	52.50	44.63	56.57	54.30	42.54	63.93	40.40	55.72	55.06	58.11
Fe/(Fe+Mg)	0.21	0.24	0.27	0.23	0.20	0.22	0.22	0.18	0.22	0.20	0.48	0.55	0.43	0.46	0.57	0.36	0.60	0.44	0.45	0.42
Mg/(Mg+Fe)	0.79	0.76	0.73	0.77	0.80	0.78	0.78	0.82	0.78	0.80	0.52	0.45	0.57	0.54	0.43	0.64	0.40	0.56	0.55	0.58
muscovite cat	0.78	0.78	0.79	0.79	0.78	0.78	0.78	0.79	0.80	0.79	0.79	0.81	0.84	0.82	0.79	0.86	0.82	0.80	0.84	0.83
paragonite	0.21	0.21	0.21	0.21	0.22	0.22	0.22	0.21	0.20	0.21	0.20	0.19	0.16	0.18	0.21	0.14	0.18	0.19	0.16	0.17
margarite	0.00	0.00	0.00	0.00	0.00	0.00	0.00	0.00	0.00	0.00	0.00	0.00	0.00	0.00	0.00	0.00	0.00	0.01	0.00	0.00
paragonite	21.45	21.39	21.03	20.88	21.52	21.91	22.20	21.00	20.26	20.87	20.52	18.54	16.30	18.21	21.27	14.08	18.13	19.14	16.12	16.73
celadonite	24.78	22.56	23.10	26.68	23.35	24.18	22.20	24.92	26.07	26.35	7.47	4.44	11.69	9.31	2.80	20.66	12.72	14.52	18.01	16.95
muskovite	53.77	56.05	55.88	52.44	55.13	53.91	55.61	54.08	53.67	52.79	72.00	77.01	72.00	72.48	75.93	65.26	69.15	66.35	65.87	66.31

Appendix B: Electron microprobe analyses of white mica; grt-cld-chl-micaschist [samples G99/26, GR99/40], micaschist [M99/13]

sample	GR99/26	GR99/40	GR99/40	GR99/40	GR99/40	GR99/40	GR99/40	GR99/40	GR99/40	GR99/40	GR99/40	GR99/40	GR99/40	GR99/40	GR99/40	GR99/40	GR99/40	GR99/40	GR99/40	GR99/40
analysis	wm5_2	wm1-1	wm1-2	wm1-3	wm2	wm3-1	wm3-2	wm3-3	wm3-4	wm4-1	wm4-2	wm4-3	wm5-1	wm5-2	wm5-3	wm6_1	wm6_2	wm6_3	wm7_1	wm7_2
Na2O	1.11	0.80	1.34	1.16	1.11	1.26	1.16	1.09	1.34	1.27	1.11	0.97	1.39	1.17	1.35	0.99	0.91	0.90	0.99	0.87
K2O	9.49	9.52	9.17	9.45	9.43	9.32	9.30	9.45	8.96	8.89	9.23	9.20	9.03	9.33	9.21	8.76	8.96	8.78	8.75	8.60
CaO	0.04	0.00	0.00	0.01	0.01	0.00	0.00	0.02	0.00	0.03	0.01	0.02	0.02	0.00	0.01	0.00	0.01	0.01	0.02	0.02
SiO2	47.25	49.99	48.31	49.60	48.71	49.26	49.11	49.53	48.52	48.26	48.77	49.41	48.29	48.87	48.91	49.27	49.17	49.33	49.40	49.27
Al2O3	31.95	31.64	34.62	34.01	34.83	33.99	33.46	33.28	34.15	34.04	33.06	32.38	34.47	33.62	34.36	31.42	30.65	31.18	31.67	30.72
TiO2	0.40	0.34	0.21	0.32	0.34	0.33	0.33	0.34	0.27	0.39	0.29	0.30	0.16	0.35	0.21	0.32	0.35	0.29	0.23	0.34
FeO	2.98	2.20	1.49	1.74	1.36	1.41	1.52	1.70	1.44	1.55	1.73	1.77	1.59	1.58	1.50	2.19	2.18	2.12	2.07	2.01
MgO	1.49	1.84	0.98	1.18	0.87	1.02	1.22	1.34	1.00	1.09	1.28	1.55	1.00	1.19	1.03	1.79	1.82	1.86	1.66	1.87
MnO	0.00	0.00	0.00	0.00	0.05	0.03	0.00	0.02	0.00	0.00	0.00	0.02	0.05	0.00	0.00	0.07	0.05	0.00	0.02	0.01
Cr2O3	0.00	0.00	0.00	0.00	0.00	0.00	0.00	0.00	0.00	0.00	0.00	0.00	0.00	0.00	0.00	0.00	0.00	0.00	0.00	0.00
total	94.74	96.33	96.12	97.48	96.70	96.61	96.10	96.77	95.67	95.53	95.50	95.63	96.00	96.11	96.59	94.85	94.15	94.50	94.93	93.81
number of cations based on 11 oxygen atoms (H2O free)																				
Na	0.14	0.10	0.17	0.14	0.14	0.16	0.15	0.14	0.17	0.16	0.14	0.12	0.18	0.15	0.17	0.13	0.12	0.12	0.13	0.11
K	0.81	0.80	0.77	0.78	0.78	0.77	0.78	0.78	0.75	0.75	0.78	0.77	0.76	0.78	0.77	0.74	0.77	0.75	0.74	0.73
Ca	0.00	0.00	0.00	0.00	0.00	0.00	0.00	0.00	0.00	0.00	0.00	0.00	0.00	0.00	0.00	0.00	0.00	0.00	0.00	0.00
total	0.96	0.90	0.94	0.92	0.92	0.93	0.92	0.92	0.92	0.91	0.92	0.90	0.93	0.93	0.94	0.87	0.88	0.86	0.87	0.85
Si	3.18	3.28	3.16	3.21	3.17	3.21	3.21	3.22	3.19	3.18	3.22	3.25	3.17	3.20	3.19	3.27	3.29	3.28	3.27	3.30
AlIV	0.82	0.72	0.84	0.79	0.83	0.79	0.79	0.78	0.81	0.82	0.78	0.75	0.83	0.80	0.81	0.73	0.71	0.72	0.73	0.70
AlVI	1.71	1.72	1.84	1.80	1.84	1.81	1.80	1.78	1.83	1.82	1.79	1.76	1.83	1.80	1.82	1.73	1.71	1.73	1.75	1.73
Al tot.	2.53	2.44	2.67	2.59	2.67	2.61	2.58	2.55	2.64	2.64	2.57	2.51	2.66	2.60	2.64	2.46	2.42	2.45	2.48	2.43
Ti	0.02	0.02	0.01	0.02	0.02	0.02	0.02	0.02	0.01	0.02	0.01	0.02	0.01	0.02	0.01	0.02	0.02	0.01	0.01	0.02
Cr3+	0.00	0.00	0.00	0.00	0.00	0.00	0.00	0.00	0.00	0.00	0.00	0.00	0.00	0.00	0.00	0.00	0.00	0.00	0.00	0.00
Fe2+	0.17	0.12	0.08	0.09	0.07	0.08	0.08	0.09	0.08	0.09	0.10	0.10	0.09	0.09	0.08	0.12	0.12	0.12	0.11	0.11
Mg	0.15	0.18	0.10	0.11	0.08	0.10	0.12	0.13	0.10	0.11	0.13	0.15	0.10	0.12	0.10	0.18	0.18	0.18	0.16	0.19
Mn	0.00	0.00	0.00	0.00	0.00	0.00	0.00	0.00	0.00	0.00	0.00	0.00	0.00	0.00	0.00	0.00	0.00	0.00	0.00	0.00
Fe + Mg	0.32	0.30	0.18	0.21	0.16	0.18	0.20	0.22	0.18	0.19	0.22	0.25	0.19	0.20	0.18	0.30	0.30	0.30	0.28	0.30
various cation ratios																				
mg number	47.18	59.89	53.96	54.72	53.30	56.22	58.85	58.38	55.31	55.66	56.87	60.98	52.95	57.24	55.10	59.68	59.80	60.99	58.83	62.38
Fe/(Fe+Mg)	0.53	0.40	0.46	0.45	0.47	0.44	0.41	0.42	0.45	0.44	0.43	0.39	0.47	0.43	0.45	0.40	0.40	0.39	0.41	0.38
Mg/(Mg+Fe)	0.47	0.60	0.54	0.55	0.53	0.56	0.59	0.58	0.55	0.56	0.57	0.61	0.53	0.57	0.55	0.60	0.60	0.61	0.59	0.62
muscovite cat	0.85	0.89	0.82	0.84	0.85	0.83	0.84	0.85	0.82	0.82	0.84	0.86	0.81	0.84	0.82	0.85	0.87	0.87	0.85	0.86
paragonite	0.15	0.11	0.18	0.16	0.15	0.17	0.16	0.15	0.18	0.18	0.15	0.14	0.19	0.16	0.18	0.15	0.13	0.13	0.15	0.13
margarite	0.00	0.00	0.00	0.00	0.00	0.00	0.00	0.00	0.00	0.00	0.00	0.00	0.00	0.00	0.00	0.00	0.00	0.00	0.00	0.00
paragonite	15.07	11.35	18.18	15.68	15.17	16.99	15.95	14.89	18.49	17.85	15.49	13.75	18.96	16.00	18.17	14.61	13.32	13.43	14.66	13.35
celadonite	17.90	27.57	16.30	20.56	16.87	20.62	21.50	22.46	18.57	17.58	21.68	25.12	16.61	20.18	18.57	27.11	29.30	28.36	27.49	30.04
muskovite	67.03	61.08	65.51	63.77	67.95	62.39	62.55	62.65	62.94	64.57	62.84	61.13	64.43	63.82	63.25	58.28	57.37	58.21	57.85	56.60

Appendix B: Electron microprobe analyses of white mica; grt-cld-chl-micaschist [sample GR99/40], micaschist [M99/13]

sample	GR99/40	GR99/40	GR99/40	GR99/40	GR99/40	GR99/40	GR99/40	GR99/40	GR99/40	GR99/40	GR99/40	GR99/40	M99/13	M99/13	M99/13	M99/13	M99/13	M99/13	M99/13	M99/13
analysis	wm7_3	wm8_1	wm8_2	wm9_1	wm9_2	wm9_3	wm10	wm11_1	wm11_2	wm12_1	wm12_2	wm12_3	wm1_1	wm1_2	wm1_3	wm2_1	wm2_2	wm3	wm4	wm5
Na2O	0.88	0.98	1.28	1.02	1.14	1.46	1.19	1.19	1.21	1.13	1.17	1.12	0.06	0.07	0.06	0.10	0.10	0.08	0.08	0.06
K2O	8.60	8.60	8.08	8.73	8.59	8.34	8.78	9.02	9.00	9.11	9.13	9.03	10.12	10.13	10.39	10.26	10.15	10.61	10.60	10.51
CaO	0.02	0.09	0.08	0.00	0.00	0.01	0.00	0.02	0.00	0.00	0.00	0.01	0.02	0.01	0.03	0.01	0.01	0.01	0.00	0.02
SiO2	49.71	49.13	47.32	47.58	47.92	46.62	48.75	49.25	48.79	49.21	47.71	49.45	49.85	50.24	51.88	51.20	50.99	50.07	50.51	50.53
Al2O3	31.15	31.41	33.98	32.15	32.82	33.94	33.03	32.92	33.07	32.97	35.05	32.70	28.42	28.18	28.01	27.58	27.49	29.00	28.45	28.27
TiO2	0.36	0.35	0.32	0.36	0.29	0.30	0.27	0.33	0.34	0.34	0.25	0.33	0.52	0.64	0.68	0.68	0.75	0.43	0.59	0.50
FeO	1.91	2.16	1.47	1.63	1.66	1.48	1.66	1.77	1.62	1.67	1.19	1.65	3.71	3.66	3.58	3.59	3.67	4.06	3.68	3.65
MgO	1.81	1.76	0.83	1.34	1.26	0.77	1.25	1.35	1.36	1.35	0.65	1.45	2.60	2.62	2.84	2.78	2.83	2.46	2.50	2.63
MnO	0.01	0.04	0.03	0.05	0.00	0.00	0.01	0.10	0.00	0.06	0.00	0.00	0.00	0.03	0.01	0.01	0.00	0.03	0.04	0.03
Cr2O3	0.00	0.00	0.00	0.00	0.00	0.00	0.00	0.00	0.00	0.00	0.00	0.00	0.00	0.00	0.00	0.00	0.00	0.00	0.00	0.00
total	94.48	94.61	93.41	92.90	93.72	92.94	94.93	95.96	95.39	95.83	95.18	95.73	95.31	95.58	97.47	96.22	96.01	96.75	96.44	96.20
number of cations based on 11 oxygen atoms (H2O free)																				
Na	0.11	0.13	0.17	0.13	0.15	0.19	0.15	0.15	0.16	0.14	0.15	0.14	0.01	0.01	0.01	0.01	0.01	0.01	0.01	0.01
K	0.73	0.73	0.69	0.75	0.73	0.72	0.74	0.75	0.76	0.76	0.77	0.76	0.86	0.86	0.87	0.87	0.86	0.90	0.90	0.89
Ca	0.00	0.01	0.01	0.00	0.00	0.00	0.00	0.00	0.00	0.00	0.00	0.00	0.00	0.00	0.00	0.00	0.00	0.00	0.00	0.00
total	0.84	0.86	0.86	0.89	0.88	0.91	0.89	0.91	0.91	0.91	0.92	0.90	0.87	0.87	0.88	0.88	0.87	0.91	0.91	0.90
Si	3.30	3.27	3.17	3.22	3.21	3.15	3.22	3.23	3.22	3.23	3.15	3.25	3.34	3.35	3.39	3.39	3.39	3.32	3.35	3.36
AlIV	0.70	0.73	0.83	0.78	0.79	0.85	0.78	0.77	0.78	0.77	0.85	0.75	0.66	0.65	0.61	0.61	0.61	0.68	0.65	0.64
AlVI	1.74	1.73	1.85	1.79	1.80	1.85	1.80	1.78	1.79	1.78	1.87	1.78	1.58	1.57	1.55	1.55	1.54	1.58	1.57	1.57
Al tot.	2.44	2.46	2.68	2.57	2.59	2.70	2.58	2.55	2.57	2.55	2.73	2.53	2.24	2.22	2.16	2.15	2.15	2.27	2.22	2.21
Ti	0.02	0.02	0.02	0.02	0.01	0.02	0.01	0.02	0.02	0.02	0.01	0.02	0.03	0.03	0.03	0.03	0.04	0.02	0.03	0.02
Cr3+	0.00	0.00	0.00	0.00	0.00	0.00	0.00	0.00	0.00	0.00	0.00	0.00	0.00	0.00	0.00	0.00	0.00	0.00	0.00	0.00
Fe2+	0.11	0.12	0.08	0.09	0.09	0.08	0.09	0.10	0.09	0.09	0.07	0.09	0.21	0.20	0.20	0.20	0.20	0.22	0.20	0.20
Mg	0.18	0.17	0.08	0.13	0.13	0.08	0.12	0.13	0.13	0.13	0.06	0.14	0.26	0.26	0.28	0.27	0.28	0.24	0.25	0.26
Mn	0.00	0.00	0.00	0.00	0.00	0.00	0.00	0.01	0.00	0.00	0.00	0.00	0.00	0.00	0.00	0.00	0.00	0.00	0.00	0.00
Fe + Mg	0.29	0.29	0.17	0.23	0.22	0.16	0.21	0.23	0.22	0.22	0.13	0.23	0.47	0.46	0.47	0.47	0.48	0.47	0.45	0.46
various cation ratios																				
mg number	62.81	59.22	50.24	59.36	57.53	48.17	57.26	57.65	59.87	59.06	49.44	61.00	55.58	56.06	58.57	57.98	57.88	51.92	54.76	56.22
Fe/(Fe+Mg)	0.37	0.41	0.50	0.41	0.42	0.52	0.43	0.42	0.40	0.41	0.51	0.39	0.44	0.44	0.41	0.42	0.42	0.48	0.45	0.44
Mg/(Mg+Fe)	0.63	0.59	0.50	0.59	0.58	0.48	0.57	0.58	0.60	0.59	0.49	0.61	0.56	0.56	0.59	0.58	0.58	0.52	0.55	0.56
muscovite cat	0.86	0.85	0.80	0.85	0.83	0.79	0.83	0.83	0.83	0.84	0.84	0.84	0.99	0.99	0.99	0.98	0.98	0.99	0.99	0.99
paragonite	0.13	0.15	0.19	0.15	0.17	0.21	0.17	0.17	0.17	0.16	0.16	0.16	0.01	0.01	0.01	0.01	0.01	0.01	0.01	0.01
margarite	0.00	0.01	0.01	0.00	0.00	0.00	0.00	0.00	0.00	0.00	0.00	0.00	0.00	0.00	0.00	0.00	0.00	0.00	0.00	0.00
paragonite	13.46	14.75	19.45	15.08	16.80	21.01	17.03	16.71	17.00	15.85	16.35	15.80	0.92	1.10	0.81	1.43	1.49	1.16	1.06	0.89
celadonite	29.99	26.91	17.01	22.06	21.10	14.90	22.43	23.00	21.65	22.99	14.80	24.54	33.83	35.32	39.16	39.29	38.70	31.78	34.94	35.69
muskovite	56.55	58.34	63.54	62.86	62.11	64.08	60.54	60.29	61.35	61.16	68.86	59.66	65.24	63.58	60.03	59.28	59.81	67.06	64.00	63.42

Appendix B: Electron microprobe analyses of white mica; micaschist [sample M99-13]

sample	M99/13	M99/13	M99/13	M99/13
analysis	wm6_1	wm6_2	wm7_1	wm7_2
Na2O	0.10	0.08	0.08	0.07
K2O	10.61	10.61	10.59	10.63
CaO	0.02	0.00	0.01	0.01
SiO2	50.76	51.72	51.81	50.62
Al2O3	28.19	27.47	27.74	28.04
TiO2	0.34	0.72	0.62	0.53
FeO	3.57	3.60	3.49	3.57
MgO	2.72	2.93	2.75	2.58
MnO	0.04	0.04	0.02	0.02
Cr2O3	0.00	0.00	0.00	0.00
total	96.35	97.17	97.10	96.09
number of cations based on 11 oxygen atoms (H2O free)				
Na	0.01	0.01	0.01	0.01
K	0.90	0.89	0.89	0.90
Ca	0.00	0.00	0.00	0.00
total	0.91	0.90	0.90	0.91
Si	3.37	3.40	3.40	3.37
AlIV	0.63	0.60	0.60	0.63
AlVI	1.57	1.53	1.55	1.57
Al tot.	2.20	2.13	2.15	2.20
Ti	0.02	0.04	0.03	0.03
Cr3+	0.00	0.00	0.00	0.00
Fe2+	0.20	0.20	0.19	0.20
Mg	0.27	0.29	0.27	0.26
Mn	0.00	0.00	0.00	0.00
Fe + Mg	0.47	0.48	0.46	0.45
various cation ratios				
mg number	57.59	59.19	58.41	56.29
Fe/(Fe+Mg)	0.42	0.41	0.42	0.44
Mg/(Mg+Fe)	0.58	0.59	0.58	0.56
muscovite cat	0.99	0.99	0.99	0.99
paragonite	0.01	0.01	0.01	0.01
margarite	0.00	0.00	0.00	0.00
paragonite	1.34	1.10	1.09	1.05
celadonite	36.71	39.95	40.30	36.77
muskovite	61.95	58.95	58.61	62.18

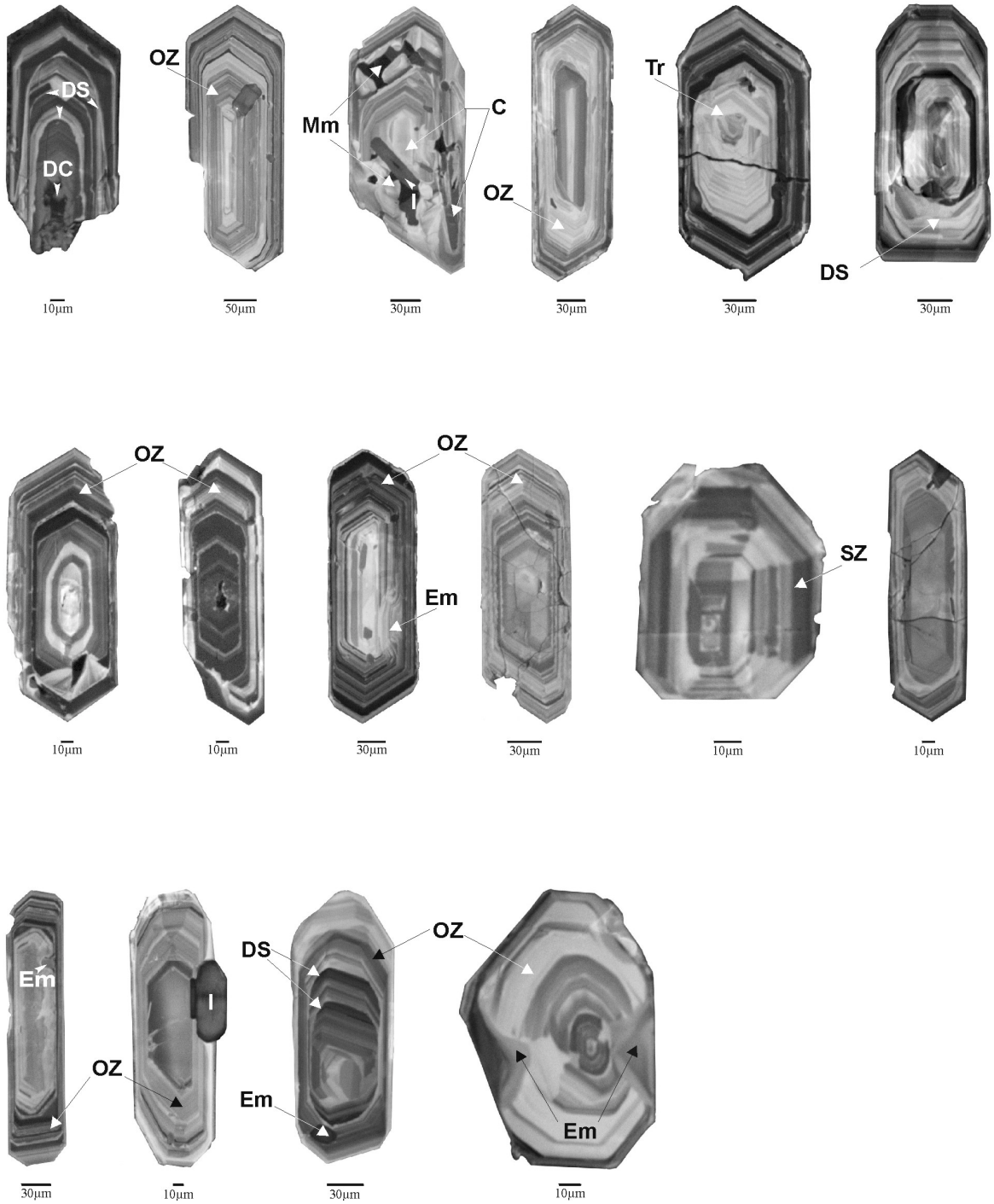

Appendix C-1: Cathodoluminescence images of zircons from East Pelagonian granite (sample 8-4). C=Core, DC=Dissolved Core, DS=Disolution Surface, Em=Embayment, I=Inclusion, Mm=Metamict, OZ=Oscillatory Zoning, SZ=Sector Zoning, Tr=Truncation.

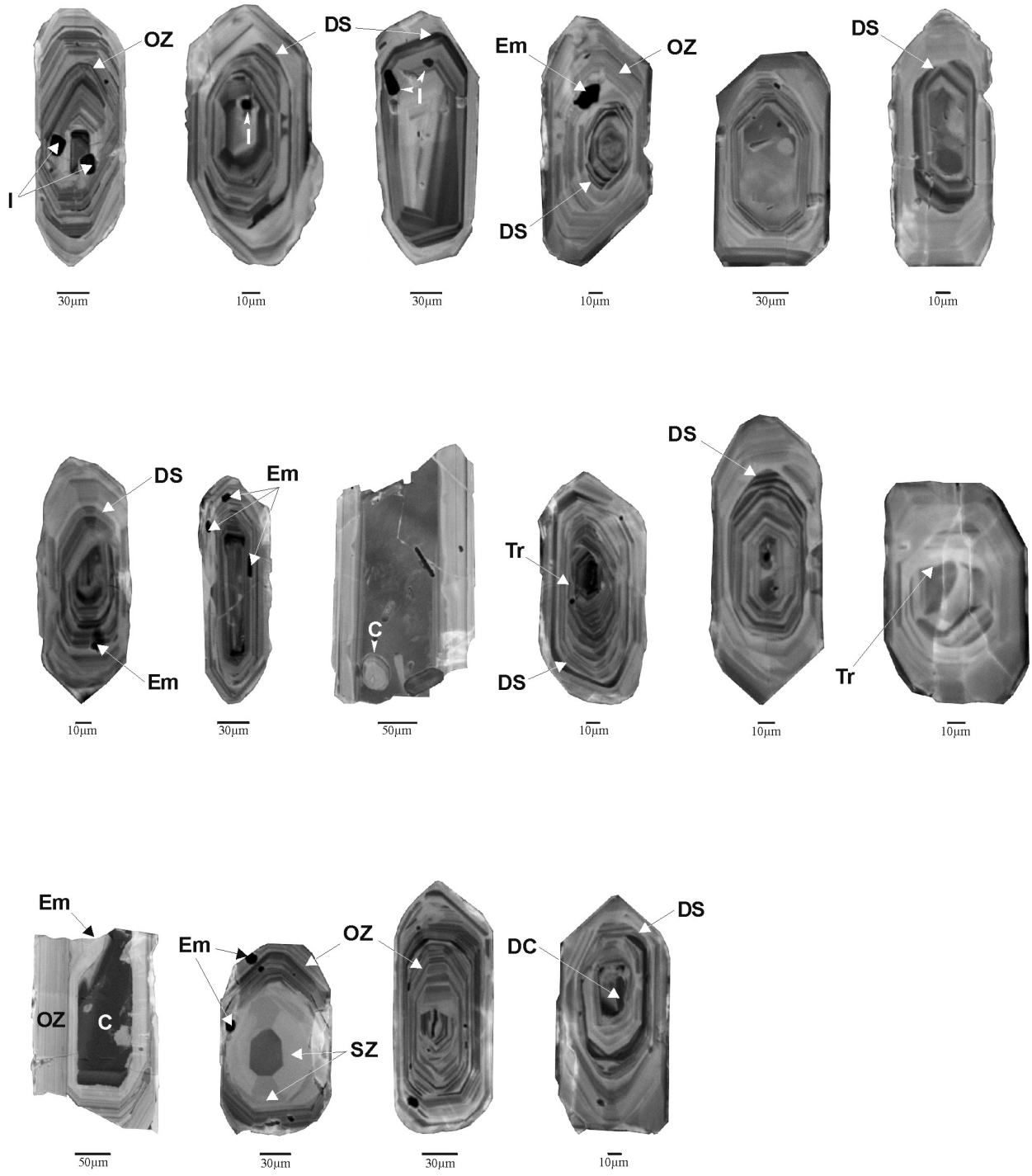

Appendix C-2: Cathodoluminescence images of zircons from East Pelagonian granite (sample M98-17). C=Core, DC=Dissolved Core, DS=Disolution Surface, Em=Embayment, I=Inclusion, Mm=Metamict, OZ=Oscillatory Zoning, SZ=Sector Zoning, Tr=Truncation.

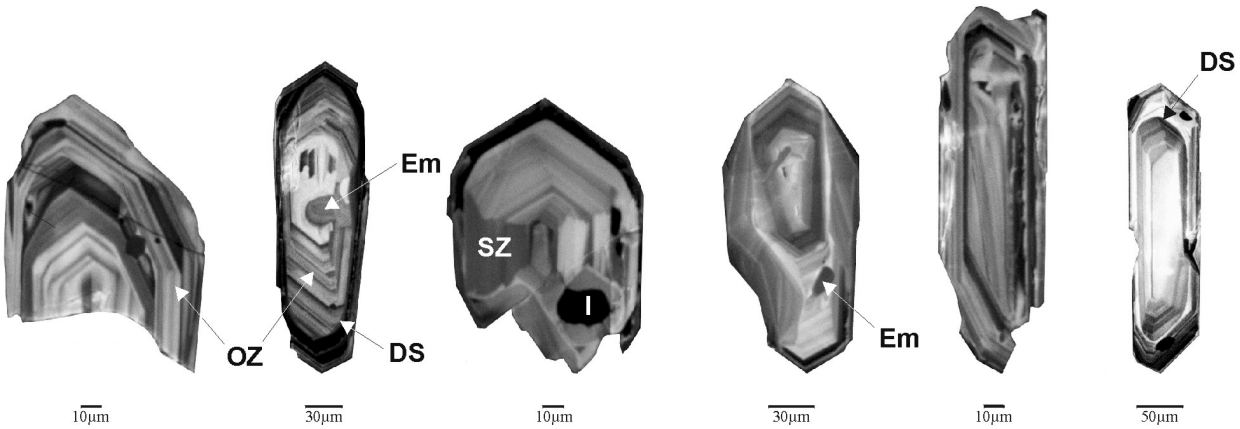

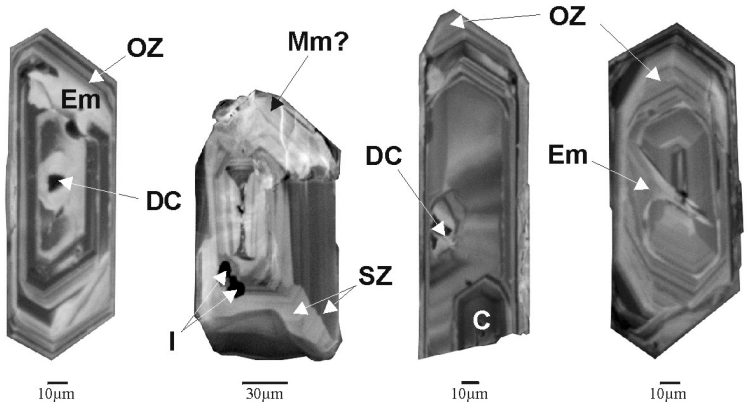

Appendix C-3: Cathodoluminescence images of zircons from East Pelagonian granite (sample M99-12). C=Core, DC=Dissolved Core, DS=Disolution Surface, Em=Embayment, I=Inclusion, Mm=Metamict, OZ=Oscillatory Zoning, SZ=Sector Zoning, Tr=Truncation.

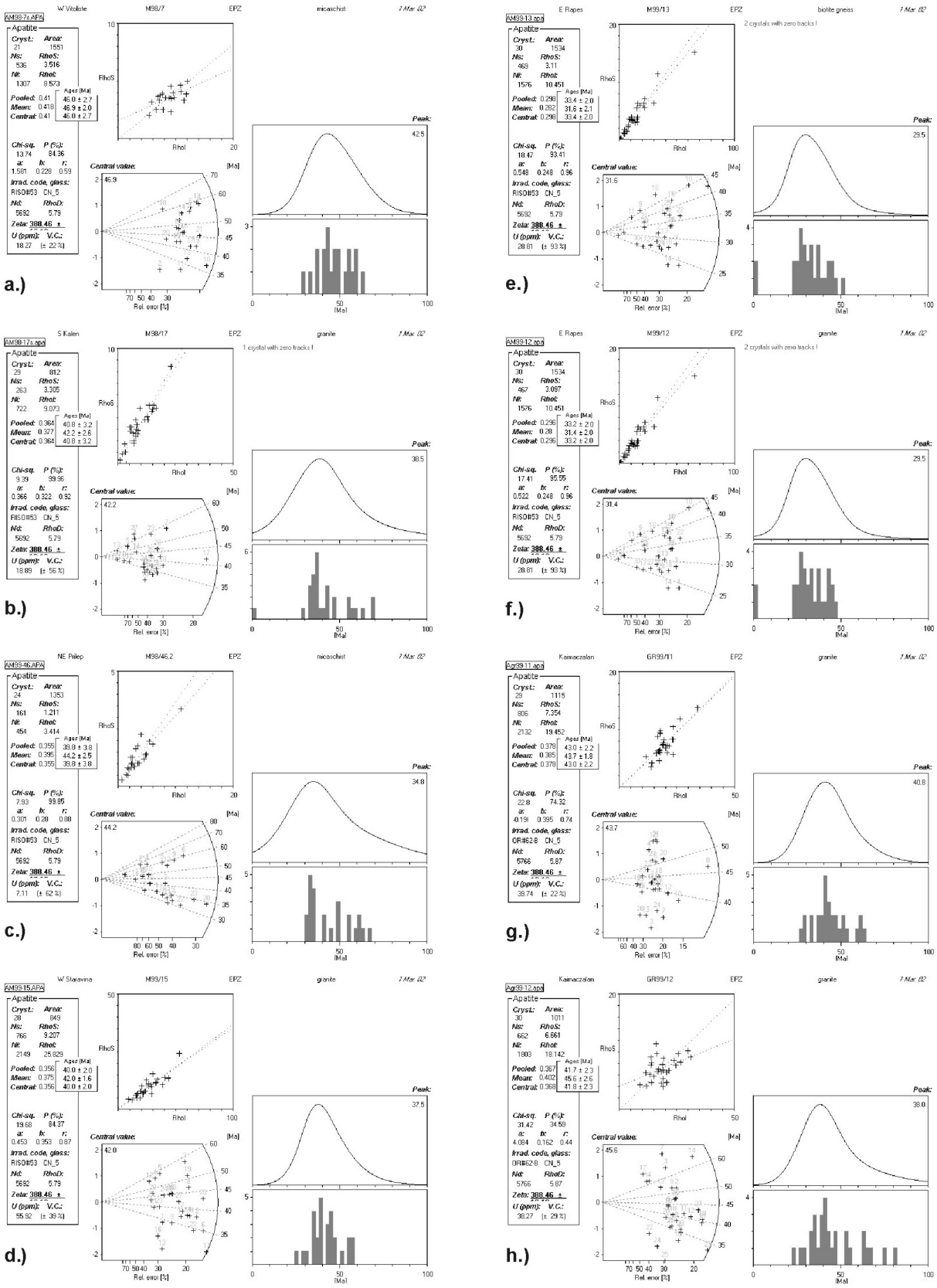

Appendix-D1: Apatite fission track data evaluation with TRACKKEY 4.1 software program (Dunkl, 2002). Fig. a.-k. East Pelagonian Zone, l.-o. West Pelagonian Zone, p.-t. Vardar Zone and u.-x. Olympos-Kranea area. Continues.

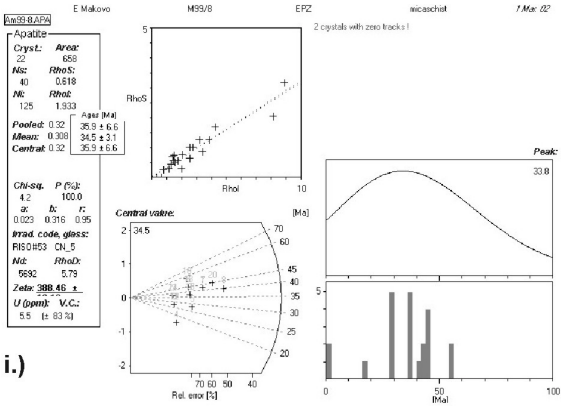

i.)

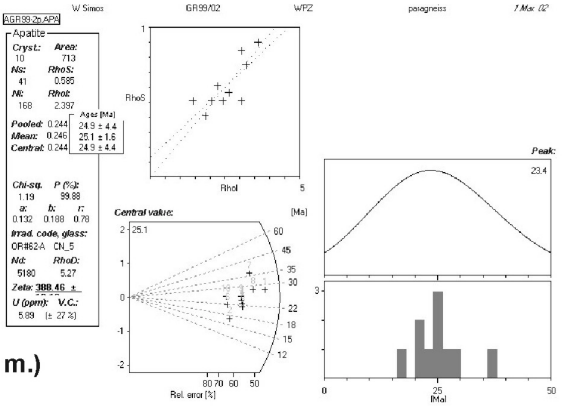

m.)

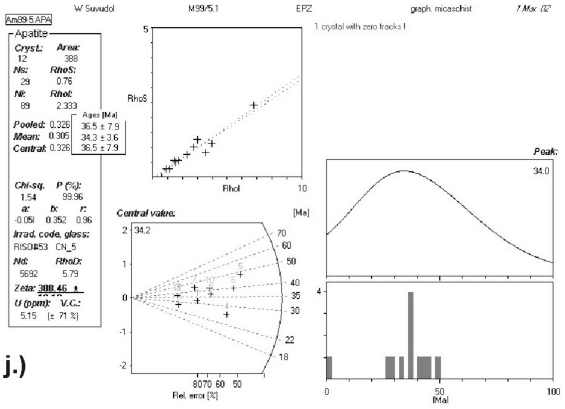

j.)

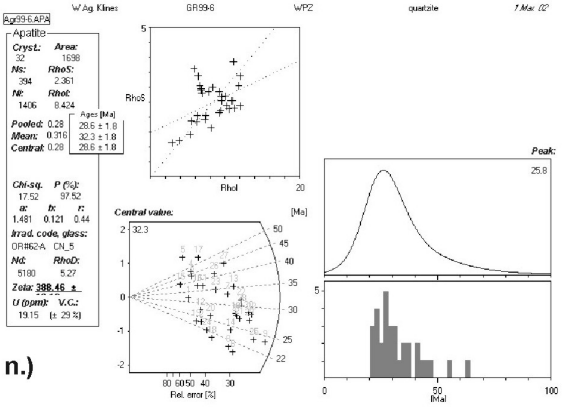

n.)

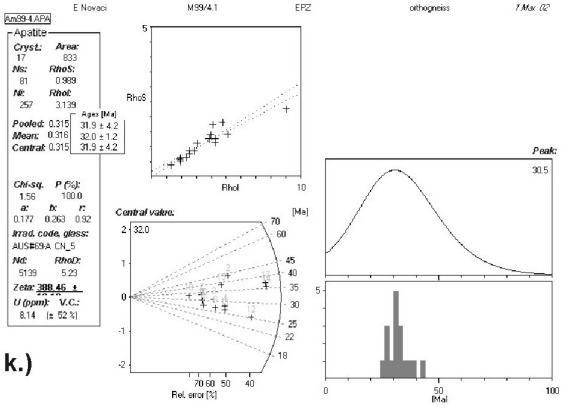

k.)

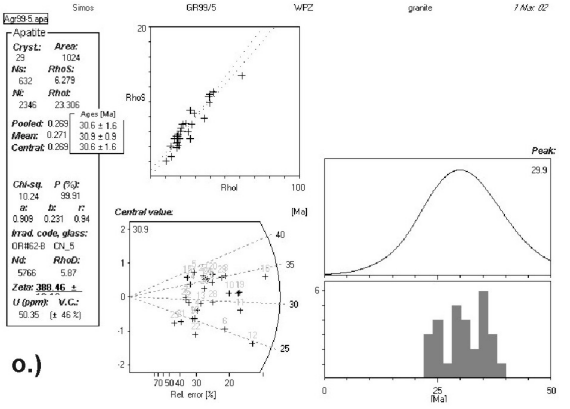

o.)

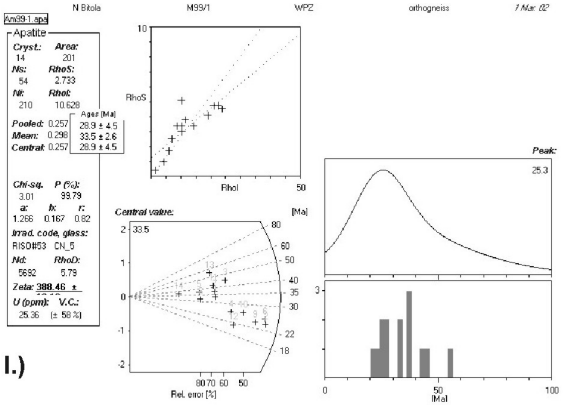

l.)

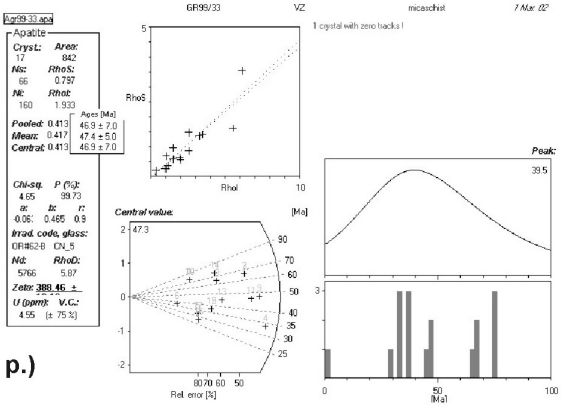

p.)

Appendix-D1: continues.

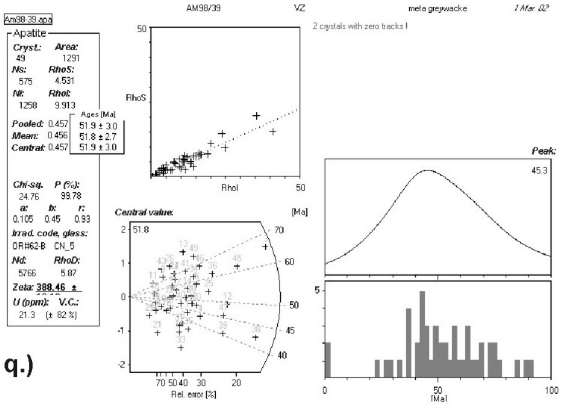

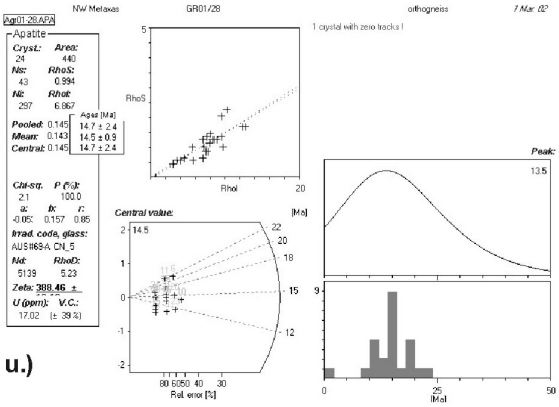

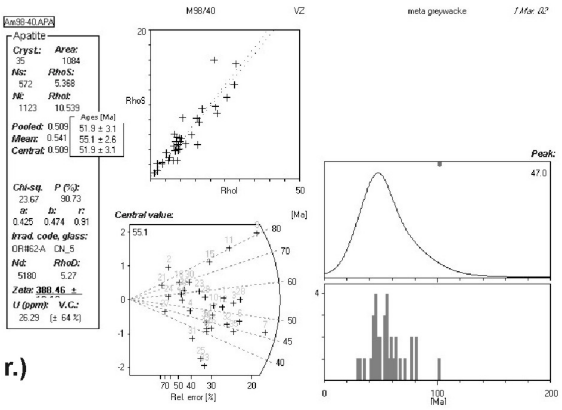

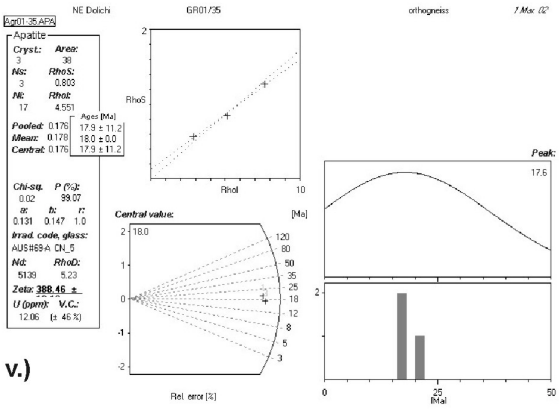

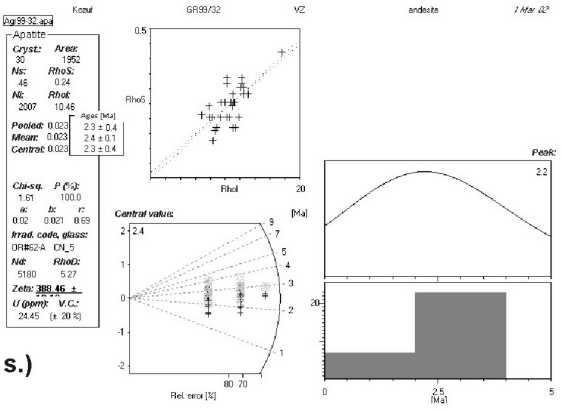

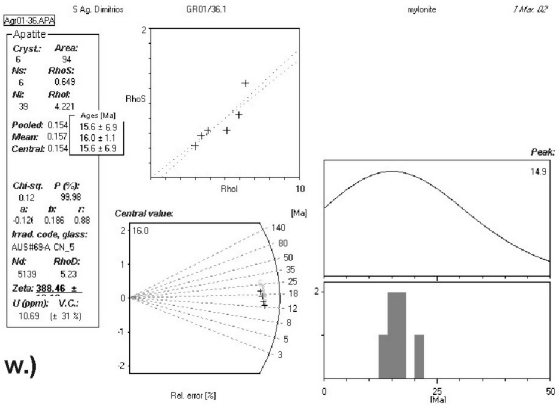

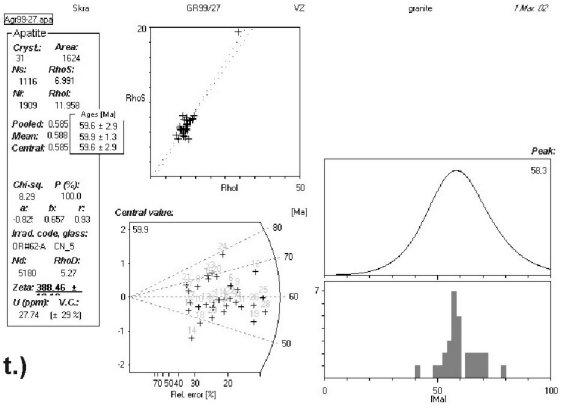

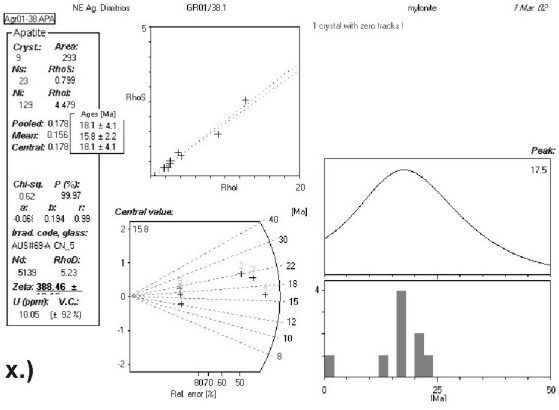

Appendix-D1: continued.

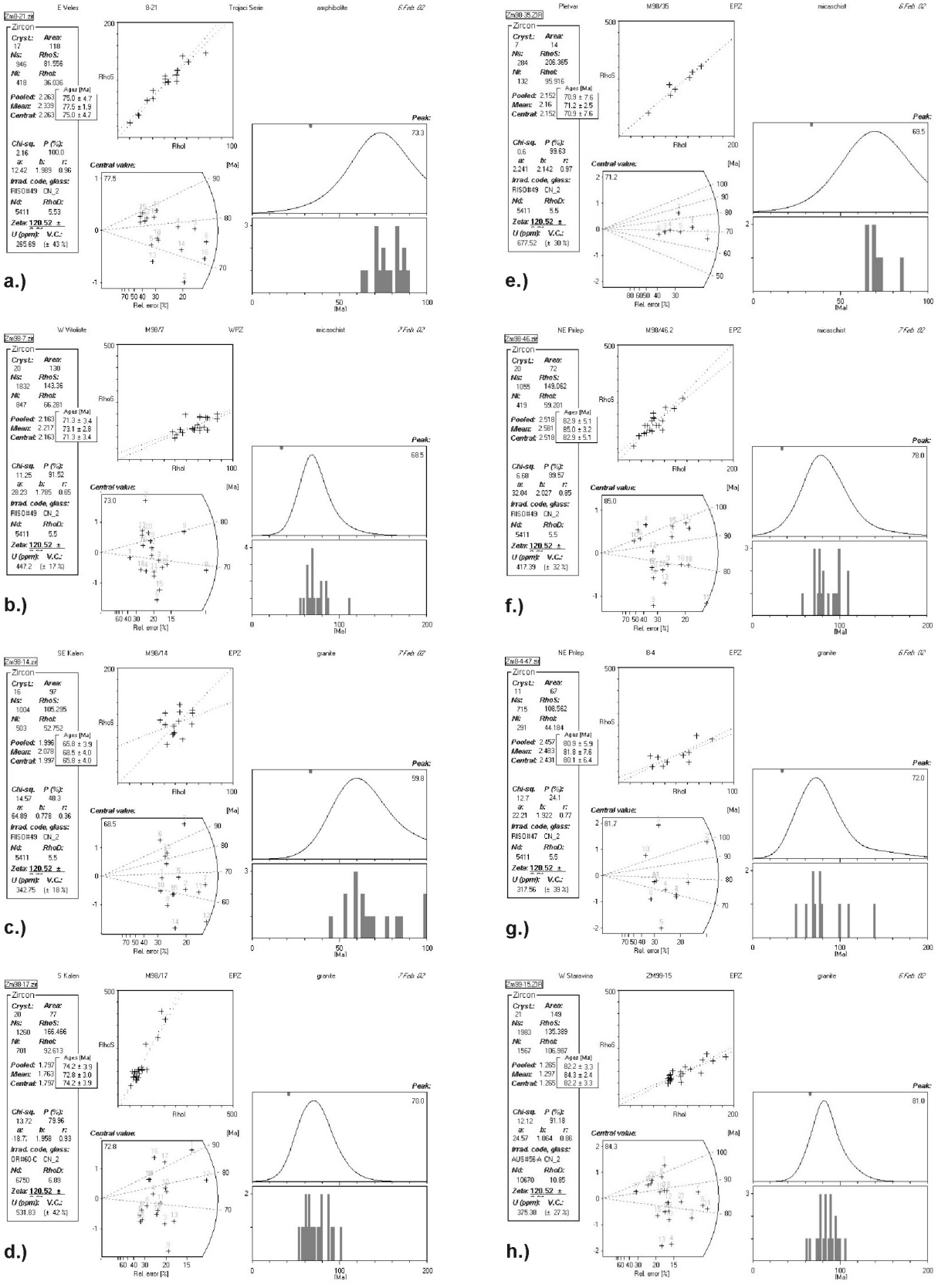

Appendix D2: Zircon fission track data evaluation with TRACKKEY 4.1 software program (Dunkl, 2001). Fig. a.-n. East Pelagonian Zone, o.-s. West Pelagonian Zone, t.-v. Vardar Zone and w.-za. Olympos-Kranea area. Continues.

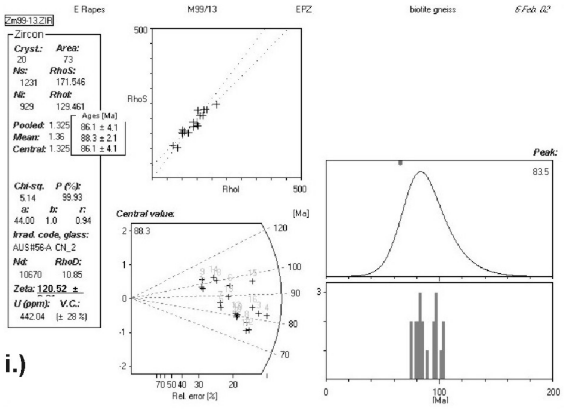

i.)

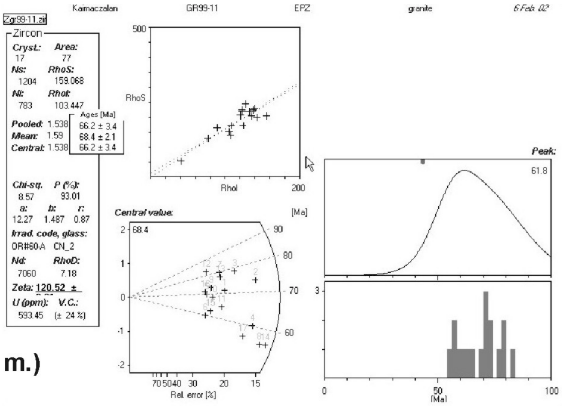

m.)

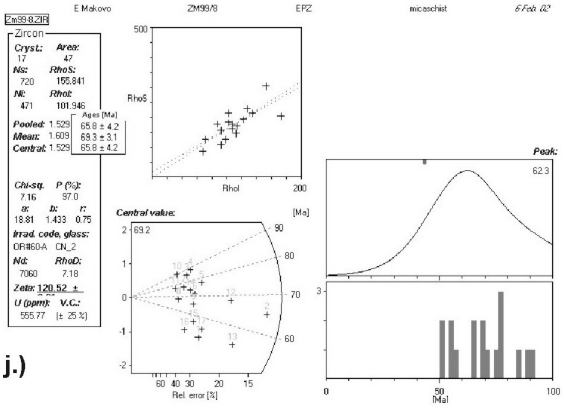

j.)

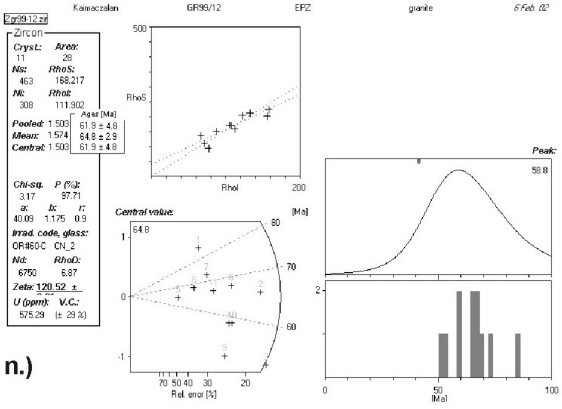

n.)

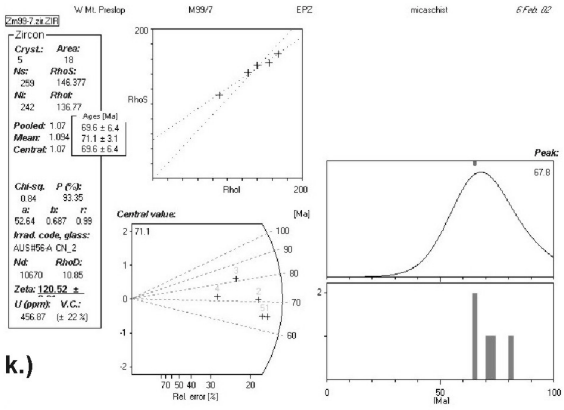

k.)

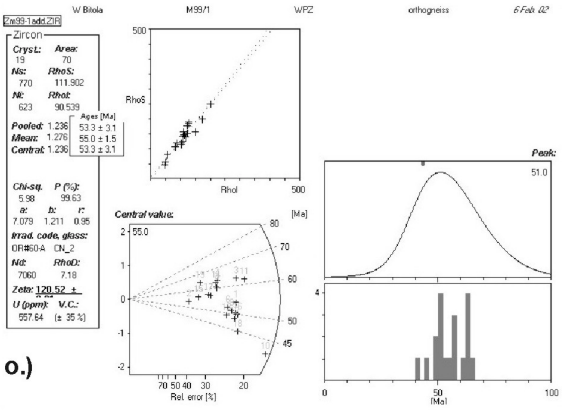

o.)

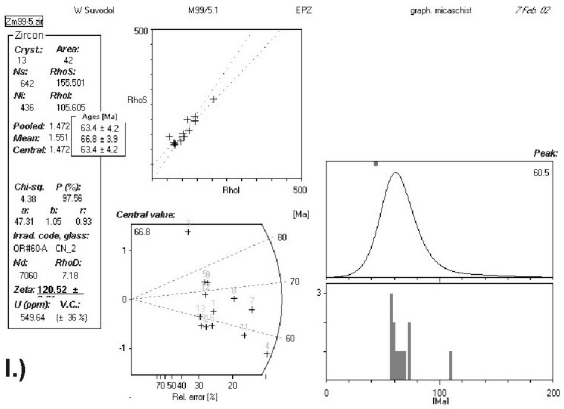

l.)

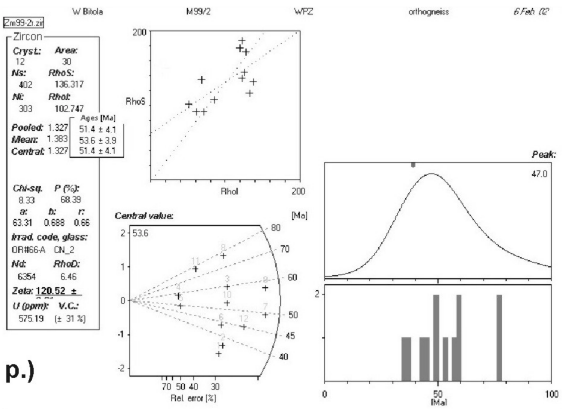

p.)

Appendix D2: Continues.

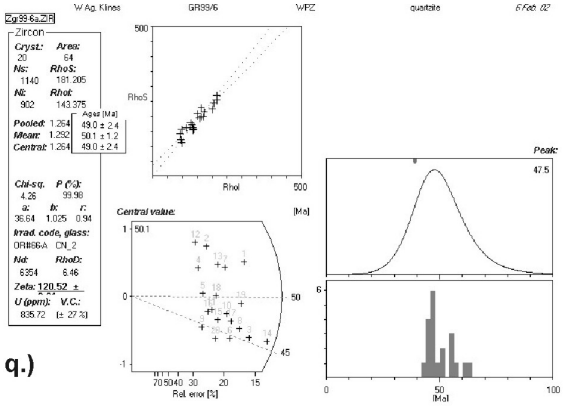

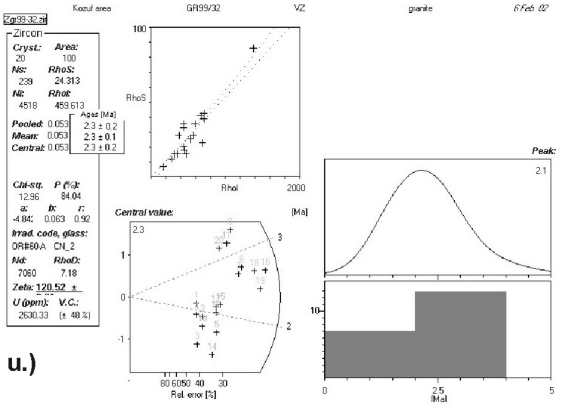

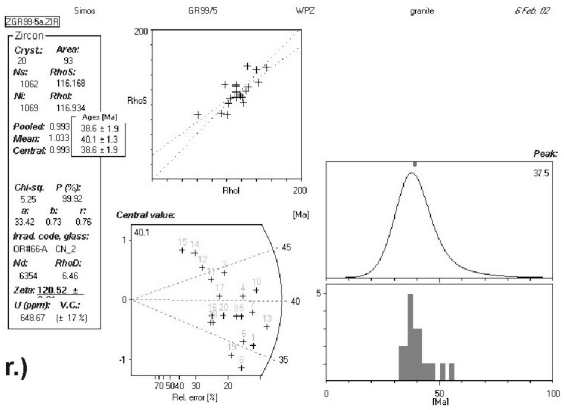

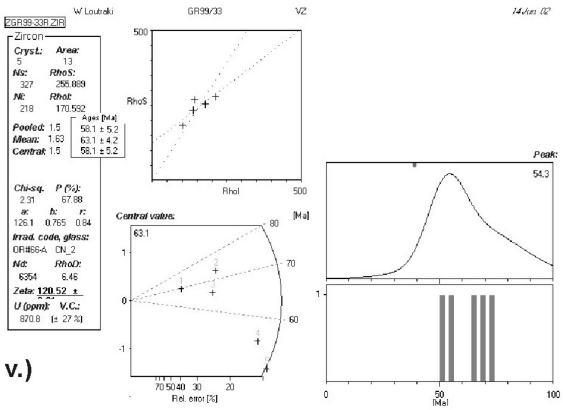

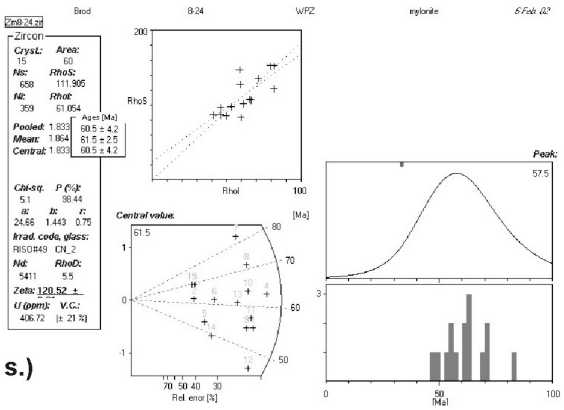

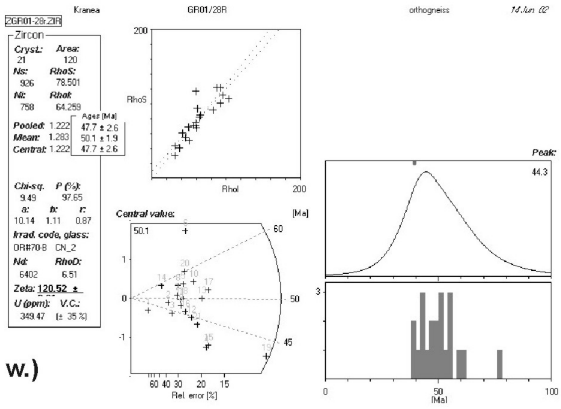

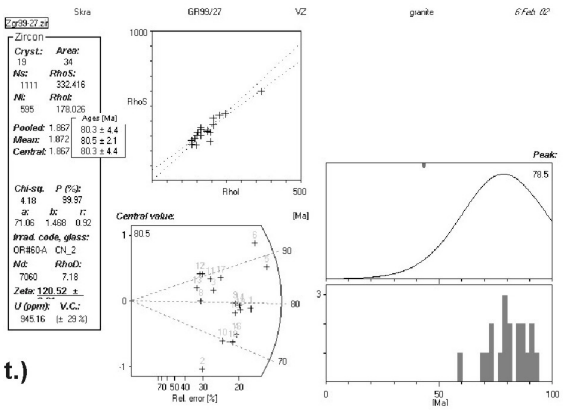

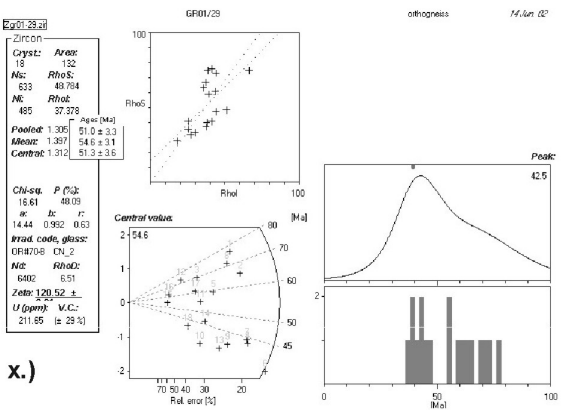

Appendix D2: Continues.

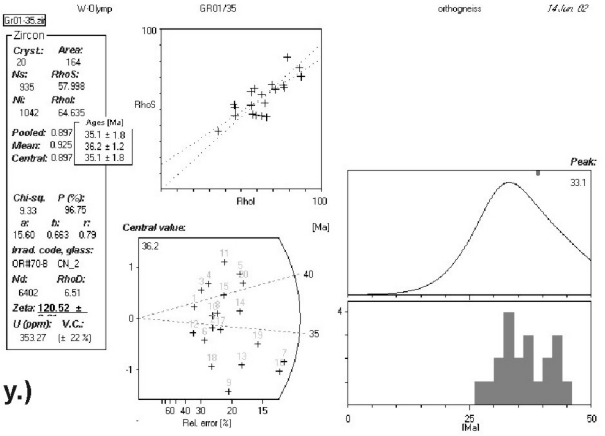

y.)

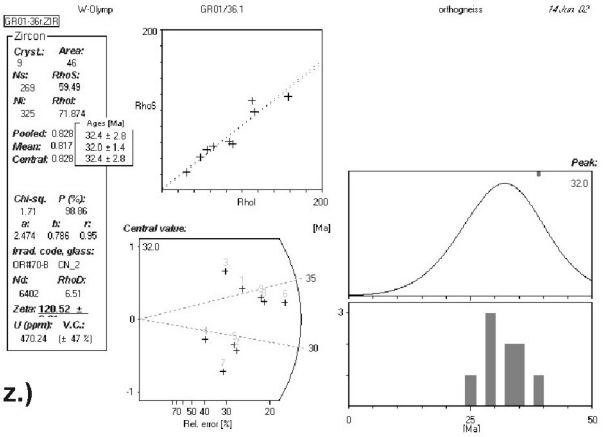

z.)

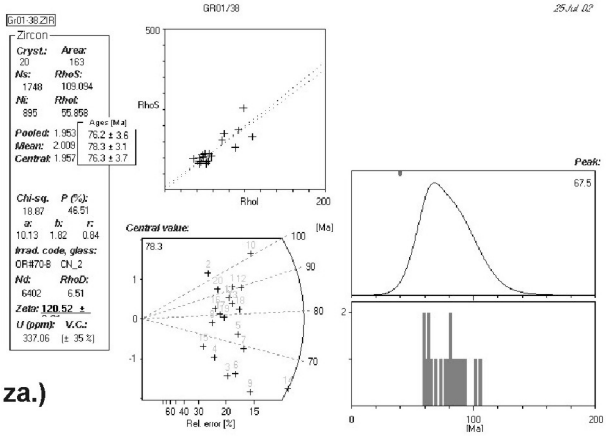

za.)

Appendix D2: Continued.

Appendix D3: $^{40}Ar/^{39}Ar$ step heating analytical data. All errors refer to the last digit.

Sample M99/13 biotite (weight = 0.0649g; J = 0.00104)

step	Temp. [°C]	Ar 40 tot. ± s x10-8	Ar 40 * x10-8	Ar 39 ± s x10-12	Ar 39 %	Ar 38 ± s x10-12	Cl x10-12	Ar 37 ± s x10-12	Ar 36 ± s x10-12	39 / 40 ± s	36 / 40 ± s x10-4	Ca / K ± s x10-1	Cl/K	Age [Ma] ± s
1	442	0.735 ± 1.80	0.442	84.2 ± 2.80	3.49	4.090 ± 5.40	1.250	0.861 ± 547	9.930 ± 4.4	0.0114 ± 0.47	1.350 ± 0.69	0.0205 ± 130	0.00340	95.89 ± 0.47
2	562	1.680 ± 0.17	1.460	213 ± 0.31	8.81	4.880 ± 5.70	0.991	0.695 ± 18	7.390 ± 3.0	0.0127 ± 0.22	0.441 ± 1.08	0.0065 ± 17	0.00107	124.18 ± 0.22
3	629	2.620 ± 0.03	2.490	342 ± 0.30	14.16	7.080 ± 4.70	2.230	-0.907 - 478	4.460 ± 2.5	0.0130 ± 0.12	0.170 ± 0.97	-0.0053 - 28	0.00150	131.75 ± 0.12
4	687	2.490 ± 0.25	2.440	330 ± 0.44	13.67	5.360 ± 1.50	1.140	0.338 ± 231	1.790 ± 1.5	0.0133 ± 0.19	0.072 ± 6.00	0.0021 ± 14	0.00080	133.47 ± 0.19
5	740	1.250 ± <0.01	1.200	165 ± 0.15	6.83	3.870 ± 0.69	1.630	2.360 ± 41	1.590 ± 3.3	0.0132 ± 0.12	0.128 ± 2.70	0.0286 ± 50	0.00228	131.75 ± 0.16
6	788	0.961 ± 0.96	0.912	125 ± 0.15	5.18	2.490 ± 1.30	0.713	-0.455 - 300	1.650 ± 1.8	0.0130 ± 0.15	0.172 ± 1.90	-0.0073 - 48	0.00131	131.8 ± 0.17
7	833	0.848 ± 0.08	0.798	110 ± 0.10	4.56	2.400 ± 1.30	0.781	0.138 ± 275	1.710 ± 1.8	0.0130 ± 0.12	0.201 ± 2.20	0.0025 ± 50	0.00163	131.06 ± 0.14
8	882	1.160 ± 0.01	1.110	153 ± 0.14	6.33	2.940 ± 2.90	0.812	0.917 ± 504	1.780 ± 2.1	0.0131 ± 0.12	0.153 ± 1.53	0.0120 ± 66	0.00122	131.37 ± 0.13
9	969	1.960 ± 0.03	1.900	259 ± 0.24	10.74	4.830 ± 1.40	1.410	-0.435 - 453	2.010 ± 2.1	0.0132 ± 0.12	0.103 ± 0.11	-0.0034 - 35	0.00125	132.48 ± 0.13
10	1070	3.880 ± 0.06	3.810	514 ± 0.46	21.31	9.030 ± 5.10	2.520	-1.010 - 41	2.490 ± 2.3	0.0132 ± 0.12	0.061 ± 5.80	-0.0039 - 16	0.00113	133.84 ± 0.12
11	1190	0.824 ± 0.08	0.814	108 ± 0.10	4.48	2.040 ± 2.40	0.695	-0.007 - 2760	0.363 ± 26.0	0.0131 ± 0.12	0.044 ± 32	-0.0001 - 51	0.00148	135.83 ± 0.17
12	1422	0.082 ± 0.15	0.078	10.3 ± 0.26	0.43	0.354 ± 27	0.204	-0.550 - 247	0.154 ± 18.0	0.0125 ± 0.32	0.187 ± 21	-0.1070 - 480	0.00456	136.42 ± 0.94

Sample M99/13 white mica (weight = 0.0741g; J = 0.00104)

step	Temp. [°C]	Ar 40 tot. ± s x10-8	Ar 40 * x10-8	Ar 39 ± s x10-12	Ar 39 %	Ar 38 ± s x10-12	Cl x10-12	Ar 37 ± s x10-12	Ar 36 ± s x10-12	39 / 40 ± s	36 / 40 ± s x10-4	Ca / K ± s x10-1	Cl/K	Age [Ma] ± s
1	456	0.161 ± 0.99	0.054	13.6 ± 1.9	0.42	0.146 ± 70	0.069	1.110 ± 88.2	3.630 ± 85	0.0084 ± 0.53	2.25 ± 5.5	0.1640 ± 1300	0.00117	73.01 ± 3.40
2	520	0.147 ± 0.11	0.100	15.0 ± 2.1	0.47	0.547 ± 30	0.072	3.120 ± 14.2	1.600 ± 16	0.0102 ± 0.16	1.09 ± 1.1	0.4160 ± 190	0.00111	120.56 ± 0.59
3	600	0.538 ± 0.05	0.451	61.2 ± 5.9	1.90	1.470 ± 3.7	0.203	0.587 ± 520	2.940 ± 34	0.0114 ± 0.11	0.547 ± 6.4	0.0192 ± 170	0.00076	133.13 ± 0.31
4	662	0.796 ± 0.25	0.705	96.4 ± 8.7	2.99	1.980 ± 3.8	0.277	1.210 ± 47.7	3.060 ± 28	0.0121 ± 0.12	0.384 ± 3.5	0.0252 ± 99	0.00066	132.24 ± 0.19
5	713	0.992 ± 0.24	0.828	112.0 ± 1.5	3.49	2.830 ± 3.3	0.474	0.563 ± 275	5.540 ± 23	0.0113 ± 0.16	0.559 ± 2.3	0.0100 ± 49	0.00097	133.23 ± 0.21
6	735	1.640 ± 0.02	1.320	181.0 ± 1.8	5.61	4.720 ± 3.9	0.573	0.150 ± 298	10.800 ± 470	0.0110 ± 0.11	0.659 ± 2.9	0.0017 ± 33	0.00073	132.38 ± 0.19
7	780	4.100 ± 0.03	3.650	496.0 ± 4.5	15.40	9.530 ± 5.1	0.876	0.172 ± 347	15.100 ± 550	0.0121 ± 0.11	0.368 ± 1.4	0.0007 ± 14	0.00041	133.02 ± 0.13
8	819	5.050 ± 0.02	4.790	651.0 ± 5.9	20.20	8.330 ± 11	0.100	1.740 ± 65.1	8.940 ± 36	0.0129 ± 0.12	0.177 ± 0.7	0.0054 ± 20	0.00004	132.94 ± 0.12
9	865	3.150 ± 0.04	2.940	400.0 ± 3.6	12.43	6.910 ± 3.7	0.885	0.374 ± 260	7.040 ± 34	0.0127 ± 0.11	0.224 ± 1.1	0.0019 ± 13	0.00051	132.70 ± 0.12

continues

Appendix D3: $^{40}Ar/^{39}Ar$ step heating analytical data. All errors refer to the last digit.

Sample M99/13 continued

step	Temp. [°C]	Ar 40 tot. ± s x10-8	Ar 40 * x10-8	Ar 39 ± s x10-12	Ar 39 %	Ar 38 ± s x10-12	Cl x10-12	Ar 37 ± s x10-12	Ar 36 ± s x10-12	39 / 40 ± s	36 / 40 ± s x10-4	Ca / K ± s x10-1	Cl/K	Age [Ma] ± s
10	907	3.770 ± 0.00	3.390	464.0 ± 4.1	14.39	8.770 ± 1.9	0.886	0.054 ± 3250	13.000 ± 500	0.0123 ± 0.11	0.345 ± 1.3	0.0002 ± 14	0.00044	132.13 ± 0.12
11	968	3.680 ± 0.01	3.460	475.0 ± 4.2	14.76	8.330 ± 1.9	1.400	9.310 ± 57.1	7.170 ± 35	0.0129 ± 0.11	0.195 ± 1	0.0391 ± 24	0.00068	131.77 ± 0.12
12	1110	1.780 ± 0.00	1.730	236.0 ± 2.1	7.33	3.560 ± 2.8	0.502	3.820 ± 60.2	1.510 ± 27	0.0133 ± 0.12	0.0848 ± 15	0.0323 ± 51	0.00049	132.55 ± 0.13
13	1370	0.156 ± 0.00	0.148	19.7 ± 3.3	0.61	0.197 ± 23	0.008	0.293 ± 227	0.251 ± 17	0.0127 ± 0.21	0.161 ± 11.0	0.0296 ± 230	0.00010	135.52 ± 0.50

Sample 8-9 white mica (weight = 0.0601g; J = 0.00104)

step	Temp. [°C]	Ar 40 tot. ± s x10-8	Ar 40 * x10-8	Ar 39 ± s x10-12	Ar 39 %	Ar 38 ± s x10-12	Cl x10-12	Ar 37 ± s x10-12	Ar 36 ± s x10-12	39 / 40 ± s	36 / 40 ± s x10-4	Ca / K ± s x10-1	Cl/K	Age [Ma] ± s
1	428	0.202 ± 0.15	0.112	17.5 ± 28	0.70	1.550 ± 39	0.774	7.762 ± 578	3.058 ± 26	0.0087 ± 0.15	1.511 ± 13.0	0.886 ± 66	0.01015	116.05 ± 0.78
2	517	0.127 ± 0.41	0.105	14.0 ± 55	0.56	0.385 ± 19	0.084	12.331 ± 525	0.741 ± 28	0.0110 ± 0.56	0.580 ± 22.0	1.762 ± 75	0.00137	135.98 ± 1.20
3	587	0.334 ± 0.19	0.297	36.5 ± 67	1.46	0.948 ± 35	0.289	8.125 ± 365	1.235 ± 14	0.0109 ± 0.21	0.369 ± 4.3	0.445 ± 20	0.00182	146.66 ± 0.34
4	657	0.901 ± 0.07	0.833	100.4 ± 93	4.01	1.871 ± 16	0.258	6.112 ± 151	2.319 ± 23	0.0111 ± 0.10	0.257 ± 2.6	0.122 ± 3	0.00059	149.32 ± 0.18
5	714	3.392 ± 0.21	3.038	370.0 ± 330	14.79	7.297 ± 21	0.701	1.651 ± 176	11.998 ± 47	0.0109 ± 0.10	0.354 ± 1.4	0.009 ± 0.95	0.00044	147.79 ± 0.14
6	740	4.712 ± 0.18	4.591	557.6 ± 490	22.29	8.706 ± 28	1.382	0.529 ± 418	4.086 ± 23	0.0118 ± 0.10	0.087 ± 0.5	0.002 ± 1.5	0.00057	148.21 ± 0.13
7	766	3.175 ± 0.33	3.091	372.7 ± 330	14.90	5.029 ± 19	0.109	-0.786 - 447	2.860 ± 24	0.0117 ± 0.10	0.090 ± 0.8	-0.004 - 2.4	0.00007	149.24 ± 0.13
8	790	1.276 ± 0.21	1.228	148.1 ± 140	5.92	2.082 ± 18	0.037	-0.895 - 637	1.615 ± 21	0.0116 ± 0.11	0.127 ± 1.6	-0.012 - 8.6	0.00006	149.24 ± 0.15
9	816	0.950 ± 0.08	0.912	110.2 ± 100	4.41	1.604 ± 23	0.063	-0.603 - 176	1.308 ± 24	0.0116 ± 0.11	0.138 ± 2.5	-0.011 - 3.2	0.00013	148.89 ± 0.17
10	859	1.363 ± 0.11	1.320	158.8 ± 140	6.35	2.355 ± 19	0.215	0.735 ± 429	1.452 ± 24	0.0117 ± 0.10	0.107 ± 1.7	0.009 ± 5.4	0.00031	149.57 ± 0.15
11	965	4.202 ± 0.62	4.099	496.6 ± 440	19.85	6.981 ± 22	0.484	0.270 ± 596	3.503 ± 29	0.0118 ± 0.11	0.083 ± 1	0.001 ± 2.4	0.00022	148.57 ± 0.13
12	1100	0.804 ± 0.04	0.783	93.4 ± 85	3.73	1.516 ± 32	0.289	-0.844 - 369	0.690 ± 17	0.0116 ± 0.11	0.086 ± 2	-0.018 - 7.9	0.00071	150.92 ± 0.16
13	1370	0.231 ± 0.09	0.209	25.8 ± 44	1.03	0.726 ± 18	0.285	1.156 ± 271	0.735 ± 19	0.0112 ± 0.19	0.318 ± 8.1	0.090 ± 21	0.00254	146.19 ± 0.44

Appendix D3: $^{40}Ar/^{39}Ar$ step heating analytical data. All errors refer to the last digit.

Sample GR99/38 white mica (weight = 0.0527g; J = 0.00104)

step	Temp. [°C]	Ar 40 tot. ± s x10-8	Ar 40 * x10-8	Ar 39 ± s x10-12	Ar 39 %	Ar 38 ± s x10-12	Cl x10-12	Ar 37 ± s x10-12	Ar 36 ± s x10-12	39 / 40 ± s	36 / 40 ± s x10-4	Ca / K ± s x10-1	Cl/K	Age [Ma] ± s
1	444	0.102 ± 1.00	0.021	8.3 ± 1.20	0.46	0.811 ± 12.0	0.198	0.248 ± 248	2.76445 ± 32	0.0081 ± 1.4	2.703 ± 42	0.608205 ± 60	0.00551	46.09 ± 2.20
2	558	0.112 ± 0.65	0.065	14.6 ± 0.90	0.81	0.645 ± 13.0	0.180	0.337 ± 337	1.57167 ± 15	0.0131 ± 1.1	1.406 ± 16	0.472608 ± 46	0.00282	81.79 ± 0.87
3		0.321 ± 0.02	0.240	45.1 ± 0.44	2.50	1.278 ± 78.0	0.237	0.429 ± 429	2.7305 ± 21	0.0141 ± 0.1	0.851 ± 6	0.135105 ± 19	0.00121	97.15 ± 0.26
4	640	7.440 ± 0.08	6.868	1125.8 ± 9.90	62.32	22.058 ± 41.0	5.206	0.270 ± 27	19.3161 ± 73	0.0151 ± 0.1	0.260 ± 1	0.034498 ± 0	0.00106	110.97 ± 0.10
5	684	0.436 ± 0.03	0.411	66.0 ± 0.62	3.65	1.126 ± 32.0	0.195	-0.168 - 168	0.82671 ± 21	0.0151 ± 0.1	0.190 ± 5	-0.00539 - 5	0.00068	113.38 ± 0.20
6	739	0.182 ± 0.02	0.174	29.1 ± 0.45	1.61	0.449 ± 24.0	0.057	0.597 ± 597	0.26558 ± 17	0.0160 ± 0.3	0.146 ± 9	0.059653 ± 41	0.00045	108.79 ± 0.35
7	791	0.345 ± 0.01	0.337	55.9 ± 0.56	3.09	1.074 ± 23.0	0.366	-0.307 - 307	0.27099 ± 23	0.0162 ± 0.2	0.079 ± 7	-0.0276 - 11	0.00151	109.72 ± 0.24
8	840	0.345 ± 0.03	0.336	55.8 ± 0.57	3.09	1.095 ± 11.0	0.379	0.390 ± 390	0.32138 ± 32	0.0161 ± 0.2	0.093 ± 9	0.08099 ± 14	0.00156	109.62 ± 0.32
9	886	0.600 ± 0.07	0.593	96.8 ± 0.93	5.36	1.642 ± 29.0	0.460	-0.726 - 726	0.2297 ± 26	0.0161 ± 0.2	0.038 ± 4	-0.01888 - 15	0.00109	111.39 ± 0.18
10	970	1.010 ± 0.01	0.986	162.0 ± 1.50	8.97	2.671 ± 25.0	0.645	-0.275 - 275	0.63865 ± 21	0.0161 ± 0.2	0.064 ± 2	-0.01685 - 3	0.00092	110.75 ± 0.12
11	1067	0.799 ± 0.09	0.783	127.9 ± 1.20	7.08	2.119 ± 24.0	0.514	0.550 ± 5500	0.53705 ± 14	0.0160 ± 0.2	0.067 ± 2	0.006587 ± 9	0.00092	111.33 ± 0.11
12	1193	0.068 ± 0.15	0.061	10.2 ± 0.30	0.57	0.246 ± 18.0	0.083	0.307 ± 307	0.23075 ± 19	0.0150 ± 0.4	0.338 ± 28	0.365708 ± 60	0.00186	109.21 ± 1.00
13	1420	0.055 ± 0.18	0.049	8.9 ± 2.00	0.49	0.040 ± 30.0	0.010	-0.665 - 665	0.20181 ± 21	0.0162 ± 0.4	0.369 ± 39	-0.24854 - 150	0.00026	100.57 ± 1.30

Sample GR99/33 white mica (weight = 0.01g; J = 0.00104)

step	Temp. [°C]	Ar 40 tot. ± s x10-8	Ar 40 * x10-8	Ar 39 ± s x10-12	Ar 39 %	Ar 38 ± s x10-12	Cl x10-12	Ar 37 ± s x10-12	Ar 36 ± s x10-12	39 / 40 ± s	36 / 40 ± s x10-4	Ca / K ± s x10-1	Cl/K	Age [Ma] ± s
1	440	0.081 ± 0.78	0.029	10.2 ± 0.7	0.60	0.802 ± 6	0.350	3.165 ± 613	1.778 ± 26	0.0126 ± 1.4	2.184 ± 38	0.6195 ± 1200	0.00788	52.24 ± 1.50
2	523	0.025 ± 0.57	0.015	4.3 ± 0.1	0.26	0.219 ± 97	0.102	4.371 ± 496	0.358 ± 16	0.0170 ± 3.8	1.404 ± 71	2.0248 ± 2300	0.00541	63.50 ± 2.50
3	595	0.049 ± 0.33	0.031	8.4 ± 0.1	0.50	0.461 ± 21	0.247	1.915 ± 415	0.619 ± 18	0.0171 ± 1.2	1.261 ± 38	0.4565 ± 990	0.00678	67.50 ± 1.30
4	657	0.086 ± 0.05	0.059	15.4 ± 0.3	0.91	0.299 ± 35	0.006	0.639 ± 479	0.926 ± 22	0.0179 ± 0.3	1.072 ± 26	0.0827 ± 620	0.00008	70.34 ± 0.78
5	713	0.111 ± 0.01	0.089	21.4 ± 0.4	1.27	0.402 ± 12	0.012	-1.360 - 278	0.737 ± 22	0.0193 ± 0.4	0.664 ± 20	-0.1270 - 260	0.00013	76.54 ± 0.57
6	738	0.113 ± 0.05	0.094	22.6 ± 0.2	1.34	0.095 ± 49	0.029	0.167 ± 407	0.631 ± 18	0.0200 ± 0.2	0.558 ± 16	0.0148 ± 360	0.00029	76.77 ± 0.42
7	764	0.050 ± 0.04	0.042	10.2 ± 0.1	0.60	0.145 ± 52	0.003	-0.334 - 361	0.276 ± 19	0.0203 ± 0.3	0.550 ± 38	-0.0657 - 710	0.00006	75.85 ± 1.00

continues

Appendix D3: $^{40}Ar/^{39}Ar$ step heating analytical data. All errors refer to the last digit.

Sample GR99/33 continued

step	Temp. [°C]	Ar 40 tot. ± s x10-8	Ar 40 * x10-8	Ar 39 ± s x10-12	Ar 39 %	Ar 38 ± s x10-12	Cl x10-12	Ar 37 ± s x10-12	Ar 36 ± s x10-12	39 / 40 ± s	36 / 40 ± s x10-4	Ca / K ± s x10-1	Cl/K	Age [Ma] ± s
8		0.061 ± 0.01	0.053	11.8 ± 0.3	0.70	0.254 ± 5.3	0.063	-1.219 - 277	0.280 ± 16	0.0193 ± 0.4	0.459 ± 26	-0.2068 - 470	0.00122	82.20 ± 0.72
9	684	3.759 ± 1.50	3.226	575.5 ± 5.4	34.05	9.293 ± 20	0.085	0.594 ± 662	18.040 ± 120	0.0153 ± 0.2	0.480 ± 3.2	0.0021 ± 23	0.00003	102.21 ± 0.15
10	711	0.338 ± 0.02	0.310	54.3 ± 0.6	3.21	0.978 ± 32	0.160	0.314 ± 407	0.962 ± 20	0.0161 ± 0.2	0.284 ± 5.8	0.0115 ± 150	0.00068	103.89 ± 0.22
11	738	0.225 ± 0.03	0.214	38.2 ± 0.4	2.26	0.549 ± 38	0.033	1.449 ± 573	0.363 ± 16	0.0170 ± 0.2	0.161 ± 7	0.0759 ± 300	0.00020	102.35 ± 0.25
12	774	0.344 ± 0.06	0.318	58.4 ± 0.6	3.45	0.928 ± 14	0.077	1.237 ± 350	0.879 ± 20	0.0170 ± 0.2	0.256 ± 6	0.0424 ± 120	0.00030	99.36 ± 0.21
13	811	0.332 ± 0.04	0.313	55.4 ± 0.6	3.28	1.022 ± 22	0.251	1.384 ± 238	0.643 ± 21	0.0167 ± 0.2	0.194 ± 6.2	0.0500 ± 86	0.00104	102.95 ± 0.22
14	857	0.395 ± 0.08	0.374	66.3 ± 0.6	3.92	1.046 ± 15	0.138	-0.604 - 255	0.681 ± 31	0.0168 ± 0.2	0.173 ± 7.9	-0.0182 - 77	0.00048	102.95 ± 0.26
15	906	0.780 ± 0.09	0.737	131.7 ± 1.2	7.79	1.956 ± 12	0.136	0.818 ± 277	1.453 ± 21	0.0169 ± 0.2	0.186 ± 2.7	0.0124 ± 42	0.00024	102.03 ± 0.13
16	968	0.817 ± 0.11	0.791	141.7 ± 1.3	8.38	2.009 ± 22	0.179	0.611 ± 524	0.874 ± 24	0.0173 ± 0.2	0.107 ± 3	0.0086 ± 74	0.00029	101.83 ± 0.13
17	1100	0.633 ± 0.10	0.577	106.8 ± 1.0	6.32	1.876 ± 22	0.265	2.965 ± 342	1.902 ± 18	0.0169 ± 0.2	0.300 ± 2.8	0.0555 ± 64	0.00057	98.63 ± 0.13
18	1373	2.196 ± 0.50	2.021	357.9 ± 3.3	21.17	5.803 ± 18	0.482	0.338 ± 412	5.944 ± 37	0.0163 ± 0.2	0.271 ± 1.7	0.0019 ± 23	0.00031	102.94 ± 0.11

CURRICULUM VITAE

Name:	Thomas Most
Geburtsdatum / -ort:	17. Juni 1969, Rüsselsheim

Schule:

1975 – 1979	Grundschule Edermünde
1979 – 1981	Georg-August-Zinn Gesamtschule Gudensberg
1981 – 1986	Leimborn Gesamtschule Kassel, Realschulabschluß
1986 – 1990	Jacob Grimm Oberstufengymnasium Kassel, Abitur
1990 – 1991	Grundwehrdienst

Studium:

1991 – 1997	Studium der Geologie / Paläontologie an der Geowissenschaftlichen Fakultät der Georg-August Universität, Göttingen. Abschluß: Diplom-Geologe.
1998 – 2003	Promotionsstudium am Institut für Geowissenschaften der Eberhardt-Karls Universität Tübingen.